

---

# **Studies on Caged Nitrogen Compounds**

A thesis presented to the University of London in partial fulfilment of the  
requirements for the degree of Doctor of Philosophy

**Catherine Elizabeth Lipton**

University College London, 2003

---

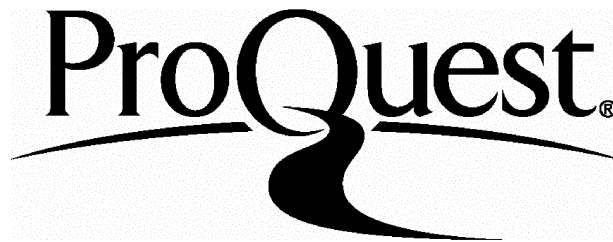
ProQuest Number: U643324

All rights reserved

INFORMATION TO ALL USERS

The quality of this reproduction is dependent upon the quality of the copy submitted.

In the unlikely event that the author did not send a complete manuscript and there are missing pages, these will be noted. Also, if material had to be removed, a note will indicate the deletion.



ProQuest U643324

Published by ProQuest LLC(2016). Copyright of the Dissertation is held by the Author.

All rights reserved.

This work is protected against unauthorized copying under Title 17, United States Code.  
Microform Edition © ProQuest LLC.

ProQuest LLC  
789 East Eisenhower Parkway  
P.O. Box 1346  
Ann Arbor, MI 48106-1346

# Abstract

---

This thesis describes studies on caged nitrogen compounds, in particular hexamethylenetetramine. Thus, Chapter One presents an introduction to the synthesis and chemistry of hexamethylenetetramine.

Chapter Two describes efforts to synthesise new caged nitrogen compounds using the synthesis of hexamethylenetetramine as a model. First, studies of the reaction of formaldehyde and ammonia in the presence of a number of metal amine complexes are described. Secondly, investigations into the use of some macrocyclic metal amine complexes as precursors to high energy compounds are reported.

In Chapter Three it has been shown that hexamethylenetetramine acts as a ligand on organometallic compounds of ruthenium and rhodium. The ligand can bind in a monodentate fashion, as in  $[\text{Ru}(\eta^3\text{-}\eta^3\text{-C}_{10}\text{H}_{16})\text{Cl}(\text{hmt})]$  or  $[\text{Ru}(\eta^6\text{-}p\text{-cymene})\text{Cl}_2(\text{hmt})]$ ; the latter has been characterised using X-ray crystallography. Binuclear complexes have also been prepared, with hexamethylenetetramine bound terminally, as in the chloride bridged salt  $[(\eta^6\text{-C}_6\text{H}_6)\text{ClRu}(\mu\text{-Cl})_2\text{Ru}(\eta^6\text{-C}_6\text{H}_6)(\text{hmt})\text{Cl}]$ , or bound as a bridging ligand, as in  $[\{\text{Rh}(\eta^5\text{-C}_5\text{Me}_5)\text{Cl}\}_2(\mu\text{-hmt})]$ .

Chapter Four presents reactions of hexamethylenetetramine with *bis*(benzotrile)palladium(II)dichloride to produce  $[\text{Pd}(\text{hmt})_2\text{Cl}_2]$  and  $[\text{Pd}(\text{hmt})_2\text{Cl}_2]_n$ . The complex  $[\text{Pd}(\text{hmt})_2\text{Cl}_2]$  has been shown by X-ray crystallography to exist as the *trans* isomer in the solid state. The reaction of chloro(2-methyl- $\eta^3$ -allyl)palladium(II) with hexamethylenetetramine gave  $[\text{PdCl}(\eta^3\text{-C}_4\text{H}_7)(\text{C}_6\text{H}_{12}\text{N}_4)]$  and  $[\text{Pd}_2\text{Cl}_2(\eta^3\text{-C}_4\text{H}_7)_2(\mu\text{-C}_6\text{H}_{12}\text{N}_4)]$ , both of which have been characterised using X-ray crystallography and low temperature  $^1\text{H}$

NMR spectroscopy. Variable temperature  $^1\text{H}$  NMR studies and computer simulation of spectra have given an insight into the solution dynamics of these compounds. Low temperature  $^1\text{H}$  NMR studies have established the existence of  $[\text{Pd}_4\text{Cl}_4(\eta^3\text{-C}_4\text{H}_7)_4(\mu^4\text{-C}_6\text{H}_{12}\text{N}_4)]$ , where hexamethylenetetramine acts as a tetradentate ligand.

Chapter Five reports the synthesis of  $[\text{Rh}_2(\text{O}_2\text{CCH}_2\text{CH}_3)_4(\text{hmt})_2]$  and  $[\text{Rh}_2(\text{O}_2\text{CCH}_2\text{CH}_3)_4(\text{hmt})]_n$ . The redox properties of both complexes have been investigated using cyclic voltammetry. Using these electrochemical results, the donor ability of a number of ligands has been determined as  $\text{hmt} > [\text{PdCl}(\eta^3\text{-C}_4\text{H}_7)(\text{hmt})] > [\text{Rh}_2(\text{O}_2\text{CCH}_2\text{CH}_3)_4(\text{hmt})]$ . A simple rationale for this ordering has been suggested.

# Table of Contents

---

<b>Abstract</b>	<b>2</b>
<b>Table of Contents</b>	<b>4</b>
<b>Table of Figures</b>	<b>9</b>
<b>Table of Schemes</b>	<b>12</b>
<b>Table of Tables</b>	<b>13</b>
<b>Abbreviations</b>	<b>15</b>
<b>Acknowledgements</b>	<b>16</b>
<b>Chapter One Introduction</b>	<b>17</b>
<hr/>	
<b>1.1 Background</b>	<b>18</b>
<b>1.2 Hexamethylenetetramine, an introduction</b>	<b>18</b>
1.2.1 Synthesis and general chemistry of hexamethylenetetramine	18
1.2.2 The solid-state structure of hexamethylenetetramine	19
1.2.3 The formation of hexamethylenetetramine from formaldehyde and ammonia	21
1.2.4 Selected reactions of hexamethylenetetramine	27
<b>1.3 Interactions of hexamethylenetetramine with metals</b>	<b>29</b>
<b>1.4 Nitrogen rich cages as precursors to energetic materials</b>	<b>34</b>
<b>1.5 Present Work</b>	<b>37</b>
<b>Chapter Two Investigations into the metal-mediated synthesis of caged nitrogen compounds</b>	<b>38</b>
<hr/>	
<b>2.1 Introduction</b>	<b>39</b>
2.1.1 Metal-mediated condensation reactions	39

<b>2.2</b>	<b>Reactions of formaldehyde with metal amine complexes</b>	<b>45</b>
2.2.1	Reactions of metal amine complexes and formaldehyde in aqueous solution	45
2.2.2	The reaction of methylaluminium <i>bis</i> (2,6-diphenylphenoxide) with [Ni(NH <sub>3</sub> ) <sub>6</sub> ]Br <sub>2</sub>	50
2.2.3	Reactions of [Ni(NH <sub>3</sub> ) <sub>6</sub> ]Br <sub>2</sub> with gaseous formaldehyde.	52
<b>2.3</b>	<b>Synthesis of metal encapsulating amines</b>	<b>53</b>
2.3.1	Introduction	53
2.3.2	Synthesis of non-metallated diaminosarcophagine	54
2.3.3	<i>Tert</i> -butoxycarbonyl protection of diaminosarcophagine	58
<b>2.4</b>	<b>Conclusions</b>	<b>59</b>
<b>2.5</b>	<b>Experimental</b>	<b>59</b>
2.5.1	Physical Measurements	59
2.5.2	Materials	60
2.5.3	Reaction of formaldehyde with <i>hexakis</i> (amino)cobalt(III)chloride	60
2.5.4	Reaction of methylaluminium <i>bis</i> (2,6-diphenylphenoxide) (MAPH) with <i>hexakis</i> (amino)nickel(II)bromide in inert atmosphere	61
2.5.5	Reaction of <i>hexakis</i> (amino)nickel(II)bromide with paraformaldehyde	62
2.5.6	Synthesis of [Co(sep)]Cl <sub>3</sub>	62
2.5.7	Synthesis of [Co{(NO <sub>2</sub> ) <sub>2</sub> sar}]Cl <sub>3</sub>	63
2.5.8	Synthesis of [Co{(NH <sub>3</sub> ) <sub>2</sub> sar}]Cl <sub>5</sub>	63
2.5.9	Synthesis of (NH <sub>2</sub> ) <sub>2</sub> sar.H <sub>2</sub> O	64
2.5.10	Reaction of (NH <sub>2</sub> ) <sub>2</sub> sar with di- <i>tert</i> -butyl dicarbonate	64
2.5.11	Reaction of piperazine with di- <i>tert</i> -butyl dicarbonate	65
<b>Chapter Three Ruthenium and rhodium complexes of hexamethylenetetramine</b>		<b>66</b>
<b>3.1</b>	<b>Introduction</b>	<b>67</b>
3.1.1	The synthesis and reactions of “Ru(η <sup>6</sup> -arene)” complexes	67
3.1.2	The synthesis and reactions of “Rh(η <sup>5</sup> -C <sub>5</sub> Me <sub>5</sub> )” complexes	72

3.1.3	<i>Bis</i> (allyl)ruthenium(IV) complexes	77
<b>3.2</b>	<b>Results and discussion</b>	<b>82</b>
3.2.1	Complexes of “Ru( $\eta^6$ - <i>p</i> -cymene)” with hexamethylenetetramine	82
3.2.2	Complexes of “Ru( $\eta^6$ -C <sub>6</sub> H <sub>6</sub> )” with hexamethylenetetramine	90
3.2.3	Complexes of “Rh( $\eta^5$ -C <sub>5</sub> Me <sub>5</sub> )” with hexamethylenetetramine	93
3.2.4	Complexes of “Ru( $\eta^3$ : $\eta^3$ -C <sub>10</sub> H <sub>16</sub> )” with hexamethylenetetramine	94
<b>3.3</b>	<b>Conclusions</b>	<b>95</b>
<b>3.4</b>	<b>Experimental</b>	<b>96</b>
3.4.1	Starting materials	96
3.4.2	Crystallography	96
3.4.3	Synthesis of [Ru( $\eta^6$ - <i>p</i> -cymene)(hmt)Cl <sub>2</sub> ]	97
3.4.4	Synthesis of [( $\eta^6$ -C <sub>6</sub> H <sub>6</sub> )ClRu( $\mu$ -Cl) <sub>2</sub> Ru(hmt)( $\eta^6$ -C <sub>6</sub> H <sub>6</sub> )]Cl	97
3.4.5	Synthesis of [{Rh( $\eta^5$ -C <sub>5</sub> Me <sub>5</sub> )Cl <sub>2</sub> ] <sub>2</sub> ( $\mu$ -hmt)]	98
3.4.6	Synthesis of [Ru( $\eta^3$ : $\eta^3$ -C <sub>10</sub> H <sub>16</sub> )Cl <sub>2</sub> (hmt)]	98
3.4.7	Crystallographic Data	99
<b>Chapter Four Palladium(II) complexes with hexamethylenetetramine</b>		<b>103</b>
<b>4.1</b>	<b>Introduction</b>	<b>104</b>
<b>4.2</b>	<b>Reactions of bis(benzonitrile)palladium(II)dichloride with hexamethylenetetramine</b>	<b>104</b>
4.2.1	Background	104
4.2.2	Reactions of <i>bis</i> (benzonitrile)palladium(II)dichloride with hexamethylenetetramine	105
<b>4.3</b>	<b>Complexes of chloro(2-methyl-<math>\eta^3</math>-allyl)palladium(II) with hexamethylenetetramine</b>	<b>110</b>
4.3.1	Background	110
4.3.2	Synthesis of hexamethylenetetramine derivatives of chloro(2-methyl- $\eta^3$ -allyl)palladium(II)	115

4.3.3	Variable temperature $^1\text{H}$ NMR studies of hexamethylenetetramine derivatives of chloro(2-methyl- $\eta^3$ -allyl)palladium(II)	124
4.3.3.1	Introduction	124
4.3.3.2	Analysis of variable temperature $^1\text{H}$ NMR spectra for $[\text{Pd}_2\text{Cl}_2(\eta^3\text{-C}_4\text{H}_7)_2(\mu\text{-hmt})]$	126
4.3.3.3	Analysis of variable temperature $^1\text{H}$ NMR spectra for $[\text{PdCl}(\eta^3\text{-C}_4\text{H}_7)(\text{C}_6\text{H}_{12}\text{N}_4)]$	131
4.3.3.4	Conclusions from analysis of variable temperature $^1\text{H}$ NMR spectra	133
<b>4.4</b>	<b>Reactions of hexamethylenetetramine with 1,3,6,8-tetraazatricyclo[4.4.1.1.<sup>3,8</sup>]-dodecane</b>	<b>134</b>
<b>4.5</b>	<b>Conclusions</b>	<b>137</b>
<b>4.6</b>	<b>Experimental</b>	<b>138</b>
4.6.1	Crystallography	138
4.6.2	Synthesis of $[\text{Pd}(\text{hmt})_2\text{Cl}_2]$ , <b>(44)</b>	138
4.6.3	Synthesis of $[\text{Pd}(\text{hmt})\text{Cl}_2]_n$ ,	139
4.6.4	Synthesis of $[\text{PdCl}(\eta^3\text{-C}_4\text{H}_7)(\text{hmt})]$ , <b>(46)</b>	139
4.6.5	Synthesis of $[\text{Pd}_2\text{Cl}_2(\eta^3\text{-C}_4\text{H}_7)_2(\mu\text{-hmt})]$ , <b>(47)</b>	139
4.6.6	Attempted synthesis of $[\text{Pd}_4\text{Cl}_4(\eta^3\text{-C}_4\text{H}_7)_4(\mu^4\text{-hmt})]$	140
4.6.7	Synthesis of $[\text{Pd}_2\text{Cl}_2(\eta^3\text{-C}_4\text{H}_7)_2(\mu\text{-C}_8\text{H}_{16}\text{N}_4)]$ , <b>(49)</b>	140
4.6.8	Crystallographic data for $[\text{Pd}(\text{hmt})_2\text{Cl}_2]$ , <b>(44)</b>	142
4.6.9	Crystallographic data for $[\text{PdCl}(\eta^3\text{-C}_4\text{H}_7)(\text{hmt})]$ , <b>(46)</b>	145
4.6.10	Crystallographic data for $[\text{Pd}_2\text{Cl}_2(\eta^3\text{-C}_4\text{H}_7)_2(\mu\text{-hmt})]$ , <b>(47)</b>	148

---

**Chapter Five Studies on complexes of rhodium(II) carboxylates with hexamethylenetetramine 151**

---

<b>5.1</b>	<b>Introduction</b>	<b>152</b>
5.1.1	Dirhodium tetracarboxylate complexes	152
5.1.2	Bonding in $[\text{Rh}_2(\text{O}_2\text{CR})_4]$ complexes	154
5.1.3	Lewis base adducts of $[\text{Rh}_2(\text{O}_2\text{CR})_4]$ compounds	156



5.1.3.1	A general overview of 1:2 adducts	156
5.1.3.2	1:2 adducts with nitrogen-donor ligands	157
5.1.3.3	Polymeric complexes of $[\text{Rh}_2(\text{O}_2\text{CR})_4]$ with nitrogen donor ligands	159
5.1.3.4	Adducts of $[\text{Rh}_2(\text{O}_2\text{CR})_4]$ with metallo-ligands	162
5.1.4	Electrochemical studies on $[\text{Rh}_2(\text{O}_2\text{CR})_4\text{L}_2]$ complexes	163
<b>5.2</b>	<b>Results and discussion</b>	<b>164</b>
5.2.1	Synthetic investigations	164
5.2.2	Electrochemical Investigations	166
<b>5.3</b>	<b>Conclusions</b>	<b>171</b>
<b>5.4</b>	<b>Experimental</b>	<b>171</b>
5.4.1	Reaction of $[\text{Rh}_2(\text{O}_2\text{CCH}_2\text{CH}_3)_4]$ with two equivalents of hexamethylenetetramine	171
5.4.2	General electrochemical procedure	172
5.4.3	Cyclic voltammetry: results	173
	<b>References</b>	<b>174</b>

# Table of Figures

Figure 1.1	Structures for hexamethylenetetramine as suggested by Lösekann, van't Hoff and Dominikiewicz	20
Figure 1.2	Representation of bond length distortion in substituted hexamethylenetetramine, the molecule now has $C_{3v}$ symmetry.	21
Figure 1.3	Coordination polymer of CuI and hexamethylenetetramine	30
Figure 1.4	Three-dimensional silver-hexamethylenetetramine complex	30
Figure 1.5	A section of an infinite 2-D layer found in $[Ag_2(\mu^3\text{-hmt})(NO_2)]_n$	31
Figure 1.6	A representation of the polymeric structure of $[Ag_2(\mu^4\text{-hmt})(NO_2)_2]_n$ .	32
Figure 1.7	Chain polymer made up of $[Cu_2(O_2CCH_3)_4(\text{hmt})]_n$ units	33
Figure 2.1	Tetraaza macrocycle formed <i>via</i> metal-template synthesis	40
Figure 2.2	Hexaaza macrocycle formed from one-pot metal template synthesis	40
Figure 2.3	Possible products from reaction of ammonia and formaldehyde	47
Figure 3.1	Geometry about ruthenium in $[(\eta^6\text{-C}_6\text{H}_6)\text{RuCl}_2(\text{PMePh}_2)]^{90}$	69
Figure 3.2	$[\text{Ru}(\eta^6\text{-arene})\text{Cl}(\text{triazine})]\text{Cl}$ , (arene = benzene or <i>p</i> -cymene)	72
Figure 3.3	Structure of $[\{\text{Ru}(\eta^3:\eta^3\text{-C}_{10}\text{H}_{16})\text{Cl}_2\}_2(\mu\text{-C}_4\text{H}_4\text{N}_2)]$ as determined by X-ray diffraction	82
Figure 3.4	$^1\text{H}$ NMR spectrum of $[(\eta^6\text{-}p\text{-cymene})\text{RuCl}_2(\text{hmt})]$ at 298 K	83
Figure 3.5	The three inequivalent sets of protons, of hexamethylenetetramine in a 1:1 adduct	84
Figure 3.6	$^1\text{H}$ NMR spectra of $[(\eta^6\text{-}p\text{-cymene})\text{RuCl}_2(\text{hmt})]$ , 211 – 298 K	85
Figure 3.7	$^1\text{H}$ NMR spectrum of $[(\eta^6\text{-}p\text{-cymene})\text{RuCl}_2(\text{hmt})]$ and a second product, 253 K	86
Figure 3.8	Solid state structure of $[(\eta^6\text{-}p\text{-cymene})\text{RuCl}_2(\text{hmt})]$ as determined by single crystal X-ray diffraction	88
Figure 3.9	$^1\text{H}$ NMR spectrum of “ $\text{Ru}(\eta^6\text{-C}_6\text{H}_6)$ ”-hmt adduct at 298 K	91
Figure 3.10	Chemical environments of hexamethylenetetramine protons in $[\{\eta^6\text{-C}_6\text{H}_6\}\text{RuCl}_2]_2(\mu\text{-hmt})]$	91
Figure 3.11	$^1\text{H}$ NMR spectrum of “ $\text{Ru}(\eta^6\text{-C}_6\text{H}_6)$ ”-hmt adduct at 253 K	92
Figure 3.12	Equatorial adduct $[\text{Ru}(\eta^3:\eta^3\text{-C}_{10}\text{H}_{16})\text{Cl}_2(\text{hmt})]$	95

Figure 4.1	Solid state structure of <i>trans</i> -[Pd(hmt) <sub>2</sub> Cl <sub>2</sub> ] as determined by single crystal X-ray diffraction	106
Figure 4.2	Possible chain polymer [PdCl <sub>2</sub> hmt] <sub>n</sub>	109
Figure 4.3	Possible ring-type structures of [PdCl <sub>2</sub> hmt] <sub>n</sub>	109
Figure 4.4	Temperature dependence of NMR spectra of PPh <sub>3</sub> adduct of chloro(allyl)palladium(II)	114
Figure 4.5	Multinuclear species containing two allylpalladium units	115
Figure 4.6	<sup>1</sup> H NMR of [PdCl(η <sup>3</sup> -C <sub>4</sub> H <sub>7</sub> )(hmt)] at 298 K, CDCl <sub>3</sub> solvent	116
Figure 4.7	<sup>1</sup> H NMR of [PdCl(η <sup>3</sup> -C <sub>4</sub> H <sub>7</sub> )(hmt)] at 223 K, CDCl <sub>3</sub> solvent	116
Figure 4.8	Solid state structure of [PdCl(η <sup>3</sup> -C <sub>4</sub> H <sub>7</sub> )(hmt)]	118
Figure 4.9	<sup>1</sup> H NMR of [Pd <sub>2</sub> Cl <sub>2</sub> (η <sup>3</sup> -C <sub>4</sub> H <sub>7</sub> ) <sub>2</sub> (μ-hmt)] at 298 K, CDCl <sub>3</sub> solvent	121
Figure 4.10	Expected <sup>1</sup> H NMR signals for hexamethylenetetramine in [Pd <sub>2</sub> Cl <sub>2</sub> (η <sup>3</sup> -C <sub>4</sub> H <sub>7</sub> ) <sub>2</sub> (μ-hmt)]	122
Figure 4.11	<sup>1</sup> H NMR of [Pd <sub>2</sub> Cl <sub>2</sub> (η <sup>3</sup> -C <sub>4</sub> H <sub>7</sub> ) <sub>2</sub> (μ-hmt)] at 298 K, CDCl <sub>3</sub> solvent	122
Figure 4.12	Solid state structure of [Pd <sub>2</sub> Cl <sub>2</sub> (η <sup>3</sup> -C <sub>4</sub> H <sub>7</sub> ) <sub>2</sub> (μ-hmt)]	123
Figure 4.13	<sup>1</sup> H NMR spectra for [Pd <sub>2</sub> Cl <sub>2</sub> (η <sup>3</sup> -C <sub>4</sub> H <sub>7</sub> ) <sub>2</sub> (μ-hmt)], 223 – 298 K	127
Figure 4.14	Fit of experimental spectra for [Pd <sub>2</sub> Cl <sub>2</sub> (η <sup>3</sup> -C <sub>4</sub> H <sub>7</sub> ) <sub>2</sub> (μ-hmt)] over a range of temperatures	129
Figure 4.15	Arrhenius plot of ln k against 1/T for [Pd <sub>2</sub> Cl <sub>2</sub> (η <sup>3</sup> -C <sub>4</sub> H <sub>7</sub> ) <sub>2</sub> (μ-hmt)]	130
Figure 4.16	Eyring plot of ln (k/T) against 1/T for [Pd <sub>2</sub> Cl <sub>2</sub> (η <sup>3</sup> -C <sub>4</sub> H <sub>7</sub> ) <sub>2</sub> (μ-hmt)]	131
Figure 4.17	<sup>1</sup> H NMR spectra for [PdCl(η <sup>3</sup> -C <sub>4</sub> H <sub>7</sub> )(hmt)], 223 – 298 K	132
Figure 4.18	[Pd <sub>2</sub> Cl <sub>2</sub> (η <sup>3</sup> -C <sub>4</sub> H <sub>7</sub> ) <sub>2</sub> (μ-C <sub>8</sub> H <sub>16</sub> N <sub>4</sub> )] ; hydrogen atom labelling corresponds to NMR shown in Figure 4.19	136
Figure 4.19	<sup>1</sup> H NMR of [Pd <sub>2</sub> Cl <sub>2</sub> (η <sup>3</sup> -C <sub>4</sub> H <sub>7</sub> ) <sub>2</sub> (μ-C <sub>8</sub> H <sub>16</sub> N <sub>4</sub> )] recorded at 178 K in CD <sub>2</sub> Cl <sub>2</sub>	136
Figure 5.1	Examples of dirhodium tetracarboxylate complexes with bulky bridging ligands	153
Figure 5.2	Chains formed by [Rh <sub>2</sub> (O <sub>2</sub> CR) <sub>4</sub> ], R = C <sub>3</sub> H <sub>7</sub> or CF <sub>3</sub> ,	154
Figure 5.3	Effect of oxidation on the electronic configuration of [Rh <sub>2</sub> (O <sub>2</sub> CR) <sub>4</sub> ]	155
Figure 5.4	Complexes isolated from the reaction of [Rh <sub>2</sub> (O <sub>2</sub> CCH <sub>3</sub> ) <sub>4</sub> ] with 2-amino-6-methylpyridine	159
Figure 5.5	Repeating unit of polymeric [Rh <sub>2</sub> (O <sub>2</sub> CCH <sub>3</sub> ) <sub>4</sub> (aamp)] <sub>n</sub>	160
Figure 5.6	Macrocyclic nitrogen-donor ligands	161

Figure 5.7	1:2 adduct of $[\text{Rh}_2(\text{O}_2\text{CR})_4]$ with a rhenium containing ligand	163
Figure 5.8	$^1\text{H}$ NMR spectrum at 223 K, of $[\text{Rh}_2(\text{O}_2\text{CCH}_2\text{CH}_3)_4(\text{hmt})_2]$ and $[\{\text{Rh}_2(\text{O}_2\text{CCH}_2\text{CH}_3)_4\}_2(\mu\text{-hmt})]$ between 4.6 and 6.2 ppm	165
Figure 5.9	The complex $[\{\text{Rh}_2(\text{O}_2\text{CCH}_2\text{CH}_3)_4\}_2(\mu\text{-hmt})]$	166
Figure 5.10	Cyclic voltammogram recorded in DCM (0.1 M TBABF <sub>4</sub> supporting electrolyte) for $[\text{Rh}_2(\text{O}_2\text{CCH}_2\text{CH}_3)]$ and hexamethylenetetramine	167
Figure 5.11	Cyclic voltammogram recorded in DCM (0.2 M TBABF <sub>4</sub> supporting electrolyte) $[\text{Rh}_2(\text{O}_2\text{CCH}_2\text{CH}_3)(\text{hmt})_2]$ over a range of scan rates	169

# Table of Schemes

---

Scheme 3.1	Suggested equilibrium for $\{[\text{RhCl}_2(\eta^5\text{-C}_5\text{Me}_5)]_2(\text{NH}_2\text{NHMe})\}$ in solution	76
Scheme 3.2	Suggested dynamic process occurring in solution for $[(\eta^6\text{-}i\text{-p-cymene})\text{RuCl}_2(\text{hmt})]$	87
Scheme 3.3	Proposed equilibrium in solution for $[(\eta^6\text{-C}_6\text{H}_6)\text{ClRu}(\mu\text{-Cl})_2\text{Ru}(\text{hmt})(\eta^6\text{-C}_6\text{H}_6)]^+$	93
Scheme 4.1	Reaction of chloro( $\eta^3$ -allyl)palladium(II) in DMSO	111
Scheme 4.2	Suggested fluxional processes occurring in solution : (a) ligand exchange (b) $\pi$ to $\sigma$ equilibrium (c) head-over-tail equilibrium	113
Scheme 4.3	Equilibrium process rendering $\text{H}_a$ and $\text{H}_a'$ equivalent and $\text{H}_b$ and $\text{H}_b'$ equivalent	117
Scheme 4.4	Proposed mechanism leading to equivalence of all 12 protons on hexamethylenetetramine ligand in solution at 298 K	128

# Table of Tables

Table 1.1	Selected properties of RDX and HMX.	34
Table 2.1	Reactions of metal amine complexes with formaldehyde at room temp.	46
Table 2.2	Reactions of metal amine complexes with formaldehyde at reflux	48
Table 3.1	Neutral, monomeric arene-ruthenium amine complexes: [( $\eta^6$ -arene)RuCl <sub>2</sub> (NHRR')]	70
Table 3.2	Cationic arene-ruthenium amine complexes: [( $\eta^6$ -arene)RuCl(NH <sub>2</sub> R) <sub>2</sub> ] <sup>+</sup>	71
Table 3.3	“RhCl( $\eta^5$ -C <sub>5</sub> Me <sub>5</sub> )” complexes with aromatic amines	74
Table 3.4	Complexes of “( $\eta^5$ -C <sub>5</sub> Me <sub>5</sub> )Rh” with hydrazines	75
Table 3.5	<sup>1</sup> H NMR data obtained on dissolution of {Ru( $\eta^3$ : $\eta^3$ -C <sub>10</sub> H <sub>16</sub> )Cl( $\mu$ -Cl)} <sub>2</sub> in CDCl <sub>3</sub> at 298 K	78
Table 3.6	Adducts of “Ru( $\eta^3$ : $\eta^3$ -C <sub>10</sub> H <sub>16</sub> )” with aromatic primary amines	81
Table 3.7	Selected bond lengths [Å] and angles [°] for [( $\eta^6$ - <i>p</i> -cymene)RuCl <sub>2</sub> (hmt)]	88
Table 3.8	Crystallographic data for [( $\eta^6$ - <i>p</i> -cymene)RuCl <sub>2</sub> (hmt)].CH <sub>2</sub> Cl <sub>2</sub>	99
Table 3.9	Atomic coordinates (x 10 <sup>4</sup> ) and equivalent isotropic displacement parameters (Å <sup>2</sup> x 10 <sup>3</sup> ) for [( $\eta^6$ - <i>p</i> -cymene)RuCl <sub>2</sub> (hmt)].CH <sub>2</sub> Cl <sub>2</sub>	100
Table 3.10	Bond lengths [Å] and angles [°] for [( $\eta^6$ - <i>p</i> -cymene)RuCl <sub>2</sub> (hmt)].CH <sub>2</sub> Cl <sub>2</sub>	101
Table 4.1	Selected bond lengths [Å] and angles [°] for <i>trans</i> -[Pd(hmt) <sub>2</sub> Cl <sub>2</sub> ]	106
Table 4.2	Selected bond lengths [Å] for a range of dichloropalladium complexes with tertiary amine ligands	108
Table 4.3	Selected bond lengths [Å] and angles [°] for [PdCl( $\eta^3$ -C <sub>4</sub> H <sub>7</sub> )(hmt)]	118
Table 4.4	Selected bond lengths [Å] for a range of $\eta^3$ -allylpalladium complexes, H atoms on allyl ligand omitted for clarity.	120
Table 4.5	Selected bond lengths [Å] and angles [°] for [Pd <sub>2</sub> Cl <sub>2</sub> ( $\eta^3$ -C <sub>4</sub> H <sub>7</sub> ) <sub>2</sub> ( $\mu$ -hmt)]	124
Table 4.6	Selected activation parameters for ligand exchange of nitrogen donor ligands on allylpalladium complexes	134
Table 4.7	Crystal data and structure refinement for [Pd(hmt) <sub>2</sub> Cl <sub>2</sub> ], <b>(44)</b>	142
Table 4.8	Atomic coordinates (x 10 <sup>4</sup> ) and equivalent isotropic displacement parameters (Å <sup>2</sup> x 10 <sup>3</sup> ) for [Pd(hmt) <sub>2</sub> Cl <sub>2</sub> ], <b>(44)</b>	143
Table 4.9	Bond lengths [Å] and angles [°] for [Pd(hmt)Cl <sub>2</sub> ], <b>(44)</b>	144
Table 4.10	Crystal data and structure refinement for [PdCl( $\eta^3$ -C <sub>4</sub> H <sub>7</sub> )(hmt)]	145

Table 4.11	Atomic coordinates ( $\times 10^4$ ) and equivalent isotropic displacement parameters ( $\text{\AA}^2 \times 10^3$ ) for $[\text{PdCl}(\eta^3\text{-C}_4\text{H}_7)(\text{hmt})]$ , <b>(46)</b>	146
Table 4.12	Bond lengths [ $\text{\AA}$ ] and angles [ $^\circ$ ] for $[\text{PdCl}(\eta^3\text{-C}_4\text{H}_7)(\text{hmt})]$ , <b>(46)</b>	147
Table 4.13	Crystal data and structure refinement for $[\text{Pd}_2\text{Cl}_2(\eta^3\text{-C}_4\text{H}_7)_2(\mu\text{-hmt})]$ , <b>(47)</b>	148
Table 4.14	Atomic coordinates ( $\times 10^4$ ) and equivalent isotropic displacement parameters ( $\text{\AA}^2 \times 10^3$ ) for $[\text{Pd}_2\text{Cl}_2(\eta^3\text{-C}_4\text{H}_7)_2(\mu\text{-hmt})]$ , <b>(47)</b>	149
Table 4.15	Bond lengths [ $\text{\AA}$ ] and angles [ $^\circ$ ] for $[\text{Pd}_2\text{Cl}_2(\eta^3\text{-C}_4\text{H}_7)_2(\mu\text{-hmt})]$ , <b>(47)</b>	150
Table 5.1	Overlaps of d-orbitals and their resulting molecular orbitals	154
Table 5.2	Bond lengths [ $\text{\AA}$ ] for selected $[\text{Rh}_2(\text{O}_2\text{CCH}_3)_4\text{L}_2]$	156

# Abbreviations

---

BOC	<i>tert</i> -butoxycarbonyl
Cp*	pentamethylcyclopentadienyl
$\delta$	chemical shift/ppm
d	doublet
DCM	dichloromethane
DMSO	dimethylsulfoxide
E <sub>pa</sub>	anodic peak potential
E <sub>pc</sub>	cathodic peak potential
E <sub>1/2</sub>	half-wave potential
Et	ethyl
hmt	hexamethylenetetramine
HMX	1,3,5,7-tetranitro-1,3,5,7-tetraazacyclooctane
I <sub>pa</sub>	anodic current
I <sub>pc</sub>	cathodic current
IR	infrared
<i>i</i> Pr	isopropyl
Me	methyl
NMR	nuclear magnetic resonance
<i>p</i> -cymene	1-methyl-4-isopropylbenzene
q	quartet
R	organic substituent
RDX	cyclo-1,3,5-trimethylene-2,4,6-trinitramine
s	singlet
sar	sarcophagine, 3,6,10,13,16,19-hexaazabicyclo[6.6.6]eicosane
sep	sepulchrane, 1,3,6,8,10,13,16,19-octaazabicyclo[6.6.6]eicosane
sept	septet
TATD	1,3,6,8-tetraazatricyclo[4.4.1.1. <sup>3,8</sup> ]-dodecane
TBABF <sub>4</sub>	tetrabutylammonium tetrafluoroborate
<i>t</i> Bu	tertiary butyl
THF	tetrahydrofuran
t	triplet



# Acknowledgements

---

appreciation recognition gratitude gratefulness thanks

During the time spent carrying out the research for this Ph.D. thesis I have made many friends and received assistance from a number of people. First, of course thanks goes to my supervisor, Dr. Derek Tocher, who has been a great source of ideas, enthusiasm and encouragement. I am also very grateful to Professor Tony Deeming for his interesting and helpful discussions and for assistance with gNMR. Input of ideas from Dr. Rob Claridge (QinetiQ) is also greatly appreciated. Members of the UCL chemistry department who deserve particular mention are Dr. Abil Aliev and Professor Edgar Anderson for help with NMR experiments and interpretation, Dr. Darren Caruana for assistance with electrochemical experiments and Mr Phil Hayes for loans of chemicals, equipment and help with instrumentation. Thanks also to Dr. Jon Steed (Kings College) who performed some of the single crystal structure determinations.

Funding from the EPSRC and QinetiQ (formerly DERA) is gratefully acknowledged.

Special thanks goes to Abul Ali, Caroline Forth and Sarah Brown, fellow members of the lab that time forgot, for making 301M a good, if slightly mad, place to work. Thanks also to all members of lab 301, past and present, for being good friends and helpful chemists. Thank you to my organic consultant, Kason Bala, and major thanks to Mark Field for being a great friend, as well as a computer genius.

Warmest thanks to my parents and all of my family, for their love and encouragement.

Finally, to Warren Cross, Blur, Track 7. Say no more.

---

# Chapter One

## Introduction

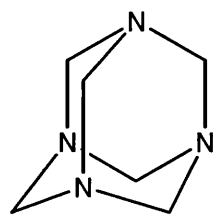
## 1.1 Background

The research described in this thesis derives from interest in caged nitrogen compounds as both precursors to energetic materials and versatile ligands in organometallic and coordination chemistry. The caged compound hexamethylenetetramine has been the main focus of this work. First, the synthesis of hexamethylenetetramine has been used as a starting point for efforts to prepare new nitrogen cage compounds using metal template synthesis as described in Chapter Two. Secondly, the suitability of hexamethylenetetramine as a ligand in organometallic and coordination compounds has been investigated and a range of adducts have been prepared. The structure, solution dynamics and redox properties of these adducts are described in Chapters Three, Four and Five. Thus, the remainder of this introductory chapter presents the synthesis and general chemistry of hexamethylenetetramine, followed by a brief survey of metallo-hexamethylenetetramine complexes and a description of how the compound is used as a precursor to energetic materials.

## 1.2 Hexamethylenetetramine, an introduction

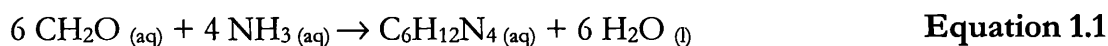
### 1.2.1 Synthesis and general chemistry of hexamethylenetetramine

Hexamethylenetetramine, 1,3,5,7-tetraazatricyclo-(3.3.1.1<sup>3,7</sup>)-decane (**1**) was first synthesised in 1859<sup>1</sup> and has been widely studied, as described in a number of reviews.<sup>2,3</sup> Hexamethylenetetramine is also known as hexamine, aminoform, formin, urotropine or methenamine and is abbreviated to hmt in this thesis.



(1)

Hexamethylenetetramine is commonly prepared *via* the condensation reaction of stoichiometric amounts of aqueous formaldehyde and ammonia, **Equation 1.1**.<sup>4</sup>



In order to precipitate the product from aqueous solution, excess ammonia may be added, alternatively evaporation of the water on a steam bath yields the crude product. The colourless solid, which may be recrystallised from ethanol, does not melt but sublimes at 280 °C, with slight decomposition.<sup>5</sup> Hexamethylenetetramine is readily soluble in water, with solubility decreasing with increasing water temperature a phenomenon attributed to decreasing association of the amine with water at higher temperatures.<sup>2</sup>

The wide-ranging chemistry of hexamethylenetetramine is a consequence of its ‘dual-nature’. For instance, hexamethylenetetramine acts as a tertiary amine when forming salts and complexes analogous to those seen for pyridine. However, the use of hexamethylenetetramine as a source of anhydrous formaldehyde is also reported.<sup>2</sup> This latter property leads to the use of hexamethylenetetramine in the manufacture of synthetic resins, for example in the final hardening of phenol-formaldehyde resins where liberation of water would lead to bubble formation.<sup>2</sup>

In addition to its use in the resin industry, hexamethylenetetramine is widely used for medical purposes as a urinary antiseptic.<sup>6</sup> The commercial use of hexamethylenetetramine of most relevance to this research is its application in the synthesis of energetic materials, which is discussed in section 1.2.4.

### 1.2.2 The solid-state structure of hexamethylenetetramine

Hexamethylenetetramine crystallises as rhombic dodecahedrons and belongs to the cubic spacegroup  $I4_3m$ , which utilises the full tetrahedral symmetry of the nearly spherical hexamethylenetetramine molecule.<sup>7</sup> The crystal structure of

hexamethylenetetramine was first determined in 1923, and in fact was the first analysis of the structure of an organic molecule.<sup>8</sup> This work reports the use of spectral and Laue photographs to deduce the structure, with all carbon and all nitrogen atoms equivalent, and confirms (1) as the solid state structure of hexamethylenetetramine, reporting a C-N bond length of 1.44 Å. Although this structure had been proposed previously,<sup>9</sup> it was one of a number of potential candidates, some of which are illustrated in **Figure 1.1**.

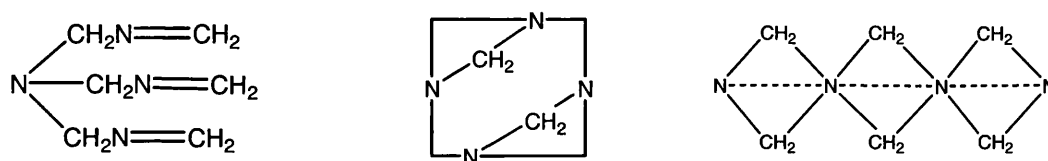


**Figure 1.1** Structures for hexamethylenetetramine as suggested by Lösekann,<sup>10</sup> van't Hoff<sup>11</sup> and Dominikiewicz<sup>12</sup>

Since the first structural determination there have been numerous reports of structure determinations of hexamethylenetetramine under various conditions. These include investigations of hexamethylenetetramine in the gas phase,<sup>13</sup> neutron diffraction studies<sup>14,15</sup> and the collection of X-ray data at low-temperature.<sup>7,16</sup> An accurate determination of atomic parameters of hexamethylenetetramine using X-ray data collected at 120 K reported a C-N bond length of 1.469(2) Å, with angles for C-N-C and N-C-N of 107.88(9) ° and 112.58(8) °, respectively.<sup>16</sup>

Quaternisation of one of the nitrogen atoms of hexamethylenetetramine significantly affects its tetrahedral geometry, as illustrated in **Figure 1.2**. The quaternary nitrogen-carbon bonds become longer relative to the C-N length in the unsubstituted hexamethylenetetramine. The C-N bonds making up the six-membered ring in the basal plane of the molecule remain the same and the C-N bonds linking this ring and the 'cap' of the molecule are shortened. This phenomenon has been illustrated using crystallographic studies of the protonated,<sup>17</sup> methylated,<sup>18</sup> N-oxide<sup>19</sup>, borine adducts<sup>20</sup> and metal coordinated<sup>21</sup> hexamethylenetetramine. A survey of this data concluded that the cage distortion

decreases in the order methylation > borine adduct formation  $\cong$  N-oxide formation  $\cong$  protonation > metal coordination.<sup>21</sup>

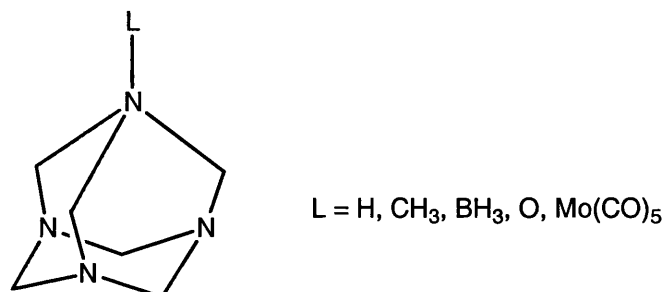
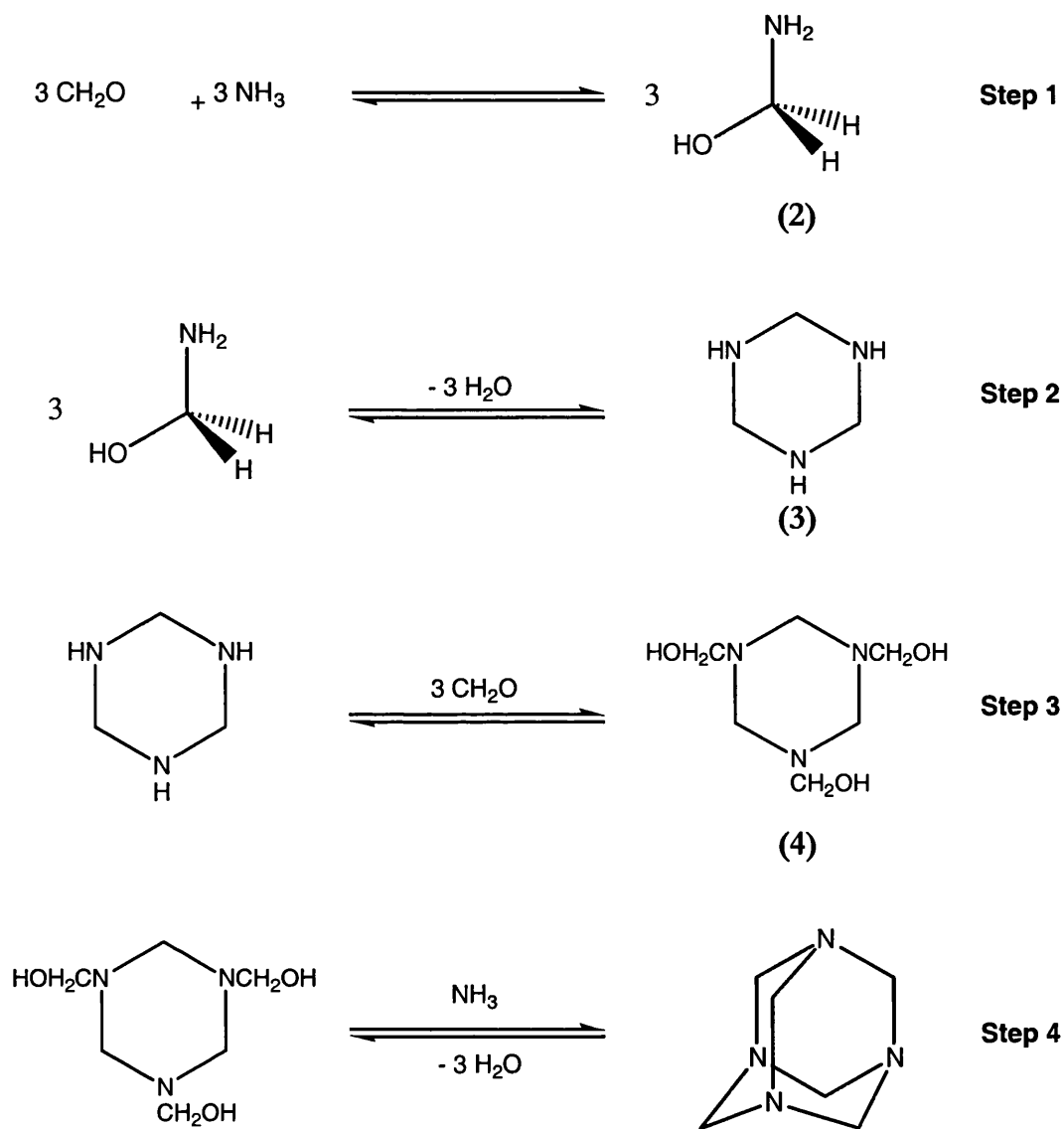


**Figure 1.2** Representation of bond length distortion in substituted hexamethylenetetramine, the molecule now has  $C_{3v}$  symmetry.

### 1.2.3 The formation of hexamethylenetetramine from formaldehyde and ammonia

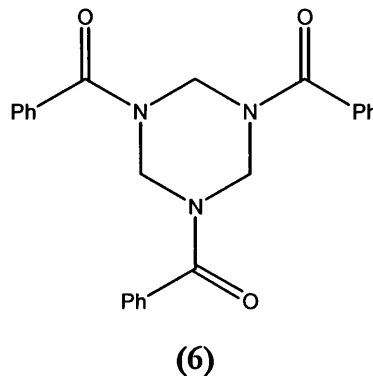
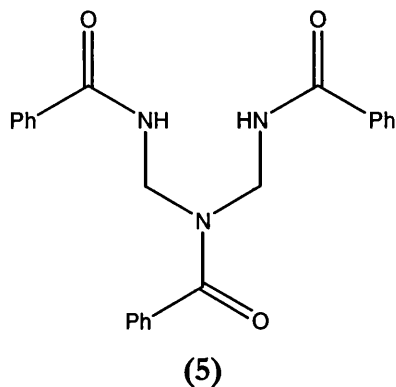
The mechanism of formation of hexamethylenetetramine from formaldehyde and ammonia has been of interest for many years. An investigation in 1895 by Duden and Scharff<sup>9</sup> assigned cyclotrimethylenetriamine (1,3,5-hexahydrotriazine) **(3)** as a reaction intermediate and postulated the mechanism illustrated in **Scheme 1.1**. This mechanism suggests that an initial condensation of formaldehyde and ammonia yields aminomethanol **(2)**, which then trimerises to cyclotrimethylenetriamine. Subsequent methylation of cyclotrimethylenetriamine produces trimethylolcyclotrimethylenetriamine **(4)**, which on condensation with ammonia produces hexamethylenetetramine.



**Scheme 1.1 Proposed mechanism for hexamethylenetetramine formation**

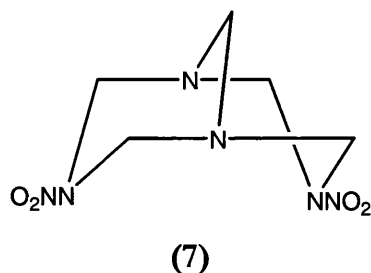
In 1948, Richmond *et al.*<sup>22</sup> re-examined the formaldehyde-ammonia system producing results in agreement with Duden and Scharff. Both groups obtained evidence for the presence of (3) as an intermediate by comparing aqueous hexamethylenetetramine solutions with freshly prepared formaldehyde/ammonia solutions. In these freshly prepared solutions an aqueous solution of ammonium chloride with an excess of sodium hydroxide served as the ammonia source; the resulting excess of sodium hydroxide raised the pH of the solution to 12.2 where hexamethylenetetramine formation is quite slow, thus allowing observation of intermediates. The researchers found that when treated with benzoyl chloride the hexamethylenetetramine solution gave 1,3,5-tribenzoyl-1,3,5-triazapentane

(5), whereas the formaldehyde/ammonia solution gave 1,3,5-tribenzoyl-1,3,5-triazacyclohexane (6) with only a trace of (5).



In addition, Richmond *et al.* investigated the first step of the reaction mechanism, by studying the changing pH of a solution of ammonia and formaldehyde at 0 °C. The pH of the initial water-ammonia solution was recorded as 12.5; the reading of 11.0 immediately after formaldehyde addition indicates reaction of the majority of the ammonia present in the solution. Reaction of dimethylnitramide with a formaldehyde/ammonia solution may be used as a test for the completion of the reaction to form hexamethylenetetramine. This is because a fresh formaldehyde-ammonia solution gives 1,5-endomethylene-3,7-dinitro-1,3,5,7-tetraazacyclooctane (DPT), (7) when reacted with benzoyl chloride, but a solution containing only hexamethylenetetramine does not. Thus, using the synthesis of DPT as a guide, the researchers concluded that conversion to hexamethylenetetramine was not complete. In addition, the pH of a solution of hexamethylenetetramine at the same concentration is *ca.* 7.2, a value not reached by the test solution until 274 minutes after formaldehyde addition. These results indicate that during mixing of formaldehyde and ammonia a fast reaction occurs, producing cyclotrimethylenetriamine (1,3,5-triazinane) (3). It was then proposed that the remaining formaldehyde reacts more slowly to yield trimethylolcyclotrimethylenetriamine (1,3,5-triazinane-1,3,5-triyltrimethanol) (4), which reacts in a final step with the remaining ammonia to give hexamethylenetetramine.<sup>22</sup>

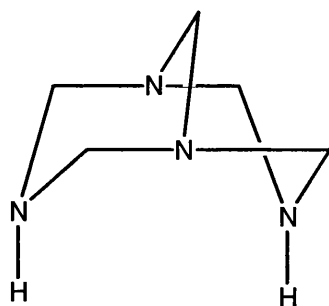




The theory that trimethylolcyclotrimethylenetriamine is a reaction intermediate is not supported by more recent studies using NMR spectroscopy.<sup>23</sup> These investigations by Nielsen and co-workers agree with earlier studies that cyclotrimethylenetriamine forms rapidly upon mixing formaldehyde and ammonia, and is ultimately the principal species present in solution other than hexamethylenetetramine, but NMR evidence indicates the presence of other significant reaction intermediates.<sup>23</sup>

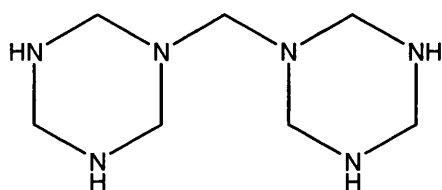
Both <sup>1</sup>H and <sup>13</sup>C NMR were used to investigate the species present at various times in D<sub>2</sub>O solutions of ammonium-*d*<sub>4</sub> hydroxide and formaldehyde at 25°C. Altering the molar ratio of formaldehyde:ammonia (from 3:2 to 1:4) had no effect on the products formed, although the relative distribution of the products at a given time had changed slightly. The <sup>1</sup>H NMR spectra show formation of hexamethylenetetramine and cyclotrimethylenetriamine, and indicate the presence of additional reaction intermediates. The resonance of the methylene protons of hexamethylenetetramine are observed at 4.75 ppm. The remaining methylene signals are grouped in two principal regions: sharp signals at 3.5-4.0 ppm, assigned as NCH<sub>2</sub>N-type methylenes, and broad signals at *ca.* 4.5 ppm attributed to NCH<sub>2</sub>O-type methylenes. Of these a sharp singlet at 3.95 ppm is assigned to cyclotrimethylenetriamine, and a collapsed AB quartet at 3.86 ppm and a singlet at 3.81 ppm are attributed to 1,3,5,7-tetraazabicyclo[3.3.1]nonane (**8**). The broad signals at 4.5 ppm, which disappear more rapidly over time than those of cyclotrimethylenetriamine and 1,3,5,7-tetraazabicyclo[3.3.1]nonane, are attributed to *N*-methylol-*O-d* derivatives.

The remaining NMR signals are attributed to intermediates present in much smaller quantities.

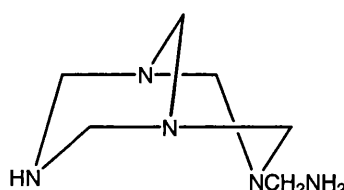


(8)

The  $^{13}\text{C}$  NMR spectra were in agreement with the assignments made using the  $^1\text{H}$  NMR spectra. In addition two sets of signals were observed that decreased in intensity with time. These signals of relative intensity 4:2:1 and 2:2:1:1, were postulated to arise from the compounds (9) and (10).

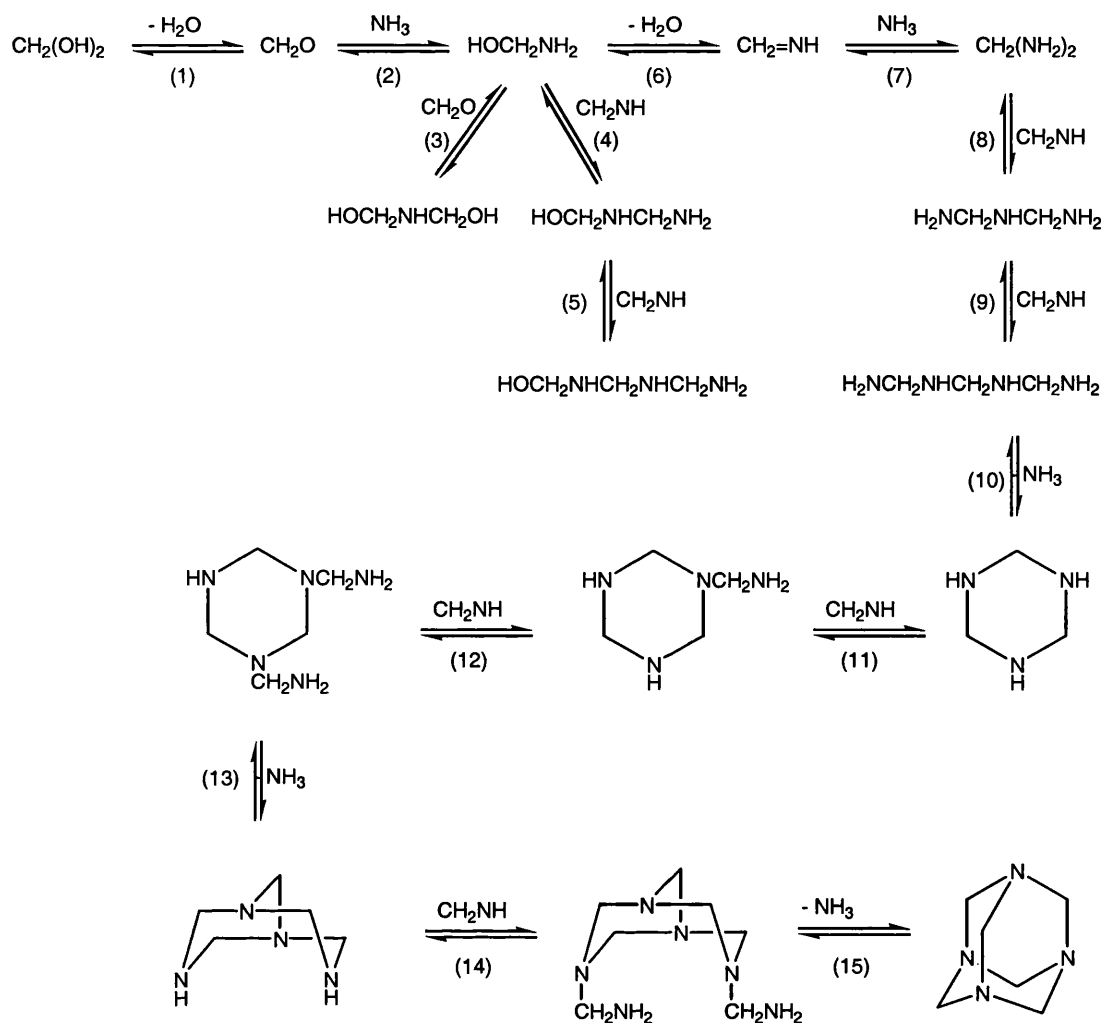


(9)



(10)

Using this NMR evidence a much more detailed mechanism for hexamethylenetetramine formation from formaldehyde and ammonia, was postulated and is illustrated in **Scheme 1.2**.<sup>23</sup>



**Scheme 1.2** A simplified mechanism for the formation of hexamethylenetetramine from formaldehyde and ammonia.

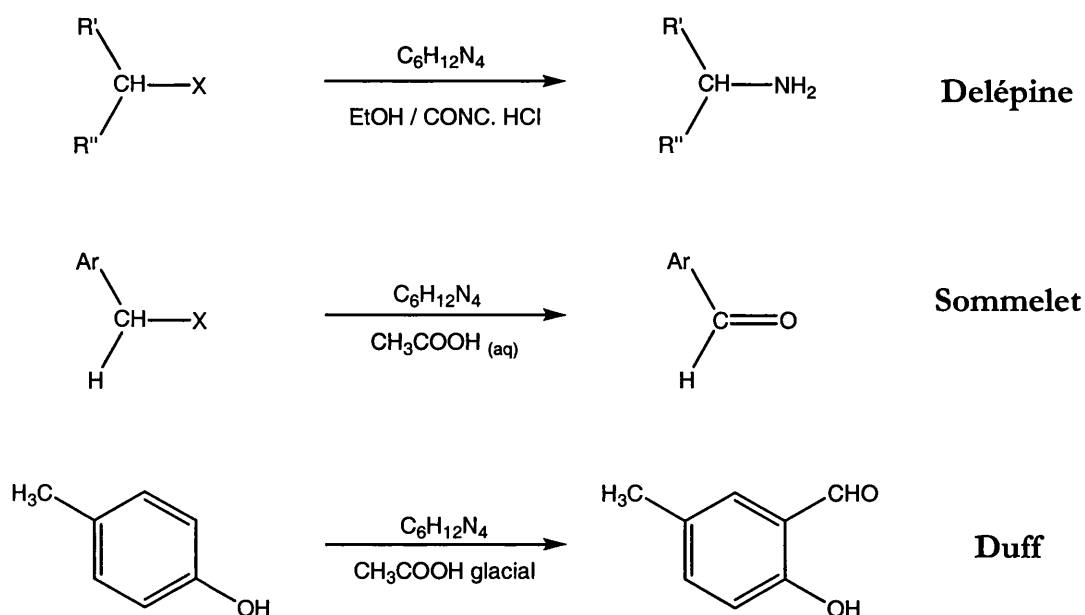
The kinetics of the formaldehyde – ammonia reaction have been investigated by a number of researchers.<sup>24-29</sup> The reaction was found to be first order with respect to ammonia and second order with respect to formaldehyde. Naturally, these studies consider the various mechanisms of hexamethylenetetramine formation, in particular the rate-determining step, which is assigned as the reaction of formaldehyde and aminomethanol to form iminodimethanol.<sup>25, 27, 29</sup> This step was noted as significant in the publications of the three groups discussed previously and is illustrated in **Scheme 1.1**, step two and **Scheme 1.2**, step three. The kinetic studies, all published prior to the NMR studies of Nielsen *et al.*, suggest numerous routes from iminodimethanol to

hexamethylenetetramine, *via* intermediates including cyclotrimethylenetriamine and 1,3,5,7-tetraazacyclooctane.<sup>27</sup>

Evidently, the reaction of formaldehyde and ammonia is a complex one affected by factors such as concentration of reactants, temperature and pH. NMR spectroscopy has been useful in identifying reaction intermediates, but the major product isolated from the reaction is always hexamethylenetetramine.

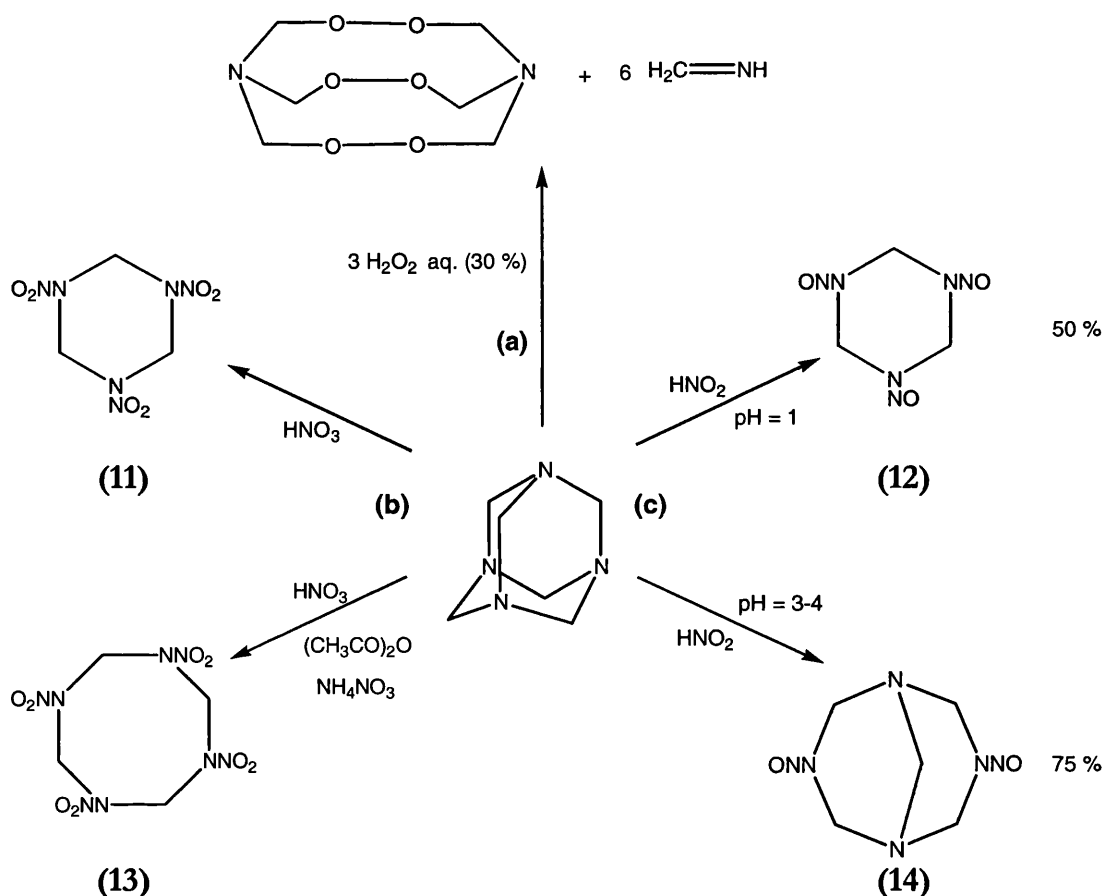
#### 1.2.4 Selected reactions of hexamethylenetetramine

Hexamethylenetetramine has an extensive chemistry, acting both as a source of formaldehyde and as a tertiary amine. The hydrolysis of hexamethylenetetramine occurs *via* reaction with strong acids in aqueous solution. Indeed, the reaction of hexamethylenetetramine with sulphuric acid has been used as a quantitative analysis for hexamethylenetetramine.<sup>30</sup> Hexamethylenetetramine is also used as a reagent in three well-known organic preparations illustrated in **Scheme 1.3**.<sup>31</sup> The Delépine reaction involves the conversion of alkyl halides into primary amines under strongly acidic conditions.<sup>32</sup> Reaction of hexamethylenetetramine with benzylic halides in aqueous acetic acid gives the benzylic aldehyde, this is known as the Sommelet reaction.<sup>33</sup> The Duff reaction uses hexamethylenetetramine as a reagent to introduce a formyl group onto a phenol with ortho selectivity.<sup>34</sup>



**Scheme 1.3** General examples of the Delépine, Sommelet and Duff reactions

Of particular relevance to the research discussed in Chapter Two of this thesis is the fact that hexamethylenetetramine can act as a precursor to energetic materials, **Scheme 1.4**. The nitrosation of hexamethylenetetramine is performed by addition of dilute HCl and sodium nitrite to an aqueous solution of hexamethylenetetramine, which produces trimethylenetrinitrosamine (**12**) or dinitrosopentamethylenetetramine (**14**), depending on the pH of the solution.<sup>37</sup> Compound (**12**) the sole product at pH 1-2 is a powerful explosive.<sup>37</sup> When hexamethylenetetramine is treated with hydrogen peroxide, in the presence of excess acid, hexamethylenetriperoxidediamine is produced.<sup>35</sup> This material is a primary explosive detonating violently when the dry material is subject to mechanical shock. The nitration of hexamethylenetetramine produces the nitramines RDX, (**11**) (cyclo-1,3,5-trimethylene-2,4,6-trinitramine, cyclonite) and HMX, (**13**) (1,3,5,7-tetranitro-1,3,5,7-tetraazacyclooctane, octogen) depending upon the nitration conditions.<sup>36</sup> Both RDX and HMX have been utilised by the military and their properties are discussed in section 1.4.



**Scheme 1.4** Reactions of hexamethylenetetramine yielding energetic materials; (a) reaction with hydrogen peroxide;<sup>35</sup> (b) nitration;<sup>36</sup> (c) nitrosation<sup>37</sup>

### 1.3 Interactions of hexamethylenetetramine with metals

In addition to the organic chemistry discussed in section 1.2.4, coordination compounds of hexamethylenetetramine with transition metals are also known. The majority of reports published to date involve the synthesis of coordination polymers from solutions of hexamethylenetetramine and simple metal salts. In these compounds hexamethylenetetramine has been observed to act in bidentate, tridentate and tetradentate fashions. The variation in the resulting polymeric networks (*i.e.* two or three dimensional with different cavity types) is a consequence of the pH of the reaction solution, molar ratio of reactants and the identity of the counter-ion.<sup>38</sup>

**Figure 1.3** depicts a coordination polymer in which hexamethylenetetramine acts as a bidentate ligand. The polymer  $[(\text{CuI})_2\text{hmt}]$  is obtained *via* addition of hexamethylenetetramine to a solution of  $\text{CuI}$  in acetonitrile.<sup>38</sup> As shown in the figure there are alternating bridges of iodide ions and hexamethylenetetramine ligands linking pairs of copper ions, resulting in the formation of a two-dimensional sheet structure.

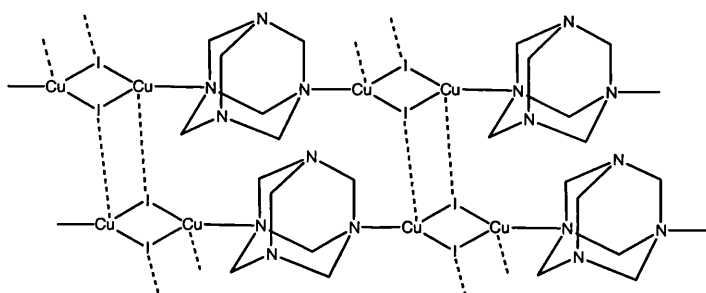


**Figure 1.3** Coordination polymer of  $\text{CuI}$  and hexamethylenetetramine

Hexamethylenetetramine also acts as a bidentate ligand in the three-dimensional complex polymer produced upon diffusion of an ethanolic solution of  $\text{AgPF}_6$  into a chloroform solution of hexamethylenetetramine **Figure 1.4**.<sup>39</sup>

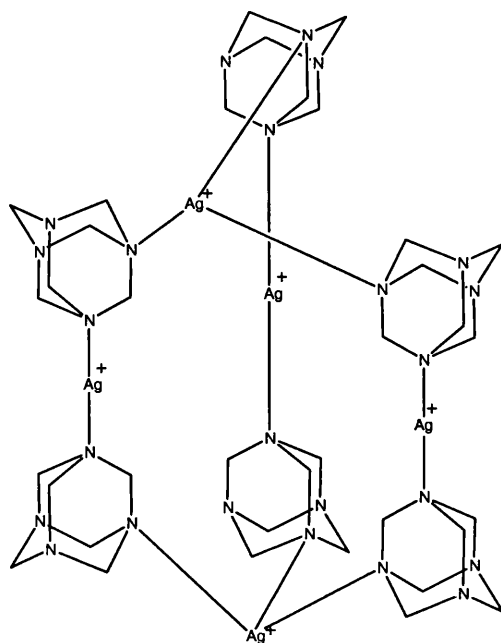


**Figure 1.4** Three-dimensional silver-hexamethylenetetramine complex

In contrast, hexamethylenetetramine acts as a tridentate ligand in the two-dimensional network formed by hexamethylenetetramine and silver ions in the complex  $[\text{Ag}_2(\mu^3\text{-hmt})(\text{NO}_2)_2]$ , which contains hexagonal cavities, **Figure 1.5.**<sup>40</sup>

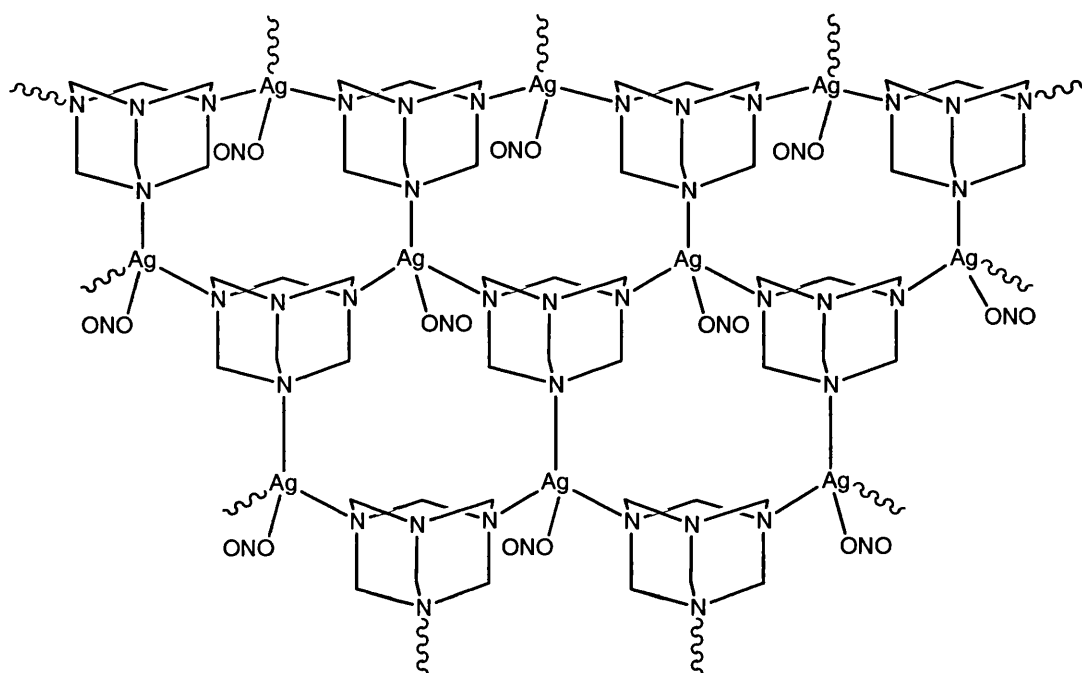


**Figure 1.5** A section of an infinite 2-D layer found in  $[\text{Ag}_2(\mu^3\text{-hmt})(\text{NO}_2)]_n$

An example of the tetradentate coordination of hexamethylenetetramine is observed in the two-dimensional coordination polymer  $[\text{Ag}_2(\mu^4\text{-hmt})(\text{NO}_2)_2]_n$ . This compound, synthesised by reaction of  $\text{AgNO}_2$  and hexamethylenetetramine in an acetonitrile-water mixture, exhibits a structure where the four nitrogen atoms of each hexamethylenetetramine molecule are coordinated to a different silver atom. Thus, a two-dimensional network with square cavities is formed, **Figure 1.6.**<sup>41</sup> The complex contains silver atoms in two different geometries; the geometry around one type of silver atom is linear with coordination by two nitrogen atoms each from a hexamethylenetetramine molecule. The other silver atom is in a triangular prism geometry coordinated by two nitrogen atoms and four oxygen atoms, from two hexamethylenetetramine molecules and two  $\text{NO}_2^-$



molecules respectively. Three-dimensional polymeric structures containing tetradentate hexamethylenetetramine are also known, for example in the compound  $[\text{Ag}_3(\mu^4\text{-hmt})_2(\text{H}_2\text{O})_2](\text{SO}_4)(\text{HSO}_4) \cdot 2 \text{H}_2\text{O}$ .<sup>40</sup>

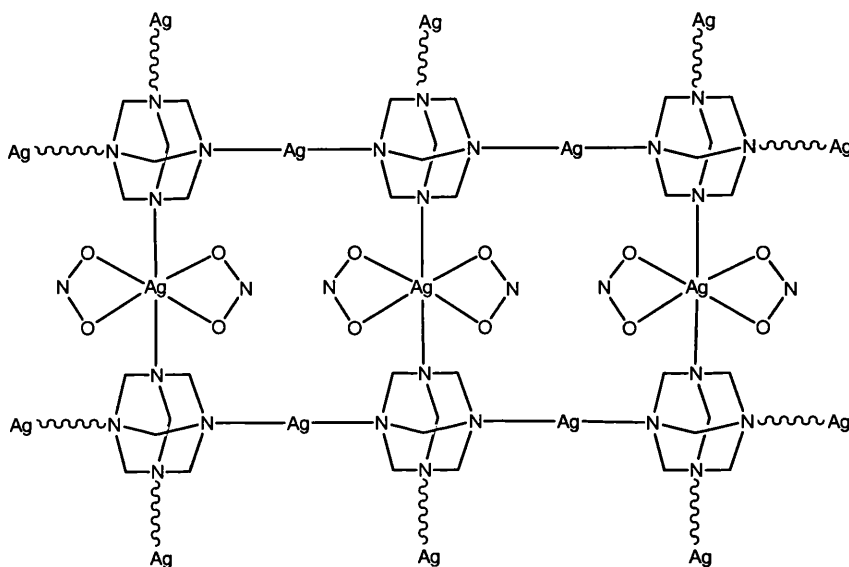


**Figure 1.6** A representation of the polymeric structure of  $[\text{Ag}_2(\mu^4\text{-hmt})(\text{NO}_2)_2]_n$ .

The compounds discussed so far involve the low coordinate metals copper and silver. Metals with potential for tetrahedral or octahedral coordination, however, are of particular interest due to the new structural motifs that may arise in products formed using polydentate ligands such as hexamethylenetetramine. In order to investigate such possibilities, reactions using Ni(II), Zn(II) and Co(II) have been performed. Each experiment involved addition of an aqueous solution of hexamethylenetetramine to an aqueous solution of NaNCS and either  $\text{M}(\text{NO}_3)_2 \cdot 6\text{H}_2\text{O}$  ( $\text{M} = \text{Co}^{42}$  or  $\text{Ni}^{43}$ ) or  $\text{ZnSO}_4 \cdot 7\text{H}_2\text{O}$ .<sup>44</sup> A crystalline product was obtained in each case, after leaving the solutions to stand for several days. Interestingly, only the nickel complex is polymeric, with each hexamethylenetetramine molecule acting as a bidentate ligand to bridge two nickel atoms and form a one-dimensional zigzag chain structure:  $[\text{Ni}(\mu\text{-hmt})(\text{NCS})_2(\text{H}_2\text{O})_2]_n$ . Hexamethylenetetramine also acts as a bridging ligand in the zinc complex,  $[\text{Hhmt}]_2[\text{Zn}_2(\mu\text{-hmt})(\text{NCS})_6]$ , with two protonated

hexamethylenetetramine molecules acting as counter-cations. In the cobalt compound  $[\text{Co}(\text{NCS})_2(\text{hmt})_2(\text{H}_2\text{O})_2][\text{Co}(\text{NCS})_2(\text{H}_2\text{O})_4]\cdot\text{H}_2\text{O}$ , hexamethylenetetramine acts as a monodentate ligand, with the ligands around each cobalt atom having an octahedral arrangement. An analogous compound,  $[\text{Co}(\text{hmt})_2(\text{H}_2\text{O})_4][\text{Co}(\text{H}_2\text{O})_6][\text{SO}_4]_2\cdot\text{H}_2\text{O}$  has been prepared by evaporation of a mixture of water, dioxane and acetone containing hexamethylenetetramine and  $\text{CoSO}_4\cdot 7\text{H}_2\text{O}$ .<sup>45</sup>

Reports of the use of hexamethylenetetramine as a ligand in organometallic complexes are not common, examples include the monomeric compound  $[\text{Mo}(\text{CO})_5(\text{hmt})]^{21}$  and a range of adducts of hexamethylenetetramine with trimethylgallium and trimethylaluminium.<sup>46</sup> The 1:1, 2:1, 3:1 and 4:1 adducts of trimethylgallium and hexamethylenetetramine and the 3:1 and 2:1 adducts of trimethylaluminium and hexamethylenetetramine were obtained as colourless needle crystals in near quantitative yield *via* addition of a stoichiometric quantity of  $\text{Me}_3\text{Ga}$  or  $\text{Me}_3\text{Al}$  to hexamethylenetetramine in toluene.<sup>46</sup>

In the complex  $[\text{Cu}_2(\text{O}_2\text{CCH}_3)_4(\text{hmt})]_n$ , illustrated in **Figure 1.7**, the copper ions are six coordinate and a chain polymer is formed, with hexamethylenetetramine acting as a bridging ligand.<sup>47</sup> The synthesis and redox properties of similar dirhodium complexes are discussed in Chapter Five of this thesis.

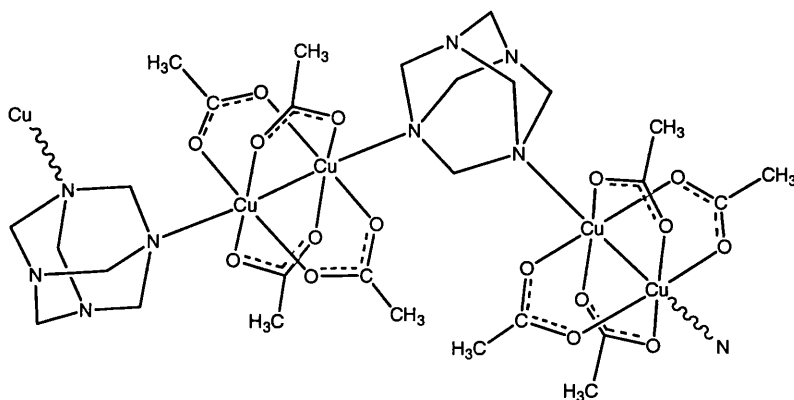


**Figure 1.7** Chain polymer made up of  $[\text{Cu}_2(\text{O}_2\text{CCH}_3)_4(\text{hmt})]_n$  units

### 1.4 Nitrogen rich cages as precursors to energetic materials

Energetic materials may be classified according to their performance and uses. This classification scheme uses the descriptions primary explosive, (detonated easily by heat or shock), secondary explosive, (cannot be detonated by heat or shock) and propellant, (burns only, does not explode). All military explosives are considered secondary explosives since they cannot be detonated readily by heat or shock. In fact the shock from the detonation of a primary explosive is necessary in order to initiate detonation of explosives such as RDX and HMX (Scheme 1.4: (11) and (13) respectively). After this initiation the secondary explosive completely dissociates into its more stable components. Some secondary explosives have such large activation energies that they can actually be set on fire without detonating.

An explosive must contain a fuel and an oxidiser. The energy released originates from the oxidation of the fuel, thus ideally both oxidiser and fuel will be contained in the same molecule. The basic carbon skeleton of the molecule acts as the fuel portion of the explosive. The oxidising component of the explosive is in the form of attached functional groups that contain oxygen atoms. Explosives may also be classified as aliphatic or aromatic by reference to their carbon skeleton. For example, RDX is an aliphatic energetic material with nitro groups acting as oxidisers.

Efficient explosives are required to be dense materials with high detonation velocities. Both RDX and HMX fulfil these criteria, Table 1.1.

**Table 1.1 Selected properties of RDX and HMX.<sup>48</sup>**

	Density/ g cm <sup>-3</sup>	Detonation Velocity/ m s <sup>-1</sup>	Melting Point/ °C
RDX	1.82	8750	204
HMX	1.96	9100	275

RDX and HMX have similar properties, which, as well as high density and detonation velocity, include melting points that are close to their ignition temperatures, therefore they cannot be melted safely. Due to its slightly higher density and detonation velocity, HMX has the better explosive performance of the two compounds. It has been shown that the detonation velocity at the shockwave front is proportional to the square of the density of the energetic material.<sup>49</sup> Thus, in order to improve upon known explosives such as HMX and RDX materials with greater densities must be produced.

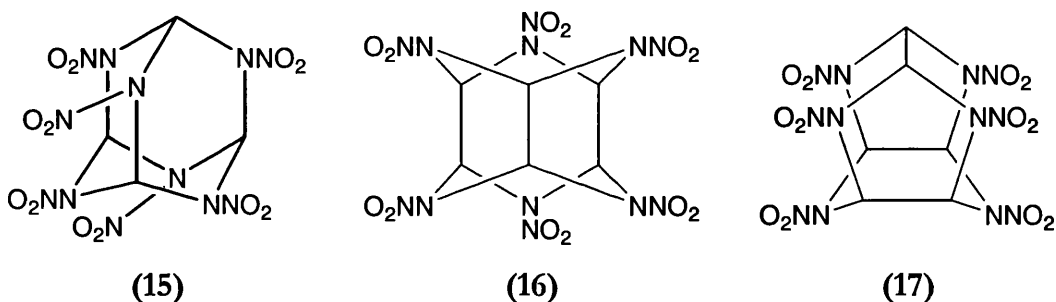
There are various approaches to optimising structures in order to increase density. As well as having high symmetry, and thus better crystal packing, the molecule should have an optimum number of quaternary or tertiary carbon atoms, tertiary nitrogen atoms and condensed rings. The observed increase in density between the monocycles cyclobutane, ( $0.70 \text{ g cm}^{-3}$ ), and cyclopentane, ( $0.74 \text{ g cm}^{-3}$ ) and their corresponding caged molecules, cubane, ( $1.28 \text{ g cm}^{-3}$ ) and dodecahedrane, ( $1.45 \text{ g cm}^{-3}$ ) illustrates the comparatively high density of polycyclic caged molecules.<sup>50, 51, 52</sup> In fact, the highest density polycyclic molecules are those with condensed polycyclic cages.

Consequently, a successful improvement upon the monocyclic nitramines RDX and HMX may be approached by the synthesis of caged nitramine compounds. Firstly a caged amine with the desired parent structure and the desired number of endocyclic amino groups would be synthesised. This molecule could then be nitrated in order to produce a polycyclic caged structure with the general formula  $(\text{CHNNO}_2)_n$ .<sup>49</sup>

As is evident in the synthesis of RDX and HMX from hexamethylenetetramine, nitrating a caged nitramine does not necessarily yield a caged product. This is because the nitrogen atoms of the cage are situated at bridgeheads and nitration at these nitrogen atoms breaks the cage structure, producing cyclic products. Thus, it would be preferable to synthesise a polyaza caged ring system where the amino groups to be nitrated are not situated at bridgeheads. A method would

then be found to introduce nitro groups onto all of the endocyclic nitrogen atoms of the cage. Unfortunately, the reaction conditions employed in current nitration methods facilitate ring opening reactions, destroying the cage structure. A useful goal in this area therefore, would be the development of new nitration procedures which circumvent this problem.

Three target molecules calculated to have higher densities, and consequently higher detonation velocities, than RDX and HMX are hexanitrohexaazadamantane (15), hexanitrohexaazawurtzitane (16) and hexanitrohexaazaisowurtzitane (17). These compounds have calculated densities of  $2.1 \text{ g cm}^{-3}$  and calculated detonation velocities of around  $9500 \text{ m s}^{-1}$ ; a significant improvement on those found for RDX and HMX.<sup>53, 54.</sup>



Recent papers describe the preparation of hexanitrohexaazaisowurtzitane (17) *via* a three-step reaction.<sup>55</sup> Step one is the condensation of benzylamine with glyoxal, forming hexabenzylhexaazaisowurtzitane, (HBIW). It is thought that glyoxal reacts with the amine to yield a diimine as an intermediate, the diimines then polymerise ultimately producing the caged compound.<sup>56</sup> This may be considered analogous to the reaction of ammonia and formaldehyde to form hexamethylenetetramine. Catalytic hydrogenolysis followed by debenzylation of HBIW, and subsequent nitrolysis produces hexanitrohexaazaisowurtzitane.<sup>55</sup> Subsequent tests on this compound have shown it to be the most energetic compound yet known.<sup>57</sup> However, of its four polymorphic forms only the  $\epsilon$ -hexanitrohexaazaisowurtzitane polymorph is of suitable high density and

workable insensitivity, with the other polymorphs having significantly reduced performance.<sup>58</sup>

### ***1.5 Present Work***

There are two major themes to the research discussed in this thesis. First, the use of metal-mediated synthesis to produce caged nitrogen compounds and secondly the use of hexamethylenetetramine as a ligand in organometallic/coordination complexes. Chapter Two describes attempts to synthesise high-energy caged nitrogen compounds, beginning with reactions of formaldehyde and ammonia in the presence of a metal and concluding with investigations into the suitability of some known polycyclic caged amine complexes as precursors toward nitrated cage species. In Chapter Three, the synthesis and structure of some 1:1 and 1:2 adducts of hexamethylenetetramine with organometallic ruthenium and rhodium complexes are described. Chapter Four discusses investigations into the solution dynamics of adducts of hexamethylenetetramine with  $[\text{Pd}(\eta^3\text{-C}_4\text{H}_7)\text{Cl}_2]$  using variable temperature  $^1\text{H}$  NMR spectroscopy. In Chapter Five the synthesis and redox properties of adducts of hexamethylenetetramine with  $[\text{Rh}_2(\text{O}_2\text{CR})_4]$  are examined.

---

# Chapter Two

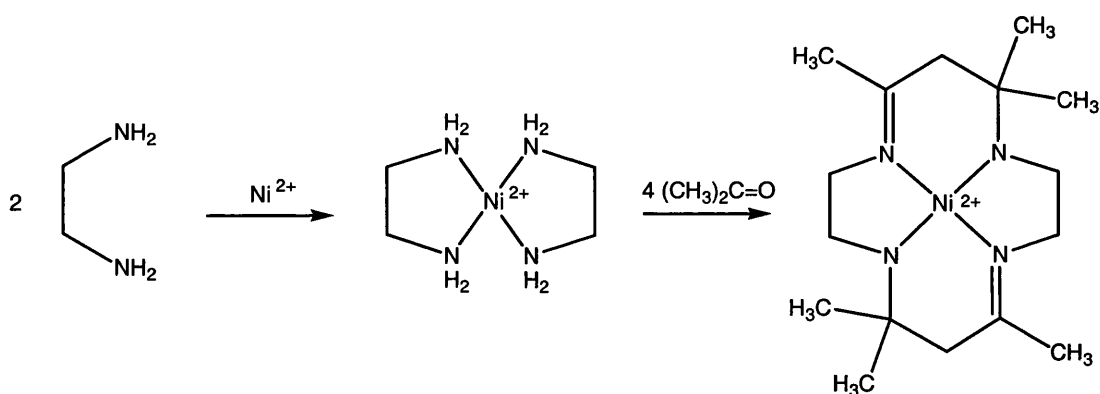
## Investigations into the metal-mediated synthesis of caged nitrogen compounds

## 2.1 Introduction

The work discussed in this chapter is in two parts. First, section 2.2 describes efforts to synthesise new cage nitrogen compounds using the synthesis of hexamethylenetetramine as a model. Within this section studies of the reaction of formaldehyde and ammonia in the presence of a number of metal amine complexes are described. Secondly, in section 2.3 investigations into the use of some macrocyclic metal amine complexes as precursors to high energy compounds are discussed.

### 2.1.1 Metal-mediated condensation reactions

Template syntheses of cyclic and polycyclic amines are ubiquitous in inorganic coordination chemistry.<sup>59, 60</sup> No attempt to cover the field is made here; instead a few particularly relevant examples are discussed. A well-known route to the synthesis of macrocyclic amines is *via* a Schiff base condensation reaction, **Equation 2.1**. A classic example of this is illustrated in **Scheme 2.1**.



**Scheme 2.1** A macrocyclic complex formed *via* the Schiff base route <sup>61</sup>

Often, metal-mediated condensations can be templated by a number of different metals, for example the macrocyclic complex illustrated in **Figure 2.1** is produced *via* reaction of *bis*acetylacetonone-ethylenediimine with *o*-phenylenediamine, in the presence of an iron, copper or nickel salt.<sup>62</sup>



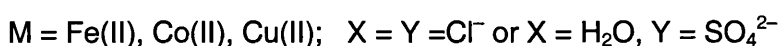
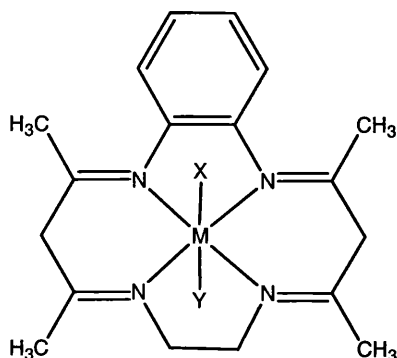


**Figure 2.1** Tetraaza macrocycle formed *via* metal-temple synthesis

A wide range of non-Schiff base macrocyclic amines are also prepared using metal template synthesis. An example is the aliphatic macrocycle formed from the reaction of formaldehyde, ethylenediamine and methylamine in the presence of the nickel(II) ion, **Figure 2.2**.<sup>63</sup>

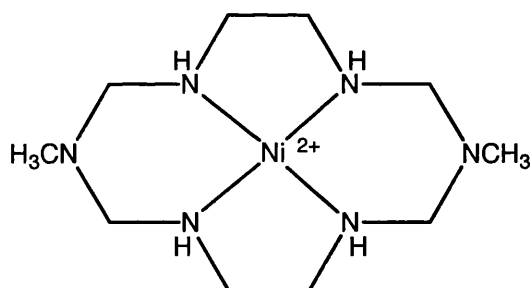
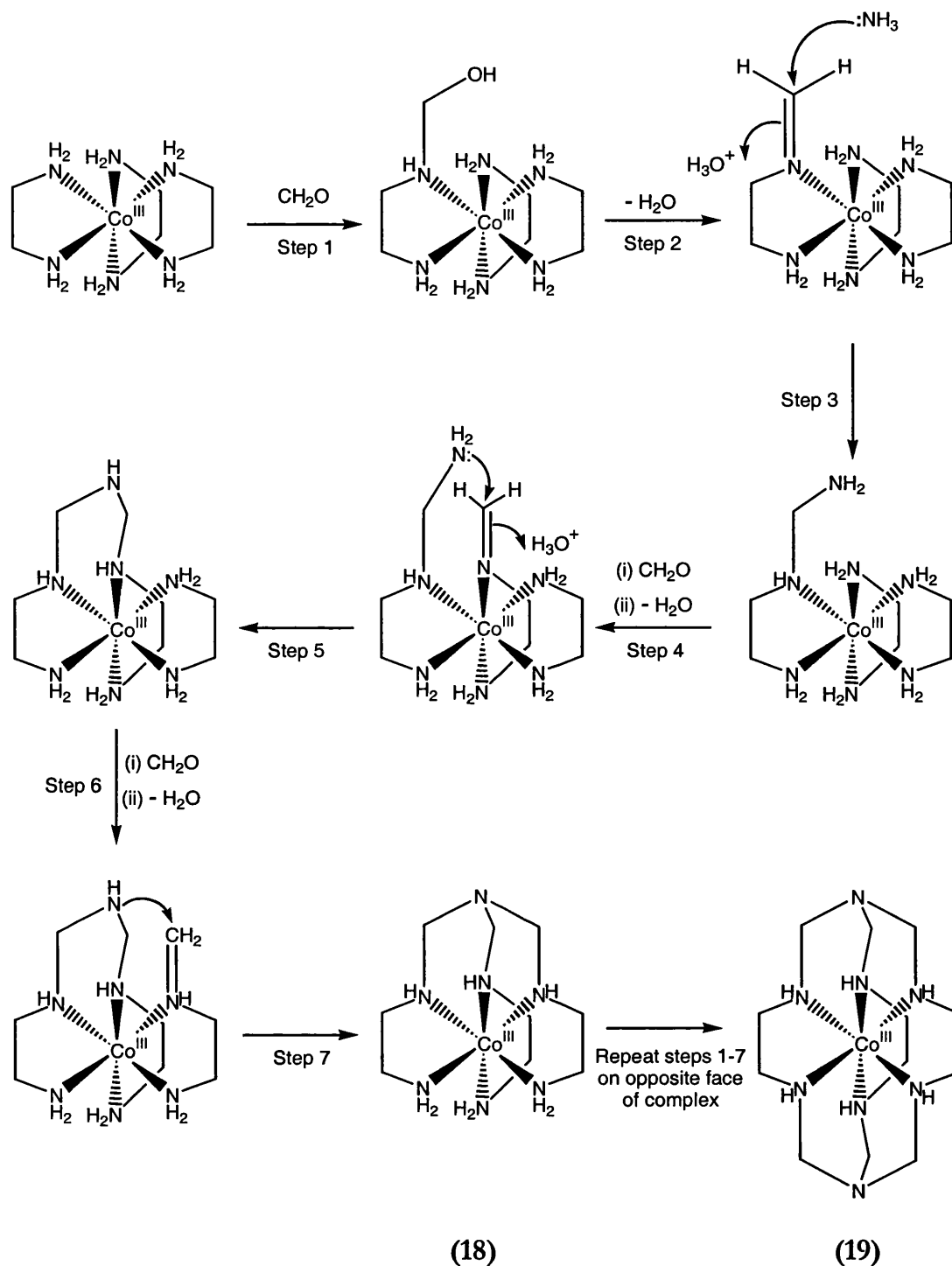


**Figure 2.2** Hexaaza macrocycle formed from one-pot metal template synthesis

Sargeson and co-workers have made great use of the metal templating effect in their synthesis of cage complexes such as [Co(sep)]Cl<sub>3</sub>, **(19)** (sep = sepulchrate, 1,3,6,8,10,13,16,19-octaazabicyclo[6.6.6]eicosane).<sup>64</sup> The synthesis of [Co(sep)]Cl<sub>3</sub> uses the synthesis of hexamethylenetetramine as a model, and involves the reaction of [Co(en)<sub>3</sub>]<sup>3+</sup>, formaldehyde and ammonia. The proposed mechanism for the synthesis of [Co(sep)]Cl<sub>3</sub> is illustrated in **Scheme 2.2**.

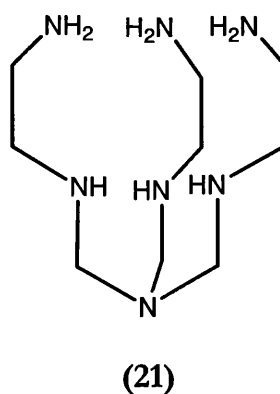
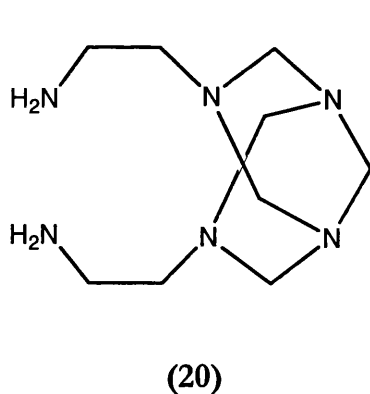


**Scheme 2.2** Proposed mechanism for synthesis of  $[\text{Co}(\text{sep})]^{3+}$  <sup>65</sup>

The first step in the mechanism involves condensation of formaldehyde with a bound deprotonated amine to yield the coordinated carbinolamine, the elimination of water then produces the imine.<sup>64</sup> The imine is subsequently attacked by ammonia yielding the *gem*-diamine. Intramolecular condensation of the *gem*-diamine with a second imine then produces one of the six-membered

rings. Formation of another imine followed by intramolecular condensation with the secondary amine of the previously formed six-membered ring produces the completed cap (step five). Repetition of this process on the opposite face of the octahedral complex affords the completely encapsulated metal ion (**19**). Evidence for this route has been obtained by isolation of reaction intermediates such as the 'semi-sepulchrates' (**18**).<sup>64</sup> In order to produce the compound in large yields from this one-pot procedure, a continuous supply and excess of both formaldehyde and ammonia are required.

In addition to cobalt, other metals including rhodium, iridium and platinum have been encapsulated in the sepulchrates using the above method.<sup>66, 67</sup> However, the major product isolated from the reaction of ethylenediamine, ammonia and formaldehyde in the presence of nickel(II)chloride is  $[\text{Ni}(\mathbf{20})][\text{ClO}_4]_2$ , and the secondary product is  $[\text{Ni}(\mathbf{21})][\text{ClO}_4]_2$ , where (**21**) is the semi-sepulchrates ligand.<sup>68</sup> Deliberate synthesis of  $[\text{Ni}(\mathbf{21})][\text{ClO}_4]_2$  has been achieved in 70 % yield.<sup>69</sup> The synthesis of  $[\text{Ni}(\text{sep})][\text{ClO}_4]_2$  has been achieved, but yields of this complex are less than 1 %.<sup>68</sup>

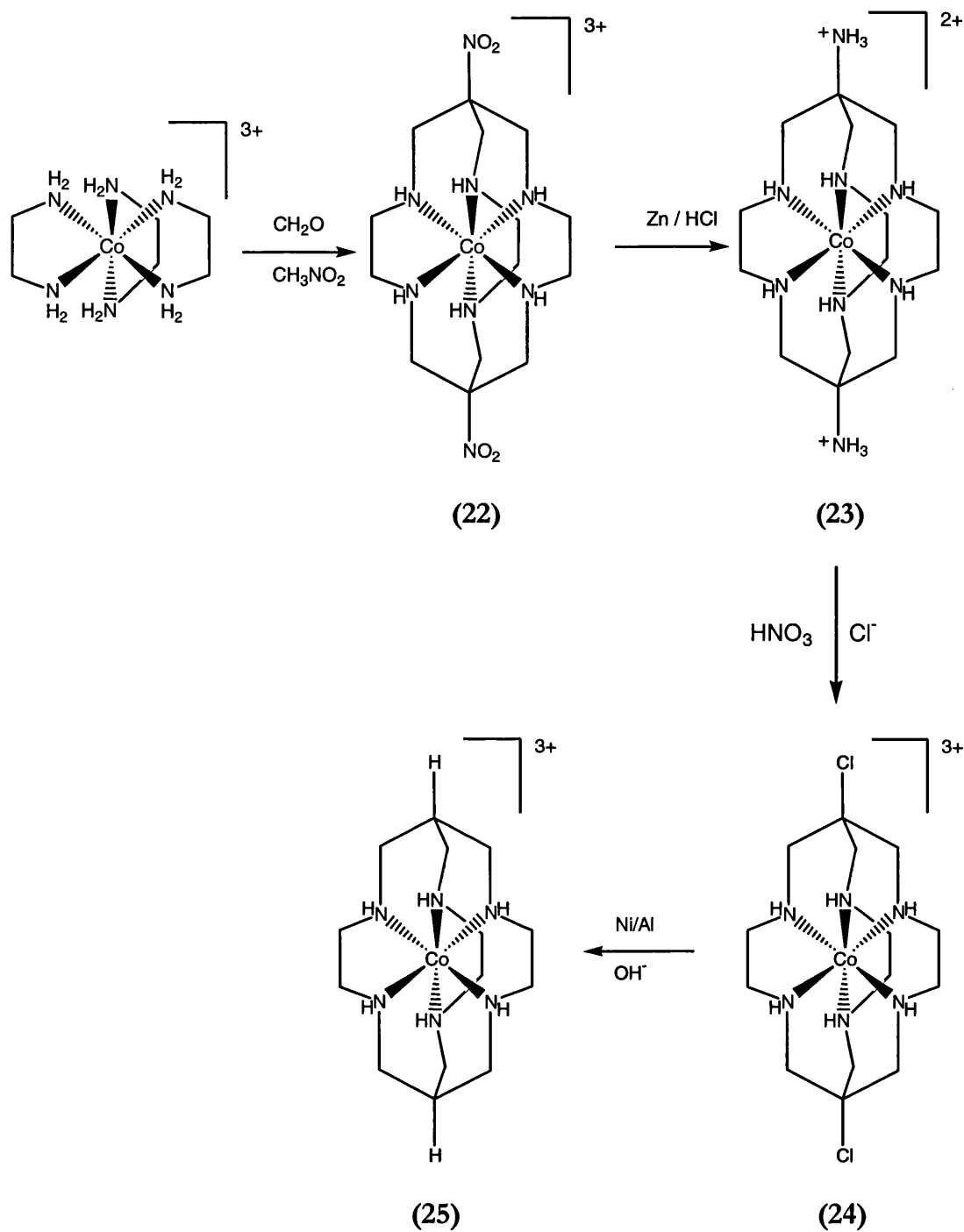


In order to encapsulate a larger range of metals within the sepulchrates cage attempts have been made to decomplex the template cation and produce the free ligand for reaction with other metal cations. However, the removal of the kinetically inert cobalt(III) ion from the caged complex proved unachievable, even when reduced to Co(II), the cation could not be extracted from the sepulchrates cage (which contains bridgehead nitrogen atoms) without cage

decomposition.<sup>70</sup> An alternative strategy investigated for generation of a free ligand of very similar structure was by removal of the cobalt ion from the structurally related carbon-bridgehead sarcophagine complexes  $[\text{Co}(\text{sar})]\text{Cl}_3$  (**25**) (sar = sarcophagine, 3,6,10,13,16,19-hexaazabicyclo[6.6.6]eicosane) and  $[\text{Co}\{(\text{NH}_3)_2\text{sar}\}]\text{Cl}_4$ , (**23**) ( $\{(\text{NH}_3)_2\text{sar}\} = 1,8\text{-diamino-sar}$ ). These complexes are derivatives of  $[\text{Co}\{(\text{NO}_2)_2\text{sar}\}]\text{Cl}_3$  (**22**) which is prepared by reaction of  $[\text{Co}(\text{en})_3]\text{Cl}_3$  with nitromethane and formaldehyde, **Scheme 2.3**.<sup>71</sup>

The complexes  $[\text{Co}\{(\text{NH}_3)_2\text{sar}\}]\text{Cl}_5$  and  $[\text{Co}(\text{sar})]\text{Cl}_3$  generated in this way may be used as sources of the free ligands,  $(\text{NH}_2)\text{sar}$  and sar, by reduction to their Co(II) forms followed by reaction in concentrated acids at elevated temperatures or reaction in hot aqueous solutions containing an excess of cyanide ion.<sup>71</sup> Direct reaction of the protonated ligands with aqueous solutions of metal salts allowed complexation of kinetically labile cations.<sup>72</sup> Using this method sarcophagine and diaminosarcophagine complexes of numerous metal ions have been synthesised, including chromium(III),<sup>73</sup> manganese(II) and manganese(III),<sup>74</sup> vanadium(IV) and nickel(II) complexes.<sup>60</sup>

A number of substituents can be introduced at the apical position of the cage to form ligands with  $-\text{NO}$ ,  $\text{N}(\text{CH}_3)_3^+$ ,  $-\text{OH}$ ,  $\text{COOR}$ ,  $\text{NHCOCH}_3$ ,  $-\text{CN}$ ,  $-\text{CONH}_2$  or  $\text{CH}_2\text{OH}$  groups in the capping positions.<sup>75, 76</sup> As a consequence a wide range of cage complexes are available by altering the metal and the apical substituents.



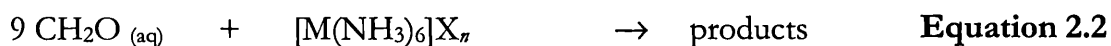
Scheme 2.3 Synthesis of cobalt sarcophagine complexes

## 2.2 Reactions of formaldehyde with metal amine complexes

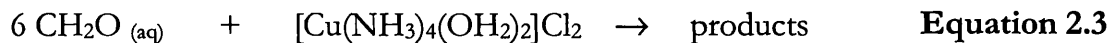
The reaction of ammonia with formaldehyde to form hexamethylenetetramine has been extensively studied, as described in Chapter One. However, whether this reaction is influenced by the presence of other species is not well studied. Indeed, the presence of metal ions in the reaction mixture might lead to the synthesis of nitrogen cages other than hexamethylenetetramine. Hence an aim of this research was to study the affect of metal ions on the reaction between formaldehyde and ammonia. Section 2.2.1 describes the reactions of a number of metal amine complexes with formaldehyde under analogous conditions to those used for the synthesis of hexamethylenetetramine. Although initial investigations indicated that products other than hexamethylenetetramine were formed, these were generally found in very small quantities and were extremely difficult to separate or characterise reliably. Performing the reactions at elevated temperatures served only to increase the number of products formed rather than increase the yields of individual components. Consequently, it was proposed that increasing reaction times while at ambient temperature might give favourable results. However this proved not to be the case. The preparation of hexamethylenetetramine is carried out in aqueous solution and it became apparent that this reaction was dominating the chemistry despite the presence of the metal ion. Therefore, it was decided to investigate reactions of metal complexes with formaldehyde under anhydrous conditions, these studies are described in sections 2.2.2 and 2.2.3.

### 2.2.1 Reactions of metal amine complexes and formaldehyde in aqueous solution

The reaction of the metal amine complexes *hexakis*(amino)nickel(II)bromide, *hexakis*(amino)cobalt(III)chloride and *tetrakis*(amino)*bis*(aquo)copper(II)chloride with formaldehyde were investigated, **Equation 2.2** and **Equation 2.3**. The metal amines were prepared using well-documented literature methods.<sup>77, 78, 79</sup>



M = Ni<sup>2+</sup>, Co<sup>3+</sup>; X = Cl, Br; n = 2, 3



First a series of reactions was studied in aqueous solution at room temperature. In each case the reaction mixture was extracted with dichloromethane and the resulting organic layer reduced to dryness to yield a small amount of colourless solid. These solid products were characterised using <sup>1</sup>H NMR spectroscopy and mass spectrometry. The remaining aqueous solution was characterised using electronic spectroscopy. The results of these studies are summarised in **Table 2.1**.

**Table 2.1** Reactions of metal amine complexes with formaldehyde at room temperature

Reaction	2.1.1	2.1.2	2.1.3
<b>Metal Amine</b>	[Co(NH <sub>3</sub> ) <sub>6</sub> ] <sup>3+</sup>	[Ni(NH <sub>3</sub> ) <sub>6</sub> ] <sup>2+</sup>	[Cu(NH <sub>3</sub> ) <sub>4</sub> (OH <sub>2</sub> ) <sub>2</sub> ] <sup>2+</sup>
<b>Aqueous layer:</b>			
<b>electronic spectra</b>	[Co(NH <sub>3</sub> ) <sub>6</sub> ] <sup>3+</sup>	[Ni(OH <sub>2</sub> ) <sub>6</sub> ] <sup>2+</sup>	[Cu(NH <sub>3</sub> ) <sub>4</sub> (OH <sub>2</sub> ) <sub>2</sub> ] <sup>2+</sup>
<b>Organic layer:</b>	4.67 (s)	4.67 (s)	4.67 (s)
<b><sup>1</sup>H NMR (4 – 5 ppm)</b>	4.71 (s)	4.72 (m)	4.72 (m)
	4.89 (m)	4.87-4.89(m)	4.86-4.89(m)

The electronic spectra of the aqueous solutions from reactions **2.1.1** and **2.1.3** confirm the presence of the unreacted metal-amine complex, suggesting either no reaction, or a slow incomplete reaction had occurred. The electronic spectrum from the aqueous extract of reaction **2.1.2** is that of the nickel(II) hexaquo ion, indicating loss of all ammonia ligands from the metal centre.

The  $^1\text{H}$  NMR spectra recorded of the colourless solids obtained from each reaction mixture exhibit a singlet resonance at  $\delta$  4.67 ppm, which is attributed to hexamethylenetetramine. In addition, there are two further sets of resonances observed at *ca.* 4.72 and 4.89 ppm. These multiplets are assigned to two different species since the relative integrals change independently with the metal present during synthesis. The metal complex also appears to have an effect on the amount of hexamethylenetetramine formed, the reaction of *hexakis(amino)nickel(II)bromide* with formaldehyde gives the largest yield of isolated hexamethylenetetramine; this is unsurprising when considering that only the nickel complex loses all its ammonia ligands during the course of the reaction. Furthermore, all of the  $^1\text{H}$  NMR spectra exhibit resonances in the region 7.0-8.5 ppm; these signals may arise from protons such as found in RN-CHO fragments or protons on imines.

Although the identities of the products other than hexamethylenetetramine are not clear, they are likely to be compounds of the type shown in **Figure 2.3**. These molecules were reported by Richmond *et al.*<sup>22</sup> and Okawara<sup>80</sup> as side products and intermediates formed during the reaction of formaldehyde and ammonia.

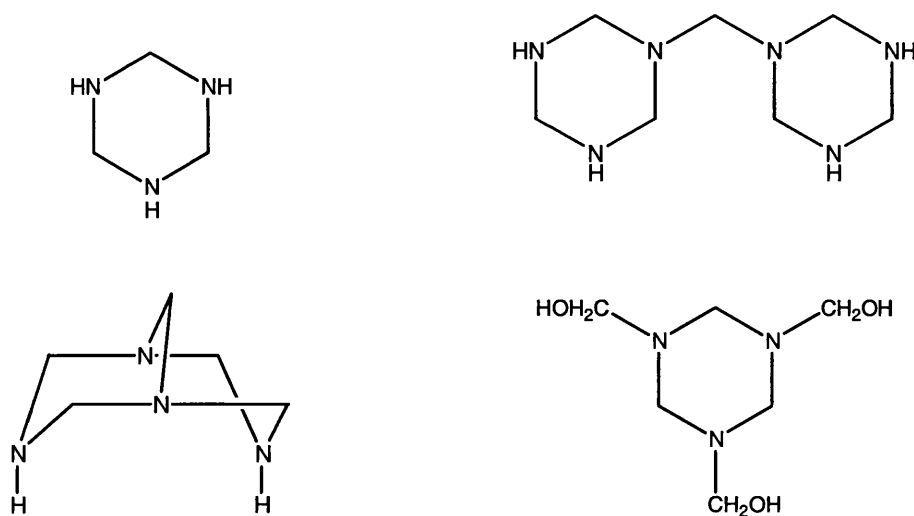


**Figure 2.3** Possible products from reaction of ammonia and formaldehyde



The mass spectra obtained for the products of each reaction mixture are very similar. In each case hexamethylenetetramine is clearly present. Interestingly, each spectrum contains peaks around  $m/z = 662$  consistent with the presence of a large cage of unknown structure. The lack of any metal isotope pattern in the spectra and the absence of colour in the dichloromethane solutions suggests the products are purely organic. Thus, no metal coordination complexes were isolated from the organic phase after work-up.

The quantities of isolated materials from reactions 2.1.1, 2.1.2 and 2.1.3 were particularly low (a few tens of milligrams at most) which added to the difficulty of separation and purification of the products. In an attempt to increase the product yields the reactions were repeated at gentle reflux, with an excess of formaldehyde present. The work-up was carried out as for the room-temperature procedures. The results obtained are summarised in **Table 2.2**.

**Table 2.2** Reactions of metal amine complexes with formaldehyde at reflux

Reaction	2.2.1	2.2.2	2.2.3
<b>Metal Amine</b>	$[\text{Co}(\text{NH}_3)_6]^{3+}$	$[\text{Ni}(\text{NH}_3)_6]^{2+}$	$[\text{Cu}(\text{NH}_3)_4(\text{OH}_2)_2]^{2+}$
<b>Aqueous layer: electronic spectra</b>	$[\text{Co}(\text{OH}_2)_6]^{3+}$	$[\text{Ni}(\text{OH}_2)_6]^{2+}$	$[\text{Cu}(\text{OH}_2)_6]^{2+}$
<b>Organic layer from DCM extraction: <math>^1\text{H}</math> NMR (4 – 5 ppm)</b>	4.24(s), 4.39(s), 4.59(s), 4.71(s), 4.78-4.84(m), 4.86-4.88(m)	4.40(s), 4.40(s), 4.42 (s), 4.52(s), 4.65(s), 4.66(s), 4.79(s), 4.88(s), 4.97(s)	4.20(s), 4.40(s), 4.61(s), 4.67(s), 4.71(s), 4.72(s), 4.86-4.87(m), 4.88-4.89(m)

In contrast to the room temperature reactions the electronic spectrum of the aqueous layer confirms the presence of the metal in the form of its hexaaquo

complex, indicating liberation of the ammonia from the metal, in all three reactions. The  $^1\text{H}$  NMR spectra differ significantly from those obtained from the room temperature reactions. In particular, there is no hexamethylenetetramine signal in the  $^1\text{H}$  NMR spectra obtained from reactions 2.2.1 and 2.2.2, and although a signal is observed for reaction 2.2.3, it is very weak. There are also a number of signals present that were not observed in the spectra obtained from the room temperature reactions. Two possible reasons for this are the occurrence of additional reactions at this elevated temperature or the decomposition of some of the products formed at lower temperatures. The  $^1\text{H}$  NMR spectra contain similar resonances in the region 7.0-8.5 ppm as those observed when the reactions were performed at room temperatures.

Although the electronic spectra of the aqueous extracts confirm cleavage of all ammonia ligands from the metal centre at high temperatures, there is no significant increase in the mass of the organic products isolated from the dichloromethane solution. Hexamethylenetetramine is soluble in dichloromethane but is also extremely soluble in water (probably owing to the fact that the molecule is at least partially protonated in aqueous solution). Thus, it is possible that hexamethylenetetramine and related organic compounds are not being extracted from the reaction solution efficiently. In order to address this issue the work-up procedure was altered: the water was removed *in vacuo* leaving the metal salt and any organic products as a solid mixture. This mixture was suspended in dichloromethane and stirred for two hours. The remaining solid was then filtered off and the dichloromethane solution evaporated *in vacuo*. This work-up led to small increases in the mass of the products isolated. However, the overall composition of the mixture of products did not differ significantly from that obtained from the first extraction with dichloromethane.

In summary, the reactions of metal amine complexes and formaldehyde discussed above have given only small amounts of mixtures of organic products, the main product being hexamethylenetetramine. The minor organic products were impossible to separate and, therefore, characterise fully.

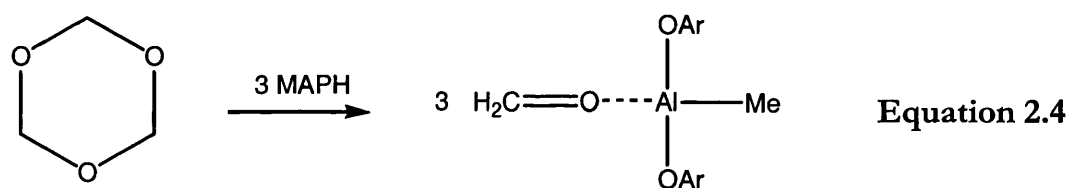
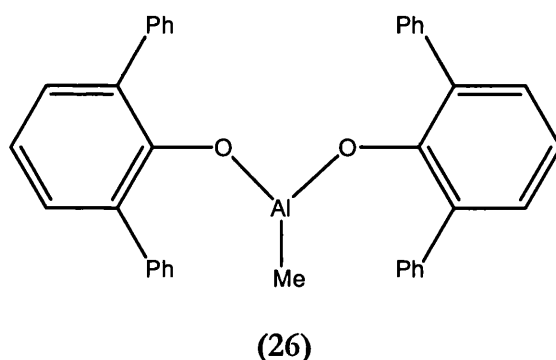
The reactions described so far have involved fairly short reaction times. To investigate whether different products were obtained over a longer period a series of studies was made whereby the aqueous solutions of metal amine salts and formaldehyde were left at room temperature for 15-20 weeks. The result of these investigations can be broadly summarised as follows. In the case of reaction between  $[\text{Co}(\text{NH}_3)_6]\text{Cl}_3$  and formaldehyde the majority of the metal complex is recovered intact and small amounts of coloured precipitate which formed were shown to be  $\text{CoCl}_2$ . Essentially no organic product was recovered. In the case of reactions with  $[\text{Ni}(\text{NH}_3)_6]\text{Cl}_2$  and  $[\text{Cu}(\text{NH}_3)_4]\text{Cl}_2$  the aqueous solutions contained the ions  $[\text{M}(\text{OH}_2)_6]\text{Cl}_2$  after 20 weeks. Work-up of the solutions gave hexamethylenetetramine as the sole organic product, as confirmed by  $^1\text{H}$  NMR spectroscopy.

The observations described so far imply that exchange of ammonia ligands for water reduces the opportunity for condensation reactions to occur on ammonia ligands coordinated to the metal. Consequently, a method for investigating this reaction under anhydrous conditions was developed.

### 2.2.2 The reaction of methylaluminium*bis*(2,6-diphenylphenoxide) with $[\text{Ni}(\text{NH}_3)_6]\text{Br}_2$

Aqueous solutions of formaldehyde and ammonia were used in the experiments described in section 2.2.1. Thus, in order to carry out reactions of formaldehyde and ammonia under anhydrous conditions an alternative source of both reactants was needed. A readily available form of anhydrous ammonia is, of course, ammonia gas. However, the situation with formaldehyde is more complex. Paraformaldehyde can be used to generate gaseous formaldehyde by thermal depolymerisation,<sup>81</sup> but because of the awkward nature of this process (involving very high temperatures) an alternative route to anhydrous formaldehyde was pursued. Formaldehyde polymerises readily in organic solvents, however, the complex methylaluminium*bis*(2,6-diphenylphenoxide), MAPH (**26**) is known to

prevent formaldehyde polymerisation.<sup>70</sup> **Equation 2.4** illustrates the reaction of trioxane (a trimer of formaldehyde) with MAPH to produce a formaldehyde-MAPH complex. A space filling model of this complex suggests that the aldehyde may be electronically stabilised by the  $\pi$ -stacking of two parallel phenyl groups of the phenoxide ligands.<sup>70</sup>



OAr = 2,6-diphenylphenoxide

A solution of the formaldehyde-MAPH complex was prepared and was added to a suspension of  $[\text{Ni}(\text{NH}_3)_6]\text{Br}_2$  in dry dichloromethane at  $0^\circ\text{C}$ . After stirring at  $0^\circ\text{C}$  for two hours the solvent was removed *in vacuo* to give a blue solid that was air/moisture sensitive. This solid turned pink after approximately 30 seconds in air, suggesting metal complexation. The  $^1\text{H}$  NMR spectrum of the solid in deuterated dichloromethane was consistent with that for a paramagnetic material, with numerous signals between 0 and -3 ppm and distortion of the resonances ascribed to the aromatic protons of MAPH. Addition of  $\text{D}_2\text{O}$  to the sample brought about a change in colour from blue to pink and produced a spectrum with aromatic resonances resembling those of uncoordinated MAPH. These observations suggest the initial product was a nickel coordination compound of MAPH or aluminium *bis*(2,6-diphenylphenoxide). No evidence of organic products (*i.e.* hexamethylenetetramine or other condensation products) was

observed in the spectra before or after the addition of D<sub>2</sub>O. As a result of this disappointing observation, the use of paraformaldehyde as an alternative source of anhydrous formaldehyde was pursued.

### 2.2.3 Reactions of [Ni(NH<sub>3</sub>)<sub>6</sub>]Br<sub>2</sub> with gaseous formaldehyde.

In the initial investigations discussed in section 2.2.1 the lack of success cannot be completely attributed to exchange of ammonia ligands for water ligands: since in the case of [Co(NH<sub>3</sub>)<sub>6</sub>]Cl<sub>3</sub> the ammonia ligands are not lost even after extended reaction periods. As described in the introduction to this chapter the azacryptand [Co(sep)]Cl<sub>3</sub> (**19**) is only obtained in high yields when formaldehyde and ammonia are supplied in excess to the *tris*(ethylenediamine)cobalt(III)chloride solution.<sup>70</sup> Thus, using the synthesis of (**19**) as a model, it was decided to supply formaldehyde and ammonia in excess to a solution of [Ni(NH<sub>3</sub>)<sub>6</sub>]Br<sub>2</sub>, in an anhydrous solvent.

Pre-dried paraformaldehyde was heated in an oil bath at 180-200 °C to produce formaldehyde in the vapour phase, which was carried into a reaction vessel containing [Ni(NH<sub>3</sub>)<sub>6</sub>]Br<sub>2</sub> in pre-dried ethanol by a stream of nitrogen. Ammonia gas was bubbled into the reaction mixture at an approximately equal rate to the gaseous formaldehyde and the reaction was terminated after 3.5 hours, upon consumption of the paraformaldehyde. A white solid and a purple solid were observed, suspended in the ethanolic solution. The solids were removed by filtration and the residue washed with water to produce a blue solution, which was reduced *in vacuo* to yield a pale green solid. The <sup>1</sup>H NMR spectrum of this solid exhibited a single resonance at 4.67 ppm attributed to hexamethylenetetramine. The absence of other signals and the pale green colour of the solid suggest it is a mixture of hexamethylenetetramine and the solvated nickel halide salt. The presence of the nickel bromide is explained by the decomposition of [Ni(NH<sub>3</sub>)<sub>6</sub>]Br<sub>2</sub> whilst the blue solution was concentrated by heating *in vacuo*. The ethanolic solution was also reduced *in vacuo* to yield a white solid confirmed by <sup>1</sup>H NMR spectroscopy to be hexamethylenetetramine. The

sole organic product of this reaction is therefore hexamethylenetetramine, presumably due to a rapid reaction between the gaseous formaldehyde and ammonia, leaving the metal complex as a passive spectator. In an attempt to encourage reaction between the metal amine complex and the gaseous formaldehyde the procedure was repeated without the addition of gaseous ammonia.

A suspension of  $[\text{Ni}(\text{NH}_3)_6]\text{Br}_2$  in pre-dried ethanol was stirred for two hours at room temperature, while formaldehyde vapour, generated from the depolymerisation of paraformaldehyde, was bubbled through the solution. After this time the originally purple mixture became green in colour, suggesting loss of the ammonia ligands from the complex and generation of the  $[\text{Ni}(\text{EtOH})_6]^{2+}$  ion. Removal of the solvent *in vacuo* produced a green solid – solvated  $\text{NiBr}_2$ . The  $^1\text{H}$  NMR spectrum of this solid redissolved in  $\text{D}_2\text{O}$  confirmed hexamethylenetetramine as the only organic product.

In conclusion, the research described in section 2.2 indicates that the presence of the metal ions makes little or no difference to the reaction between formaldehyde and ammonia, with hexamethylenetetramine being the major isolated product in every case. However, the reaction of formaldehyde and ammonia in the presence of metal complexes with bidentate amine ligands has been utilised to produce caged compounds other than hexamethylenetetramine. Investigations into the suitability of such complexes as precursors to energetic materials are described in section 2.3.

## ***2.3 Synthesis of metal encapsulating amines***

### **2.3.1 Introduction**

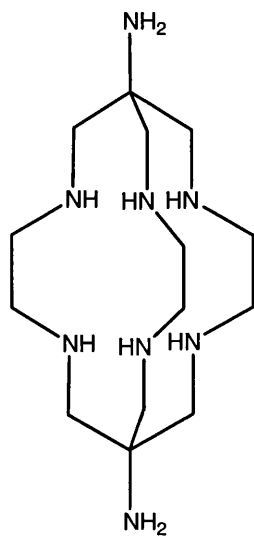
The research discussed in this section concerns the synthesis and reactions of metal encapsulated amines previously prepared by Sargeson *et al.*<sup>60</sup> and discussed

in section 2.1.1. The ultimate aim was to prepare the non-metallated cage  $(\text{NH}_2)_2\text{sar}$  (**27**) and study its nitration.

### 2.3.2 Synthesis of non-metallated diaminosarcophagine

The complex  $[\text{Co}\{(\text{NO}_2)_2\text{sar}\}]\text{Cl}_3$  was synthesised, following published methods,<sup>71</sup> *via* addition of an excess of formaldehyde and nitromethane (in a 6:2 ratio) to a solution of *tris*(ethylenediamine)cobalt(III) chloride. After cooling the solution in ice, a solution of sodium hydroxide was added and the resulting solution stirred for twenty five minutes. After this time addition of concentrated HCl gave  $[\text{Co}\{(\text{NO}_2)_2\text{sar}\}]\text{Cl}_3$  as an orange precipitate. The product was characterised using  $^1\text{H}$  NMR spectroscopy. The high symmetry of the complex is evident from the  $^1\text{H}$  NMR spectrum where two overlapping quartets are observed. One quartet has the characteristic appearance of an AB spin system and is attributed to the methylene groups of the cap. The other is a more complex AA'BB' spin system and arises from the ethylenediamine methylene protons.<sup>82</sup>

The next step in the synthetic methodology was the conversion of  $[\text{Co}\{(\text{NO}_2)_2\text{sar}\}]\text{Cl}_3$  to  $[\text{Co}\{(\text{NH}_3)_2\text{sar}\}]\text{Cl}_5\cdot\text{H}_2\text{O}$  *via* reduction with zinc and concentrated acid. This procedure involved considerable care due to the extreme sensitivity of Co(II) to oxygen, in fact the complex is isolated as the Co(III) form. Obtaining the free ligand  $(\text{NH}_2)_2\text{sar}$  (**27**) from  $[\text{Co}\{(\text{NH}_3)_2\text{sar}\}]\text{Cl}_5\cdot\text{H}_2\text{O}$  is a difficult task. The chelating effect of the six Co-N linkages as well as the inert character of the cobalt(III) ion generates an extremely inert complex. However, removal of the ligand can be achieved *via* two routes, both involving an initial reduction of the complex to its cobalt(II) analogue. These are reaction with concentrated acid at high temperature or reaction with an excess of potassium cyanide solution in hot aqueous media.<sup>71</sup>



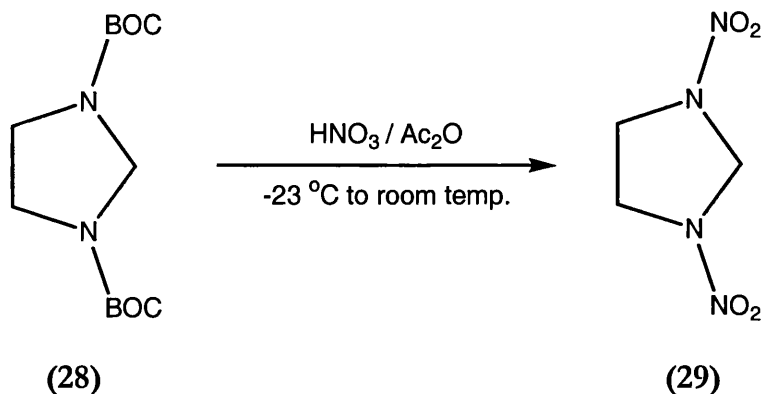
(27)

The diaminosarcophagine compound described herein was obtained using the potassium cyanide method, fully described in experimental section 2.5.9. The reaction vessel was kept under nitrogen at all times and deoxygenated water used as solvent since conversion of  $\text{Co}^{2+}$  back to  $\text{Co}^{3+}$  will terminate the reaction. Following the addition of an excess of potassium cyanide the mixture was heated at  $70\text{ }^{\circ}\text{C}$  for six hours after which time the solution became colourless. The solvent was removed and the resulting solid extracted with boiling acetonitrile. Concentration of the acetonitrile solution yielded the diaminosarcophagine as a white solid. Spectroscopic data, see experimental section 2.5.9, were consistent with that reported previously.<sup>85</sup>

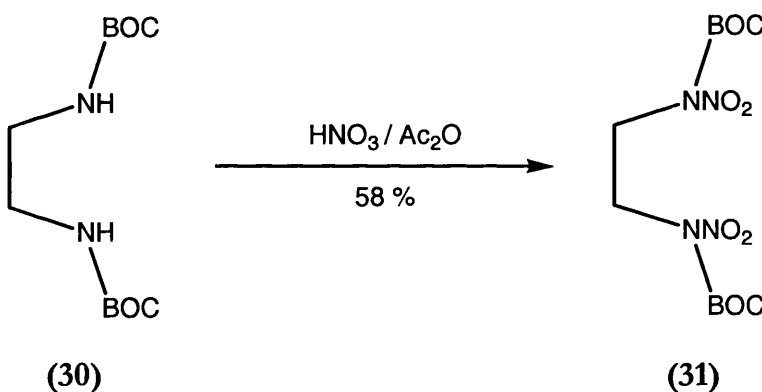
Before nitration of (27) could be attempted the following factors had to be considered. Diaminosarcophagine (27) contains two primary amines, nitration of which will produce thermally unstable primary nitramines. In order to avoid formation of primary nitramines, the use of a protecting group was employed. Since (27) also contains secondary amines it was important to choose a protecting group which would not affect their susceptibility to nitration. The protecting group chosen was the *tert*-butoxycarbonyl (BOC) group, well known for its use as an acid-labile amine protecting group.<sup>83</sup> The specific reasons for



choosing this protecting route are explained with reference to **Scheme 2.4** and **Scheme 2.5**.

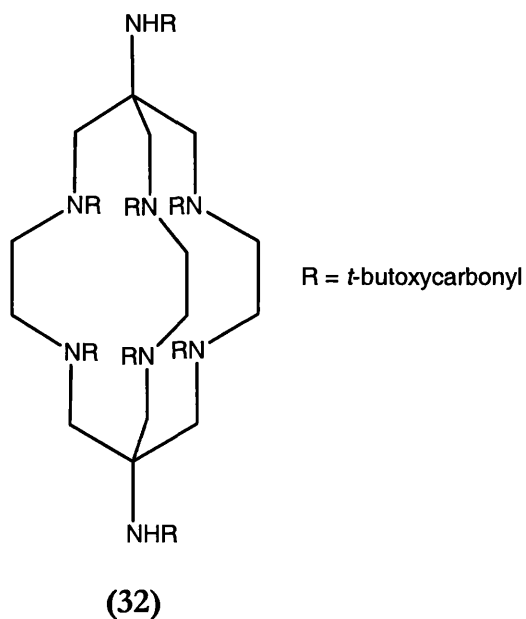


**Scheme 2.4** Nitrolysis of *tert*-butoxycarbonyl protected tertiary amines.

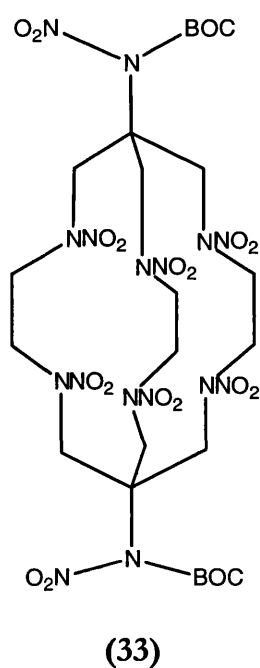


**Scheme 2.5** Nitrolysis of *tert*-butoxycarbonyl protected secondary amines

**Scheme 2.4** shows the nitrolysis of 1,3-*bis*-BOC-1,3-diazacyclopentane (**28**).<sup>84</sup> Although nitration takes place at a tertiary nitrogen atom, the cyclic skeleton of the molecule remains intact because the *tert*-butoxycarbonyl group is replaced in preference to breaking C-N bonds of the ring. This is an important point because (**32**), the target molecule in the protection of diaminosarcophagine, contains six unprotected tertiary nitrogen atoms.



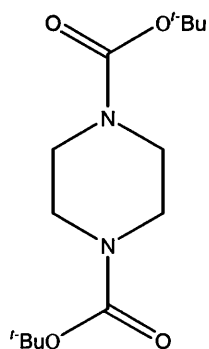
Scheme 2.5 illustrates the product of successful nitration of a *tert*-butoxycarbonyl protected primary amine.<sup>84</sup> The importance of this example with respect to the nitration of (32) is that the *tert*-butoxycarbonyl groups are neither cleaved nor nitrolysed. Thus, in an analogous nitration of (32) the problem of synthesising primary nitramines would be avoided yielding a product such as (33).



### 2.3.3 Tert-butoxycarbonyl protection of diaminosarcophagine

An excess of di-*tert*-butyl dicarbonate was added to a solution of diaminosarcophagine and sodium hydroxide in THF/water. The reaction mixture was stirred at room temperature for three days then extracted with ethyl acetate. A colourless oil was obtained from this extraction. After extraction of the colourless oil, the reaction mixture was acidified and an ethyl acetate extraction of the acidified mixture produced an off-white solid.

The  $^1\text{H}$  NMR spectra of the two samples obtained above is quite complex. The absence of signals due to the methylene groups of the diaminosarcophagine indicates modification of the compound. Signals at 1.47 ppm attributable to *t*-butyl groups strengthen this view. The absence of the expected  $-\text{CH}_2-$  signals is taken to imply that the diaminosarcophagine has decomposed. In order to further examine the viability of the protection reaction a study of the BOC protection of piperazine was undertaken. Piperazine was chosen because of its structural similarity to the diaminosarcophagine, *i.e.* secondary amines linked by ethylene groups. The di-*tert*-butyl dicarbonate was added to a solution of piperazine in water/THF at 0 °C. After stirring for 1 hour a white precipitate was observed and collected by filtration. The  $^1\text{H}$  NMR spectrum of this material confirms it to be the *tert*-butoxycarbonyl derivative (34). The spectrum contains a singlet at 3.27 ppm due to 8 methylene protons, along with a second singlet resonance at 1.49 ppm due to 18 tertiary butyl protons.



(34)

Despite success with the model reaction, repeated attempts to extend this procedure to the polycyclic cage molecule were consistently unreliable and eventually abandoned. No clear reason for these difficulties was apparent.

## ***2.4 Conclusions***

Although the research described in this chapter did not lead to new nitrogen rich cage compounds, it did, in hexamethylenetetramine, produce an obvious candidate for developing a new direction for the thesis. Hexamethylenetetramine is a potentially very interesting ligand for transition metals due to its rigid structure and four potential binding sites. Although some coordination chemistry of hexamethylenetetramine has been investigated, most of the published studies involve polymer networks with simple metal salts. Therefore, it was decided that studies of the coordination chemistry, and in particular organometallic chemistry, of hexamethylenetetramine would provide a good opportunity to carry out some interesting and novel work. Hence, the following three chapters describe the synthesis of metallo-hexamethylenetetramine complexes and investigations into their chemistry.

## ***2.5 Experimental***

### **2.5.1 Physical Measurements**

<sup>1</sup>H NMR spectra were recorded on a Bruker AMX-400 or DMX-300 instrument at 400 and 300 MHz respectively. All spectra were referenced internally to residual protio-solvent (<sup>1</sup>H) resonances. Chemical shifts are quoted in ppm and coupling constants in Hertz (Hz). Infrared spectra were recorded as thin films between NaCl or CsI plates, or as KBr discs on a Shimadzu FTIR 8700 infrared spectrophotometer or a Perkin-Elmer 457 grating infrared spectrophotometer. Electronic spectra were obtained using quartz cells on a Shimadzu UV-2401 PC

instrument. Mass spectrometry measurements were carried out by the UCL mass spectrometry service and were obtained by EI (electron impact) or FAB (fast atom bombardment) as stated. Elemental analyses were carried out by the UCL departmental service.

## 2.5.2 Materials

All reagents were obtained from Aldrich Chemical Company and used without further purification unless stated otherwise. Dried solvents were distilled over appropriate drying agents; sodium/benzophenone – hydrocarbons; calcium hydride - chlorinated solvents, alcohols.

## 2.5.3 Reaction of formaldehyde with *hexakis(amino)cobalt(III)chloride*

This reaction was studied under three sets of conditions.

### A. Reactions at room temperature

Formaldehyde (0.25 cm<sup>3</sup>, 40 % aqueous solution, 9 eq.) was added dropwise with stirring to a solution of [Co(NH<sub>3</sub>)<sub>6</sub>]Cl<sub>3</sub> , (0.10 g, 0.37 mmol, 1 eq.) in water (5.0 cm<sup>3</sup>) at room temperature for two hours. The solution was extracted with dichloromethane (3 x 10 cm<sup>3</sup>). The clear organic layer was dried over magnesium sulfate, decanted from the solid and reduced *in vacuo* to yield a colourless solid.

Reactions of formaldehyde with *hexakis(amino)nickel(II)bromide* (1.00 g, 3.12 mmol) and *tetrakis(amino)copper(II)chloride* (0.50 g, 2.10 mmol) were performed in an analogous fashion. Relevant spectroscopic data are described in section 2.2.1.

### B. Reactions at reflux with an excess of formaldehyde

Formaldehyde (1.00 cm<sup>3</sup>, 18 eq.) was added dropwise with stirring to a solution of [Co(NH<sub>3</sub>)<sub>6</sub>]Cl<sub>3</sub> , (0.20 g, 0.75 mmol, 1 eq.) in water (6.0 cm<sup>3</sup>). After refluxing for 9 h the solution was cooled and extracted with dichloromethane (3 x 10 cm<sup>3</sup>). The clear organic layer was dried over magnesium sulfate, decanted from the

solid and reduced *in vacuo* to yield an oily product. Reduction of the aqueous layer *in vacuo* gave a solid, which was suspended in DCM (50 cm<sup>3</sup>), stirred for 2 h then filtered through celite. The colourless solution was reduced *in vacuo* producing a colourless solid.

Reactions with *hexakis*(amino)nickel(II)bromide (1.00 g, 3.12 mmol) and *tetrakis*(amino)copper(II)chloride (0.50 g, 2.10 mmol) were performed in an analogous fashion. See section 2.2.1 for characterisation of the products.

### C. Reactions over extended time periods

Formaldehyde (10.0 cm<sup>3</sup>, excess) was added dropwise with stirring to a solution of [Co(NH<sub>3</sub>)<sub>3</sub>]Cl<sub>3</sub>, (0.10 g, 0.37 mmol, 1 eq.) in water (10.0 cm<sup>3</sup>) at room temperature. The solution was stirred at room temperature for two days, then left in a sealed vessel for 20 weeks. A pink/red precipitate was observed and removed by filtration. Analysis of this solid using electronic spectroscopy showed it to be CoCl<sub>2</sub>. The nature of the aqueous layer was then investigated using electronic spectroscopy. Reduction of the remaining aqueous layer *in vacuo* gave a solid, which was suspended in DCM (50 cm<sup>3</sup>), stirred for 2 h then filtered through celite. Reduction of the DCM layer gave a colourless product.

Reactions with *hexakis*(amino)nickel(II)bromide (1.00 g, 3.12 mmol) and *tetrakis*(amino)copper(II)chloride (0.50 g, 2.10 mmol) were performed in an analogous fashion, however no precipitate was observed in these cases. Characterisation of products is discussed in section 2.2.1.

#### 2.5.4 Reaction of methylaluminium*bis*(2,6-diphenylphenoxide) (MAPH) with *hexakis*(amino)nickel(II)bromide in inert atmosphere

2,6-diphenylphenol (0.74 g, 3 mmol) was dissolved in dichloromethane (15 cm<sup>3</sup>). To this solution was added trimethylaluminium (0.75 cm<sup>3</sup>, 1.5 mmol, 2 M in hexanes). The pale yellow solution was stirred at room temperature for one hour. Trioxane (50 mg, 0.5 mmol) in dichloromethane (0.2 cm<sup>3</sup>) was added at 0 °C. The resulting solution was stirred for one hour then was added to a

suspension of  $[\text{Ni}(\text{NH}_3)_6]\text{Br}_2$  (50 mg, 0.17 mmol) in dichloromethane ( $15 \text{ cm}^3$ ) at  $0^\circ\text{C}$ . After stirring for 20 minutes the solution was blue in colour. The solution was stirred for a total of two hours in which time no further colour change was observed. The solvent was removed *in vacuo* yielding a blue solid. Upon exposure to air the solid became pink in colour.

$\delta_{\text{H}}$  (400 MHz;  $\text{CD}_2\text{Cl}_2$ ; 298 K) various signals from  $-3$  to  $2.0$ ,  $6.46$ - $7.49$  (m, aromatic H, MAPH). See section 2.2.2 for discussion of NMR data.

$m/z$  (FAB +) 246 (m (2,6-diphenylphenol + 1)).

### 2.5.5 Reaction of *hexakis(amino)nickel(II)bromide* with paraformaldehyde

Paraformaldehyde (5.0 g, excess, pre-dried over phosphorus pentoxide) was heated to  $140^\circ\text{C}$ , in a nitrogen atmosphere. The formaldehyde gas generated was carried in a nitrogen gas stream and bubbled into a purple suspension of  $[\text{Ni}(\text{NH}_3)_6]\text{Br}_2$  (2.5 g, 7.80 mmol) in pre-dried ethanol ( $150 \text{ cm}^3$ ). The reaction mixture was stirred at room temperature for 2 h until the paraformaldehyde was consumed. The ethanol solution now appeared green. The solution was reduced *in vacuo* to give a green solid, solvated  $\text{NiBr}_2$ .

$\delta_{\text{H}}$  (400 MHz;  $\text{D}_2\text{O}$ ; 298 K) 4.67 (s, hexamethylenetetramine-H).

### 2.5.6 Synthesis of $[\text{Co}(\text{sep})]\text{Cl}_3$ <sup>64</sup>

Lithium carbonate (3.97 g) was added to a solution of *tris*(ethylenediamine)cobalt(III) chloride (2.89 g, 8.70 mmol) in water ( $20 \text{ cm}^3$ ). Aqueous ammonia (397 mmol,  $52.24 \text{ cm}^3$  diluted to  $97 \text{ cm}^3$ ) and formaldehyde solution (1191 mmol,  $97 \text{ cm}^3$ ) were added simultaneously over a period of 0.5 h. The resulting mixture was stirred for 2 h. The lithium carbonate was removed by filtration. The pH of the filtrate was adjusted to  $\sim 3$  using perchloric acid. The solution was sorbed onto an ion-exchange column (DOWEX 50W-X2, 200-400 mesh,  $\text{H}^+$  form,  $5 \times 5 \text{ cm}$ ). The column was eluted with trisodium citrate ( $900 \text{ cm}^3$ , 0.2 M) to remove a pink species that was then discarded. The column

was washed with water and HCl (550 cm<sup>3</sup> 1 M) to remove Na<sup>+</sup>. Finally, the column was eluted with HCl (500 cm<sup>3</sup> 3 M) to obtain an orange species. The eluant was reduced *in vacuo* at 50 °C. The orange solid obtained was recrystallised by dissolving in water (90 °C) and adding acetone dropwise whilst cooling in ice. Orange crystals were obtained. Yield 2.14 g, 4.80 mmol, 55 %.

$\delta_{\text{H}}$  (300 MHz; D<sub>2</sub>O; 298 K) 2.51, 3.15 (12H, AA'BB', HNCH<sub>2</sub>CH<sub>2</sub>NH), 3.51, 4.10 (12H, AB q,  $J = 14\text{Hz}$ , CH<sub>2</sub> of cap).

Anal. Calc. for CoC<sub>12</sub>H<sub>30</sub>N<sub>8</sub>Cl<sub>3</sub>: C, 31.91; H, 6.69; N, 24.81 %, found: C, 30.81; H, 6.88; N, 23.69 %.

### 2.5.7 Synthesis of [Co{(NO<sub>2</sub>)<sub>2</sub>sar}]Cl<sub>3</sub><sup>82</sup>

Aqueous formaldehyde (11.10 cm<sup>3</sup>, 148 mmol) and nitromethane (2.45 cm<sup>3</sup>, 96 mmol) were added to a solution of [Co(en)<sub>3</sub>]Cl<sub>3</sub> (4.62 g, 13.9 mmol) in water (7.8 cm<sup>3</sup>). The resulting orange solution was cooled to 5 °C. A cooled solution of sodium hydroxide (1.85 g) in water (11.5 cm<sup>3</sup>) was added to the solution of the metal complex. The mixture was stirred in an ice bath for 25 minutes, then HCl (15.40 cm<sup>3</sup>, 10 M) was added to quench the reaction. After cooling in ice for 1 h, an orange precipitate was collected. Yield 5.37 g, 10.10 mmol, 72 %.

$\delta_{\text{H}}$  (300 MHz; D<sub>2</sub>O; 298 K) 2.73, 3.35 (12H, AA'BB', HNCH<sub>2</sub>CH<sub>2</sub>NH), 3.16, 3.69 (12H, AB q,  $J = 13.8\text{ Hz}$ , CH<sub>2</sub> of cap).

Anal. Calc. for CoC<sub>14</sub>H<sub>30</sub>N<sub>8</sub>O<sub>4</sub>Cl<sub>3</sub>: C, 31.12; H, 5.60; N, 20.76%, found: C, 30.86; H, 5.66; N, 19.68 %.

### 2.5.8 Synthesis of [Co{(NH<sub>3</sub>)<sub>2</sub>sar}]Cl<sub>5</sub><sup>85</sup>

[Co{(NO<sub>2</sub>)<sub>2</sub>sar}]Cl<sub>3</sub> (5.0 g, 9.3 mmol) was dissolved in deoxygenated water (250 cm<sup>3</sup>) under a nitrogen atmosphere. Zinc dust (5.0 g) was added to the solution, followed by dropwise addition of HCl (deoxygenated, 10 M, 25 cm<sup>3</sup>). The mixture was stirred for 1.5 h at room temperature. The reduction to Co(II) was monitored by withdrawing a few drops of the reaction mixture, adding a drop of 30 % H<sub>2</sub>O<sub>2</sub> to oxidise the complex to the Co(III) state, and separating



the components by chromatography on a microcolumn of Na<sup>+</sup> SP Sephadex C25 with NaCl eluant (0.3 M). When a single orange band was detected H<sub>2</sub>O<sub>2</sub> (30 %, 7.0 cm<sup>3</sup>), was added to the bulk solution. The resulting orange solution was warmed on a steam bath for 15 minutes. The solution was absorbed on H<sup>+</sup> Dowex 50 WX2 cation-exchange resin. The resin was washed with water (225 cm<sup>3</sup>) then HCl (1 M, 225 cm<sup>3</sup>) to remove Zn<sup>2+</sup>. Elution with HCl (3 M) gave an orange solution. This solution was reduced *in vacuo* at 50 °C until crystallisation commenced and deposition was completed by the addition of ethanol. The complex was recrystallised as large yellow-orange plates by dissolution in warm HCl (1 M), addition of ethanol to the point of turbidity and slow cooling. Yield 2.10 g, 3.80 mmol, 41 %.

$\delta_{\text{H}}$  (400 MHz; D<sub>2</sub>O; 298 K) 2.68 (12H, m, CH<sub>2</sub>), 3.29 (12H, m, CH<sub>2</sub>).

Electronic spectrum:  $\lambda_{\text{max}}$  in HCl (0.1 M), nm: 475, 343.

Anal. Calc. for CoC<sub>14</sub>H<sub>36</sub>N<sub>8</sub>Cl<sub>5</sub>: C, 30.41; H, 6.56; N, 20.27 %, found: C, 29.58; H, 6.68; N, 19.39 %.

### 2.5.9 Synthesis of (NH<sub>2</sub>)<sub>2</sub>sar.H<sub>2</sub>O <sup>71</sup>

[Co((NH<sub>3</sub>)<sub>2</sub>sar)]Cl<sub>5</sub> (2.0 g, 3.6 mmol), NaOH (0.281 g) and CoCl<sub>2</sub>.6H<sub>2</sub>O (0.877 g) were dissolved in deoxygenated water (30 cm<sup>3</sup>). Potassium cyanide (4.30 g) was added to the solution and a green precipitate was observed. The reaction mixture was heated at 70 °C under nitrogen for 6 hours. The solution was then taken to dryness *in vacuo* and the residue was extracted with boiling acetonitrile (3 x 20 cm<sup>3</sup>). The extract was filtered then reduced to produce a white solid. The product was recrystallised from acetonitrile. Yield 0.16 g, 0.48 mmol, 13 %.

$\delta_{\text{H}}$  (400 MHz; D<sub>2</sub>O; 298 K) 2.48 (12H, s), 2.57 (12H, s).

Anal. Calc. for C<sub>14</sub>H<sub>36</sub>N<sub>8</sub>O: C, 50.57; H, 10.91; N, 33.70 %, found: C, 50.92; H, 10.69; N, 33.99 %.

### 2.5.10 Reaction of (NH<sub>2</sub>)<sub>2</sub>sar with di-*tert*-butyl dicarbonate

The diaminosarcophagine cage (NH<sub>2</sub>)<sub>2</sub>sar.H<sub>2</sub>O (0.04 g, 0.12 mmol) was dissolved in tetrahydrofuran (2.5 cm<sup>3</sup>) and water (2.5 cm<sup>3</sup>). Solid NaOH (0.04 g) was then

added to the mixture followed by di-*tert*-butyl dicarbonate (0.444 g). After stirring for 3 days the reaction mixture appeared to contain oily droplets. The mixture was extracted with ethyl acetate (3 x 5 cm<sup>3</sup>), and the solution evaporated to give a colourless oil. The aqueous layer was then acidified to pH 2 and extracted with ethyl acetate (3 x 5 cm<sup>3</sup>). Evaporation of the solvent gave an off-white solid. See section 2.3.3 for discussion of the characterisation.

#### **2.5.11 Reaction of piperazine with di-*tert*-butyl dicarbonate**

Piperazine (0.2 g, 2.32 mmol) was dissolved in tetrahydrofuran (5 cm<sup>3</sup>) and water (5 cm<sup>3</sup>). Solid NaOH (0.19 g, 4.64 mmol) was added to the mixture, which was then cooled in ice to 0 °C. Di-*tert*-butyl dicarbonate (2.02 g, 4 eq) was added to the cooled mixture with stirring. After stirring for 15 minutes the mixture was allowed to warm to room temperature, at which point formation of a precipitate was observed. The mixture was stirred at room temperature for a further 2 h then the white precipitate obtained by filtration and washed with water. Yield 0.37 g, 1.45 mmol, 63 %.

$\delta_{\text{H}}$  (400 MHz; CDCl<sub>3</sub>; 298 K) 1.47 (18H, s, <sup>t</sup>Bu), 3.27 (8H, s, CH<sub>2</sub>).

---

# **Chapter Three**

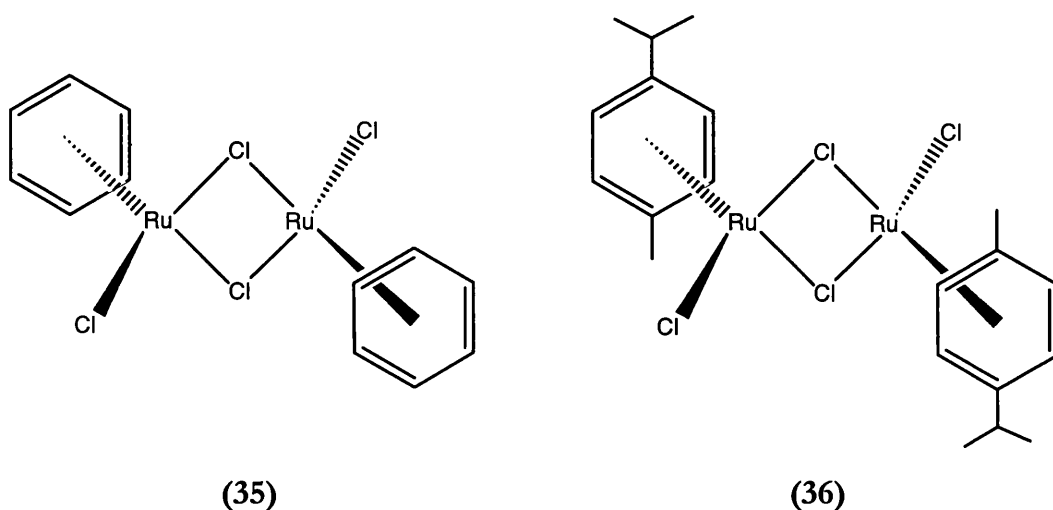
## **Ruthenium and rhodium complexes of hexamethylenetetramine**

### 3.1 Introduction

This chapter describes investigations into the reactions of hexamethylenetetramine with a range of dichloride bridged ruthenium and rhodium complexes, namely, the ruthenium(II) complexes,  $[\{\text{Ru}(\eta^6\text{-C}_6\text{H}_6)\text{Cl}(\mu\text{-Cl})\}_2]$  and  $[\{\text{Ru}(\eta^6\text{-}i\text{-p-cymene})\text{Cl}(\mu\text{-Cl})\}_2]$ ; the ruthenium(IV) complex  $[\{\text{Ru}(\eta^3:\eta^3\text{-C}_{10}\text{H}_{16})\text{Cl}(\mu\text{-Cl})\}_2]$ ; and the rhodium(III) complex  $[\{\text{Rh}(\eta^5\text{-C}_5\text{Me}_5)\text{Cl}(\mu\text{-Cl})\}_2]$ . The products of these reactions have been characterised using  $^1\text{H}$  NMR spectroscopy, infrared spectroscopy and microanalytical data. In addition, low temperature  $^1\text{H}$  NMR spectroscopy has been used to investigate the nature of the products in solution. A brief introduction to the chemistry of these complexes, and in particular their reactions with nitrogen donor ligands, is provided in sections 3.1.1 - 3.1.3.

#### 3.1.1 The synthesis and reactions of “Ru( $\eta^6$ -arene)” complexes

In the arene-ruthenium(II) complexes  $[\{\text{Ru}(\eta^6\text{-C}_6\text{H}_6)\text{Cl}(\mu\text{-Cl})\}_2]$  (35) and  $[\{\text{Ru}(\eta^6\text{-}i\text{-p-cymene})\text{Cl}(\mu\text{-Cl})\}_2]$  (36) the arene ligands may be considered tridentate, occupying three adjacent sites about the octahedrally coordinated ruthenium ion.



These complexes are synthesised by reaction of hydrated ruthenium trichloride with the appropriate diene in refluxing ethanol. Synthesis of  $[\{\text{Ru}(\eta^6\text{-}p\text{-cymene})\text{Cl}(\mu\text{-Cl})\}_2]$  is achieved using  $\alpha$ -phellandrene (5-isopropyl-2-methyl-cyclohexa-1,3-diene).<sup>86</sup> The reaction of ruthenium trichloride with cyclohexa-1,4-diene gives  $[\{\text{Ru}(\eta^6\text{-C}_6\text{H}_6)\text{Cl}(\mu\text{-Cl})\}_2]$ .<sup>87</sup> Initial reports of this complex, empirical formula  $[\text{RuCl}_2(\text{C}_6\text{H}_6)]$ , postulated a polymeric chloro-bridged structure containing  $\eta^4$ -benzene and octahedrally coordinated ruthenium(II).<sup>88</sup> However, evidence from the IR spectrum of the complex, which contains one band for a terminal Ru-Cl stretch and two bridging Ru-Cl-Ru stretches, suggests that the complex exists as the dimer.<sup>89</sup> Further evidence for the dimeric structure of arene-ruthenium(II) complexes was obtained in the form of a molecular weight determination of  $[\text{RuCl}_2(p\text{-cymene})]$ .<sup>90</sup> Determination of the solid-state structure of  $[\{\text{Ru}(\eta^6\text{-C}_6\text{Me}_6)\text{Cl}(\mu\text{-Cl})\}_2]$ , using X-ray diffraction, finally confirmed the dimeric nature of these  $[\text{RuCl}_2(\eta^6\text{-arene})]$  species.<sup>91</sup>

The reactions of these complexes with Lewis bases are wide-ranging, and are considered as being of three major types:

1) Reactions with Lewis bases giving monomeric half-sandwich complexes,  $[(\eta^6\text{-arene})\text{RuCl}_2(\text{L})]$  or  $[(\eta^6\text{-arene})\text{RuCl}(\text{L})_2]^+$ , (L = Lewis base, *eg.* pyridine,  $\text{PR}_3$ ,  $\text{P}(\text{OR})_3$ ,  $\text{AsR}_3$ ,  $\text{CNR}$ ,  $\text{CO}$  *etc.*)<sup>92, 93</sup>

2) Reactions with bidentate Lewis bases producing monomeric half-sandwich complexes containing a chelating ligand,  $[(\eta^6\text{-arene})\text{RuCl}(\text{L-L})]^+$  (L-L = 2,2'-bipy, 1,10-phenanthroline, ethylenediamine)<sup>94, 95</sup> or  $[(\eta^6\text{-arene})\text{RuCl}(\text{L-L})]$ , (L-L =  $\text{O}_2\text{CR}$ , acac, 2-hydroxypyridinate)<sup>96, 97, 98</sup>

3) Reactions with bifunctional Lewis bases producing binuclear half-sandwich complexes with a bridging ligand,  $[\{(\eta^6\text{-arene})\text{RuCl}_2\}_2(\mu\text{-L-L})]$ , (L-L = pyrazine,  $\text{Ph}_2\text{PCH}_2\text{CH}_2\text{PPh}_2$ )<sup>99, 100</sup>

For these three reaction types, the nature of the solvent affects the products formed. In non-polar solvents cleavage of the chloride bridge occurs leaving one vacant coordination site for the incoming base; in polar solvents loss of a

chloride ion occurs and thus two coordination sites are available on the metal centre. The reactions may be carried out using the Lewis base as both solvent and reactant, and compounds formed by this method include  $[(\eta^6\text{-C}_6\text{H}_6)\text{RuCl}_2\text{L}]$  ( $\text{L} = \text{PR}_3$ ,  $\text{P}(\text{OR})_3$  or  $\text{py}$ ).<sup>87, 89</sup> Single-crystal X-ray diffraction studies on  $[(\eta^6\text{-C}_6\text{H}_6)\text{RuCl}_2(\text{PMePh}_2)]$  and  $[(\eta^6\text{-}i\text{-cymene})\text{RuCl}_2(\text{PMePh}_2)]$  illustrate the piano-stool geometry, common for this type of complex. The arene rings and the other three ligands are mutually staggered, with the arene ring slightly but significantly non-planar.<sup>90</sup> **Figure 3.1** illustrates the geometry around ruthenium in  $[(\eta^6\text{-}i\text{-cymene})\text{RuCl}_2(\text{PMePh}_2)]$ , which is common for arene-ruthenium complexes  $[(\eta^6\text{-arene})\text{RuCl}_2\text{L}]$ .

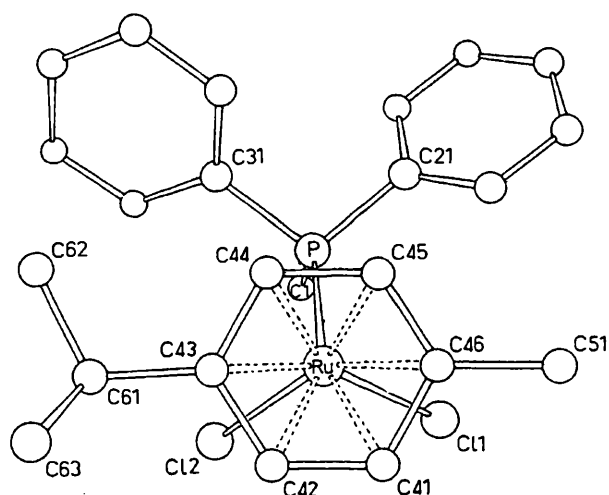


**Figure 3.1** Geometry about ruthenium in  $[(\eta^6\text{-C}_6\text{H}_6)\text{RuCl}_2(\text{PMePh}_2)]$ <sup>90</sup>

Reports of arene-ruthenium complexes with nitrogen and phosphorus donor ligands are abundant and the reactions of arene-ruthenium complexes with Lewis bases have been the subject of a number of reviews<sup>101, 102, 103, 104</sup> The remainder of this introduction concentrates specifically on arene-ruthenium complexes with amine ligands. Although reactions of arene-ruthenium dimers with nitrogen donor ligands such as pyridine, hydrazines and ammonia have been well-studied, reactions with simple amines have not been studied so extensively.<sup>105</sup> The limited number of reported reactions of arene-ruthenium complexes with primary and secondary amines resulting in neutral, monomeric complexes are

summarised in **Table 3.1**. There are currently no literature reports of reactions of arene-ruthenium complexes with tertiary amines.

**Table 3.1** Neutral, monomeric arene-ruthenium amine complexes:  
[[ $\eta^6$ -arene)RuCl<sub>2</sub>(NHRR')]

arene	R	R'	ref.
<i>p</i> -cymene	H	CH(CH <sub>3</sub> )CH <sub>2</sub> CH <sub>3</sub>	106, 107
<i>p</i> -cymene	H	C <sub>6</sub> H <sub>4</sub> Me	108
<i>p</i> -cymene	H	Ph	109
<i>p</i> -cymene	H	PhOH	110
<i>p</i> -cymene	H	CH(Me)Ph	111
<i>p</i> -cymene	Et	Et	105
C <sub>6</sub> H <sub>6</sub>	H	CH(CH <sub>3</sub> )CH <sub>2</sub> CH <sub>3</sub>	106
C <sub>6</sub> H <sub>6</sub>	H	Ph	109
C <sub>6</sub> H <sub>6</sub>	H	Et	112
C <sub>6</sub> H <sub>6</sub>	H	<sup>t</sup> Bu	112
C <sub>6</sub> H <sub>6</sub>	H	C <sub>6</sub> H <sub>4</sub> Me	112
C <sub>6</sub> H <sub>6</sub>	H	PhOH	110
C <sub>6</sub> H <sub>6</sub>	H	CH(Me)Ph	111
C <sub>6</sub> H <sub>6</sub>	Et	Et	109
1,3,5-Me <sub>3</sub> C <sub>6</sub> H <sub>3</sub>	H	Ph	105
1,3,5-Me <sub>3</sub> C <sub>6</sub> H <sub>3</sub>	H	CH <sub>2</sub> Ph	105
1,3,5-Me <sub>3</sub> C <sub>6</sub> H <sub>3</sub>	Et	Et	105
1,3,5-Me <sub>3</sub> C <sub>6</sub> H <sub>3</sub>	Bu	Bu	105
1,3,5-Me <sub>3</sub> C <sub>6</sub> H <sub>3</sub>	NHRR' = piperidine: C <sub>5</sub> H <sub>10</sub> NH		105
<i>o</i> -MeC <sub>6</sub> H <sub>4</sub> CO <sub>2</sub> Me	H	CH(Me)Ph	111

A number of ionic compounds, [[ $\eta^6$ -arene)RuCl(NHRR')<sub>2</sub>]<sup>+</sup>, have also been prepared from the reaction of arene-ruthenium complexes with amines, **Table 3.2**.

**Table 3.2 Cationic arene-ruthenium amine complexes:**  
 $[(\eta^6\text{-arene})\text{RuCl}(\text{NH}_2\text{R})_2]^+$

	complex	prepared in	ref.
<b>A</b>	$[(\eta^6\text{-}p\text{-cymene})\text{RuCl}(\text{NH}_2\text{C}_6\text{H}_4\text{OH})_2]\text{Cl}$	DCM	110
<b>B</b>	$[(\eta^6\text{-C}_6\text{H}_6)\text{RuCl}(\text{NH}_2\text{C}_6\text{H}_4\text{OH})_2]\text{Cl}$	DCM	110
<b>C</b>	$[(\eta^6\text{-C}_6\text{H}_6)\text{RuCl}(\text{NH}_2\text{C}_6\text{H}_4\text{Me})_2]\text{PF}_6$	THF	112
<b>D</b>	$[(\eta^6\text{-1,3,5-Me}_3\text{C}_6\text{H}_3)\text{RuCl}(\text{NH}_2\text{Ph})_2]\text{BF}_4$	DCM	105
<b>E</b>	$[(\eta^6\text{-1,3,5-Me}_3\text{C}_6\text{H}_3)\text{RuCl}(\text{NH}_2\text{CH}_2\text{Ph})_2]\text{BF}_4$	DCM	105

Although cationic, the complexes described in **Table 3.2** were not prepared in polar solvents. Complexes **A** and **B** were precipitated from dichloromethane solutions containing four equivalents of *o*-aminophenol and the arene-ruthenium complex.<sup>110</sup> In the reaction of  $[\{\text{Ru}(\eta^6\text{-C}_6\text{H}_6)\text{Cl}(\mu\text{-Cl})\}_2]$  with *p*-toluidine to produce **C**, ultrasound is used to overcome the problem of insolubility of the ruthenium starting material in non-coordinating solvents.<sup>112</sup> However, attempts to prepare complexes  $[(\eta^6\text{-C}_6\text{H}_6)\text{RuCl}(\text{NH}_2\text{R})_2]^+$ , containing the aliphatic amine ligands  $\text{NH}_2\text{Et}$  or  $\text{NH}_2\text{CMe}_3$ , were unsuccessful. This led to the conclusion that the relative softness of the ligand is of more importance in the substitution reaction than its basicity.<sup>112</sup> In contrast to examples **A-C**, complexes **D** and **E** were not prepared from  $[\{\text{Ru}(\eta^6\text{-arene})\text{Cl}(\mu\text{-Cl})\}_2]$ . Instead, aniline or benzylamine were reacted with the mono-adduct  $[(1,3,5\text{-Me}_3\text{C}_6\text{H}_3)\text{RuCl}_2(\text{amine})]$ .<sup>105</sup>

A limited number of complexes of the type  $[\text{Ru}(\eta^6\text{-arene})\text{Cl}(\text{L-L})]\text{X}$ , containing chelating bidentate amines have been reported. One example is  $[\text{Ru}(\eta^6\text{-arene})\text{Cl}(\text{en})]^+$  (en = ethylenediamine), which is precipitated from ethanol



by the addition of  $\text{NaBPh}_4$ .<sup>113</sup> Similar complexes have been prepared in dichloromethane solution, for example  $[\text{Ru}(\eta^6\text{-arene})\text{Cl}(\text{L-L})]\text{X}$  ( $\text{L-L} = o$ -phenylenediamine,  $\text{X} = \text{Cl}$  or  $\text{PF}_6$ ;  $\text{L-L} = 1,2$ -diphenyl-1,2-diaminoethane,  $\text{X} = \text{PF}_6$ ).<sup>110, 111</sup> Complexes containing asymmetric chelating ligands have also been prepared. **Figure 3.2** illustrates the structure of  $[\text{Ru}(\eta^6\text{-arene})\text{Cl}(\text{triazine})]\text{Cl}$ , which is precipitated from a dichloromethane solution of  $[\{\text{Ru}(\eta^6\text{-arene})\text{Cl}(\mu\text{-Cl})\}_2]$  and the triazine by addition of diethyl ether.<sup>114</sup>

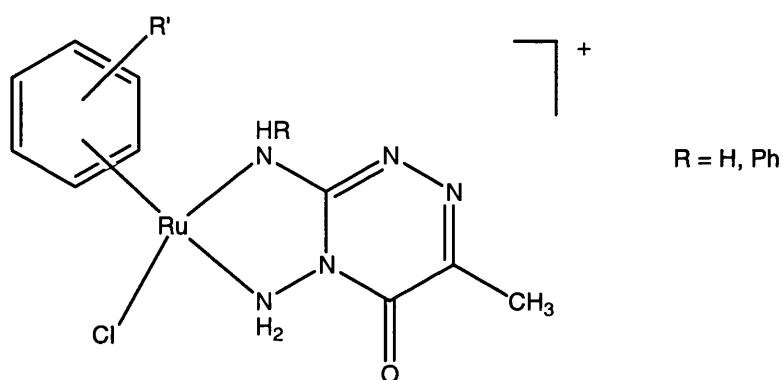


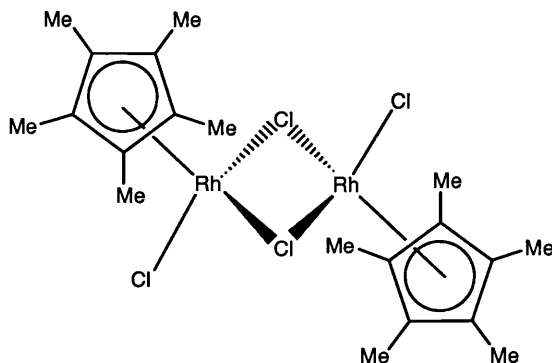
**Figure 3.2**  $[\text{Ru}(\eta^6\text{-arene})\text{Cl}(\text{triazine})]\text{Cl}$ , (arene = benzene or *p*-cymene)

Bidentate amines may also behave as bridging groups, depending upon the positions of the donor atoms in the ligand. A good illustration of this is in the reaction of  $[\{\text{Ru}(\eta^6\text{-arene})\text{Cl}(\mu\text{-Cl})\}_2]$  with *o*-phenylenediamine, which produces  $[\text{Ru}(\eta^6\text{-arene})\text{Cl}(o\text{-phenylenediamine})]^+$  with a chelating phenylenediamine ligand. In contrast, the reaction of  $[\{\text{Ru}(\eta^6\text{-arene})\text{Cl}(\mu\text{-Cl})\}_2]$  with *p*-phenylenediamine produces the bridged complex  $[\{(\eta^6\text{-arene})\text{RuCl}\}_2(\mu\text{-}p\text{-phenylenediamine})]^{2+}$ .<sup>110</sup>

### 3.1.2 The synthesis and reactions of “ $\text{Rh}(\eta^5\text{-C}_5\text{Me}_5)$ ” complexes

The complex  $[\{\text{Rh}(\eta^5\text{-C}_5\text{Me}_5)\text{Cl}(\mu\text{-Cl})\}_2]$  (**37**) is prepared in an analogous fashion to “ $\text{Ru}(\eta^6\text{-arene})$ ” complexes, by refluxing  $\text{RhCl}_3 \cdot 3\text{H}_2\text{O}$  with pentamethylcyclopentadiene.<sup>86</sup> Single crystal X-ray diffraction proves the structure is dimeric in the solid state, and the  $\text{C}_5\text{Me}_5$  ligand gives rise to a singlet

in the  $^1\text{H}$  NMR spectrum.<sup>115</sup> The reactions of  $[\{\text{Rh}(\eta^5\text{-C}_5\text{Me}_5)\text{Cl}(\mu\text{-Cl})\}_2]$  are similar to those described for “ $\text{Ru}(\eta^6\text{-arene})$ ” complexes in section 3.1.1.



(37)

Simple adducts  $[\text{Rh}(\eta^5\text{-C}_5\text{Me}_5)\text{Cl}_2\text{L}]$  can be prepared by dissolution of  $[\{\text{Rh}(\eta^5\text{-C}_5\text{Me}_5)\text{Cl}(\mu\text{-Cl})\}_2]$  in coordinating solvents, such as pyridine, acetonitrile or dimethylsulfoxide.<sup>116, 117</sup> By reaction with tertiary phosphines in non-coordinating solvents, compounds such as  $[\text{Rh}(\eta^5\text{-C}_5\text{Me}_5)\text{Cl}_2\text{L}]$  ( $\text{L} = \text{PPh}_3$ ,<sup>118</sup>  $\text{PMe}_3$ ,<sup>119</sup>  $\text{PMe}_2\text{Ph}$ ,<sup>120</sup>  $\text{PCy}_3$ ,<sup>120</sup>  $\text{PBu}_3$ <sup>120</sup>) are prepared. Cationic complexes of “ $\text{Rh}(\eta^5\text{-C}_5\text{Me}_5)$ ” are also known. These complexes may contain two neutral ligands coordinated in a monodentate fashion *i.e.*  $[\text{Rh}(\eta^5\text{-C}_5\text{Me}_5)\text{ClL}_2]\text{Cl}$  ( $\text{L} = \text{PMe}_2\text{Ph}$ ,<sup>121</sup>) or one chelating neutral ligand as in  $[\text{Rh}(\eta^5\text{-C}_5\text{Me}_5)\text{ClL-L}]\text{Cl}$  ( $\text{L-L} = \text{dppe}$ <sup>122</sup>).

As with the “ $\text{Ru}(\eta^6\text{-arene})$ ” complexes, “ $\text{Rh}(\eta^5\text{-C}_5\text{Me}_5)$ ” complexes with nitrogen donor ligands are well known. In particular, a number of reactions of  $[\{\text{Rh}(\eta^5\text{-C}_5\text{Me}_5)\text{Cl}(\mu\text{-Cl})\}_2]$  with amines have been studied. These may be separated into two broad categories: reactions with aliphatic amines and reactions with aromatic amines. Reported reactions using aliphatic amines are limited to ammonia, ethylenediamine and trimethylethylenediamine. The addition of a dichloromethane solution of  $[\{\text{Rh}(\eta^5\text{-C}_5\text{Me}_5)\text{Cl}(\mu\text{-Cl})\}_2]$  to liquid ammonia produces the insoluble cationic complex  $[\text{Rh}(\eta^5\text{-C}_5\text{Me}_5)(\text{NH}_3)_3]\text{Cl}_2$ .<sup>123</sup> Reactions with the bidentate ligands ethylenediamine and trimethylethylenediamine gave the

cationic products  $[\text{RhCl}(\eta^5\text{-C}_5\text{Me}_5)(\text{en})]\text{Cl}$  and  $[\text{Rh}(\eta^5\text{-C}_5\text{Me}_5)\text{Cl}(\text{tmen})]\text{Cl}$ , respectively.<sup>124</sup> A wider range of compounds has been formed with aromatic amine ligands and a number of examples are given in **Table 3.3**.

**Table 3.3** “ $\text{RhCl}(\eta^5\text{-C}_5\text{Me}_5)$ ” complexes with aromatic amines

ligand	product	ref.
<i>o</i> -aminophenol	$[\text{Rh}(\eta^5\text{-C}_5\text{Me}_5)\text{Cl}_2(o\text{-OHC}_6\text{H}_5\text{NH}_2)]$	124
<i>o</i> -aminothiophenol	$[\text{Rh}(\eta^5\text{-C}_5\text{Me}_5)\text{Cl}_2(o\text{-SHPhNH}_2)]$	124
<i>p</i> -phenylenediamine	$[\{\text{Rh}(\eta^5\text{-C}_5\text{Me}_5)\text{Cl}_2\}_2(\mu\text{-}p\text{-NH}_2\text{PhNH}_2)]$	124
<i>o</i> -phenylenediamine	$[\text{Rh}(\eta^5\text{-C}_5\text{Me}_5)\text{Cl}(o\text{-NH}_2\text{PhNH}_2)]\text{Cl}$	124
aniline	$[\text{Rh}(\eta^5\text{-C}_5\text{Me}_5)\text{Cl}_2(\text{C}_6\text{H}_5\text{NH}_2)]$	125
<i>p</i> -toluidine	$[\text{Rh}(\eta^5\text{-C}_5\text{Me}_5)\text{Cl}_2(p\text{-CH}_3\text{C}_6\text{H}_4\text{NH}_2)]$	118, 125
<i>p</i> -anisidine	$[\text{Rh}(\eta^5\text{-C}_5\text{Me}_5)\text{Cl}_2(p\text{-CH}_3\text{OC}_6\text{H}_4\text{NH}_2)]$	125
<i>p</i> -chloroaniline	$[\text{Rh}(\eta^5\text{-C}_5\text{Me}_5)\text{Cl}_2(p\text{-ClC}_6\text{H}_4\text{NH}_2)]$	125
<i>p</i> -bromoaniline	$[\text{Rh}(\eta^5\text{-C}_5\text{Me}_5)\text{Cl}_2(p\text{-BrC}_6\text{H}_4\text{NH}_2)]$	125

Although the majority of reported complexes of “ $\text{Rh}(\eta^5\text{-C}_5\text{Me}_5)$ ” with aromatic amine ligands are neutral, cationic species have also been prepared. One example is  $[\text{Rh}(\eta^5\text{-C}_5\text{Me}_5)\text{Cl}(o\text{-NH}_2\text{PhNH}_2)]\text{Cl}$  which contains a chelating *o*-phenylenediamine ligand.<sup>124</sup> The reaction of  $[\{\text{Rh}(\eta^5\text{-C}_5\text{Me}_5)\text{Cl}(\mu\text{-Cl})\}_2]$  with *p*-phenylenediamine however, produces  $[\{\text{Rh}(\eta^5\text{-C}_5\text{Me}_5)\text{Cl}_2\}_2(\mu\text{-}p\text{-NH}_2\text{PhNH}_2)]$  where the amine ligand bridges two “ $\text{Rh}(\eta^5\text{-C}_5\text{Me}_5)$ ” moieties.<sup>124</sup>

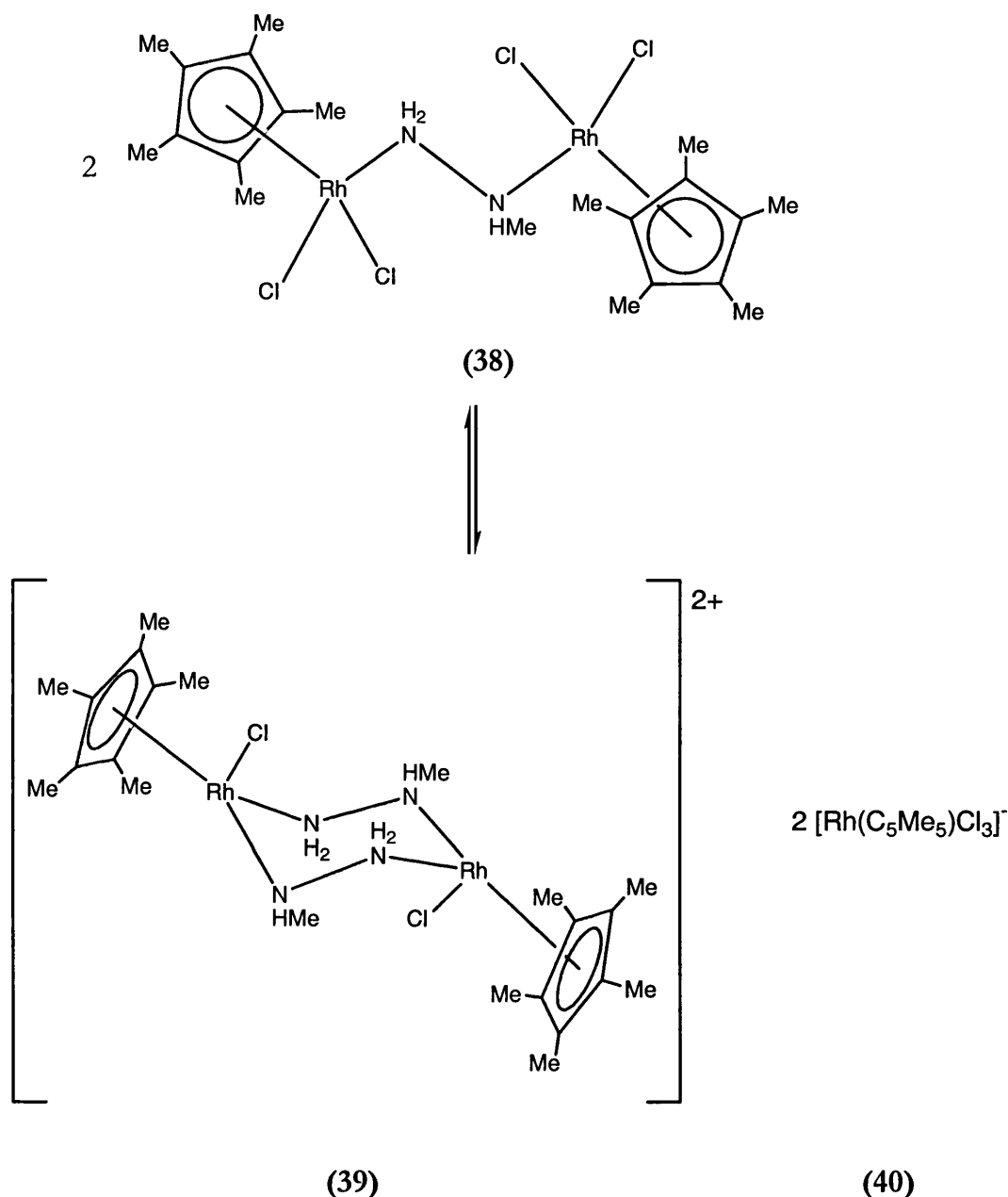
Two 1,2,4-triazine derivatives of “ $(\eta^6\text{-arene})\text{Ru}$ ” with chelating triazine ligands were described in section 3.1.1, and shown in **Figure 3.2**. Analogous compounds have been prepared containing the “ $(\eta^5\text{-C}_5\text{Me}_5)\text{Rh}$ ” moiety.<sup>114</sup>

Another category of complexes of “Rh( $\eta^5$ -C<sub>5</sub>Me<sub>5</sub>)” with nitrogen donor ligands, are those containing substituted-hydrazines. **Table 3.4** gives examples of mononuclear complexes of this type.

**Table 3.4** Complexes of “( $\eta^5$ -C<sub>5</sub>Me<sub>5</sub>)Rh” with hydrazines

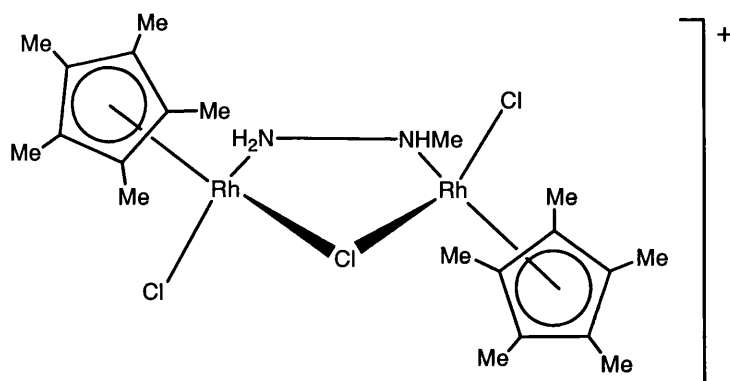
ligand, L	product	coordination	ref.
NH <sub>2</sub> NHPh	[RhCl <sub>2</sub> ( $\eta^5$ -C <sub>5</sub> Me <sub>5</sub> )(L)]	monodentate	123
	[RhCl( $\eta^5$ -C <sub>5</sub> Me <sub>5</sub> )(L) <sub>2</sub> ]Cl		
NH <sub>2</sub> NHC <sub>6</sub> F <sub>5</sub>	[RhCl <sub>2</sub> ( $\eta^5$ -C <sub>5</sub> Me <sub>5</sub> )(L)]	monodentate	123
NH <sub>2</sub> NHC <sub>6</sub> H <sub>4</sub> Me- <i>p</i>	[RhCl <sub>2</sub> ( $\eta^5$ -C <sub>5</sub> Me <sub>5</sub> )(L)]	monodentate	123
	[RhCl( $\eta^5$ -C <sub>5</sub> Me <sub>5</sub> )(L) <sub>2</sub> ]Cl		
NH <sub>2</sub> NH <sub>2</sub>	[Rh( $\eta^5$ -C <sub>5</sub> Me <sub>5</sub> )(L) <sub>3</sub> ]Cl <sub>2</sub>	monodentate	123

In addition to these mononuclear compounds, binuclear 1:2 adducts of “Rh( $\eta^5$ -C<sub>5</sub>Me<sub>5</sub>)” and hydrazines have also been prepared. For example, the reaction of [ $\{\text{Rh}(\eta^5\text{-C}_5\text{Me}_5)\text{Cl}(\mu\text{-Cl})\}_2$ ] with methylhydrazine gives [ $\{\text{Rh}(\eta^5\text{-C}_5\text{Me}_5)\text{Cl}_2\}_2(\mu\text{-NH}_2\text{NHMe})$ ].<sup>123</sup> The <sup>1</sup>H NMR spectrum of this compound at -40 °C exhibited a total of eight signals for the methylhydrazine ligands: two NHMe resonances and six NH resonances. The <sup>13</sup>C NMR spectrum recorded at -40 °C exhibited four doublets (splitting due to coupling to <sup>103</sup>Rh) due to four different “ $\eta^5$ -C<sub>5</sub>Me<sub>5</sub>” environments. In order to account for these low temperature spectra, the equilibrium illustrated in **Scheme 3.1** was postulated. The <sup>1</sup>H NMR data were assigned as follows: one NHMe resonance and three NH resonances, are ascribed to each complex, **(38)** and **(39)**. The <sup>13</sup>C NMR data was attributed to two inequivalent “ $\eta^5$ -C<sub>5</sub>Me<sub>5</sub>” moieties on **(38)**, one pair of equivalent “ $\eta^5$ -C<sub>5</sub>Me<sub>5</sub>” ligands on **(39)** and one “ $\eta^5$ -C<sub>5</sub>Me<sub>5</sub>” ligand on **(40)**.



**Scheme 3.1** Suggested equilibrium for  $[\{\text{RhCl}_2(\eta^5\text{-C}_5\text{Me}_5)\}_2(\text{NH}_2\text{NHMe})]$  in solution

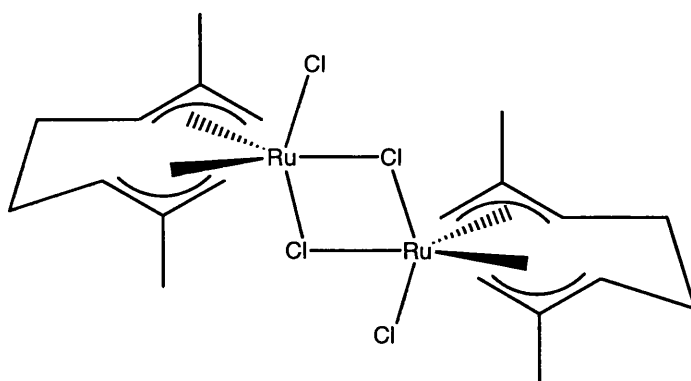
The reaction of (38) with  $\text{NH}_4\text{PF}_6$  in dichloromethane gave a cationic compound, which had a  $^1\text{H}$  NMR spectrum not affected by temperature and indicated the presence of two inequivalent “ $\text{Rh}(\eta^5\text{-C}_5\text{Me}_5)$ ” moieties and an absence of symmetry in the molecule. Consequently, the structure  $[\{\text{Rh}(\eta^5\text{-C}_5\text{Me}_5)\}_2\text{Cl}_3(\mu\text{-NH}_2\text{NHMe})][\text{PF}_6]$  (41) was suggested for this complex.<sup>123</sup> Analytical data were also consistent with this formulation.



(41)

### 3.1.3 *Bis(allyl)ruthenium(IV) complexes*

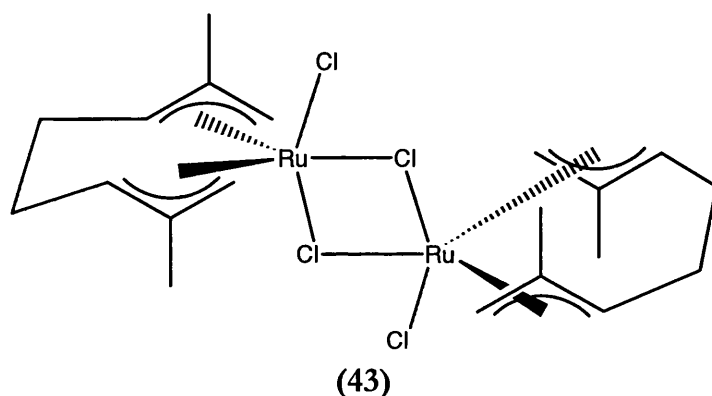
The *bis(allyl)ruthenium(IV)* chloride bridged dimer [ $\{\text{Ru}(\eta^3\text{-}\eta^3\text{-C}_{10}\text{H}_{16})\text{Cl}(\mu\text{-Cl})\}_2$ ] (**42**) is structurally similar to the arene-ruthenium complexes discussed in section 3.1.1 and is also synthesised in a similar fashion, by reaction of hydrated ruthenium trichloride with isoprene (2-methylbutadiene) in refluxing ethanol.<sup>126</sup> The structure of (**42**) in the solid state has been determined by single crystal X-ray diffraction to be of  $C_i$  molecular symmetry, the geometry around each ruthenium ion may be considered as trigonal bipyramidal, with the allyl ligand occupying two equatorial sites.<sup>127</sup> The 2,7-dimethyloctadienediyl ligands have  $C_2$  symmetry.



(42)

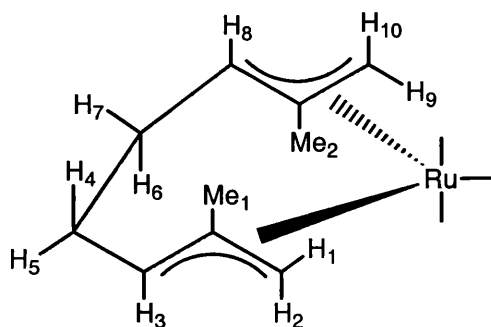
However,  $^1\text{H}$  NMR studies in non-coordinating solvents have shown [ $\{\text{Ru}(\eta^3\text{-}\eta^3\text{-C}_{10}\text{H}_{16})\text{Cl}(\mu\text{-Cl})\}_2$ ] to exist in two diastereomeric forms that

interconvert by chloride bridge rupture.<sup>128</sup> These species are the  $C_i$  isomer (**42**) and the  $C_2$  isomer (**43**) and are present in approximately equimolar proportions, ( $[C_2]/[C_i] = 1.25$  at 298 K).



The occurrence of the pair of diasereoisomers is due to the  $C_2$  symmetry adopted by the 2,7-dimethyloctadienediyl ligands, which renders the “ $(\eta^3:\eta^3-C_{10}H_{16})Ru^{2+}$ ” fragments chiral. In addition the axial and equatorial sites about ruthenium are inequivalent. Thus the  $^1H$  NMR spectrum of  $[\{Ru(\eta^3:\eta^3-C_{10}H_{16})Cl(\mu-Cl)\}_2]$  in deuterated chloroform exhibits the signals described in **Table 3.5**.

**Table 3.5**  $^1H$  NMR data obtained on dissolution of  $[\{Ru(\eta^3:\eta^3-C_{10}H_{16})Cl(\mu-Cl)\}_2]$  in  $CDCl_3$  at 298 K<sup>a</sup>



isomer	methyl <sup>c</sup> Me <sub>1</sub> , Me <sub>2</sub>	methylene chain <sup>d</sup> H <sub>4</sub> , H <sub>6</sub> , H <sub>5</sub> , H <sub>7</sub>	internal allyl <sup>d</sup> H <sub>3</sub> , H <sub>8</sub>	terminal allyl <sup>e</sup> H <sub>1</sub> , H <sub>9</sub> , H <sub>2</sub> , H <sub>10</sub>
$C_i$	2.39, 2.30	2.7-2.4	4.66, 4.51	5.73, 5.38, 5.23, 4.49
$C_2$	2.49, 2.25	2.7-2.4	4.72, 4.46	6.11, 5.09, 4.88, 4.74

<sup>a</sup>Adapted from reference <sup>128</sup> <sup>b</sup>Shifts in  $\delta$  ppm with Me<sub>4</sub>Si as reference <sup>c</sup>Singlets <sup>d</sup>Multiplets <sup>e</sup>Singlets,  $^2J(\text{syn/anti}) < 1.5$  Hz

In coordinating solvents the dimer is cleaved and both equatorially and axially solvated monomeric complexes are observed.<sup>128</sup> The complexes  $[\text{Ru}(\eta^3\text{-}\eta^3\text{-C}_{10}\text{H}_{16})\text{Cl}_2\text{L}]$  ( $\text{L} = \text{pyridine, sulfur bound-DMSO}$ ) have been isolated and NMR studies indicate formation of the equatorial adduct. In the case of  $[\text{Ru}(\eta^3\text{-}\eta^3\text{-C}_{10}\text{H}_{16})\text{Cl}_2\text{L}]$  ( $\text{L} = \text{MeCN, oxygen bound-DMF}$ ) both the axial and equatorial adducts are observed in equilibrium in solution.<sup>128</sup>

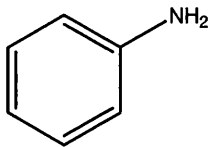
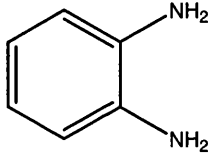
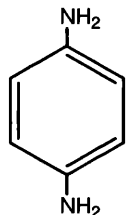
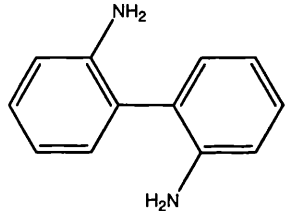
Initially derivatives of  $[\{\text{Ru}(\eta^3\text{-}\eta^3\text{-C}_{10}\text{H}_{16})\text{Cl}(\mu\text{-Cl})\}_2]$  were limited to a number of neutral monomeric adducts  $[\text{Ru}(\eta^3\text{-}\eta^3\text{-C}_{10}\text{H}_{16})\text{Cl}_2\text{L}]$  ( $\text{L} = \text{CO, PPh}_3, \text{PF}_3, \text{PF}_2(\text{NMe}_2), \text{PCl}_2(\text{CF}_3)$  or  $\text{P}(\text{OCH}_2)_3\text{CPh}$ ).<sup>129</sup> A number of complexes of “ $\text{Ru}(\eta^3\text{-}\eta^3\text{-C}_{10}\text{H}_{16})$ ” with nitrogen donor ligands are now also known, for example,  $[\text{Ru}(\eta^3\text{-}\eta^3\text{-C}_{10}\text{H}_{16})\text{Cl}_2\text{L}]$  ( $\text{L} = \text{tBuNC, iPrNC}$ ) with the nitrogen donor ligands in the axial sites.<sup>130</sup> Cationic complexes  $[\text{Ru}(\eta^3\text{-}\eta^3\text{-C}_{10}\text{H}_{16})\text{ClL}_2]^+$  ( $\text{L} = \text{MeCN, tBuNC, iPrNC}$ ) have also been synthesised, in each case the nitrogen-donor ligands lie in both axial positions.<sup>130</sup>

The studies most relevant to this work concern the reaction of various amines with  $[\{\text{Ru}(\eta^3\text{-}\eta^3\text{-C}_{10}\text{H}_{16})\text{Cl}(\mu\text{-Cl})\}_2]$ . The reactions of aromatic amines with  $[\{\text{Ru}(\eta^3\text{-}\eta^3\text{-C}_{10}\text{H}_{16})\text{Cl}(\mu\text{-Cl})\}_2]$  have been studied in dichloromethane and methanol, the results of these reactions are summarised in **Table 3.6**.<sup>131</sup> Reaction of aniline with  $[\{\text{Ru}(\eta^3\text{-}\eta^3\text{-C}_{10}\text{H}_{16})\text{Cl}(\mu\text{-Cl})\}_2]$  in methanol results in the formation of the 1:1 adduct  $[\text{Ru}(\eta^3\text{-}\eta^3\text{-C}_{10}\text{H}_{16})\text{Cl}_2(\text{NH}_2\text{Ph})]$  with the amine ligand occupying the equatorial position and the axial sites occupied by terminal chloride ligands. Hence, the <sup>1</sup>H NMR spectra of the complex exhibits three signals attributable to the allyl part of the complex, two singlets for the terminal allyl protons and one singlet for the methyl groups. Reactions of  $[\{\text{Ru}(\eta^3\text{-}\eta^3\text{-C}_{10}\text{H}_{16})\text{Cl}(\mu\text{-Cl})\}_2]$  with two mole equivalents of *o*-phenylenediamine (*o*-pda) in deoxygenated methanol did not result in cationic species but instead the neutral, monomeric 1:1 adduct  $[\text{Ru}(\eta^3\text{-}\eta^3\text{-C}_{10}\text{H}_{16})\text{Cl}_2(\textit{o}\text{-pda})]$  was formed. In



contrast, an analogous reaction in the presence of atmospheric oxygen gave the cationic complex  $[\text{Ru}(\eta^3\text{:}\eta^3\text{-C}_{10}\text{H}_{16})\text{Cl}(o\text{-pda})]\text{Cl}$  with the amine ligand coordinated in a chelating fashion through its two amine functions. The reaction of one molar equivalent of *o*-pda with  $[\{\text{Ru}(\eta^3\text{:}\eta^3\text{-C}_{10}\text{H}_{16})\text{Cl}(\mu\text{-Cl})\}_2]$  in either dichloromethane or methanol produces the bridging adduct,  $[\{\text{Ru}(\eta^3\text{:}\eta^3\text{-C}_{10}\text{H}_{16})\text{Cl}_2\}_2(\mu\text{-}o\text{-pda})]$ .  $^1\text{H}$  NMR spectroscopy studies of this compound indicate that it exists as two diastereoisomers in solution in the same way as described for the starting material  $[\{\text{Ru}(\eta^3\text{:}\eta^3\text{-C}_{10}\text{H}_{16})\text{Cl}(\mu\text{-Cl})\}_2]$ .<sup>128</sup> The reaction of *p*-phenylenediamine (*p*-pda) with  $[\{\text{Ru}(\eta^3\text{:}\eta^3\text{-C}_{10}\text{H}_{16})\text{Cl}(\mu\text{-Cl})\}_2]$  in either methanol or dichloromethane, produces  $[\text{Ru}(\eta^3\text{:}\eta^3\text{-C}_{10}\text{H}_{16})\text{Cl}_2(p\text{-pda})]$  and  $[\{\text{Ru}(\eta^3\text{:}\eta^3\text{-C}_{10}\text{H}_{16})\text{Cl}\}_2(\mu\text{-}p\text{-pda})]\text{Cl}_2$ , respectively. Again, as for  $[\{\text{Ru}(\eta^3\text{:}\eta^3\text{-C}_{10}\text{H}_{16})\text{Cl}(\mu\text{-Cl})\}_2]$  the  $^1\text{H}$  NMR studies of the binuclear adduct show that it exists as two diastereoisomeric forms, and broadening of the spectrum at room temperature is attributed to interconversion between the two forms *via* Ru-N bond fission and exchange of “ $\text{Ru}(\eta^3\text{:}\eta^3\text{-C}_{10}\text{H}_{16})\text{Cl}_2$ ” units.<sup>131</sup> The reaction of  $[\{\text{Ru}(\eta^3\text{:}\eta^3\text{-C}_{10}\text{H}_{16})\text{Cl}(\mu\text{-Cl})\}_2]$  with the larger bifunctional ligand, 2,2'-diaminodiphenyl has also been investigated. In methanol in both the presence or absence of air the cationic complex  $[\text{Ru}(\eta^3\text{:}\eta^3\text{-C}_{10}\text{H}_{16})\text{Cl}(o\text{-NH}_2\text{C}_6\text{H}_4 \cdot \text{C}_6\text{H}_4\text{NH}_2)]\text{Cl}$  is formed in this reaction. Although this complex is unexpected due to the presence of a seven-membered heterocyclic chelate ring, examination of molecular models shows that an unstrained ring may be obtained if the rings of the 2,2'-diaminodiphenyl ligand are orientated at 90 ° to each other, by rotation of the interannular C-C bond.<sup>131</sup>

Table 3.6 Adducts of “Ru( $\eta^3$ : $\eta^3$ -C<sub>10</sub>H<sub>16</sub>)” with aromatic primary amines<sup>131</sup>

ligand, L	solvent	product	ligand coordination
	MeOH <sup>a</sup>	[Ru( $\eta^3$ : $\eta^3$ -C <sub>10</sub> H <sub>16</sub> )Cl <sub>2</sub> (L)]	monodentate
	MeOH <sup>a</sup>	[Ru( $\eta^3$ : $\eta^3$ -C <sub>10</sub> H <sub>16</sub> )Cl <sub>2</sub> (L)]	monodentate
	MeOH <sup>b</sup>	[Ru( $\eta^3$ : $\eta^3$ -C <sub>10</sub> H <sub>16</sub> )Cl(L)]Cl	chelating
	DCM <sup>a</sup>	[{Ru( $\eta^3$ : $\eta^3$ -C <sub>10</sub> H <sub>16</sub> )Cl <sub>2</sub> } <sub>2</sub> ( $\mu$ -L)]	bridging
	MeOH <sup>a</sup>	[Ru( $\eta^3$ : $\eta^3$ -C <sub>10</sub> H <sub>16</sub> )Cl <sub>2</sub> (L)]	monodentate
	DCM <sup>a</sup>	[{Ru( $\eta^3$ : $\eta^3$ -C <sub>10</sub> H <sub>16</sub> )Cl <sub>2</sub> } <sub>2</sub> ( $\mu$ -L)]	bridging
	MeOH <sup>a,b</sup>	[Ru( $\eta^3$ : $\eta^3$ -C <sub>10</sub> H <sub>16</sub> )Cl(L)]Cl	chelating

<sup>a</sup> deoxygenated solvent, <sup>b</sup> oxygenated solvent

Binuclear and trinuclear complexes with bridging nitrogen donor ligands are also known. The reaction of [ $\{Ru(\eta^3$ : $\eta^3$ -C<sub>10</sub>H<sub>16</sub>)Cl( $\mu$ -Cl) $\}_2$ ] with pyrazine gives the bridged complex [ $\{Ru(\eta^3$ : $\eta^3$ -C<sub>10</sub>H<sub>16</sub>)Cl<sub>2</sub> $\}_2(\mu$ -C<sub>4</sub>H<sub>4</sub>N<sub>2</sub>)]. Interestingly, this product is obtained when anything between one and ten mole equivalents of pyrazine are added to the reaction mixture, with the monomeric 1:1 adduct being formed only when more than fifteen molar equivalents of pyrazine were used.<sup>132</sup> The <sup>1</sup>H NMR spectrum of [ $\{Ru(\eta^3$ : $\eta^3$ -C<sub>10</sub>H<sub>16</sub>)Cl<sub>2</sub> $\}_2(\mu$ -C<sub>4</sub>H<sub>4</sub>N<sub>2</sub>)] exhibits double the number of signals expected, a fact which is attributed to the presence of diastereoisomers in solution (as observed for [ $\{Ru(\eta^3$ : $\eta^3$ -C<sub>10</sub>H<sub>16</sub>)Cl( $\mu$ -Cl) $\}_2$ ]). A

single crystal X-ray study, however, showed that only one isomer is present in the solid state, that with  $C_i$  symmetry, **Figure 3.3**. Analogous reactions using 1,3,5-triazine as a ligand produced a mixture of products containing  $[\text{Ru}(\eta^3:\eta^3\text{-C}_{10}\text{H}_{16})\text{Cl}_2(\text{C}_3\text{H}_3\text{N}_3)]$ ,  $[\{\text{Ru}(\eta^3:\eta^3\text{-C}_{10}\text{H}_{16})\text{Cl}_2\}_2(\mu\text{-C}_3\text{H}_3\text{N}_3)]$  and  $[\{\text{Ru}(\eta^3:\eta^3\text{-C}_{10}\text{H}_{16})\text{Cl}_2\}_3(\mu^3\text{-C}_3\text{H}_3\text{N}_3)]$ , which interconvert in chloroform solution at room temperature.<sup>133</sup>

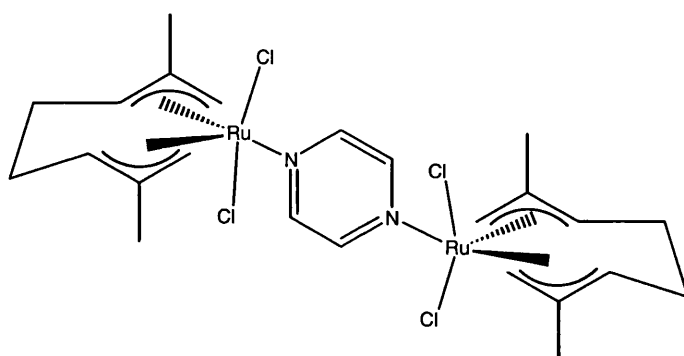


**Figure 3.3** Structure of  $[\{\text{Ru}(\eta^3:\eta^3\text{-C}_{10}\text{H}_{16})\text{Cl}_2\}_2(\mu\text{-C}_4\text{H}_4\text{N}_2)]$  as determined by X-ray diffraction

## 3.2 Results and discussion

### 3.2.1 Complexes of “ $\text{Ru}(\eta^6\text{-}p\text{-cymene})$ ” with hexamethylenetetramine

In order to prepare  $[(\eta^6\text{-}p\text{-cymene})\text{RuCl}_2(\text{hmt})]$ , two mole equivalents of hexamethylenetetramine were added to a solution of  $[\{\text{Ru}(\eta^6\text{-}p\text{-cymene})\text{Cl}(\mu\text{-Cl})\}_2]$  in dichloromethane at room temperature. Addition of diethyl ether to the reaction mixture, followed by cooling to 0 °C, gave a red-brown crystalline product. The  $^1\text{H}$  NMR spectrum of this compound, **Figure 3.4**, exhibits four resonances attributable to the  $p$ -cymene ligand, suggesting a single environment for the  $p$ -cymene ligand. These signals are, a doublet and septet for the methyl and CH of the isopropyl moiety ( $\delta$  1.29 ppm, 3.10 ppm); a singlet for the methyl group of the  $p$ -cymene ( $\delta$  2.26 ppm); and an AB quartet for the protons of the aromatic ring ( $\delta$  5.27, 5.42 ppm).

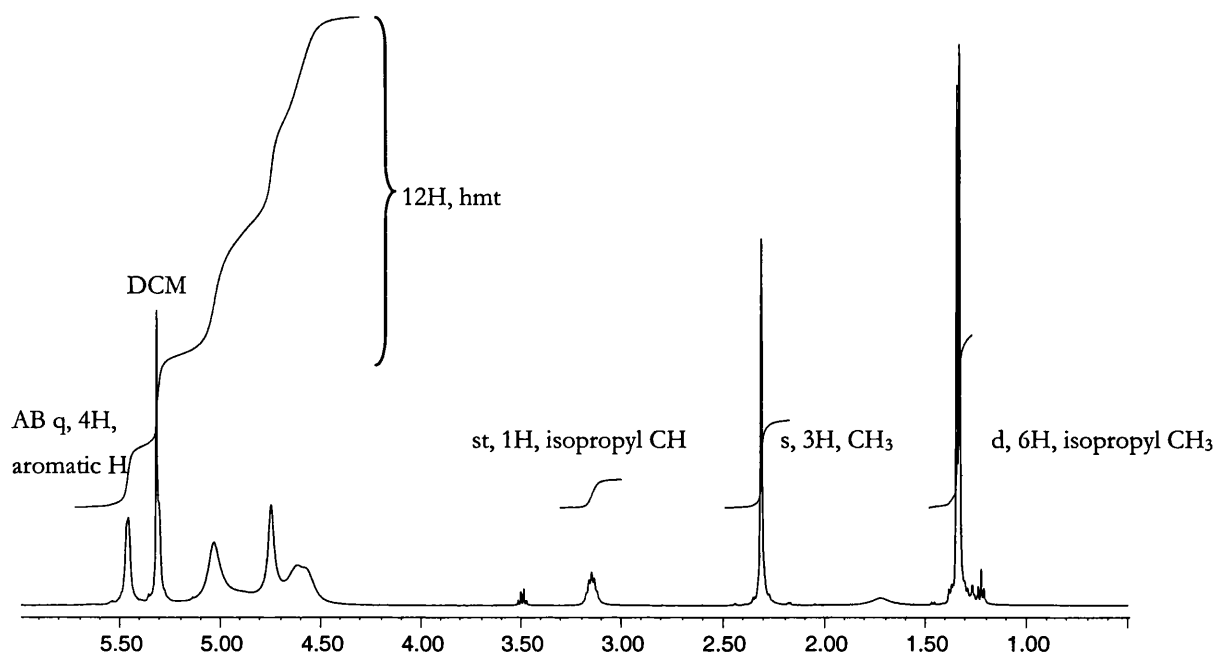


**Figure 3.4**  $^1\text{H}$  NMR spectrum of  $[(\eta^6\text{-}p\text{-cymene})\text{RuCl}_2(\text{hmt})]$  at 298 K

In addition to the signals ascribed to the *p*-cymene ligand, there are three signals attributable to hexamethylenetetramine within the spectrum, at 4.56 ppm, 4.69 ppm and 4.98 ppm. This group of three hexamethylenetetramine signals integrates against the methyl signal of the *p*-cymene ligand in a 4:1 ratio, indicating the product is the expected 1:1 adduct  $[(\eta^6\text{-}p\text{-cymene})\text{RuCl}_2(\text{hmt})]$ .

In the  $^1\text{H}$  NMR spectrum of this complex, the expected coupling pattern for the protons of hexamethylenetetramine is a singlet and an AB quartet, both integrating for an equal number of protons. **Figure 3.5** illustrates the three inequivalent protons on the hexamethylenetetramine ligand which give rise to these signals. In the figure, hexamethylenetetramine is coordinated to the metal in a monodentate fashion and may be viewed as a six membered ring, in a chair conformation, capped by three methylene groups and a nitrogen atom. The capping nitrogen atom is the one coordinated to the metal. The ligand symmetry is now reduced from  $T_d$  to  $C_{3v}$  (with the  $C_3$  axis running along the metal-nitrogen bond). This gives rise to three sets of magnetically inequivalent protons,  $H_a$ ,  $H_b$  and  $H_c$  as illustrated in **Figure 3.5**. Therefore, the expected signals in the

$^1\text{H}$  NMR spectrum are a singlet for the  $\text{H}_c$  protons and an AB quartet for protons  $\text{H}_a$  and  $\text{H}_b$ .

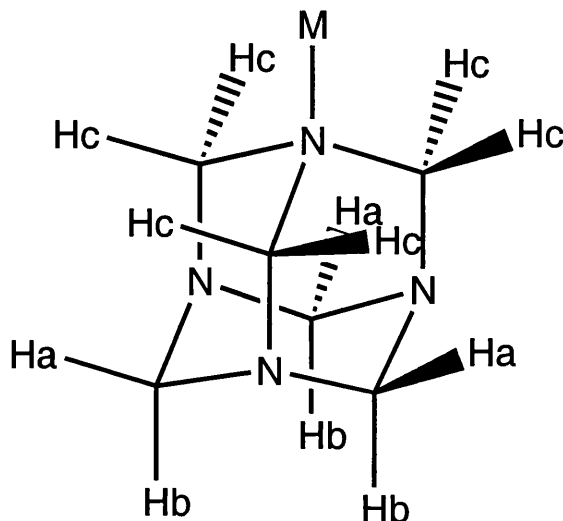


**Figure 3.5** The three inequivalent sets of protons,  $\text{H}_a$ ,  $\text{H}_b$  and  $\text{H}_c$  of hexamethylenetetramine in a 1:1 adduct

Since, the observed  $^1\text{H}$  NMR spectrum recorded at room temperature does not exhibit these signals for hexamethylenetetramine, it was proposed that a dynamic exchange process was occurring and a low temperature study was necessary in order to confirm the synthesis of the 1:1 adduct. Hence, a variable temperature  $^1\text{H}$  NMR experiment was performed in the range 298-211 K, **Figure 3.6**.

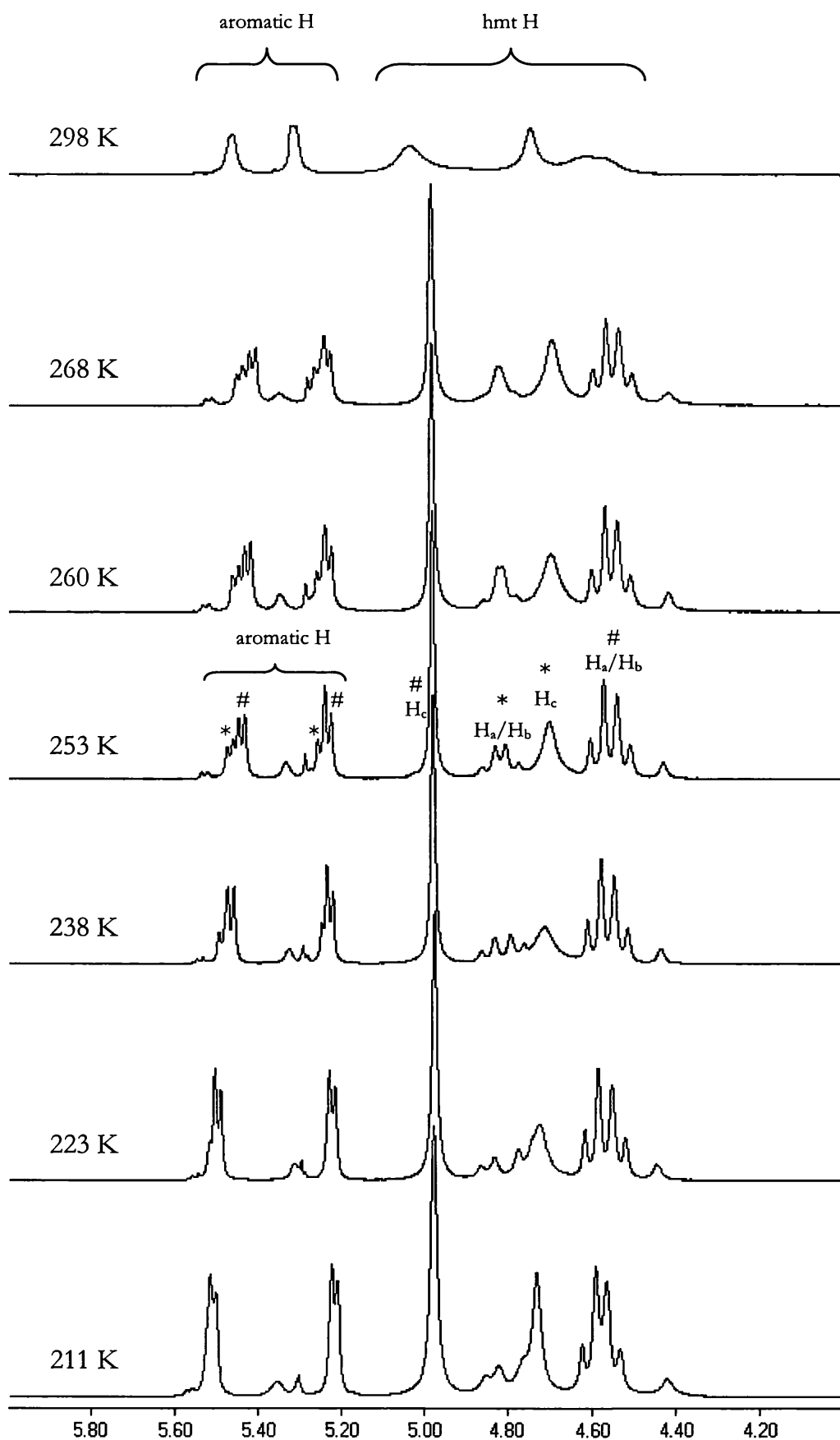
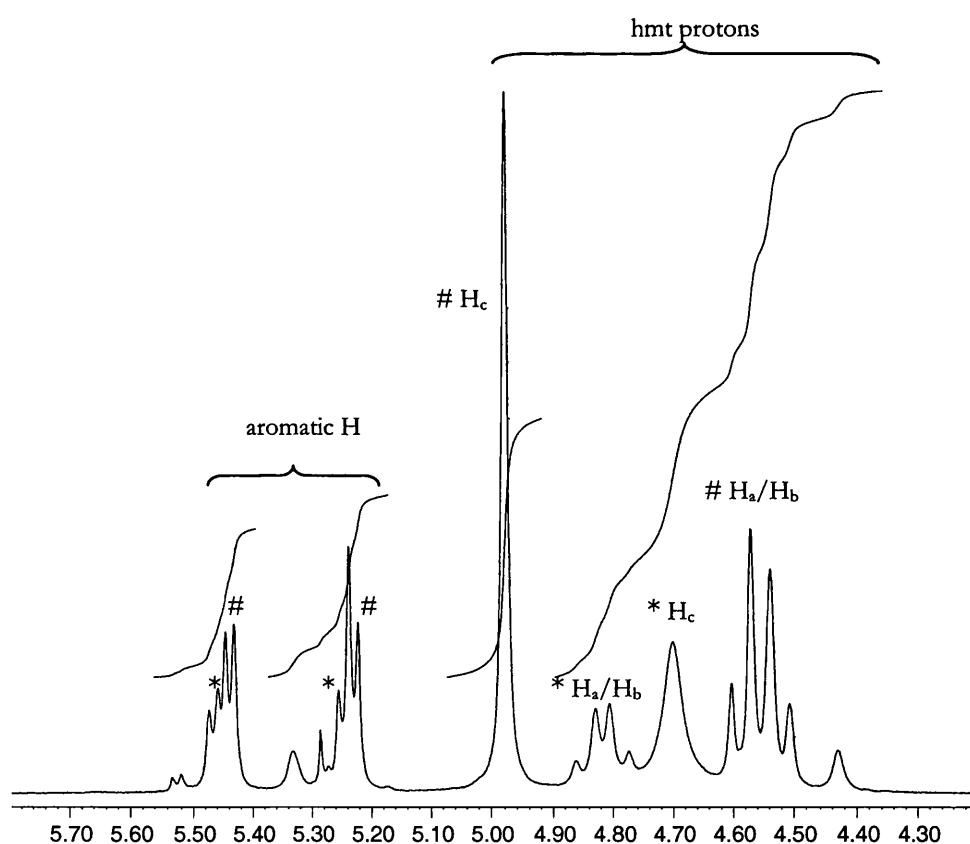


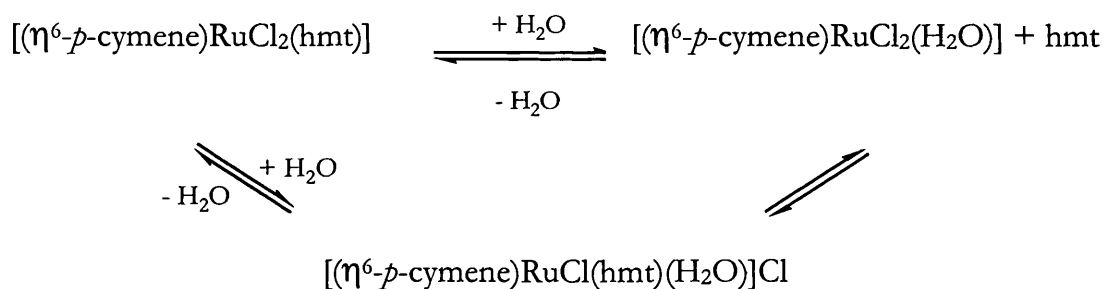
Figure 3.6  $^1\text{H}$  NMR spectra of  $[(\eta^6\text{-}p\text{-cymene})\text{RuCl}_2(\text{hmt})]$ , 211 – 298 K, in the region 4 to 6 ppm; # major product, \* minor product

Although the variable temperature NMR study gave evidence for monodenate coordination of hexamethylenetetramine to ruthenium, the overall appearance of the spectra was not as simple as expected. As the sample is cooled, the three hexamethylenetetramine resonances resolve into four distinct signals: two singlets and two AB quartets. Two AB quartets are also observed for the protons of the *p*-cymene ring at low temperatures, a second doublet, singlet and septet attributable to the Me and <sup>i</sup>Pr substituents *p*-cymene ligand are also observed. Therefore, rather than a single product it appears that two products are present in solution. Hexamethylenetetramine is coordinated to ruthenium through one nitrogen atom in both products, and it is suggested that the major product is  $[(\eta^6\text{-}p\text{-cymene})\text{RuCl}_2(\text{hmt})]$ . The presence of two products is most apparent in the spectrum recorded at 253 K, **Figure 3.7**. The integrals indicate an approximate ratio of 2:1 for the products.



**Figure 3.7** <sup>1</sup>H NMR spectrum of  $[(\eta^6\text{-}p\text{-cymene})\text{RuCl}_2(\text{hmt})]$  # and a second product \*, 253 K

As described in Section 3.1.1 polar solvents promote chloride loss from arene-ruthenium complexes, consequently, the presence of water in the NMR solvent may result in the formation of  $[(\eta^6\text{-}p\text{-cymene})\text{RuCl}(\text{hmt})_2]^+$  or  $[(\eta^6\text{-}p\text{-cymene})\text{RuCl}(\text{hmt})(\text{H}_2\text{O})]^+$ . The latter product is consistent with the ratio of “ $(\eta^6\text{-}p\text{-cymene})\text{Ru}$ ” protons to hexamethylenetetramine protons observed for the minor product in the  $^1\text{H}$  NMR spectrum. A possible mechanism for the dynamic process is described in **Scheme 3.2**. Rapid interchange between the three components would lead to equivalence of the hexamethylenetetramine protons at high temperatures.



**Scheme 3.2** Suggested dynamic process occurring in solution for  $[(\eta^6\text{-}p\text{-cymene})\text{RuCl}_2(\text{hmt})]$

The synthesis of the 1:1 adduct was confirmed by single crystal X-ray diffraction studies on the red-brown crystals obtained from dichloromethane/diethyl ether solution. The solid state structure is shown in **Figure 3.8**. Selected bond lengths and angles are presented in **Table 3.7**. The geometry about the ruthenium atom may be considered as a distorted octahedron with the arene ring occupying three sites. The resulting “piano-stool” geometry is very common for  $[(\eta^6\text{-arene})\text{RuCl}_2\text{L}]$  complexes. The Ru-N bond length, 2.234(3) Å, is somewhat longer than that observed in the similar compounds,  $[(\eta^6\text{-}p\text{-cymene})\text{RuCl}_2(p\text{-toluidine})]$ , 2.118(2) Å and  $[(\eta^6\text{-}p\text{-cymene})\text{RuCl}_2(\textit{sec}\text{-butylamine})]$ , 2.153(7) Å.<sup>108, 107</sup>



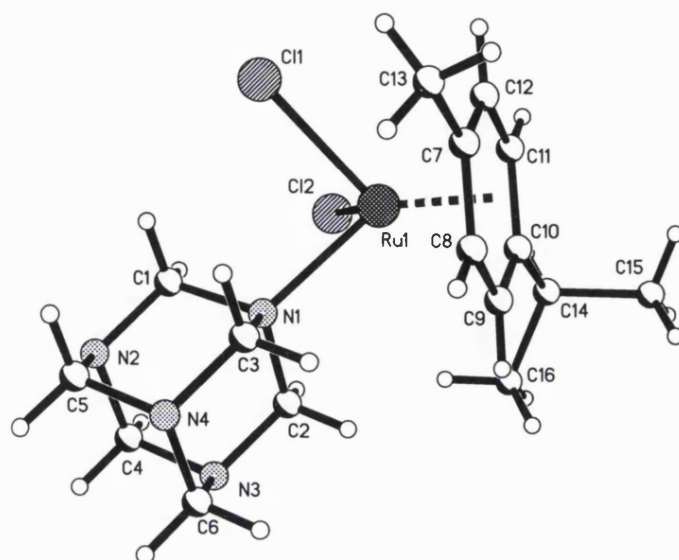


**Figure 3.8** Solid state structure of  $[(\eta^6\text{-}p\text{-cymene})\text{RuCl}_2(\text{hmt})]$  as determined by single crystal X-ray diffraction

**Table 3.7** Selected bond lengths [Å] and angles [°] for  $[(\eta^6\text{-}p\text{-cymene})\text{RuCl}_2(\text{hmt})]$

Ru(1)-N(1)	2.234(3)	N(1)-C(1)	1.522(6)
Ru(1)-Cl(2)	2.4179(12)	N(2)-C(1)	1.457(6)
Ru(1)-Cl(1)	2.4339(12)	N(2)-C(5)	1.464(6)
Ru(1)-C(11)	2.165(4)	N(2)-C(4)	1.468(6)
Ru(1)-C(12)	2.172(5)	C(2)-N(1)-C(3)	106.7(3)
Ru(1)-C(8)	2.196(4)	C(2)-N(1)-C(1)	106.6(3)
Ru(1)-C(9)	2.198(4)	C(3)-N(1)-C(1)	106.5(3)
Ru(1)-C(10)	2.204(5)	N(2)-C(1)-N(1)	112.5(4)
Ru(1)-C(7)	2.220(5)	N(3)-C(2)-N(1)	112.5(3)
N(1)-C(2)	1.501(5)	N(4)-C(3)-N(1)	111.8(4)
N(1)-C(3)	1.511(6)		

The distances Ru(1)-Cl(1) 2.4339(12) Å and Ru(1)-Cl(2) 2.4179(12) Å are significantly different to each other, but within the range observed in other

*p*-cymene-ruthenium amine complexes, 2.395(1) – 2.434(1) Å.<sup>107</sup> The Ru-C distances lie in the range 2.165(4) – 2.220(5) Å and the centre of the ring is 1.675 Å from the ruthenium atom. These values are similar to those observed in  $[(\eta^6\text{-}p\text{-cymene})\text{RuCl}_2\text{L}]$  complexes where L is *p*-toluidine,<sup>108</sup> *sec*-butylamine<sup>107</sup> or aminopyridine.<sup>134</sup> The methyl and isopropyl groups of the *p*-cymene ligand are bent towards the ruthenium atom by 2.0 ° and 3.9 °, respectively. The isopropyl group is not symmetrically placed with respect to the arene ring but forms a torsion angle, C(9)-C(10)-C(14)-C(16) of 32.2 ° with the mean plane. Coordination to ruthenium lengthens the N(1)-C bond with N(1)-C(1), N(1)-C(2) and N(1)-C(3), being in the range 1.501(5) – 1.522(6) Å, and longer than the corresponding bonds between carbon and the non-metallated nitrogen atoms, 1.464(6) – 1.470(6) Å. For comparison free hexamethylenetetramine exhibits a N-C bond length of 1.462(5) Å. The N-C-N angles of the hexamethylenetetramine ligand fall in the range 111.8(4) to 112.5(4) ° which are comparable with those in non-complexed hexamethylenetetramine, 112.4(3) °. Upon coordination the atoms around N(1) are slightly distorted from the tetrahedral geometry found in non-complexed hexamethylenetetramine (where C-N-C is 108.0(3) °) with bond angles ranging from 106.5(3) ° for C(3)-N(1)-C(1) to 106.7(3) ° for C(2)-N(1)-C(3). This effect is often observed when hexamethylenetetramine bonds to a metal and was discussed in Chapter One.

Further characterisation of the bulk product in the solid state was performed using infrared spectroscopy (as a nujol mull between caesium iodide plates). The infrared spectrum exhibited only one band in the far infrared region at 285 cm<sup>-1</sup>, this band is attributable to  $\nu(\text{Ru-Cl})$ . This IR data along with microanalytical data confirm that the second species,  $[(\eta^6\text{-}p\text{-cymene})\text{RuCl}(\text{hmt})(\text{H}_2\text{O})]\text{Cl}$ , observed in the NMR experiments, was only present in solution.

After successful synthesis of the 1:1 adduct, attempts were made to prepare the 1:2 adduct with hexamethylenetetramine bridging two *p*-cymene-ruthenium units.

However, the reaction of [ $\{\text{Ru}(\eta^6\text{-}p\text{-cymene})\text{Cl}(\mu\text{-Cl})\}_2$ ] with one mole equivalent of hexamethylenetetramine in dichloromethane gave only the 1:1 adduct and unreacted starting material. No significant changes were observed when the reaction was carried out in refluxing dichloromethane.

To further probe the reactivity of  $[\text{Ru}(\eta^6\text{-}p\text{-cymene})\text{Cl}(\mu\text{-Cl})]_2$ , it was decided to follow the work of Dyson and co-workers, who synthesised  $[\text{Ru}(\eta^6\text{-}p\text{-cymene})\text{Cl}_2(\text{pta})]$  (pta = 1,3,4-triaza-7-phosphatricyclo-[3.3.1.1]decane, an analogue of hexamethylenetetramine where one nitrogen atom is replaced by a phosphorus atom). This complex is produced *via* reaction of pta with the [ $\{\text{Ru}(\eta^6\text{-}p\text{-cymene})\text{Cl}(\mu\text{-Cl})\}_2$ ] in refluxing methanol.<sup>135</sup> The pta ligand binds to ruthenium through the phosphorus atom and this complex has been shown to exhibit pH dependent DNA binding in cancerous cells.<sup>135</sup> An analogous reaction with hexamethylenetetramine, did not produce the corresponding 1:1 adduct and no single product could be isolated. The <sup>1</sup>H NMR spectrum of the bulk material exhibited a complex set of signals for the aromatic protons of the *p*-cymene ring; evidently a mixture of products is obtained. Repeating the reaction under less forcing conditions at room temperature made little difference, with the <sup>1</sup>H NMR spectrum also indicating a mixture of products.

### 3.2.2 Complexes of “Ru( $\eta^6\text{-C}_6\text{H}_6$ )” with hexamethylenetetramine

Having successfully prepared  $[(\eta^6\text{-}p\text{-cymene})\text{RuCl}_2(\text{hmt})]$ , attempts were made to obtain the analogous compound containing the  $\eta^6\text{-C}_6\text{H}_6$  ligand. To that end two mole equivalents of hexamethylenetetramine were reacted with [ $\{\text{Ru}(\eta^6\text{-C}_6\text{H}_6)\text{Cl}(\mu\text{-Cl})\}_2$ ] at room temperature in dichloromethane, giving a yellow-green precipitate. This material was not soluble in the usual deuterated solvents ( $\text{CDCl}_3$ ,  $\text{CD}_2\text{Cl}_2$  *etc.*), thus <sup>1</sup>H NMR spectra were recorded in  $\text{CD}_3\text{NO}_2$ . The residual protons of the NMR solvent appear as a quintet at 4.33 ppm. The <sup>1</sup>H NMR spectrum of the product at room temperature, **Figure 3.9** exhibits two broad signals for the hexamethylenetetramine protons in the region 4.8-5.4 ppm

and a broad signal at 5.74 ppm attributed to the protons of the benzene ring. These signals integrate in a 1:1 ratio, indicating formation of a product containing two moles of “Ru( $\eta^6$ -C<sub>6</sub>H<sub>6</sub>)” per mole of hexamethylenetetramine. The obvious structure of such a product has hexamethylenetetramine bridging two “Ru( $\eta^6$ -C<sub>6</sub>H<sub>6</sub>)” units, *i.e.* the 1:2 adduct. The <sup>1</sup>H NMR spectrum for the 1:2 adduct should exhibit two singlets and an AB quartet, in a 1:1:4 ratio for the hexamethylenetetramine ligand. The protons giving rise to these signals are shown in **Figure 3.10**.

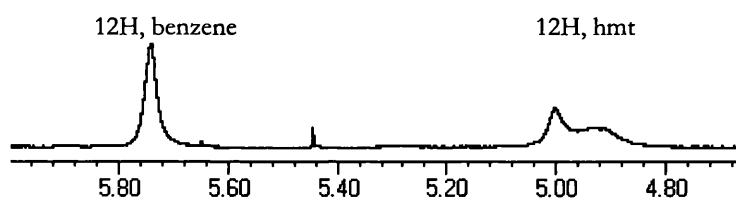


**Figure 3.9** <sup>1</sup>H NMR spectrum of “Ru( $\eta^6$ -C<sub>6</sub>H<sub>6</sub>)”-hmt adduct at 298 K

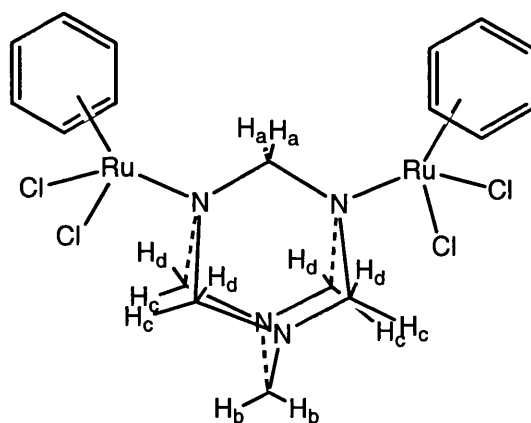


**Figure 3.10** Chemical environments of hexamethylenetetramine protons in [ $\{(\eta^6$ -C<sub>6</sub>H<sub>6</sub>)RuCl<sub>2</sub>\}<sub>2</sub>( $\mu$ -hmt)]: H<sub>a</sub> (s, 2H); H<sub>c</sub>, H<sub>d</sub> (AB q, 8H); H<sub>b</sub> (s, 2H)

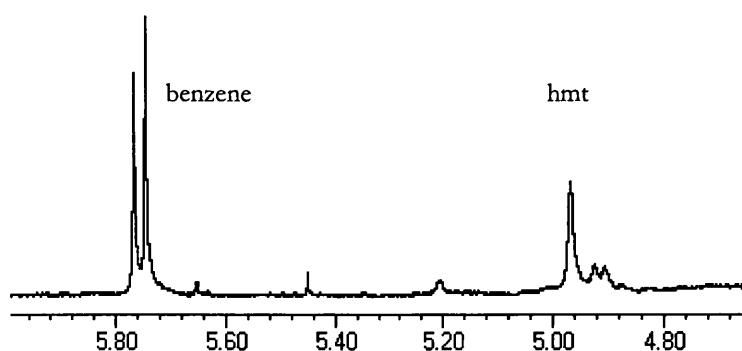
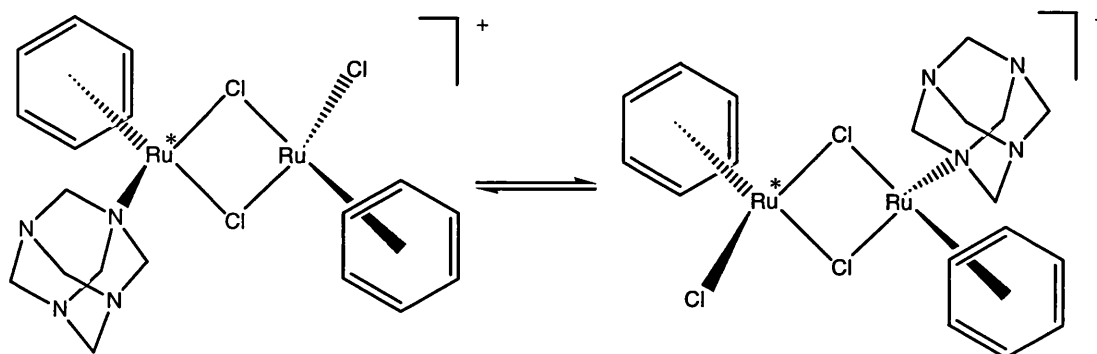


**Figure 3.11**  $^1\text{H}$  NMR spectrum of “ $\text{Ru}(\eta^6\text{-C}_6\text{H}_6)$ ”-hmt adduct at 253 K

Unfortunately the low temperature  $^1\text{H}$  NMR spectrum, **Figure 3.11** did not contain the expected signals. Instead a singlet and an AB quartet were observed, both integrating for an equal number of protons. This pair of signals is characteristic of hexamethylenetetramine coordinated to a metal through one nitrogen atom. At low temperature the singlet attributable to the benzene protons resolves into two singlets of equal integral. Possible explanations for the low temperature spectrum are the exchange of hexamethylenetetramine for solvent in the 1:1 adduct, or an equilibrium between the 1:1 adduct and  $[\{\text{Ru}(\eta^6\text{-C}_6\text{H}_6)\text{Cl}(\mu\text{-Cl})\}_2]$ , yet neither postulation accounts for the observed reproducible stoichiometry. The chloride bridged product illustrated in **Scheme 3.3**, however, would give rise to the  $^1\text{H}$  NMR spectrum observed at 253 K. In addition, fast exchange of hexamethylenetetramine between ruthenium ions at room temperature, would cause all of the hexamethylenetetramine protons to become equivalent, and render the protons of the two benzene rings equivalent. Further support for this theory is gained from the infrared spectrum of the complex, which exhibits three Ru-Cl bands, at  $301\text{ cm}^{-1}$  (terminal Ru-Cl) and at  $277\text{ cm}^{-1}$  and  $260\text{ cm}^{-1}$  (bridging Ru-Cl). Although unexpected on this occasion, compounds of this nature are not without precedent. Examples include,  $[(\eta^5\text{-C}_5\text{Me}_5)(\text{py})\text{Ru}(\mu\text{-Cl})_2\text{Ru}(\text{py})(\eta^5\text{-C}_5\text{Me}_5)]\text{PF}_6$ , which contains two chloride bridging ligands and two  $\eta^1$  pyridine molecules.<sup>136</sup> Complexes are also known which contain both chloride bridges and bridging nitrogen donor ligands. For example, the reaction of  $[\{\text{Ru}(\eta^6\text{-C}_6\text{H}_6)\text{Cl}(\mu\text{-Cl})\}_2]$

with pyrazole (pz) in appropriate molar ratio gives the dimeric complexes  $[(\eta^6\text{-C}_6\text{H}_6)\text{Ru}(\mu\text{-Cl})(\mu\text{-pz})_2\text{Ru}(\eta^6\text{-C}_6\text{H}_6)]\text{Cl}$  or,  $(\eta^6\text{-C}_6\text{H}_6)\text{Ru}(\mu\text{-Cl})_2(\mu\text{-pz})\text{Ru}(\eta^6\text{-C}_6\text{H}_6)]\text{Cl}$ .<sup>137</sup>



**Scheme 3.3** Proposed equilibrium in solution for  $[(\eta^6\text{-C}_6\text{H}_6)\text{ClRu}(\mu\text{-Cl})_2\text{Ru}(\text{hmt})(\eta^6\text{-C}_6\text{H}_6)]^+$

### 3.2.3 Complexes of “ $\text{Rh}(\eta^5\text{-C}_5\text{Me}_5)$ ” with hexamethylenetetramine

In order to prepare the 1:1 adduct of “ $\text{Rh}(\eta^5\text{-C}_5\text{Me}_5)$ ” and hexamethylenetetramine, two mole equivalents of hexamethylenetetramine were added to a dichloromethane solution of  $[\{\text{Rh}(\eta^5\text{-C}_5\text{Me}_5)\text{Cl}(\mu\text{-Cl})\}_2]$  at room temperature. Addition of diethyl ether to the solution, followed by cooling gave a yellow-orange precipitate. The  $^1\text{H}$  NMR spectrum of this solid at room temperature exhibits a singlet at 1.64 ppm assigned to the protons of the  $\eta^5\text{-C}_5\text{Me}_5$  ligand. A broad singlet is observed at 4.84 ppm due to the protons of the hexamethylenetetramine ligand. These two signals integrate in an approximate hmt: $\eta^5\text{-C}_5\text{Me}_5$  ratio of 12:30, suggesting the product is the 1:2 adduct. However, the hexamethylenetetramine signal is not resolved into the expected three signals (as discussed for  $[\{(\eta^6\text{-C}_6\text{H}_6)\text{RuCl}_2\}_2(\mu\text{-hmt})]$ , section 3.2), implying dynamic behaviour of the molecule in solution at room temperature. At 218 K the resonance ascribed to the protons of  $\eta^5\text{-C}_5\text{Me}_5$  resolve into four separate signals, indicating the presence of four species in solution. The hexamethylenetetramine resonance resolves into a number of signals at this

temperature. Unfortunately, the complexity of these signals prevents accurate characterisation of the four species present in the solution, although it is probable that they are attributable to various ionic forms of the 1:2 adduct. At room temperature, an equilibrium exists between these forms rendering the two sets of protons ( $\eta^5\text{-C}_5\text{Me}_5$  and hmt) equivalent.

In the solid state microanalytical data (see experimental data, section 3.4.5) are consistent with the 1:2 adduct. The infrared spectrum of the compound exhibits only one Rh-Cl stretch at  $275\text{ cm}^{-1}$ , also implying that the 1:2 adduct has been formed.

### 3.2.4 Complexes of “ $\text{Ru}(\eta^3\text{:}\eta^3\text{-C}_{10}\text{H}_{16})$ ” with hexamethylenetetramine

In addition to the study of the arene complexes of ruthenium(II), reactions of hexamethylenetetramine with the *bis*(allyl)Ru(IV) complex  $[\{\text{Ru}(\eta^3\text{:}\eta^3\text{-C}_{10}\text{H}_{16})\text{Cl}(\mu\text{-Cl})\}_2]$  have been investigated. The reaction of  $[\{\text{Ru}(\eta^3\text{:}\eta^3\text{-C}_{10}\text{H}_{16})\text{Cl}(\mu\text{-Cl})\}_2]$  with two equivalents of hexamethylenetetramine in dichloromethane at room temperature, produced a brown precipitate. The insolubility of this solid in the deuterated solvents available prevented characterisation by NMR spectroscopy. However, reducing the reaction mixture to dryness *in vacuo* within ten minutes of the hexamethylenetetramine addition (before the brown precipitate was apparent), afforded a solid, from which it was possible to obtain an informative  $^1\text{H}$  NMR spectrum. Comparisons of the  $^1\text{H}$  NMR spectrum of  $[\{\text{Ru}(\eta^3\text{:}\eta^3\text{-C}_{10}\text{H}_{16})\text{Cl}(\mu\text{-Cl})\}_2]$  with the  $^1\text{H}$  NMR spectrum of the solid revealed the presence of a small quantity of a new compound. The four observed signals arising from this material, are characteristic of the equatorial 1:1 adduct, **Figure 3.12**. Two singlets (4.02 ppm and 4.92 ppm) can be assigned to the terminal allyl protons and one singlet (2.27 ppm) to the two equivalent methyl groups. The coordinated hexamethylenetetramine appears as a singlet at 4.72 ppm. Observation of the resonances arising from the internal allyl

protons and the ethylene protons was not possible due to the presence of  $[\{\text{Ru}(\eta^3:\eta^3\text{-C}_{10}\text{H}_{16})\text{Cl}(\mu\text{-Cl})\}_2]$ .

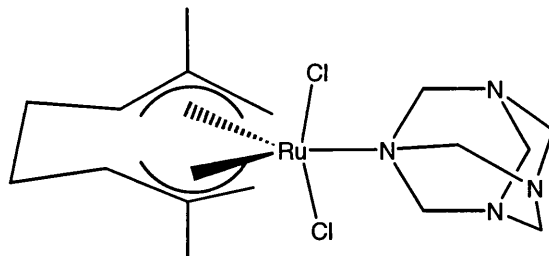


**Figure 3.12** Equatorial adduct  $[\text{Ru}(\eta^3:\eta^3\text{-C}_{10}\text{H}_{16})\text{Cl}_2(\text{hmt})]$

Considering that the brown precipitate was most likely formed as a result of decomposition of the 1:1 adduct due to air or moisture sensitivity, the reaction was repeated using pre-dried and degassed dichloromethane. Careful analysis indicated that the product still contained a mixture of unreacted  $[\{\text{Ru}(\eta^3:\eta^3\text{-C}_{10}\text{H}_{16})\text{Cl}\}_2(\mu\text{-Cl})_2]$  and the 1:1 adduct  $[\{\text{Ru}(\eta^3:\eta^3\text{-C}_{10}\text{H}_{16})\text{Cl}(\text{hmt})]$ . Subsequent reactions, in pre-dried and degassed toluene, produced a pink-brown solid after thirty minutes of refluxing. The  $^1\text{H}$  NMR spectrum of this solid confirms the presence of two species,  $[\{\text{Ru}(\eta^3:\eta^3\text{-C}_{10}\text{H}_{16})\text{Cl}\}_2(\mu\text{-Cl})_2]$  and  $[\text{Ru}(\eta^3:\eta^3\text{-C}_{10}\text{H}_{16})\text{Cl}_2(\text{hmt})]$ , although with a higher ratio of product to starting material than observed in earlier experiments. Various attempts to drive the reaction to completion without decomposition were unsuccessful and it was not possible to isolate the 1:1 adduct in analytically pure form to confirm its successful synthesis.

### 3.3 Conclusions

It has been shown that hexamethylenetetramine acts as a ligand for organometallic compounds of ruthenium and rhodium. The ligand can bind in a monodentate fashion, as in  $[\text{Ru}(\eta^6\text{-}p\text{-cymene})\text{Cl}_2(\text{hmt})]$  and  $[\text{Ru}(\eta^3:\eta^3\text{-C}_{10}\text{H}_{16})\text{Cl}(\text{hmt})]$ . Binuclear complexes have also been prepared with



hexamethylenetetramine acting as a bridging ligand to two metals as in  $[\{\text{Rh}(\eta^5\text{-C}_5\text{Me}_5)\text{Cl}\}_2(\mu\text{-hmt})]$  or with a chloride bridge and hexamethylenetetramine bound in a monodentate fashion, as in the cationic compound  $[(\eta^6\text{-C}_6\text{H}_6)\text{ClRu}(\mu\text{-Cl})_2\text{Ru}(\eta^6\text{-C}_6\text{H}_6)(\text{hmt})]\text{Cl}$ . Although attempts were made to prepare both  $[\text{M}(\pi\text{-ligand})(\text{hmt})\text{Cl}_2]$  and  $[\{\text{M}(\pi\text{-ligand})\text{Cl}\}_2(\mu\text{-hmt})]$  from each starting material only a single adduct was obtained in each particular case.

Due to the complexity of the dynamic processes operating in solution for this group of compounds, no detailed thermodynamic data could be extracted from the variable temperature NMR measurements. The search for a system amenable to such a study led to the work on the palladium complexes described in Chapter Four.

### 3.4 Experimental

#### 3.4.1 Starting materials

Ruthenium trichloride hydrate was obtained on loan from Johnson Matthey PLC and was purified by dissolution in water followed by boiling to dryness. The complexes  $[\{\text{Ru}(\eta^6\text{-}i\text{-p-cymene})\text{Cl}(\mu\text{-Cl})\}_2]$ ,  $[\{\text{Ru}(\eta^6\text{-C}_6\text{H}_6)\text{Cl}(\mu\text{-Cl})\}_2]$ ,  $[\{\text{Ru}(\eta^5\text{-C}_5\text{Me}_5)\text{Cl}(\mu\text{-Cl})\}_2]$  and  $[\{\text{Ru}(\eta^3\text{-}\eta^3\text{-C}_{10}\text{H}_{16})\text{Cl}\}_2(\mu\text{-Cl})_2]$  prepared using literature methods.<sup>86, 87, 126</sup>

#### 3.4.2 Crystallography

Crystallographic measurements were recorded with a Nonius Kappa CCD diffractometer equipped with graphite monochromated Mo K $\alpha$  radiation. Integration was carried out by the program DENZO-SMN.<sup>138</sup> Data were corrected for Lorentz and polarisation effects, and the effects of absorption, using the program SCALEPACK.<sup>138</sup> The data were corrected for Lorentz and polarisation effects and for absorption, based on additional azimuthal scan data.

Structures were solved using direct methods (SHELXS-86)<sup>139</sup> and developed using alternating cycles of least-squares refinement and difference Fourier synthesis (SHELXL-93).<sup>140</sup> All non-hydrogen atoms were refined anisotropically, whilst the hydrogen atoms were fixed in idealised positions and allowed to ride on the atom to which they were attached.

### 3.4.3 Synthesis of [Ru( $\eta^6$ -*p*-cymene)(hmt)Cl<sub>2</sub>]

[{Ru( $\eta^6$ -*p*-cymene)Cl( $\mu$ -Cl)}<sub>2</sub>] (70 mg, 0.11 mmol) was dissolved in dichloromethane (10 cm<sup>3</sup>). Hexamethylenetetramine (32 mg, 0.23 mmol, 2 eq.) was added to the orange solution with stirring. After 18 h at room temperature the solution was reduced *in vacuo* to approximately half volume and diethyl ether added. The solution was cooled for 36 h, after which time brown-red crystals were obtained. Yield 74 mg, 0.17 mmol, 73 %.

$\delta_{\text{H}}$  (400 MHz; CDCl<sub>3</sub>; 298 K) 1.29 (6H, d, *J* 6.9 Hz, isopropyl CH<sub>3</sub>), 2.26 (3H, s, CH<sub>3</sub>), 3.10 (1H, sept, *J* = 6.75 Hz, isopropyl CH), 4.56 (br, hmt), 4.70 (br, hmt), 4.99 (br, hmt) 5.27, 5.42 (4H, AB q, *J* = 5.7 Hz, *p*-cymene ring).

$\delta_{\text{H}}$  (400 MHz; CDCl<sub>3</sub>; 253 K) 1.27 (d, *J* = 6.8 Hz, isopropyl CH<sub>3</sub>), 2.26 (s, CH<sub>3</sub>), 2.29 (s, CH<sub>3</sub>), 3.10 (m, isopropyl CH), 4.53, 4.59 (AB q, *J* = 12.7 Hz, hmt), 4.70 (s, hmt), 4.79, 4.85 (AB q, *J* = 12.7 Hz, hmt), 4.98 (s, hmt), 5.23, 5.44 (4H, AB q, *J* = 5.7 Hz, *p*-cymene ring), 5.25, 5.47 (4H, AB q, *J* = 5.8 Hz, *p*-cymene ring).

Anal. Calc. for RuC<sub>16</sub>H<sub>26</sub>N<sub>4</sub>Cl<sub>2</sub>[0.25(CH<sub>2</sub>Cl<sub>2</sub>): C 41.74, H 5.73, N 11.98 %, found: C 41.56, H 5.78, N 11.98 % (Dichloromethane was observed in the crystal and is taken into account when calculating the microanalytical data.).

### 3.4.4 Synthesis of [( $\eta^6$ -C<sub>6</sub>H<sub>6</sub>)ClRu( $\mu$ -Cl)<sub>2</sub>Ru(hmt)( $\eta^6$ -C<sub>6</sub>H<sub>6</sub>)]Cl

[{Ru( $\eta^6$ -C<sub>6</sub>H<sub>6</sub>)Cl( $\mu$ -Cl)}<sub>2</sub>] (70 mg, 0.14 mmol) was suspended in dichloromethane (10 cm<sup>3</sup>). Hexamethylenetetramine (39 mg, 0.28 mmol) was added to the suspension with stirring at room temperature. After 2 h a yellow-green precipitate

was observed and isolated from the solution by filtration. Yield 81 mg, 0.21 mmol, 74 %.

$\delta_{\text{H}}$  (400 MHz;  $\text{CDCl}_3$ ; 298 K) 4.8-5.4 (12H, br, hmt), 5.74 (12H, s,  $\text{C}_6\text{H}_6$ ).

$\delta_{\text{H}}$  (400 MHz;  $\text{CDCl}_3$ ; 253 K) 4.90, 4.94 (6H, AB q,  $J$  7.2 Hz, hmt), 4.97 (6H, s, hmt), 5.74 (6H, s,  $\text{C}_6\text{H}_6$ ), 5.77 (6H, s,  $\text{C}_6\text{H}_6$ ).

Anal. Calc. for  $\text{Ru}_2\text{C}_{18}\text{H}_{24}\text{N}_4\text{Cl}_4$  : C 33.76, H 3.78, N 8.75 %, found: C 32.87, H 4.13, N 11.41 %.

### 3.4.5 Synthesis of $[\{\text{Rh}(\eta^5\text{-C}_5\text{Me}_5)\text{Cl}_2\}_2(\mu\text{-hmt})]$

$[\{\text{Ru}(\eta^5\text{-C}_5\text{Me}_5)\text{Cl}(\mu\text{-Cl})\}_2]$  (70 mg, 0.10 mmol) was dissolved in dichloromethane ( $5\text{ cm}^3$ ) and hexamethylenetetramine (29 mg, 0.20 mmol) was added to the solution. After stirring at room temperature for 2 h the solution was reduced *in vacuo* to ca.  $2\text{ cm}^3$  and diethyl ether was added. The solution was cooled overnight, after which a yellow precipitate formed and was isolated by filtration. Yield 38 mg, 0.05 mmol, 50 %.

$\delta_{\text{H}}$  (400 MHz;  $\text{CDCl}_3$ ; 298 K) 1.64 (30H, s,  $\text{C}_5\text{Me}_5$ ), 4.84 (12H, s, hmt).

Anal. Calc. for  $\text{Rh}_2\text{C}_{16}\text{H}_{27}\text{N}_4\text{Cl}_2$  C 41.18, H 5.58, N 7.39 %, found C 40.76, H 4.90, N 7.01 %.

### 3.4.6 Synthesis of $[\text{Ru}(\eta^3\text{:}\eta^3\text{-C}_{10}\text{H}_{16})\text{Cl}_2(\text{hmt})]$

$[\{\text{Ru}(\eta^3\text{:}\eta^3\text{-C}_{10}\text{H}_{16})\text{Cl}\}_2(\mu\text{-Cl})_2]$  (70 mg, 0.14 mmol) was stirred in pre-dried toluene ( $30\text{ cm}^3$ ), with hexamethylenetetramine (40 mg, 0.29 mmol) at reflux under nitrogen for 30 minutes. The solution was reduced to dryness *in vacuo* to produce a pink-brown solid. Repeated attempts to separate this product from the starting material were unsuccessful.

$\delta_{\text{H}}$  (400 MHz;  $\text{CDCl}_3$ ; 298 K) 2.27 (6H, s, allyl Me), 4.02 (s, allyl), 4.72 (s, hmt), 4.86 (s, allyl).

3.4.7 Crystallographic Data <sup>141</sup>**Table 3.8** Crystallographic data for  $[(\eta^6\text{-}p\text{-cymene})\text{RuCl}_2(\text{hmt})]\cdot\text{CH}_2\text{Cl}_2$ 

Empirical formula	$\text{C}_{17}\text{H}_{28}\text{Cl}_4\text{N}_4\text{Ru}$	
Formula weight	531.30	
Temperature	100(2) K	
Wavelength	0.71073 Å	
Crystal system	Monoclinic	
Space group	$P2_1/n$	
Unit cell dimensions	$a = 10.9547(13)$ Å	$\alpha = 90^\circ$ .
	$b = 12.5494(15)$ Å	$\beta = 90.848(7)^\circ$ .
	$c = 15.5566(14)$ Å	$\gamma = 90^\circ$ .
Volume	2138.4(4) Å <sup>3</sup>	
Z	4	
Density (calculated)	1.650 Mg m <sup>-3</sup>	
Absorption coefficient	1.243 mm <sup>-1</sup>	
F(000)	1080	
Crystal size	0.40 x 0.30 x 0.10 mm <sup>3</sup>	
Theta range for data collection	2.09 to 27.50 °.	
Index ranges	$-11 \leq h \leq 14$ , $-16 \leq k \leq 14$ , $-19 \leq l \leq 18$	
Reflections collected	12392	
Independent reflections	4859 [R(int) = 0.0578]	
Completeness to theta = 27.50°	98.9 %	
Absorption correction	Multi-scan	
Max. and min. transmission	0.8858 and 0.6363	
Refinement method	Full-matrix least-squares on F <sup>2</sup>	
Data / restraints / parameters	4859 / 0 / 239	
Goodness-of-fit on F <sup>2</sup>	1.029	
Final R indices [I > 2σ(I)]	R1 = 0.0531, wR2 = 0.1127	
R indices (all data)	R1 = 0.0831, wR2 = 0.1260	
Extinction coefficient	0.0010(5)	
Largest diff. peak and hole	2.513 and -1.359 e.Å <sup>-3</sup>	
	Near to ruthenium atom	

**Table 3.9** Atomic coordinates ( $\times 10^4$ ) and equivalent isotropic displacement parameters ( $\text{\AA} \times 10^3$ ) for  $[(\eta^6\text{-}p\text{-cymene})\text{RuCl}_2(\text{hmt})]\cdot\text{CH}_2\text{Cl}_2$

U(eq) is defined as one third of the trace of the orthogonalized  $U^{ij}$  tensor.

	x	y	z	U(eq)
Ru(1)	7153(1)	8350(1)	1861(1)	29(1)
Cl(1)	6541(1)	7248(1)	3067(1)	35(1)
Cl(2)	8338(1)	6869(1)	1332(1)	34(1)
N(1)	8830(3)	8776(3)	2619(2)	28(1)
N(2)	10428(3)	8187(3)	3658(2)	34(1)
N(3)	10935(4)	9447(3)	2534(3)	43(1)
N(4)	9667(4)	10007(3)	3712(3)	41(1)
C(1)	9343(4)	7872(4)	3168(3)	35(1)
C(2)	9843(4)	9136(4)	2049(3)	36(1)
C(3)	8573(4)	9687(4)	3226(3)	39(1)
C(4)	11357(4)	8548(4)	3053(3)	42(1)
C(5)	10111(4)	9086(4)	4211(3)	40(1)
C(6)	10612(5)	10315(4)	3113(3)	47(1)
C(7)	5463(4)	9292(4)	2048(3)	40(1)
C(8)	6420(4)	9977(4)	1806(3)	37(1)
C(9)	7122(5)	9792(4)	1059(3)	38(1)
C(10)	6865(4)	8905(4)	529(3)	40(1)
C(11)	5886(4)	8206(4)	785(3)	37(1)
C(12)	5224(4)	8396(4)	1521(3)	41(1)
C(13)	4767(5)	9503(5)	2863(3)	46(1)
C(14)	7522(5)	8669(4)	-294(3)	44(1)
C(15)	6799(5)	9219(5)	-1033(3)	54(1)
C(16)	8830(5)	9013(5)	-288(3)	49(1)
Cl(1S)	7811(2)	12454(1)	-643(1)	73(1)
Cl(2S)	8351(1)	14657(1)	-157(1)	50(1)
C(1S)	8880(5)	13329(4)	-158(4)	46(1)

**Table 3.10** Bond lengths [Å] and angles [°] for  $[(\eta^6\text{-}p\text{-cymene})\text{RuCl}_2(\text{hmt})]\cdot\text{CH}_2\text{Cl}_2$ 

Ru(1)-C(11)	2.165(4)	N(3)-C(6)	1.461(7)
Ru(1)-C(12)	2.172(5)	N(4)-C(6)	1.455(7)
Ru(1)-C(8)	2.196(4)	N(4)-C(3)	1.464(6)
Ru(1)-C(9)	2.198(4)	N(4)-C(5)	1.470(6)
Ru(1)-C(10)	2.204(5)	C(7)-C(8)	1.412(7)
Ru(1)-C(7)	2.220(5)	C(7)-C(12)	1.414(7)
Ru(1)-N(1)	2.234(3)	C(7)-C(13)	1.513(7)
Ru(1)-Cl(2)	2.4179(12)	C(8)-C(9)	1.421(7)
Ru(1)-Cl(1)	2.4339(12)	C(9)-C(10)	1.412(7)
N(1)-C(2)	1.501(5)	C(10)-C(11)	1.446(7)
N(1)-C(3)	1.511(6)	C(10)-C(14)	1.506(7)
N(1)-C(1)	1.522(6)	C(11)-C(12)	1.385(7)
N(2)-C(1)	1.457(6)	C(14)-C(16)	1.497(7)
N(2)-C(5)	1.464(6)	C(14)-C(15)	1.550(7)
N(2)-C(4)	1.468(6)	Cl(1S)-C(1S)	1.767(5)
N(3)-C(2)	1.459(6)	Cl(2S)-C(1S)	1.764(5)
N(3)-C(4)	1.459(6)		
<hr/>			
C(11)-Ru(1)-C(12)	37.26(18)	C(7)-Ru(1)-Cl(1)	87.80(13)
C(11)-Ru(1)-C(8)	79.48(17)	N(1)-Ru(1)-Cl(1)	87.84(9)
C(12)-Ru(1)-C(8)	67.17(18)	Cl(2)-Ru(1)-Cl(1)	88.92(4)
C(11)-Ru(1)-C(9)	68.02(17)	C(2)-N(1)-C(3)	106.7(3)
C(12)-Ru(1)-C(9)	80.41(18)	C(2)-N(1)-C(1)	106.6(3)
C(8)-Ru(1)-C(9)	37.73(18)	C(3)-N(1)-C(1)	106.5(3)
C(11)-Ru(1)-C(10)	38.63(18)	C(2)-N(1)-Ru(1)	111.7(2)
C(12)-Ru(1)-C(10)	68.78(18)	C(3)-N(1)-Ru(1)	110.6(3)
C(8)-Ru(1)-C(10)	67.81(18)	C(1)-N(1)-Ru(1)	114.3(3)
C(9)-Ru(1)-C(10)	37.42(18)	C(1)-N(2)-C(5)	108.5(4)
C(11)-Ru(1)-C(7)	67.63(18)	C(1)-N(2)-C(4)	108.4(4)
C(12)-Ru(1)-C(7)	37.54(18)	C(5)-N(2)-C(4)	108.1(4)
C(8)-Ru(1)-C(7)	37.29(18)	C(2)-N(3)-C(4)	109.3(4)
C(9)-Ru(1)-C(7)	68.25(18)	C(2)-N(3)-C(6)	108.3(4)

C(10)-Ru(1)-C(7)	81.20(18)	C(4)-N(3)-C(6)	108.3(4)
C(11)-Ru(1)-N(1)	160.19(16)	C(6)-N(4)-C(3)	109.1(4)
C(12)-Ru(1)-N(1)	155.77(17)	C(6)-N(4)-C(5)	108.3(4)
C(8)-Ru(1)-N(1)	95.46(15)	C(3)-N(4)-C(5)	108.6(4)
C(9)-Ru(1)-N(1)	96.22(15)	N(2)-C(1)-N(1)	112.5(4)
C(10)-Ru(1)-N(1)	121.74(16)	N(3)-C(2)-N(1)	112.5(3)
C(7)-Ru(1)-N(1)	118.95(16)	N(4)-C(3)-N(1)	111.8(4)
C(11)-Ru(1)-Cl(2)	90.82(13)	N(3)-C(4)-N(2)	112.1(4)
C(12)-Ru(1)-Cl(2)	117.58(14)	N(2)-C(5)-N(4)	112.1(4)
C(8)-Ru(1)-Cl(2)	154.08(13)	N(4)-C(6)-N(3)	112.2(4)
C(9)-Ru(1)-Cl(2)	116.36(13)	C(8)-C(7)-C(12)	117.5(4)
C(10)-Ru(1)-Cl(2)	89.60(13)	C(8)-C(7)-C(13)	120.2(5)
C(7)-Ru(1)-Cl(2)	155.11(14)	C(12)-C(7)-C(13)	122.2(5)
N(1)-Ru(1)-Cl(2)	85.55(9)	C(8)-C(7)-Ru(1)	70.4(3)
C(11)-Ru(1)-Cl(1)	111.59(13)	C(12)-C(7)-Ru(1)	69.4(3)
C(12)-Ru(1)-Cl(1)	85.65(14)	C(13)-C(7)-Ru(1)	129.4(3)
C(8)-Ru(1)-Cl(1)	116.99(13)	C(7)-C(8)-C(9)	122.1(4)
C(9)-Ru(1)-Cl(1)	154.59(14)	C(7)-C(8)-Ru(1)	72.3(3)
C(10)-Ru(1)-Cl(1)	150.16(13)	C(9)-C(8)-Ru(1)	71.2(3)
C(10)-C(9)-C(8)	120.1(4)	C(12)-C(11)-Ru(1)	71.6(3)
C(10)-C(9)-Ru(1)	71.5(3)	C(10)-C(11)-Ru(1)	72.1(3)
C(8)-C(9)-Ru(1)	71.1(3)	C(11)-C(12)-C(7)	121.3(5)
C(9)-C(10)-C(11)	117.3(4)	C(11)-C(12)-Ru(1)	71.1(3)
C(9)-C(10)-C(14)	123.9(5)	C(7)-C(12)-Ru(1)	73.1(3)
C(11)-C(10)-C(14)	118.7(4)	C(16)-C(14)-C(10)	114.1(4)
C(9)-C(10)-Ru(1)	71.0(3)	C(16)-C(14)-C(15)	110.7(4)
C(11)-C(10)-Ru(1)	69.2(3)	C(10)-C(14)-C(15)	107.3(4)
C(14)-C(10)-Ru(1)	132.3(3)	Cl(2S)-C(1S)-Cl(1S)	111.8(3)
C(12)-C(11)-C(10)	121.6(4)		

---

# **Chapter Four**

## **Palladium(II) complexes**

**with**

## **hexamethylenetetramine**

---



## 4.1 Introduction

This chapter describes the synthesis of palladium(II) complexes containing hexamethylenetetramine ligands. First, in section 4.2, the preparation and characterisation of coordination complexes of hexamethylenetetramine with palladium chloride,  $[\text{Pd}(\text{hmt})_2\text{Cl}_2]_n$ , are described. Secondly, section 4.3 describes the synthesis of allylpalladium complexes,  $[\{\eta^3\text{-C}_4\text{H}_7\}\text{PdCl}]_x(\text{hmt})$ , and a study of their solution behaviour and kinetics using  $^1\text{H}$  NMR spectroscopy. Finally, section 4.4 introduces a new caged nitrogen ligand and discusses its reactions with chloro( $\eta^3$ -allyl)palladium(II) – analogous to those described for hexamethylenetetramine in section 4.3.

## 4.2 Reactions of bis(benzonitrile)palladium(II)dichloride with hexamethylenetetramine

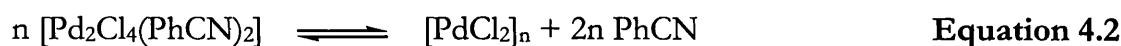
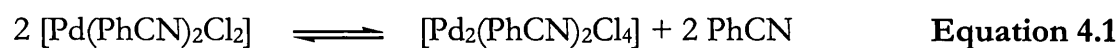
### 4.2.1 Background

Nitrogen containing ligands are often utilised in coordination chemistry and a large number of stable palladium complexes containing Pd-N bonds are known. In the majority of these complexes, the Pd-N bond is exclusively  $\sigma$  in character due to the absence of low lying *d*-orbitals on the nitrogen atom. This  $\sigma$ -character leads to the N-containing ligands being low in the *trans* influence and *trans* effect series. Hence, palladium complexes with nitrogen donor ligands, such as amines, are stable.

The most common palladium(II)-amine complexes have the general formula  $[\text{PdX}_2\text{L}_2]$ , where X = halide and L = amine. This type of complex is generally prepared from palladium(II)chloride, however since polymeric  $[\text{PdCl}_2]_n$  is insoluble in solvents that do not break the chloride bridge common routes to  $[\text{PdX}_2\text{L}_2]$  compounds involve addition of the amine to aqueous solutions of  $[\text{PdCl}_4]^{2-}$  or reaction of the amine with  $[\text{PdCl}_2]_n$  in organic solvents. Although the resulting complexes may exist in either the *cis* or *trans* form, the *cis* isomer is

thermodynamically more stable and is the preferred isomer in more polar solvents because of its higher dipole moment.<sup>142</sup> Isomerisation between the two forms has been observed in solution.<sup>143</sup>

A convenient form of soluble PdCl<sub>2</sub> is the complex *bis*(benzonitrile)palladium(II)dichloride in which the benzonitrile ligands are highly labile. In fact, PdCl<sub>2</sub> been known to crystallise from solutions of *bis*(benzonitrile)palladium(II)dichloride.<sup>144</sup> This phenomenon is attributed to the equilibria that exist in solution, **Equation 4.1** and **Equation 4.2**.<sup>145</sup>

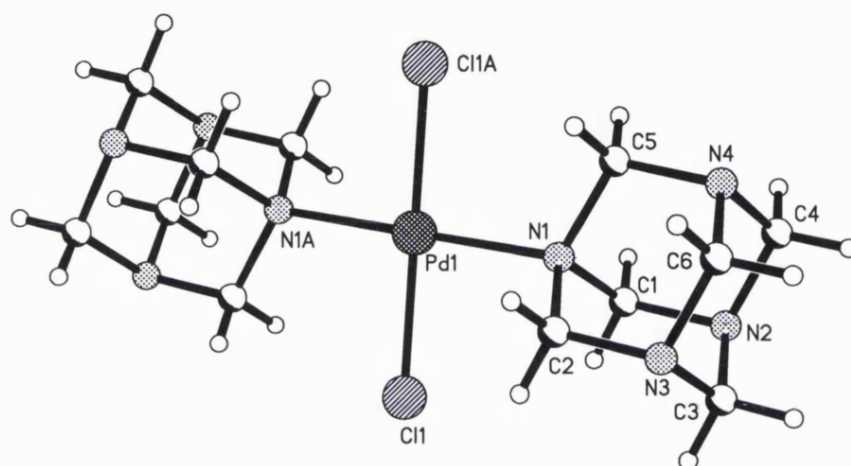


Unlike [PdCl<sub>2</sub>]<sub>n</sub> the benzonitrile complex is readily soluble in benzene, toluene and polar organic solvents, making it all the more suitable as a precursor to palladium amine complexes. The complex has been shown to exist in the *trans* configuration,<sup>146</sup> however the products formed *via* benzonitrile substitution are entirely dependent on the identity of the substituting ligand.

#### 4.2.2 Reactions of *bis*(benzonitrile)palladium(II)dichloride with hexamethylenetetramine

*Bis*(benzonitrile)palladium(II)dichloride was prepared<sup>147</sup> by heating palladium chloride in an excess of benzonitrile at 100 °C for four hours. After cooling the solution the solid yellow product was collected by filtration and washed with petroleum ether. Upon addition of two equivalents of hexamethylenetetramine to a dichloromethane solution of [Pd(PhCN)<sub>2</sub>Cl<sub>2</sub>] a pale yellow product precipitated immediately. The <sup>1</sup>H NMR spectrum for this compound in CDCl<sub>3</sub> exhibits two signals, an AB quartet at 4.46 ppm and a singlet at 5.03 ppm, which are of equal integral. This spectrum was obtained at room temperature and no dynamic process is observed. No signals are observed in the benzonitrile region of the spectrum, indicating substitution of all benzonitrile ligands as expected. Due to

the particularly insoluble nature of the product crystals were grown *via* diffusion of a solution of *bis*(benzonitrile)palladium(II)dichloride into a solution of hexamethylenetetramine in a sealed tube. The single crystal X-ray structure obtained from these yellow crystals is shown in **Figure 4.1**.



(44)

**Figure 4.1** Solid state structure of *trans*-[Pd(hmt)<sub>2</sub>Cl<sub>2</sub>] as determined by single crystal X-ray diffraction

**Table 4.1** Selected bond lengths [Å] and angles[°] for *trans*-[Pd(hmt)<sub>2</sub>Cl<sub>2</sub>]

Pd(1)-N(1)	2.122(4)	N(1A)-Pd(1)-N(1)	180.0
Pd(1)-Cl(1)	2.2980(14)	N(1A)-Pd(1)-Cl(1)	91.80(11)
N(1)-C(1)	1.501(6)	N(1)-Pd(1)-Cl(1)	88.20(10)
N(1)-C(2)	1.505(6)	Cl(1)-Pd(1)-Cl(1A)	180.0
N(1)-C(5)	1.522(7)	C(1)-N(1)-C(2)	108.4(4)
		C(1)-N(1)-C(5)	106.6(4)
		C(2)-N(1)-C(5)	106.3(4)

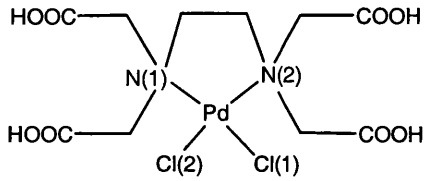
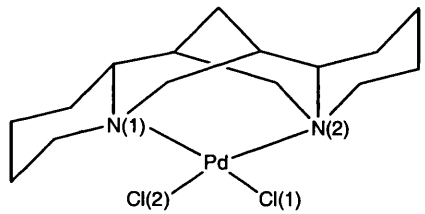
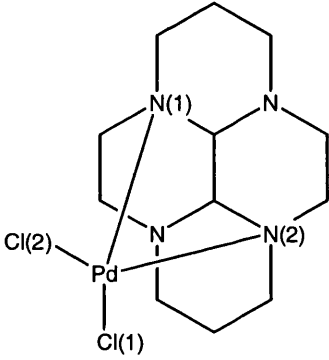
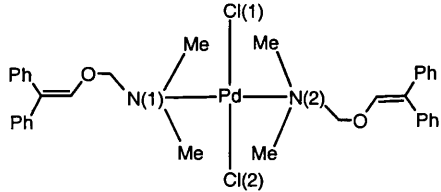
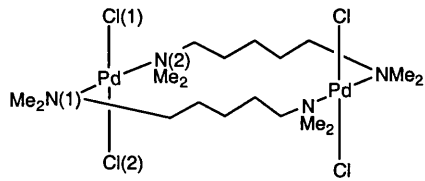
The complex crystallises with half of the molecule in the asymmetric unit, the other half of the molecule is generated by inversion through a centre of symmetry.

Due to the inversion centre, the ligating atoms all lie in a common least squares plane with the palladium ion. The geometry about palladium is almost perfectly square planar and the ligands adopt a *trans* configuration. The angles between *cis* ligands are Cl(1)-Pd(1)-N(1A) 91.80(11) ° and N(1)-Pd(1)-Cl(1) 88.20(10) °. The Pd(1)-N(1) bond length, 2.122(4) Å is comparable to the Pd-N bond lengths found in typical examples of [PdCl<sub>2</sub>(NR<sub>3</sub>)<sub>2</sub>] compounds as illustrated in **Table 4.2**.

The Pd(1)-Cl(1) bond length, 2.2980(14) Å, is significantly longer than that of 2.2857(8) Å for the Pd-Cl bond in *bis*(benzonitrile)palladium(II)dichloride<sup>148</sup> and falls just below the lower end of the range shown in **Table 4.2**.

Coordination to palladium lengthens the N(1)-C bond of hexamethylenetetramine with N(1)-C(1), N(1)-C(2) and N(1)-C(5), being 1.501(6) – 1.522(7) Å, and longer than the corresponding bonds between carbon and the non-metallated nitrogen atoms, which lie in the range 1.450(8) – 1.475(8) Å. Free hexamethylenetetramine exhibits a N-C bond length of 1.462(5) Å. The N-C-N angles of hexamethylenetetramine fall in the range 111.6(4) to 112.3(4) °, which are comparable with those in non-complexed hexamethylenetetramine, 112.4(3) °. Upon coordination the atoms around N(1) are slightly distorted from the tetrahedral geometry found in non-complexed hexamethylenetetramine (where C-N-C is 108.0(3) °) with bond angles ranging from 106.3(4) ° for C(2)-N(1)-C(5) to 108.4(4) ° for C(1)-N(1)-C(2). This effect was also observed for [(η<sup>6</sup>-*p*-cymene)RuCl<sub>2</sub>(hmt)], as described in Chapter Three.

**Table 4.2** Selected bond lengths [Å] for a range of dichloropalladium complexes with tertiary amine ligands

Complex	ref.	Pd-N(1)	Pd-N(2)	Pd-Cl(1)	Pd-Cl(2)
<i>trans</i> -[Pd(hmt) <sub>2</sub> Cl <sub>2</sub> ]	–	2.122	2.122	2.2980	2.2980
	149	2.087	2.087	2.299	2.299
	150	2.100	2.150	2.323	2.308
	151	2.114	2.099	2.300	2.312
	152	2.125	2.125	2.309	2.309
	153	2.142	2.135	2.315	2.308

Addition of only one equivalent of hexamethylenetetramine to a dichloromethane solution of  $[\text{Pd}(\text{C}_6\text{H}_5\text{CN})_2\text{Cl}_2]$  at room temperature also gave a yellow precipitate, predicted to be the polymeric compound  $[\text{Pd}(\text{hmt})_2\text{Cl}_2]_n$ . Due to the extremely insoluble nature of this product it was not possible to obtain NMR data on this compound. Dissolution was attempted in  $\text{CDCl}_3$ ,  $\text{CD}_3\text{NO}_2$ ,  $\text{CD}_2\text{Cl}_2$  and  $(\text{CD}_3)_2\text{C}=\text{O}$  without success. The use of a diffusion technique to grow crystals of this product was also unsuccessful, producing only  $[\text{Pd}(\text{hmt})_2\text{Cl}_2]$ . Mass spectrometry did not yield any useful information, all peaks observed were attributable to hexamethylenetetramine. Microanalytical data (see section 4.6.3) did indicate that a polymer with the empirical formula  $\text{PdC}_6\text{H}_{12}\text{N}_4\text{Cl}_2$  is formed. The most likely structure for this compound is the chain polymer **Figure 4.2**. However, ring structures of the types illustrated in **Figure 4.3** are also possible.

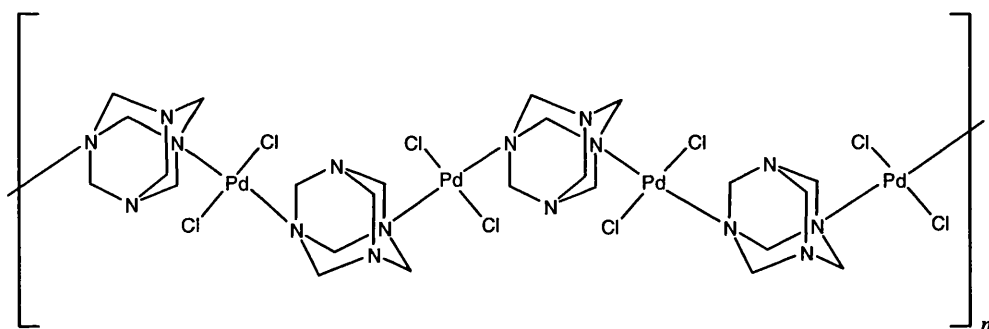


**Figure 4.2** Possible chain polymer  $[\text{PdCl}_2\text{hmt}]_n$

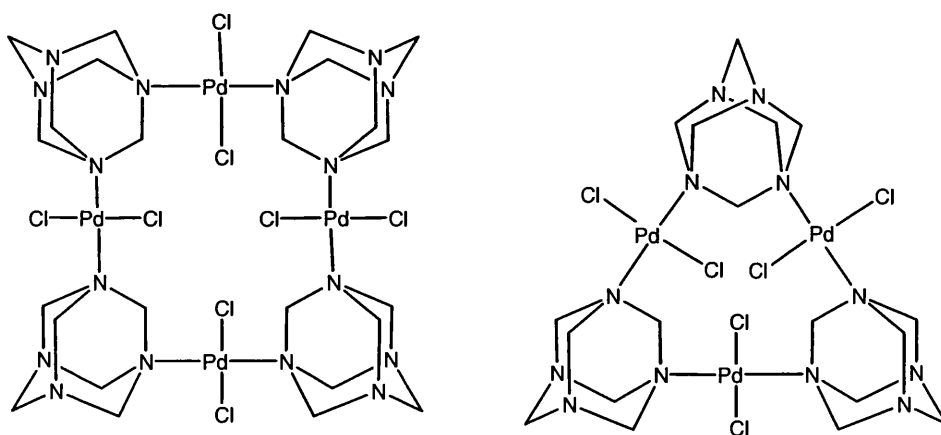
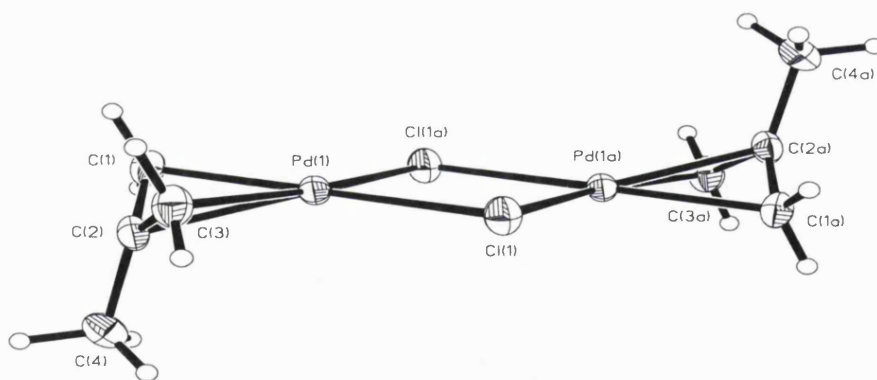


**Figure 4.3** Possible ring-type structures of  $[\text{PdCl}_2\text{hmt}]_n$

### 4.3 Complexes of chloro(2-methyl- $\eta^3$ -allyl)palladium(II) with hexamethylenetetramine

#### 4.3.1 Background

The compound chloro( $\eta^3$ -allyl)palladium(II) (**45**) provides a good starting point for an introduction to  $\eta^3$ -allyl complexes of palladium. Single crystal X-ray structure studies of this complex<sup>154</sup> have demonstrated that the allyl group is bonded to the metal in an  $\eta^3$ -fashion and is approximately symmetrically bound. The allyl moiety occupies two *cis* coordination sites on the metal, the remaining coordination sites are occupied by the bridging chloride ions. Calculations based on this X-ray data suggested that the *anti* protons are significantly closer to palladium than the *syn* protons and thus are more shielded by the palladium.<sup>154</sup> This information is frequently used when assigning the <sup>1</sup>H NMR spectra of  $\eta^3$ -allylpalladium compounds. In non-coordinating solvents, as in the solid-state, the  $\eta^3$ -allyl ligand is a bidentate ligand and the geometry about each palladium is square planar.

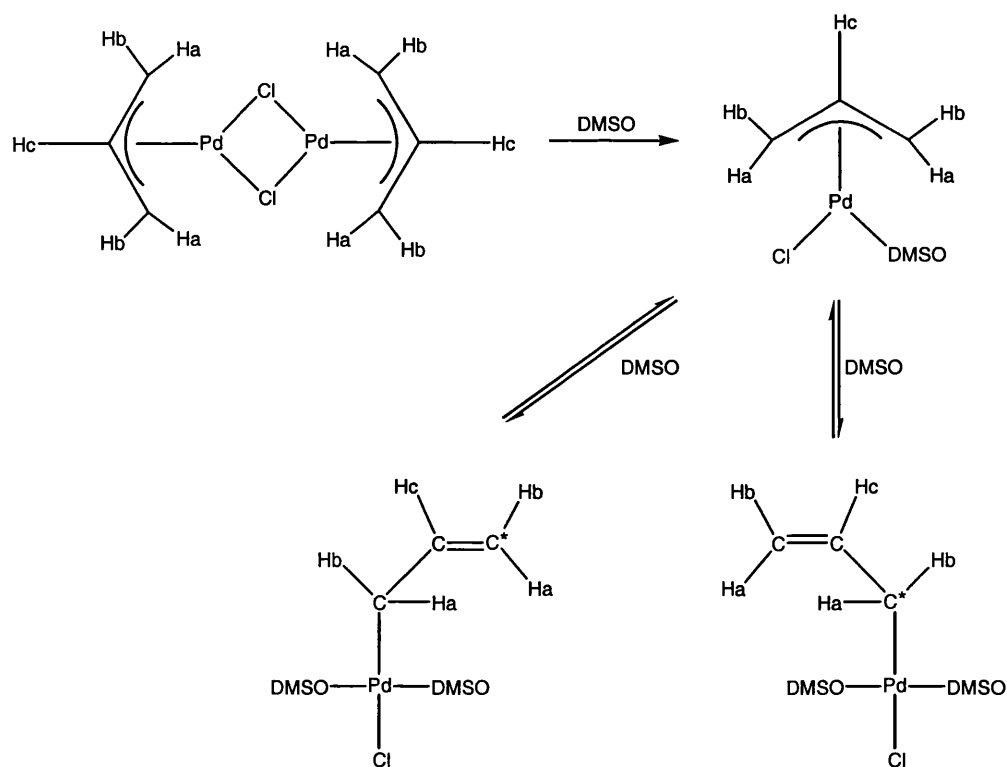


(45)

The reactions of allylpalladium complexes are numerous<sup>155</sup> and include allyl-metal bond cleavage and insertion reactions into the allyl-metal bond. In the current research, use has been made of the ease with which the chloride bridges of the complex are cleaved to give a vacant coordination site on the metal. Such bridge cleavage reactions leave the palladium to  $\pi$ -allyl bond intact, although in strongly

complexing solvents cleavage of the chloride bridge followed by complexation of solvent enables observation of the  $\eta^1/\sigma$  bonding mode for the allyl ligand.<sup>156</sup>

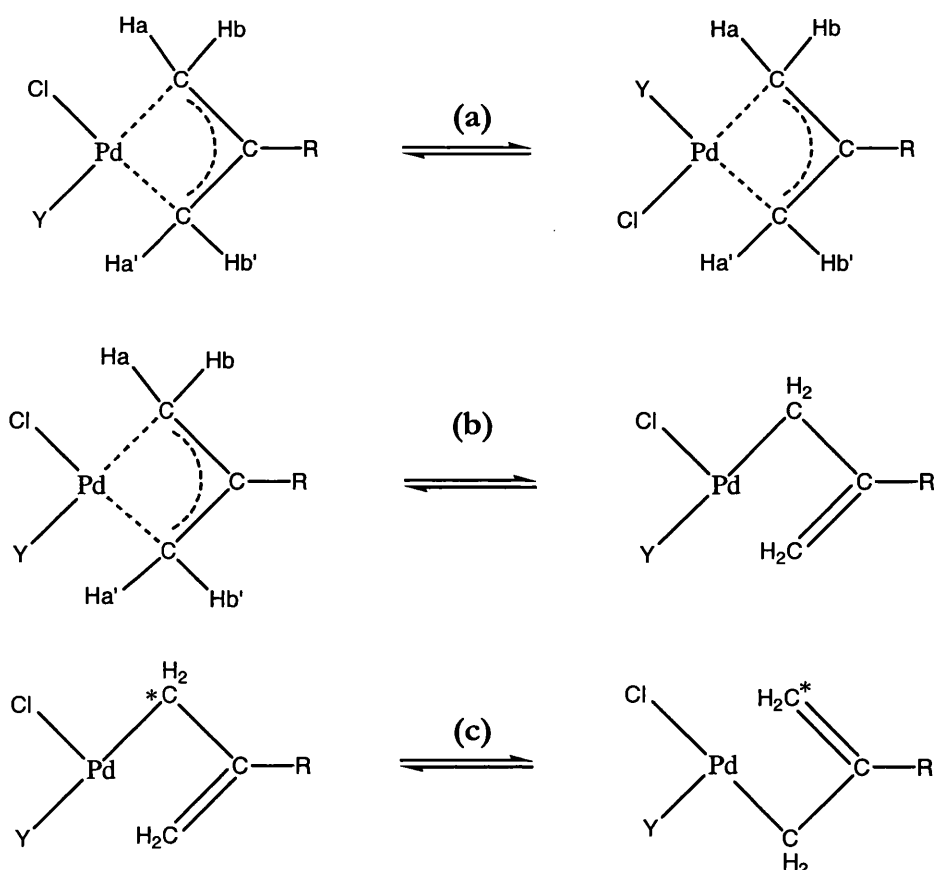
Simple investigations have been carried out to observe interconversion of  $\eta^1$  and  $\eta^3$  modes of allyl bonding in solution. Dissolution in dimethylsulfoxide (DMSO) cleaves the chloride bridge of chloro( $\eta^3$ -allyl)palladium(II) and a DMSO molecule occupies the resulting vacant coordination site, maintaining the square planar geometry around palladium.<sup>157</sup> A reversible process follows where the allyl converts from  $\pi$  to  $\sigma$ -bonding mode, allowing a second molecule of DMSO to complex with palladium. Loss of either DMSO ligand enables the allyl to become  $\pi$  bound again. This process, illustrated in **Scheme 4.1**, is easily followed by  $^1\text{H}$  NMR spectroscopy. In the  $\pi$ -bound allyl the rigidity of the ligand gives rise to three types of nonequivalent hydrogen atoms,  $\text{H}_a$  (*anti* to  $\text{H}_c$ ),  $\text{H}_b$  (*syn* to  $\text{H}_c$ ) and  $\text{H}_c$ . The  $\sigma$  mode of bonding, however, allows free rotation about the C-C bond, which is followed by a rapid equilibrium that renders  $\text{H}_a$  and  $\text{H}_b$  equivalent; as a consequence only two signals are observed in the  $^1\text{H}$  NMR spectrum.



**Scheme 4.1** Reaction of chloro( $\eta^3$ -allyl)palladium(II) in DMSO



Initial investigations of the  $\pi$ - $\sigma$  exchange<sup>158</sup> postulated that the equilibrium process (at 30 °C) was a head-over-tail mechanism of the  $\sigma$ -bound allyl group (**Scheme 4.2**), rendering the *syn* and *anti* protons equivalent. Later research investigating the NMR spectra of a number of chloro(allyl)palladium(II) complexes at lower temperatures led to the suggestion that three fluxional processes were occurring, namely the head-over-tail equilibrium,  $\pi$  to  $\sigma$  equilibrium and ligand exchange, illustrated in **Scheme 4.2**. This conclusion was based on two arguments. First, the low temperature spectra clearly show that the overall process is more complex than just a head-over-tail equilibrium, one possibility is that a  $\pi$  to  $\sigma$  equilibrium occurs first and then the head-over-tail process follows. Secondly, the low temperature spectrum of the 1:1 adduct of DMSO and chloro( $\eta^3$ -allyl)palladium(II) shows that the protons *cis* and *trans* to the DMSO ligand are equivalent, which is unexpected. These observations suggest another equilibration process is taking place, such as exchange of the chloride and DMSO ligands. This deduction is reinforced by the sensitivity of the system to the concentration of DMSO, as illustrated by the fact that coalescence occurs at lower temperatures in pure DMSO solutions, than it does in CDCl<sub>3</sub> solutions containing one mole equivalent of DMSO. This observation is taken to confirm the occurrence of a ligand exchange process.



**Scheme 4.2** Suggested fluxional processes occurring in solution : (a) ligand exchange (b)  $\pi$  to  $\sigma$  equilibrium (c) head-over-tail equilibrium

In order to study the dynamic processes in more detail, the NMR spectra of the triphenylarsine and triphenylphosphine adducts of chloro(allyl)palladium(II) were recorded at a variety of temperatures.<sup>159</sup> The spectra obtained from variable temperature <sup>1</sup>H NMR studies of the triphenylphosphine adduct are shown in **Figure 4.4**. The lowest temperature spectrum exhibits five resonances. The assignments (**Figure 4.4**) were made on the basis that *trans* couplings  $J_{P-H_b}$  or  $J_{P-H_a}$  are expected to be larger than the *cis* couplings  $J_{P-H_b'}$  or  $J_{P-H_a'}$ .<sup>160</sup> The spectrum obtained at  $-30$  °C corresponds to a 'static' structure where no exchange process is occurring. As the temperature is increased the resonances of the terminal allylic protons  $H_b$  and  $H_b'$ , along with  $H_a$  and  $H_a'$ , broaden, then coalesce. At  $90$  °C only two signals are observed for the terminal protons, because the *cis* and *trans* protons of the allyl group have become equivalent due to the exchange of the chloride and phosphine ligands. The next change observed in the NMR spectrum occurs at

140 °C, where the two broad, terminal allyl singlets coalesce into one sharp doublet. This is attributed to  $\pi$  to  $\sigma$  equilibration, (possibly followed by a head-over-tail process) which results in the equivalence of the *syn* and *anti* protons.

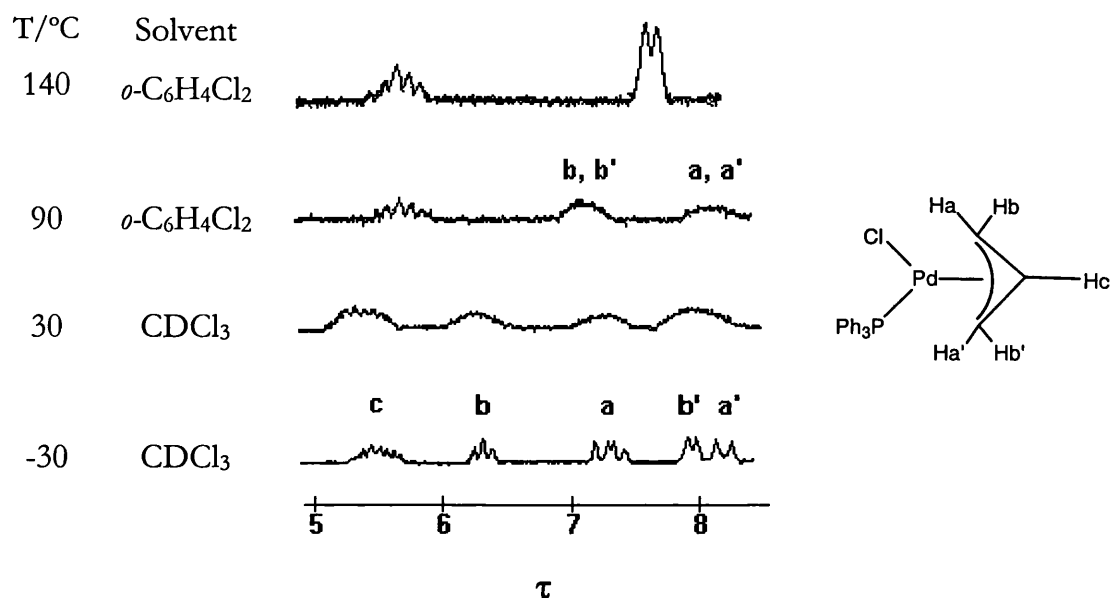


**Figure 4.4** Temperature dependence of NMR spectra of  $\text{PPh}_3$  adduct of chloro(allyl)palladium(II)<sup>159</sup>

Many complexes of the chloro(allyl)palladium(II) moiety have been synthesised with N-donor ligands, ranging from the relatively simple chloro( $\eta^3$ -allyl)palladium(2-amino-4-methylpyridine) to the more complex cation shown in **Figure 4.5**.

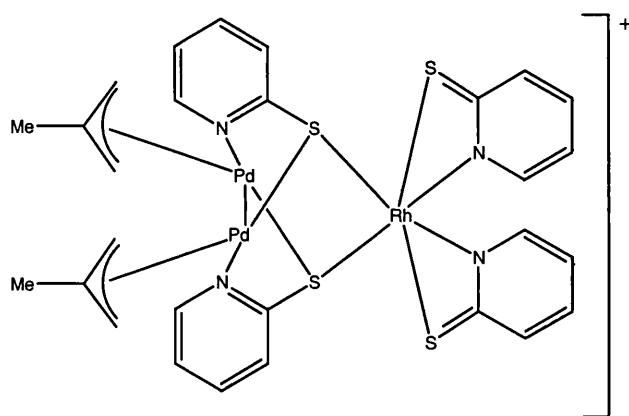


**Figure 4.5** Multinuclear species containing two allylpalladium units<sup>161</sup>

The dynamic behaviour of a number of such compounds in solution has also been investigated. For example, it has been shown that the *syn* proton pair and *anti* proton pair of chloro(allyl)palladium(II)(2-picoline) complexes, which are equivalent on the NMR timescale at room temperature, are resolved into four distinct signals at low temperatures.<sup>162</sup> The explanation for this observation was suggested as loss of amine from the palladium centre, formation of the chloro(allyl)palladium(II) dimer, and then reformation of the chloro(allyl)palladium(II)(2-picoline) complex.<sup>162, 163</sup> The overall effect of this process is ligand exchange, as illustrated in **Scheme 4.2a**. Work in this field has continued to develop and a wide range of chloro(allyl)palladium(II) complexes with N-donor ligands are known and have been studied using both solid state and solution methods.<sup>164</sup>

### 4.3.2 Synthesis of hexamethylenetetramine derivatives of chloro(2-methyl- $\eta^3$ -allyl)palladium(II)

The compound  $[\text{Pd}_2\text{Cl}_2(\eta^3\text{-C}_4\text{H}_7)_2]$  was synthesised as described in the literature,<sup>165</sup> by bubbling CO through a mixture of 2-methylallyl chloride and sodium chloropalladate in methanol/water. Dissolution of  $[\text{Pd}_2\text{Cl}_2(\eta^3\text{-C}_4\text{H}_7)_2]$  in dichloromethane followed by the addition of two equivalents of hexamethylenetetramine gave a yellow product which precipitated out of solution upon addition of diethyl ether. The <sup>1</sup>H NMR spectrum of this compound,

**Figure 4.6**, exhibits a broad signal at 4.80 ppm attributed to palladium complexed hexamethylenetetramine. This signal integrates against the three resonances of the allylic protons in a 12:7 ratio, indicating the product to be the 1:1 adduct  $[\text{PdCl}(\eta^3\text{-C}_4\text{H}_7)(\text{hmt})]$ . The observation of a broad singlet for the protons of the hexamethylenetetramine ligand suggests a dynamic exchange process is occurring at 298 K which renders all protons of the hexamethylenetetramine ligand equivalent. In order to confirm this a variable temperature NMR experiment was performed – recording  $^1\text{H}$  NMR data for the complex over the range 223 to 333 K. At 223 K exchange is slow and the hexamethylenetetramine resonance is resolved into two distinct signals, a singlet,  $\delta$  4.97 ppm and an AB quartet,  $\delta$  4.58, 4.66 ppm **Figure 4.7**. These coupling patterns are as expected for hexamethylenetetramine bound to a metal through one nitrogen only, as discussed in Chapter Three for  $[\text{Ru}(\eta^6\text{-}p\text{-cymene})(\text{hmt})\text{Cl}_2]$ .

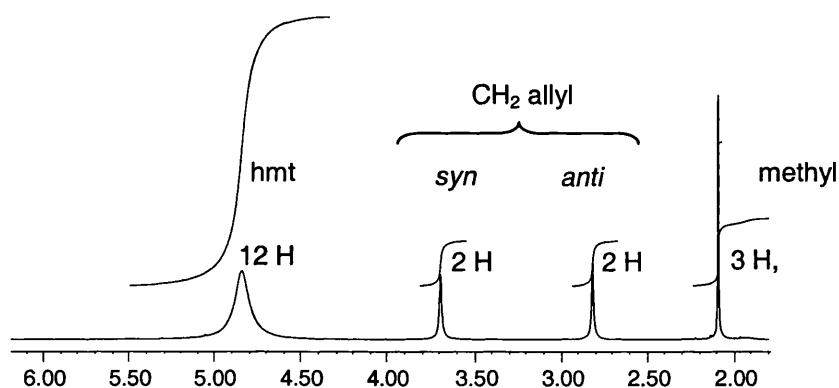


**Figure 4.6**  $^1\text{H}$  NMR of  $[\text{PdCl}(\eta^3\text{-C}_4\text{H}_7)(\text{hmt})]$  at 298 K,  $\text{CDCl}_3$  solvent

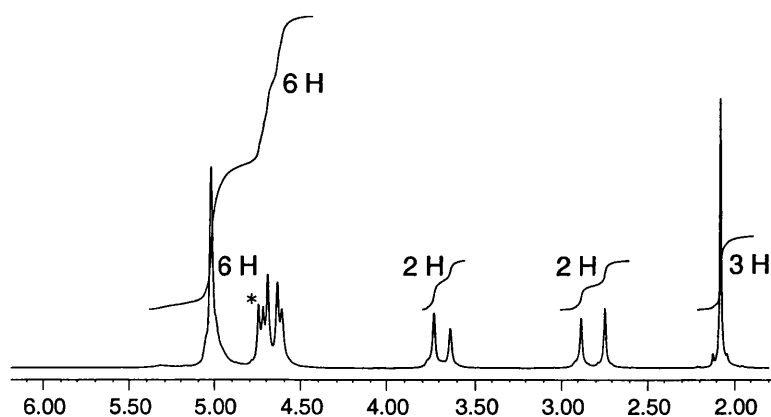
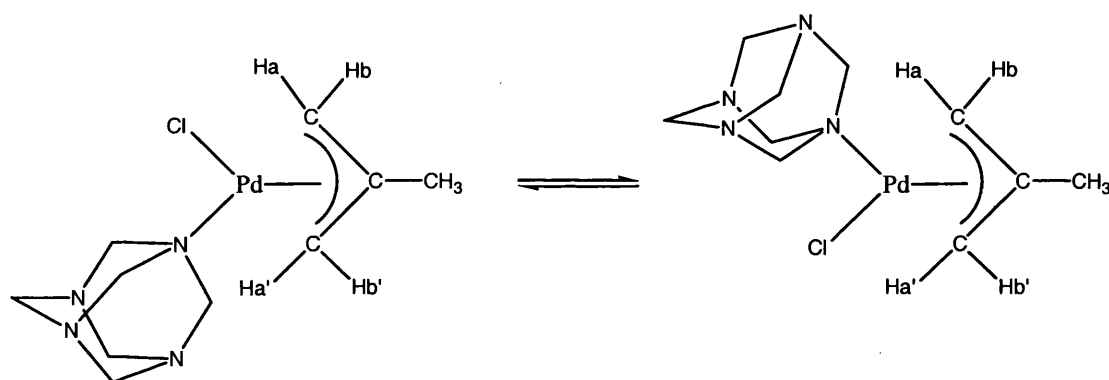


**Figure 4.7**  $^1\text{H}$  NMR of  $[\text{PdCl}(\eta^3\text{-C}_4\text{H}_7)(\text{hmt})]$  at 223 K,  $\text{CDCl}_3$  solvent,  
\* uncomplexed hexamethylenetetramine

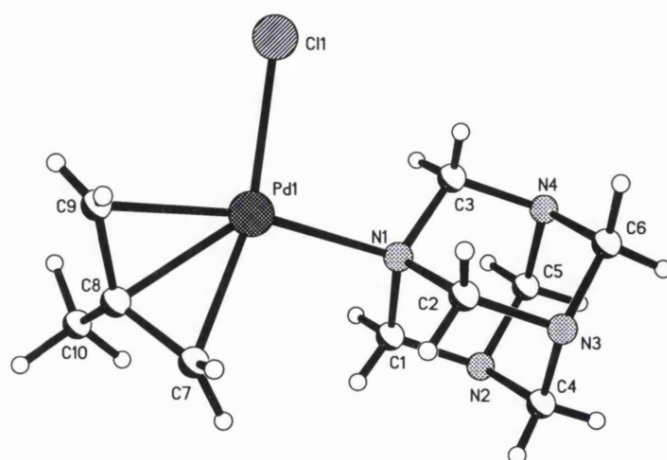
The  $^1\text{H}$  NMR chemical shifts of the allyl moiety are also temperature dependent; the *syn* and *anti* protons of the  $\text{CH}_2$  groups on the allyl are observed as two resonances at room temperature, but resolve into four singlets at lower temperatures. The equivalence of the *anti* proton pair and the *syn* proton pair at 298 K may be explained as a consequence of the ligand exchange process, as illustrated in **Scheme 4.3**. Fast exchange of hexamethylenetetramine at room temperature renders the *syn* proton pair equivalent and the *anti* proton pair equivalent. In the static structure observed at low temperatures separate resonances are observed for the protons *trans* to hexamethylenetetramine and the protons *cis* to hexamethylenetetramine.



**Scheme 4.3** Equilibrium process rendering  $\text{H}_a$  and  $\text{H}_{a'}$  equivalent and  $\text{H}_b$  and  $\text{H}_{b'}$  equivalent

Section 4.3.3 discusses the calculation of kinetic and thermodynamic data related to the observed equilibrium processes determined using data from the variable temperature NMR experiments.

Cooling of a dichloromethane/diethyl ether solution of the product gave yellow crystals suitable for single crystal X-ray diffraction studies. The solid state structure of the product determined from these studies is shown in **Figure 4.8**.



(46)

Figure 4.8 Solid state structure of  $[\text{PdCl}(\eta^3\text{-C}_4\text{H}_7)(\text{hmt})]$ Table 4.3 Selected bond lengths [Å] and angles[°] for  $[\text{PdCl}(\eta^3\text{-C}_4\text{H}_7)(\text{hmt})]$ 

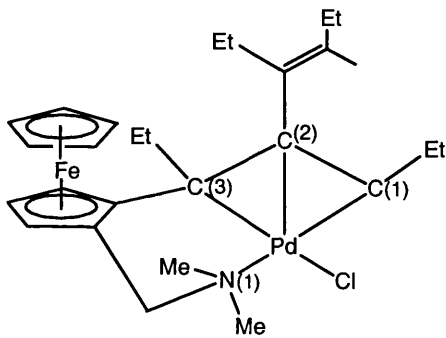
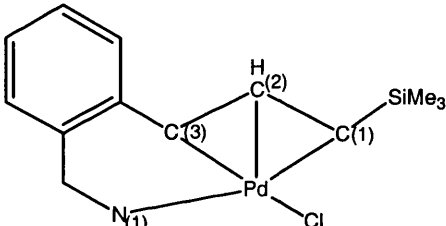
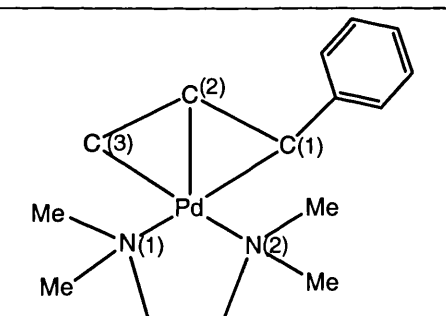
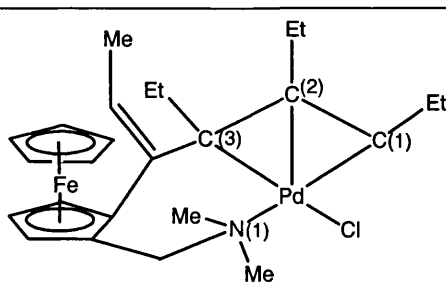
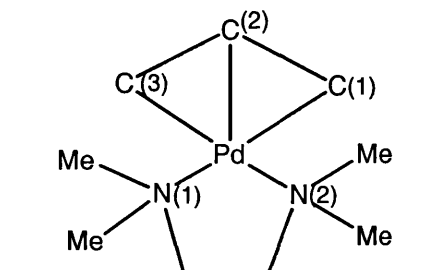
Pd(1)-N(1)	2.159(4)	N(1)-Pd(1)-Cl(1)	96.97(10)
Pd(1)-Cl(1)	2.3856(10)	C(2)-N(1)-C(3)	107.8(3)
Pd(1)-C(7)	2.141(5)	C(2)-N(1)-C(1)	107.1(3)
Pd(1)-C(8)	2.136(4)	C(3)-N(1)-C(1)	106.1(3)
Pd(1)-C(9)	2.100(5)	C(7)-Pd(1)-N(1)	98.78(17)
N(1)-C(1)	1.513(5)	C(9)-Pd(1)-Cl(1)	95.75(14)
N(1)-C(2)	1.495(5)		
N(1)-C(3)	1.506(6)		

If it is assumed that the  $\eta^3$ -allyl ligand occupies two coordination sites on palladium, then the geometry around the metal may be considered to be heavily distorted square planar. The geometry of the allyl ligand restricts the angle C(7)-Pd(1)-C(9) to 68.4(2)°, a phenomenon often observed in metal complexes with an  $\eta^3$ -allyl group.<sup>166</sup> As a consequence the Cl(1)-Pd(1)-N(1) angle opens out to 96.9(1)°. The maximum deviation from the mean plane Cl(1)-N(1)-C(7)-C(9) is 0.09 Å (C(7)). In Table 4.4 selected bond lengths for a range of allylpalladium

complexes containing nitrogen donor ligands are given. The Pd(1)-N(1) bond length in [PdCl( $\eta^3$ -C<sub>4</sub>H<sub>7</sub>)(hmt)], 2.159(4) Å, falls within the range shown in **Table 4.4**. The Pd(1)-C(7) bond which is *trans* to Cl(1), 2.141(5) Å, is longer than Pd(1)-C(9) which is *trans* to N(1), 2.100(5) Å. This is consistent with the *trans* influence of the two different donors. The Pd(1)-Cl(1) bond length, 2.3856(10) Å, lies just above the range of Pd-Cl bond lengths presented in **Table 4.4** and is significantly different from that in [Pd(hmt)<sub>2</sub>Cl<sub>2</sub>] 2.2980(14) Å. The Pd(1)-Cl(1) bond length is shorter than that in the dimeric precursor, 2.401(3) Å.<sup>167</sup> As observed in [Pd(hmt)<sub>2</sub>Cl<sub>2</sub>], distortion of the angles around N(1) occurs upon metal-complexation of hexamethylenetetramine, with the C-N(1)-C angle ranging from 106.1(3) to 107.8(3)°, compared with the C-N-C angle in free hexamethylenetetramine, 108.0(3)°.



**Table 4.4** Selected bond lengths [Å] for a range of  $\eta^3$ -allylpalladium complexes, H atoms on allyl ligand omitted for clarity.

Complex	ref.	Pd-N(1)	Pd-Cl	Pd-C(1)	Pd-C(2)	Pd-C(3)
[PdCl( $\eta^3$ -C <sub>4</sub> H <sub>7</sub> )(hmt)]	–	2.159(4)	2.3856(10)	2.100(5)	2.136(4)	2.141(5)
	168	2.16(1)	2.369(3)	2.13(1)	2.09(1)	2.11(1)
	169	2.171(4)	2.372(1)	2.183(5)	2.114(4)	2.086(4)
	170	2.146(3)	2.138(3)	2.173(3)	2.125(4)	2.124(5)
	168	2.166(5)	2.384(2)	2.155(5)	2.118(6)	2.122(6)
	171	2.16(2)	2.15(1)	2.15(2)	2.06(3)	2.15(3)

The synthesis of the 1:2 adduct, with a hexamethylenetetramine molecule bridging two palladium allyl moieties, was achieved by addition of one mole equivalent of hexamethylenetetramine to a solution of  $[\text{Pd}_2\text{Cl}_2(\eta^3\text{-C}_4\text{H}_7)_2]$  in dichloromethane at room temperature. The product was precipitated from solution by addition of diethyl ether. Integration of the  $^1\text{H}$  NMR spectrum of the yellow compound indicates it to be the 1:2 adduct, as shown in **Figure 4.9**. As was the case for the 1:1 adduct, only a broad signal was observed for the hexamethylenetetramine protons in the  $^1\text{H}$  NMR spectrum at room temperature. In the low temperature spectrum there are three signals for the hexamethylenetetramine moiety, with relative intensities 2:8:2, which are assigned as illustrated in **Figure 4.10** and **Figure 4.11**.

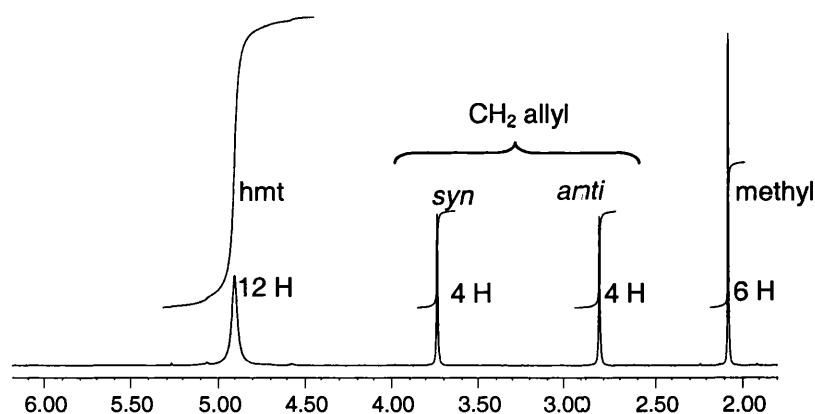


**Figure 4.9**  $^1\text{H}$  NMR of  $[\text{Pd}_2\text{Cl}_2(\eta^3\text{-C}_4\text{H}_7)_2(\mu\text{-hmt})]$  at 298 K,  $\text{CDCl}_3$  solvent

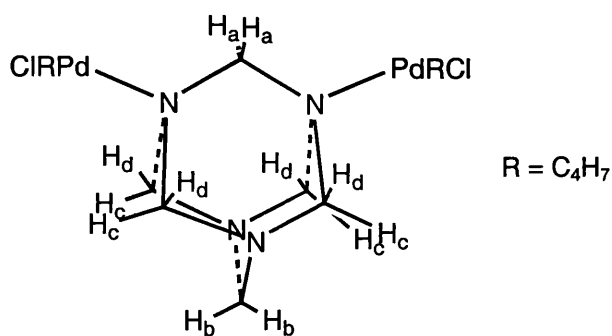


**Figure 4.10** Expected  $^1\text{H}$  NMR signals for hexamethylenetetramine in  $[\text{Pd}_2\text{Cl}_2(\eta^3\text{-C}_4\text{H}_7)_2(\mu\text{-hmt})]$ :  $\text{H}_a$  (s, 2H);  $\text{H}_c, \text{H}_d$  (AB q, 8H);  $\text{H}_b$  (s, 2H)

Although the AB quartet is not well resolved integration of the spectrum is unequivocal in confirming the structure. Microanalytical data confirm the formulation  $\text{Pd}_2\text{C}_{14}\text{H}_{26}\text{N}_4\text{Cl}_2$ , and the observation of a  $\nu(\text{Pd-Cl})$  band at  $275\text{ cm}^{-1}$  confirms that the chlorides remain terminal.

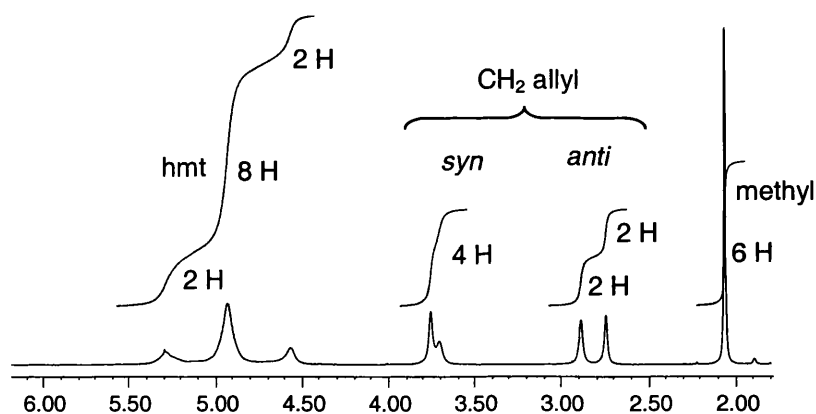
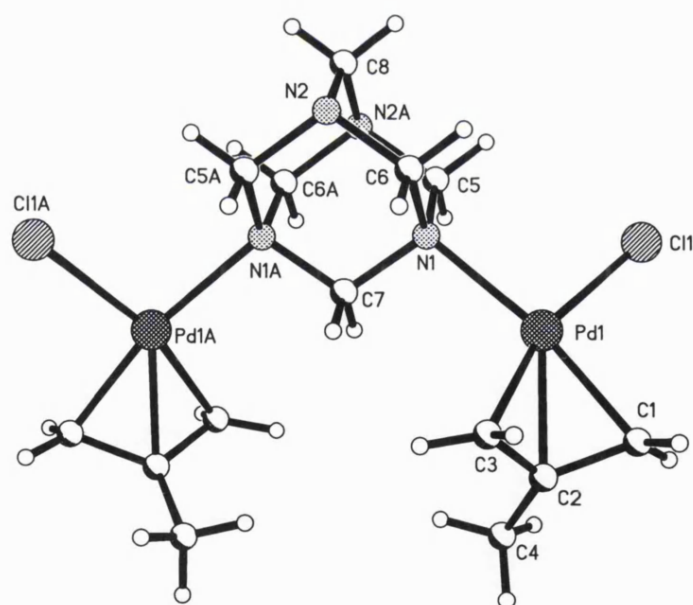


**Figure 4.11**  $^1\text{H}$  NMR of  $[\text{Pd}_2\text{Cl}_2(\eta^3\text{-C}_4\text{H}_7)_2(\mu\text{-hmt})]$  at 298 K,  $\text{CDCl}_3$  solvent

Single crystals of  $[\text{Pd}_2\text{Cl}_2(\eta^3\text{-C}_4\text{H}_7)_2(\mu\text{-hmt})]$  were grown by cooling a dichloromethane/diethyl ether solution to  $0\text{ }^\circ\text{C}$ . The solid state structure of the complex was obtained by X-ray diffraction, **Figure 4.12**.

The compound crystallises in the space group  $C2/c$ , with a  $C2$  axis intersecting the atoms  $\text{C}(8)$  and  $\text{C}(7)$ . The geometry of the allyl ligand restricts the  $\text{C}(1)\text{-Pd}(1)\text{-C}(3)$  angle to  $67.5(2)^\circ$ , consequently the  $\text{Cl}(1)\text{-Pd}(1)\text{-N}(1)$  angle opens

out to  $95.41(8)^\circ$ . Thus, as for  $[\text{PdCl}(\eta^3\text{-C}_4\text{H}_7)(\text{hmt})]$ , the geometry around each palladium atom may be considered as heavily distorted square planar. The maximum deviation from the mean plane of the atoms Pd(1)Cl(1)N(1)C(1),C(3) is  $0.11 \text{ \AA}$  (C(3)). The distance Pd(1)-Pd(1A) is  $5.86 \text{ \AA}$  consistent with no intermetallic bond. The Pd(1)-Cl(1) bond length,  $2.3767(12) \text{ \AA}$ , falls within the range of Pd-Cl bond lengths presented in **Table 4.4** and is very similar to that in  $[\text{PdCl}(\eta^3\text{-C}_4\text{H}_7)(\text{hmt})]$ ,  $2.3856(10) \text{ \AA}$ . The Pd(1)-C(3) bond that is *trans* to Cl(1),  $2.142(5) \text{ \AA}$ , is longer than Pd(1)-C(1) which is *trans* to N(1),  $2.099(4) \text{ \AA}$ , consistent with the *trans* influence of the two different donors. Once more, distortion of the angles around the metallated nitrogen atom is observed, with C-N(1)-C ranging from  $107.3(3)$  to  $107.8(2)^\circ$ . This distortion is less marked than that observed in  $[\text{PdCl}(\eta^3\text{-C}_4\text{H}_7)(\text{hmt})]$  or  $[\text{PdCl}_2(\text{hmt})_2]$ , however.



(47)

Figure 4.12 Solid state structure of  $[\text{Pd}_2\text{Cl}_2(\eta^3\text{-C}_4\text{H}_7)_2(\mu\text{-hmt})]$

**Table 4.5** Selected bond lengths [Å] and angles[°] for [Pd<sub>2</sub>Cl<sub>2</sub>(η<sup>3</sup>-C<sub>4</sub>H<sub>7</sub>)<sub>2</sub>(μ-hmt)]

Pd(1)-C(1)	2.099(4)	N(1)-Pd(1)-Cl(1)	95.41(8)
Pd(1)-C(2)	2.140(4)	C(3)-Pd(1)-N(1)	101.0(2)
Pd(1)-C(3)	2.142(5)	C(1)-Pd(1)-Cl(1)	96.31(14)
Pd(1)-N(1)	2.189(3)	C(7)-N(1)-C(5)	107.8(2)
Pd(1)-Cl(1)	2.3767(12)	C(7)-N(1)-C(6)	107.5(2)
N(1)-C(7)	1.494(4)	C(5)-N(1)-C(6)	107.3(3)
N(1)-C(5)	1.494(5)		
N(1)-C(6)	1.496(4)		

Attempts to generate the 1:4 adduct *via* reaction of two equivalents of [Pd<sub>2</sub>Cl<sub>2</sub>(η<sup>3</sup>-C<sub>4</sub>H<sub>7</sub>)<sub>2</sub>] with one equivalent of hexamethylenetetramine were only partially successful. A yellow precipitate was isolated from the reaction mixture in the same way as described above. Integration of the <sup>1</sup>H NMR spectrum recorded at room temperature suggested the product was the 1:3 adduct. Further <sup>1</sup>H NMR investigations at low temperature indicated a mixture of three products, however. The absence of well-resolved peaks in the hexamethylenetetramine region of the NMR spectrum, even at temperatures as low as 188 K, hindered the conclusive characterisation of these compounds. Nevertheless, it is tentatively suggested that the product mixture contained the 1:4 adduct as well as both the 1:1 and 1:2 adducts. Attempted separation of the products by fractional crystallisation was unsuccessful.

### 4.3.3 Variable temperature <sup>1</sup>H NMR studies of hexamethylenetetramine derivatives of chloro(2-methyl-η<sup>3</sup>-allyl)palladium(II)

#### 4.3.3.1 Introduction

Variable temperature <sup>1</sup>H NMR studies of exchange equilibria are often used to obtain kinetic data for a reaction and to deduce a value for the activation energy

for the exchange process. The NMR data is used to determine a rate constant for the exchange process at each temperature, these values are then used to plot a graph of  $\ln k$  against  $1/T$ , the Arrhenius plot. If the reaction has a rate constant that follows the Arrhenius equation (**Equation 4.3**) then a straight line should be observed. The gradient of the line equals  $-E_a / R$  and the intercept at  $1/T = 0$  is  $\ln A$ .

$$\ln k = \ln A - (E_a / RT) \quad \text{Equation 4.3}$$

$A$  = pre exponential factor,  $E_a$  = activation energy,  $R$  = universal gas constant

To enable determination of  $\Delta H^\ddagger$ ,  $\Delta S^\ddagger$  and  $\Delta G^\ddagger$  from the kinetic data, **Equation 4.4** (the Eyring equation) and **Equation 4.5** are used to give **Equation 4.6**. Thus, a plot of  $\ln(k/T)$  against  $1/T$  should give a straight line of gradient  $-\Delta H^\ddagger/R$  and an intercept at  $1/T = 0$  of  $(\Delta S^\ddagger/R) + \ln(\kappa/h)$ .

$$k = (\kappa T/h) \cdot \exp(-\Delta G^\ddagger / RT) \quad \text{Equation 4.4}$$

$\kappa$  = Boltzmann constant,  $h$  = Planck's constant

$$\Delta G^\ddagger = \Delta H^\ddagger - T\Delta S^\ddagger \quad \text{Equation 4.5}$$

$$\ln(k/T) = -(\Delta H^\ddagger/R)(1/T) + (\Delta S^\ddagger/R) + \ln(\kappa/h) \quad \text{Equation 4.6}$$

In order to determine rate data from the variable temperature NMR studies carried out here the computer program gNMR 4.1<sup>172</sup> was used. This is a program for the simulation of one-dimensional NMR spectra and the fitting of calculated and observed spectra using line-shape analysis. The initial approach involved the use of the hexamethylenetetramine portion of the  $^1\text{H}$  NMR spectra to calculate the rate constants at each temperature. Due to limitations of the computer program, however, this method could not be used for the 1:1 adduct  $\text{PdCl}(\eta^3\text{-C}_4\text{H}_7)(\text{hmt})$ , because the low symmetry of the molecule gives rise to more unique protons than the program gNMR can deal with. Thus, this

discussion begins with the consideration of the solution dynamics observed for the 1:2 adduct  $[\text{Pd}_2\text{Cl}_2(\eta^3\text{-C}_4\text{H}_7)_2(\mu\text{-hmt})]$ .

#### 4.3.3.2 Analysis of variable temperature $^1\text{H}$ NMR spectra for $[\text{Pd}_2\text{Cl}_2(\eta^3\text{-C}_4\text{H}_7)_2(\mu\text{-hmt})]$

A series of NMR spectra obtained for  $[\text{Pd}_2\text{Cl}_2(\eta^3\text{-C}_4\text{H}_7)_2(\mu\text{-hmt})]$  are shown in **Figure 4.13**. The spectra indicate a dynamic process which affects both the allyl and hexamethylenetetramine protons of the complex. At 298 K two distinct signals are observed for the *syn* and *anti* protons of the complex, but the protons *cis* and *trans* to the hexamethylenetetramine ligand remain indistinguishable. At 223 K however, the *cis* and *trans* protons have become inequivalent, thus a total of four signals are observed. The twelve protons of the hexamethylenetetramine ligand appear equivalent at 298 K, and resolve into three separate signals with a relative integral of 2:8:2 at 223 K. These changes were discussed in detail in section 4.3.2.

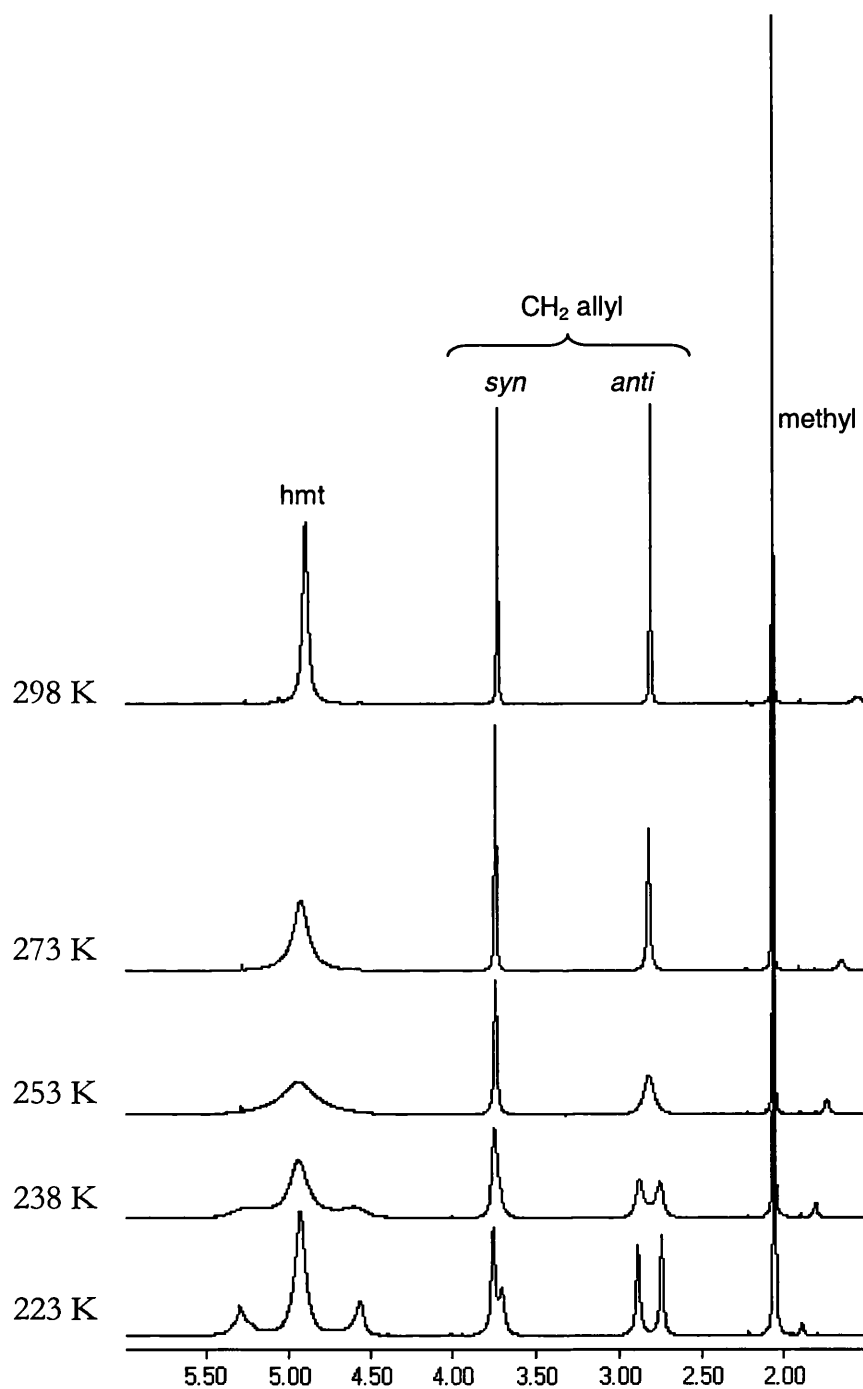
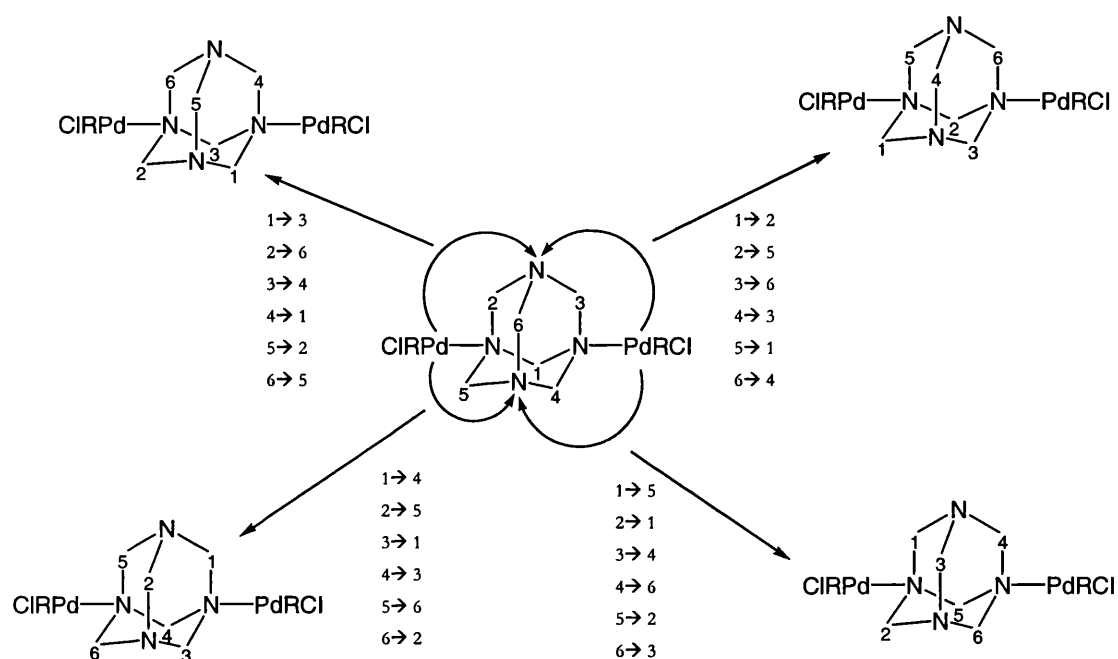


Figure 4.13  $^1\text{H}$  NMR spectra for  $[\text{Pd}_2\text{Cl}_2(\eta^3\text{-C}_4\text{H}_7)_2(\mu\text{-hmt})]$ , 223 – 298 K

Based upon these variable temperature spectra, a mechanism for the process occurring in solution was proposed. The *syn* and *anti* allyl protons remain distinct at all observed temperatures (up to 333 K), therefore in any mechanism the allyl ligand must remain  $\pi$ -bound. As both the hexamethylenetetramine protons, and the allyl protons *cis* and *trans* to hexamethylenetetramine, are equivalent at 298 K a



ligand exchange process is proposed. It is suggested that a Pd-N bond is broken and then reformed, or with equal probability, a new Pd-N bond is formed. This is illustrated in **Scheme 4.4**, where the process is simplified by treating the problem as if the two palladium allyl moieties are migrating around the hexamethylenetetramine to vacant nitrogen sites. The analysis is further simplified by considering the 12 protons of hexamethylenetetramine to be grouped as six pairs.



**Scheme 4.4** Proposed mechanism leading to equivalence of all 12 protons on hexamethylenetetramine ligand in solution at 298 K

In **Scheme 4.4** each methylene unit is identified by a number (1-6). These numbers were used when describing the exchange of each pair of protons. Using this mechanism four 'exchange permutations' were obtained, one for each exchange being considered. The program gNMR was used to confirm the proposed mechanism by following the change in appearance of the spectrum as the rate of exchange was increased from zero (static structure), in arbitrary steps. A close match was observed between the lineshapes for calculated and experimental spectra.

Line-shape analysis was then used to obtain an accurate fit between the calculated and experimental spectra. The variable temperature spectra were simulated using gNMR. Varying the rate constant for the exchange gave an excellent fit between the calculated and experimental spectra, **Figure 4.14**.

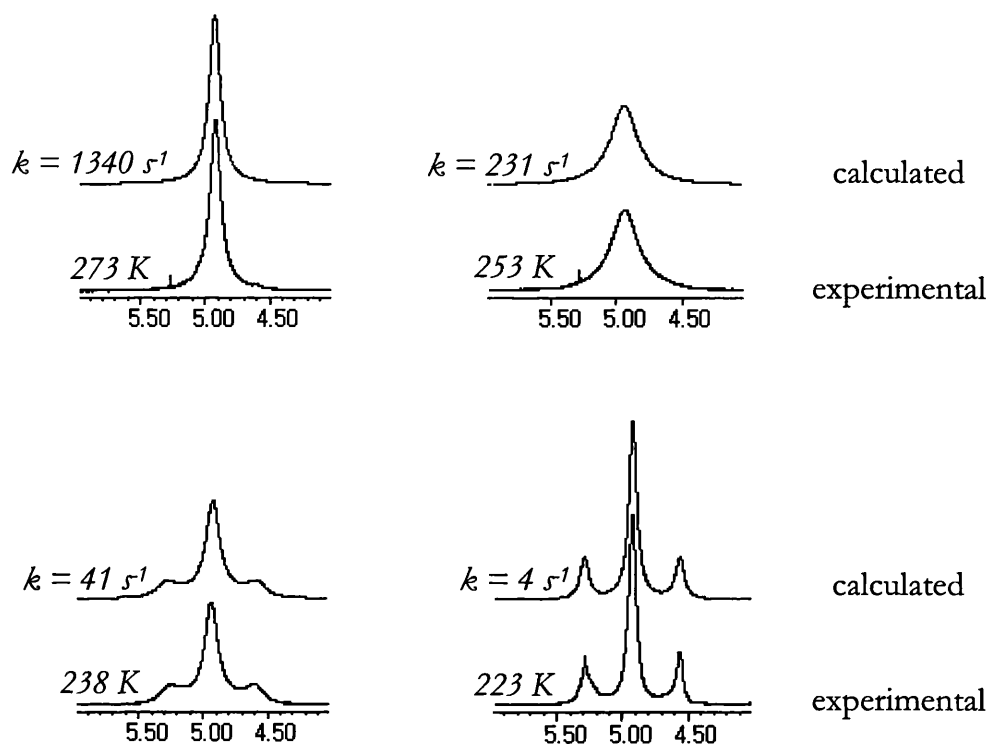


**Figure 4.14** Fit of experimental spectra for  $[\text{Pd}_2\text{Cl}_2(\eta^3\text{-C}_4\text{H}_7)_2(\mu\text{-hmt})]$  over a range of temperatures

The activation energy of the pseudo-first order process was calculated from an Arrhenius plot of the kinetic data, **Figure 4.15**. The plot has a gradient of  $-7062$  which gives a value of  $59 \text{ kJ mol}^{-1}$  for the  $E_a$  of the exchange process.

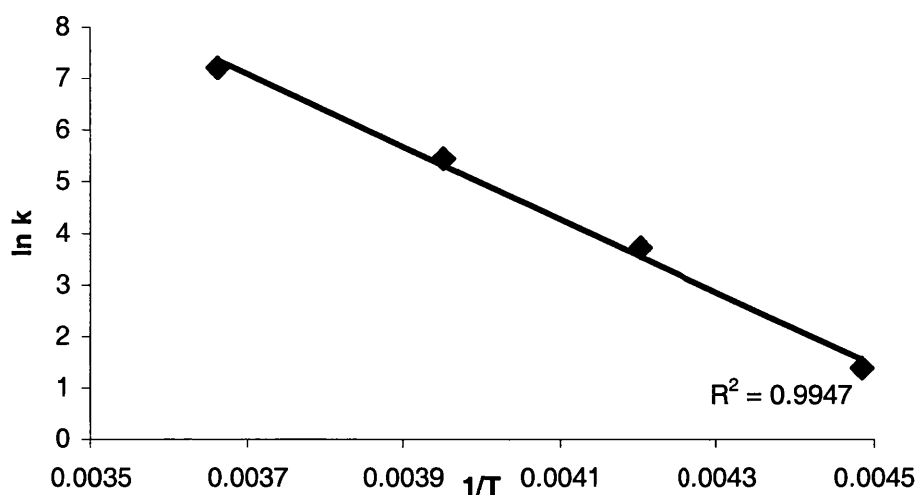


**Figure 4.15** Arrhenius plot of  $\ln k$  against  $1/T$  for  $[\text{Pd}_2\text{Cl}_2(\eta^3\text{-C}_4\text{H}_7)_2(\mu\text{-hmt})]$

An Eyring plot using the same kinetic data, gave a straight line ( $R^2 = 0.9941$ ) with a gradient of  $-6815.8$ . Thus giving  $\Delta H^\ddagger = 57 \text{ kJ mol}^{-1}$ . Using **Equation 4.7**  $\Delta H^\ddagger(298 \text{ K})$  is calculated as  $59 \text{ kJ mol}^{-1}$ , a value consistent with the value of  $E_a$  determined from the Arrhenius plot. The value of  $\Delta S^\ddagger$  determined using the Eyring plot is  $25 \text{ J mol}^{-1} \text{ K}^{-1}$ , a small positive value consistent with the proposed dissociative mechanism.

$$E_a = \Delta H^\ddagger + RT \quad \text{Equation 4.7}$$

$R$  = universal gas constant,  $8.315 \text{ J K}^{-1} \text{ mol}^{-1}$

Since the appearance of the  $^1\text{H}$  NMR spectrum of the allyl moiety is also temperature dependent the program gNMR was also used to calculate a rate constant for the 'exchange' of the allyl protons, (*i.e.* from *cis* to *trans* with respect to hexamethylenetetramine) using full lineshape analysis. A value for the activation energy was then calculated using an Arrhenius plot (a line with  $R^2$  of  $0.9974$  and a gradient of  $-7114$ ). The energy barrier determined from this plot is  $59 \text{ kJ mol}^{-1}$ , in agreement with the  $59 \text{ kJ mol}^{-1}$  calculated using data from the hexamethylenetetramine part of the NMR spectrum.

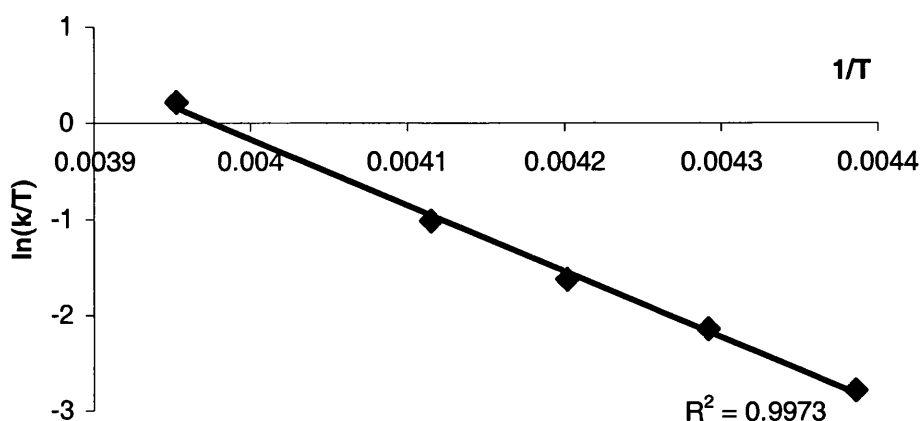


**Figure 4.16** Eyring plot of  $\ln(k/T)$  against  $1/T$  for  $[\text{Pd}_2\text{Cl}_2(\eta^3\text{-C}_4\text{H}_7)_2(\mu\text{-hmt})]$

An Eyring plot using the data calculated for the allyl exchange in  $[\text{Pd}_2\text{Cl}_2(\eta^3\text{-C}_4\text{H}_7)_2(\mu\text{-hmt})]$  gave a straight line with a gradient of  $-6873.8$ , **Figure 4.16**. Thus the value for  $\Delta H^\ddagger$  (298 K) determined from this plot is  $60 \text{ kJ mol}^{-1}$ , in agreement with the  $E_a$  calculated using the Arrhenius plot. The value of  $\Delta S^\ddagger$  determined using the Eyring plot is  $30 \text{ J mol}^{-1} \text{ K}^{-1}$ , a small positive value, again consistent with the proposed dissociative mechanism.

#### 4.3.3.3 Analysis of variable temperature $^1\text{H}$ NMR spectra for $[\text{PdCl}(\eta^3\text{-C}_4\text{H}_7)(\text{C}_6\text{H}_{12}\text{N}_4)]$

As discussed in section 4.3.2, both the allyl and hexamethylenetetramine regions of the  $^1\text{H}$  NMR spectra of the 1:1 adduct  $[\text{PdCl}(\eta^3\text{-C}_4\text{H}_7)(\text{hmt})]$  exhibit fluxional behaviour. As stated previously, lineshape analysis of the hexamethylenetetramine part of the  $^1\text{H}$  NMR spectra was not possible for  $[\text{PdCl}(\eta^3\text{-C}_4\text{H}_7)(\text{hmt})]$ , due to the limitations of the computer program gNMR. However, as described in section 4.3.3.2, calculations using the hexamethylenetetramine and allyl parts of the  $^1\text{H}$  NMR spectrum for  $[\text{Pd}_2\text{Cl}_2(\eta^3\text{-C}_4\text{H}_7)_2(\mu\text{-hmt})]$  were in good agreement. Using

this precedent, the rate constants for the *cis/trans* exchange of the allyl protons were calculated using the allyl component of the  $^1\text{H}$  NMR spectra, then these values were then used to obtain an  $E_a$  for the hexamethylenetetramine exchange process. The variable temperature  $^1\text{H}$  NMR spectra obtained for  $[\text{PdCl}(\eta^3\text{-C}_4\text{H}_7)(\text{hmt})]$  are shown in **Figure 4.17**.

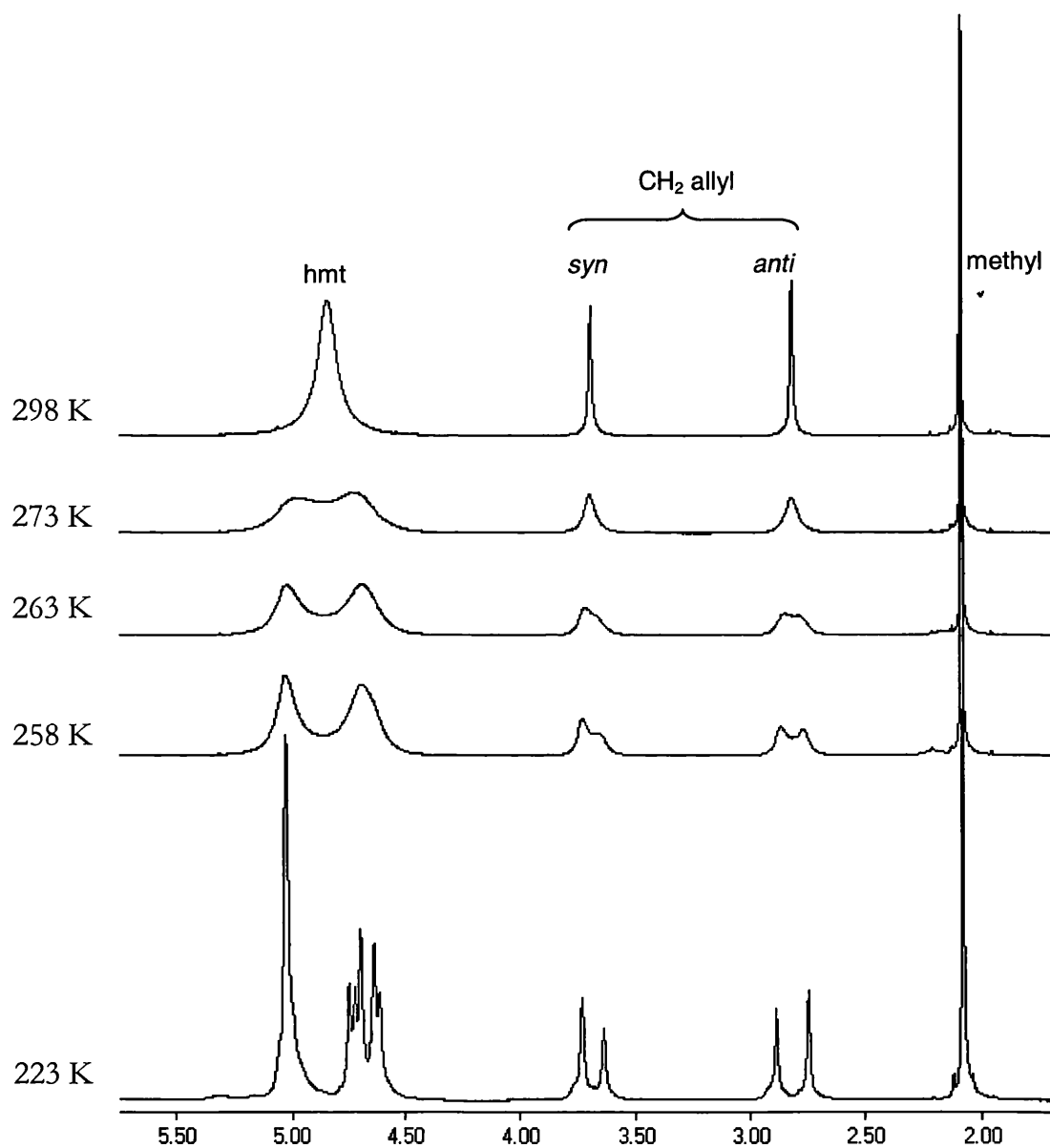


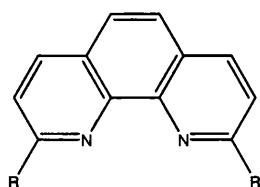
**Figure 4.17**  $^1\text{H}$  NMR spectra for  $[\text{PdCl}(\eta^3\text{-C}_4\text{H}_7)(\text{hmt})]$ , 223 – 298 K

The best fit straight line of an Arrhenius plot using rate data determined from the  $^1\text{H}$  NMR signals due to the allyl moiety of  $[\text{PdCl}(\eta^3\text{-C}_4\text{H}_7)(\text{hmt})]$  has a gradient of  $-6426$ . The  $E_a$  for hexamethylenetetramine exchange determined using this plot

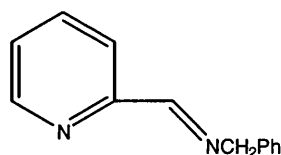
is  $53 \text{ kJ mol}^{-1}$ . An Eyring plot also gave a straight line ( $R^2 = 0.9984$ ), with a gradient of  $-6182.6$ . The Eyring plot gives a value for  $\Delta H^\ddagger$  (298 K) of  $54 \text{ kJ mol}^{-1}$  and a value of  $-6 \text{ J mol}^{-1} \text{ K}^{-1}$  for  $\Delta S^\ddagger$ .

#### 4.3.3.4 Conclusions from analysis of variable temperature $^1\text{H}$ NMR spectra

The activation parameters calculated for  $[\text{Pd}_2\text{Cl}_2(\eta^3\text{-C}_4\text{H}_7)_2(\mu\text{-hmt})]$  and  $[\text{PdCl}(\eta^3\text{-C}_4\text{H}_7)(\text{hmt})]$  are summarised in **Table 4.6**. The values determined for hexamethylenetetramine exchange for both the 1:1 adduct and the 1:2 adduct are in excellent agreement, indicating that it is very likely that a similar mechanism is operating in both cases. The table also contains thermodynamic data on other palladium allyl complexes containing nitrogen donor ligands. While these compounds bear only a passing similarity to the new compounds described here, the quoted thermodynamic data have been ascribed to a ligand exchange mechanism involving Pd-N bond cleavage, therefore comparison with data calculated in this chapter is reasonable. The values calculated for  $[\text{Pd}_2\text{Cl}_2(\eta^3\text{-C}_4\text{H}_7)_2(\mu\text{-hmt})]$  and  $[\text{PdCl}(\eta^3\text{-C}_4\text{H}_7)(\text{hmt})]$  fall within the range given in the table, suggesting that the dynamic processes do indeed involve ligand exchange *via* Pd-N bond cleavage. The compounds  $[\text{PdCl}(\eta^3\text{-C}_4\text{H}_7)(\text{L}^1)]^{173}$  and  $[\text{PdCl}(\eta^3\text{-C}_4\text{H}_7)(\text{L}^2)]$  are good indicators of the effect of steric factors upon the dynamic process.



**L<sup>1</sup>**, R = H; **L<sup>2</sup>**, R = CH<sub>3</sub>



**L<sup>3</sup>**

The complex containing the more sterically crowded ligand, **L<sub>2</sub>**, has a significantly lower barrier to exchange ( $33 \text{ kJ mol}^{-1}$ ) than its less crowded counterpart ( $55 \text{ kJ mol}^{-1}$ ). This may also explain the much larger barrier to exchange

calculated for  $[\text{PdCl}(\eta^3\text{-C}_4\text{H}_7)\{\text{NH}_2\text{CH}(\text{CH}_3)\text{Ph}\}]$ ,<sup>174</sup> which is much less sterically crowded than the other examples in the table.

**Table 4.6** Selected activation parameters for ligand exchange of nitrogen donor ligands on allylpalladium complexes

Complex	$E_a$	$\Delta H^\ddagger$ (298 K) (kJ mol <sup>-1</sup> )	$\Delta G^\ddagger$	$\Delta S^\ddagger$ (J mol <sup>-1</sup> K <sup>-1</sup> )
$[\text{Pd}_2\text{Cl}_2(\eta^3\text{-C}_4\text{H}_7)_2(\mu\text{-hmt})]^a$	59	60	51	30
$[\text{Pd}_2\text{Cl}_2(\eta^3\text{-C}_4\text{H}_7)_2(\mu\text{-hmt})]^b$	59	59	52	25
$[\text{PdCl}(\eta^3\text{-C}_4\text{H}_7)(\text{hmt})]^a$	53	54	56	-6
$[\text{PdCl}(\eta^3\text{-C}_4\text{H}_7)(\text{L}^1)]^{173}$	—	55	58	-11
$[\text{PdCl}(\eta^3\text{-C}_4\text{H}_7)(\text{L}^2)]^{173}$	—	33	48	50
$[\text{Pd}(\eta^3\text{-C}_4\text{H}_7)(\text{L}^3)]^+^{175}$	72	—	—	—
$[\text{PdCl}(\eta^3\text{-C}_4\text{H}_7)\{\text{NH}_2\text{CH}(\text{CH}_3)\text{Ph}\}]^{174}$	85	—	—	—

<sup>a</sup>calculated using allyl <sup>1</sup>H NMR data; <sup>b</sup> calculated using hexamethylenetetramine <sup>1</sup>H NMR data

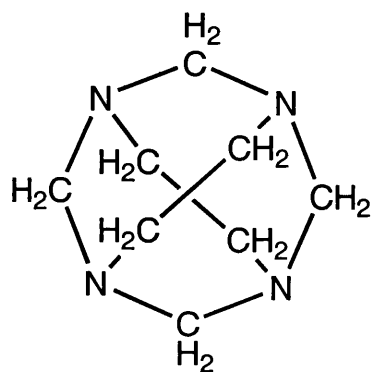
In other studies, variable temperature <sup>1</sup>H NMR spectroscopy has been used as a diagnostic tool to identify the exchange of palladium coordinated allyl ligands between  $\pi$ -bound and  $\sigma$ -bonding modes. For the complexes discussed here at temperatures up to 333 K, the resonances of the *syn* and *anti* protons of the allyl ligand remain distinct, *i.e.* the allyl ligand remains  $\pi$ -bound.

#### 4.4 Reactions of hexamethylenetetramine with

##### 1,3,6,8-tetraazatricyclo[4.4.1.1.<sup>3,8</sup>]-dodecane

The compound 1,3,6,8-tetraazatricyclo[4.4.1.1.<sup>3,8</sup>]-dodecane, TATD, is the 2:1 condensation product of formaldehyde and ethylenediamine.<sup>176</sup> TATD has been shown by single crystal X-ray diffraction to adopt the symmetrical  $D_{2d}$  structure (48) shown below.<sup>177</sup> The N-C-C-N linkage of the ethylene bridge is planar, so

the C-N and C-H bonds are eclipsed. The symmetry of the molecule in solution is confirmed by  $^1\text{H}$  NMR spectroscopy, where two sharp singlets are observed at  $\delta$  3.24 and 3.97 ppm, respectively, each integrating for eight protons.



(48)

Interest in the reactions of TATD arose due to its similarity to the caged structure of hexamethylenetetramine. Whereas hexamethylenetetramine has six methylene bridges, TATD contains four methylene and two ethylene bridges. The preparation of TATD complexes analogous to the allylpalladium hexamethylenetetramine adducts described in section 4.3, was attempted in order to give an insight into the steric and electronic factors involved in the formation of these compounds.

The reactions of chloro(2-methyl- $\eta^3$ -allyl)palladium(II) with TATD were performed in an analogous fashion to those involving hexamethylenetetramine. Thus chloro(2-methyl- $\eta^3$ -allyl)palladium(II) and TATD were reacted in a 1:1, 2:1 and 4:1 molar ratios. In each case, however only the 1:2 adduct (**49**) was isolated. As in the case of the hexamethylenetetramine adducts of chloro(2-methyl- $\eta^3$ -allyl)palladium(II), the appearance of the  $^1\text{H}$  NMR spectrum is temperature dependent. **Figure 4.19** shows the  $^1\text{H}$  NMR spectrum of the product  $[\text{Pd}_2\text{Cl}_2(\eta^3\text{-C}_4\text{H}_7)_2(\mu\text{-TATD})]$  at 178 K, establishing its identity as the 1:2 adduct. Microanalytical data are also consistent with this conclusion. The reason for the formation of the 1:2 adduct from each reaction is unclear, although it



would seem that coordination of one palladium ion to the molecule activates the nitrogen atom across the ethylene bridge, and de-activates of the other two nitrogen atoms of the cage.

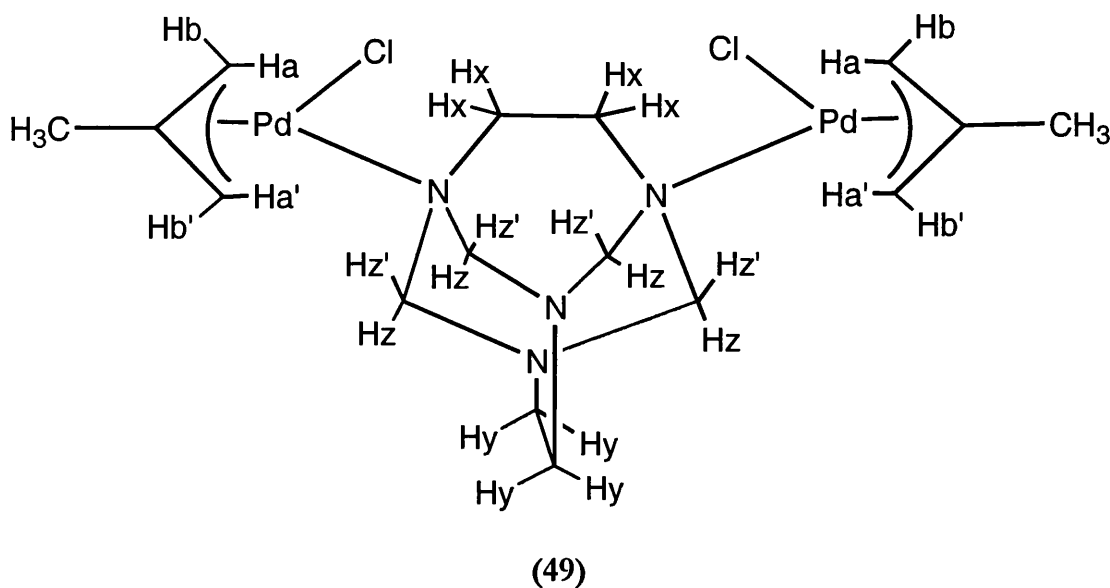


Figure 4.18  $[\text{Pd}_2\text{Cl}_2(\eta^3\text{-C}_4\text{H}_7)_2(\mu\text{-C}_8\text{H}_{16}\text{N}_4)]$ ; hydrogen atom labelling corresponds to NMR shown in Figure 4.19

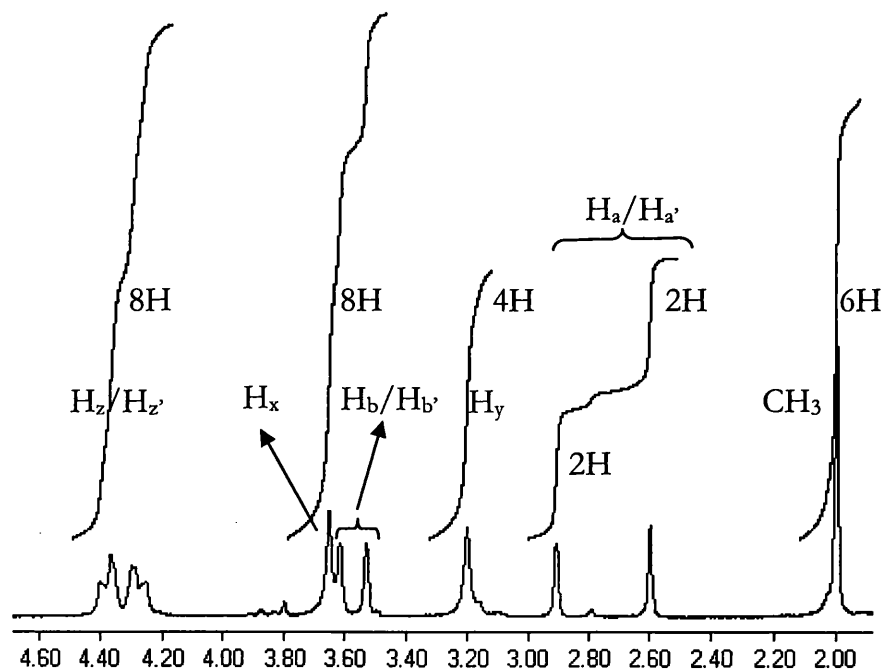


Figure 4.19  $^1\text{H}$  NMR of  $[\text{Pd}_2\text{Cl}_2(\eta^3\text{-C}_4\text{H}_7)_2(\mu\text{-C}_8\text{H}_{16}\text{N}_4)]$  recorded at 178 K in  $\text{CD}_2\text{Cl}_2$

Although a good  $^1\text{H}$  NMR spectrum was obtained at 178 K, for the static structure of  $[\text{Pd}_2\text{Cl}_2(\eta^3\text{-C}_4\text{H}_7)_2(\mu\text{-C}_8\text{H}_{16}\text{N}_4)]$ , the complexity of the spectra recorded between 298 K and 178 K prevented any lineshape analysis being performed.

#### 4.5 Conclusions

Hexamethylenetetramine acts as a ligand in coordination compounds of palladium, as proven by the synthesis of  $[\text{Pd}(\text{hmt})_2\text{Cl}_2]$  and  $[\text{Pd}(\text{hmt})_2\text{Cl}_2]_n$ . The complex  $[\text{Pd}(\text{hmt})_2\text{Cl}_2]$  was shown to exist in the *trans* form using solid state X-ray diffraction.

For the organometallic complexes a combination of  $^1\text{H}$  NMR spectroscopy and single crystal X-ray diffraction have been used to show that hexamethylenetetramine may use between one and four nitrogen atoms to bind to palladium. Hexamethylenetetramine may be coordinated in a monodentate fashion, as in  $[\text{PdCl}(\eta^3\text{-C}_4\text{H}_7)(\text{C}_6\text{H}_{12}\text{N}_4)]$  or act as a bridging ligand between two metal atoms, as in  $[\text{Pd}_2\text{Cl}_2(\eta^3\text{-C}_4\text{H}_7)_2(\mu\text{-C}_6\text{H}_{12}\text{N}_4)]$ . Variable temperature  $^1\text{H}$  NMR studies, along with computer simulation of spectra, have given an insight into the solution dynamics of these compounds. hexamethylenetetramine can also be a tetradentate ligand, as in  $[\text{Pd}_4\text{Cl}_4(\eta^3\text{-C}_4\text{H}_7)_4(\mu^4\text{-C}_6\text{H}_{12}\text{N}_4)]$  (although this complex was not isolated in pure form).

Attempts to prepare analogous complexes using TATD were only successful with the synthesis of the 1:2 adduct. The inability to prepare other adducts is possibly a result of electronic, rather than steric, effects.

## 4.6 Experimental

### 4.6.1 Crystallography

Crystallographic data for (46) were collected as described in section 3.4.2. Crystallographic data for (44) and (47) were measured at 293 K on an automated four circle diffractometer (Nicolet R3mV) equipped with graphite monochromated Mo K $\alpha$  radiation. The data were corrected for Lorentz and polarisation effects and for absorption, based on additional azimuthal scan data. Structures were solved using direct methods (SHELXS-86)<sup>178</sup> and developed using alternating cycles of least-squares refinement and difference Fourier synthesis (SHELXL-93).<sup>179</sup> All non-hydrogen atoms were refined anisotropically, whilst the hydrogen atoms were fixed in idealised positions and allowed to ride on the atom to which they were attached.

### 4.6.2 Synthesis of [Pd(hmt)<sub>2</sub>Cl<sub>2</sub>], (44)

[Pd(C<sub>6</sub>H<sub>5</sub>CN)<sub>2</sub>Cl<sub>2</sub>] (100 mg, 0.26 mmol) was dissolved in dichloromethane (5 cm<sup>3</sup>). Addition of hexamethylenetetramine (73 mg, 0.52 mmol, 2 eq.) to the solution immediately gave a yellow precipitate. The precipitate was filtered off, washed with dichloromethane and dried *in vacuo* to give a yellow microcrystalline solid. Yield 103 mg, 0.23 mmol, 87 %. Diffusion of a dichloromethane solution of hexamethylenetetramine into a dichloromethane solution of [Pd(C<sub>6</sub>H<sub>5</sub>CN)<sub>2</sub>Cl<sub>2</sub>] produced crystals of [Pd(C<sub>6</sub>H<sub>12</sub>N<sub>4</sub>)<sub>2</sub>Cl<sub>2</sub>] suitable for single crystal X-ray analysis.

$\delta_{\text{H}}$  (400 MHz; CDCl<sub>3</sub>; 298 K) 4.40, 4.52 (6H, AB q,  $J = 12.6$  Hz), 5.03 (6H, s).

Anal. Calc. for PdC<sub>12</sub>H<sub>24</sub>N<sub>8</sub>Cl<sub>2</sub>: C 31.56, H 5.30, N 24.53 %, found: C 31.33, H 5.27, N 24.24 %.

$\nu_{\text{max}}$ /cm<sup>-1</sup> 345 (Pd-Cl).

#### 4.6.3 Synthesis of [Pd(hmt)Cl<sub>2</sub>]<sub>n</sub>,

[Pd(C<sub>6</sub>H<sub>5</sub>CN)<sub>2</sub>Cl<sub>2</sub>] (50 mg, 0.13 mmol) was dissolved in dichloromethane (5 cm<sup>3</sup>). Addition of hexamethylenetetramine (18 mg, 0.13 mmol, 1 eq.) to the solution immediately gave a yellow precipitate. The pale yellow powder was filtered off, washed with dichloromethane and dried *in vacuo*. Yield 39 mg, 0.12 mmol, 93 %.

Anal. Calc. for PdC<sub>6</sub>H<sub>12</sub>N<sub>4</sub>Cl<sub>2</sub> : C 22.79, H 3.82, N 17.77, Cl 22.40%, found: C 21.91, H 3.73, N 16.34, Cl 21.88 %.

$\nu_{\max}/\text{cm}^{-1}$  345 (Pd-Cl).

#### 4.6.4 Synthesis of [PdCl( $\eta^3$ -C<sub>4</sub>H<sub>7</sub>)(hmt)], (46)

[Pd<sub>2</sub>Cl<sub>2</sub>( $\eta^3$ -C<sub>4</sub>H<sub>7</sub>)<sub>2</sub>] (60 mg, 0.15 mmol) was dissolved in dichloromethane (5.0 cm<sup>3</sup>) and hexamethylenetetramine (43 mg, 0.31 mmol, 2 eq.) was added to the pale yellow solution. The solution was stirred at room temperature for 2.5 h. The solvent was removed under vacuum to give a solid, which was redissolved in the minimum amount of dichloromethane. Subsequent addition of diethyl ether and cooling to 0 °C, produced yellow crystals. Yield 63 mg, 0.19 mmol, 61 %.

$\delta_{\text{H}}$  (400 MHz; CDCl<sub>3</sub>; 298 K) 2.05 (3H, s, CH<sub>3</sub> allyl), 2.61 (2H, s, anti H allyl), 3.65 (s, 2H, syn H allyl), 4.80 (12H, s, hmt).

$\delta_{\text{H}}$  (400 MHz; CDCl<sub>3</sub>; 223 K) 2.04 (3H, s, CH<sub>3</sub> allyl), 2.70 (1H, s, anti H allyl), 2.84 (1H, s, anti H allyl), 3.59 (1H, s, syn H allyl), 3.69 (1H, s, syn H allyl), 4.58, 4.66 (6H, AB q,  $J = 12.5$  Hz, hmt: N(non-complexed)-CH<sub>2</sub>), 4.97 (6H, s, hmt: N(complexed)-CH<sub>2</sub>).

Anal. Calc. for PdC<sub>10</sub>H<sub>19</sub>N<sub>4</sub>Cl : C 35.73, H 5.70, N 16.67 %, found: C 35.24, H 5.11, N 16.53 %.

$\nu_{\max}/\text{cm}^{-1}$  275 (Pd-Cl)

#### 4.6.5 Synthesis of [Pd<sub>2</sub>Cl<sub>2</sub>( $\eta^3$ -C<sub>4</sub>H<sub>7</sub>)<sub>2</sub>( $\mu$ -hmt)], (47)

[Pd<sub>2</sub>Cl<sub>2</sub>( $\eta^3$ -C<sub>4</sub>H<sub>7</sub>)<sub>2</sub>] (60 mg, 0.15 mmol) was dissolved in dichloromethane (5.0 cm<sup>3</sup>) and hexamethylenetetramine (22 mg, 0.15 mmol, 1 eq.) was added to the

pale yellow solution. The solution was stirred at room temperature for 2.5 h. The solvent was removed under vacuum to give a solid, which was redissolved in the minimum amount of dichloromethane. Subsequent addition of diethyl ether and cooling to 0 °C, produced a yellow microcrystalline product. Yield 35. mg, 0.69 mmol, 45 %.

$\delta_{\text{H}}$  (400 MHz; CDCl<sub>3</sub>; 298 K) 2.09 (6H, s, CH<sub>3</sub> allyl), 2.83 (4H, s, anti H allyl), 3.74 (4H, s, syn H allyl), 4.91 (12H, s, hmt).

$\delta_{\text{H}}$  (400 MHz; CDCl<sub>3</sub>; 223 K) 2.07 (6H, s, CH<sub>3</sub> allyl), 2.75 (2H, s, anti H allyl), 2.89 (2H, s, anti H allyl), 3.71 (2H, s, syn H allyl), 3.76 (2H, s, syn H allyl), 4.57 (2H, s, hmt), 4.93 (4H, s, hmt), 5.30 (2H, s, hmt).

Anal. Calc. for Pd<sub>2</sub>C<sub>12</sub>H<sub>26</sub>N<sub>4</sub>Cl<sub>2</sub> : C 28.73, H 5.16, N 11.03 %, found: C 27.68, H 4.87, N 10.78 %.

$\nu_{\text{max}}$ /cm<sup>-1</sup> 275 (Pd-Cl).

#### 4.6.6 Attempted synthesis of [Pd<sub>4</sub>Cl<sub>4</sub>( $\eta^3$ -C<sub>4</sub>H<sub>7</sub>)<sub>4</sub>( $\mu^4$ - hmt)]

[Pd<sub>2</sub>Cl<sub>2</sub>( $\eta^3$ -C<sub>4</sub>H<sub>7</sub>)<sub>2</sub>] (60 mg, 0.15 mmol) was dissolved in dichloromethane (5.0 cm<sup>3</sup>) and hexamethylenetetramine (11 mg, 0.077 mmol, 0.5 eq.) was added to the pale yellow solution. The solution was stirred at room temperature for 5 h. The solvent was reduced *in vacuo* to approximately 2 cm<sup>3</sup>, addition of diethyl ether and cooling to 0 °C, produced a fine pale yellow powder. <sup>1</sup>H NMR analysis showed the product to contain a mixture of 1:1, 1:2 and 1:4 adducts.

$\delta_{\text{H}}$  (400 MHz; CDCl<sub>3</sub>; 298 K) 2.10 (9H, s, CH<sub>3</sub> allyl), 2.84 (6H, s, anti H allyl), 3.78 (6H, s, syn H allyl), 4.92 (12H, s, hmt).

#### 4.6.7 Synthesis of [Pd<sub>2</sub>Cl<sub>2</sub>( $\eta^3$ -C<sub>4</sub>H<sub>7</sub>)<sub>2</sub>( $\mu$ -C<sub>8</sub>H<sub>16</sub>N<sub>4</sub>)], (49)

[Pd<sub>2</sub>Cl<sub>2</sub>( $\eta^3$ -C<sub>4</sub>H<sub>7</sub>)<sub>2</sub>] (50 mg, 0.13 mmol) was dissolved in dichloromethane (15.0 cm<sup>3</sup>) and 1,3,6,8-tetraazatricyclo[4.4.1.1.3<sup>8</sup>]-dodecane (43 mg, 0.26 mmol, 0.5 eq.) was added to the pale yellow solution. The solution was stirred at room temperature for 3 h. The volume of the solvent was reduced *in vacuo* to

approximately 5 cm<sup>3</sup>, addition of diethyl ether and cooling to 0 °C, produced a yellow solid. Yield 45 mg, 0.080 mmol, 63 %.

$\delta_{\text{H}}$  (400 MHz; CDCl<sub>3</sub>; 298 K) 2.11 (6H, s, CH<sub>3</sub>, allyl), 2.86 (4H, s, anti H allyl), 3.30 (8H, s, TATD), 3.81 (6H, s, syn H allyl), 4.08 (8H, s, TATD),

$\delta_{\text{H}}$  (400 MHz; CDCl<sub>3</sub>; 178 K) 1.98 (6H, s, CH<sub>3</sub> allyl), 2.59 (2H, s, anti H allyl), 2.90 (2H, s, anti H allyl), 3.19 (4H, s, TATD), 3.52 (2H, s, syn H allyl), 3.61 (2H, s, syn H allyl), 3.64 (4H, s, TATD), 4.26, 4.37 (8H, AB q,  $J = 14.6$  Hz, TATD).

Anal. Calc. for Pd<sub>2</sub>C<sub>16</sub>H<sub>30</sub>N<sub>4</sub>Cl<sub>2</sub> : C 31.36, H 5.64, N 10.65 %, found: C 34.24, H 5.15, N 9.78 %.

4.6.8 Crystallographic data for [Pd(hmt)<sub>2</sub>Cl<sub>2</sub>], (44)Table 4.7 Crystal data and structure refinement for [Pd(hmt)<sub>2</sub>Cl<sub>2</sub>], (44)

Empirical formula	C <sub>12</sub> H <sub>24</sub> N <sub>8</sub> Cl <sub>2</sub> Pd
Formula weight	457.69
Temperature	293(2) K
Wavelength	0.71073 Å
Crystal system	Monoclinic
Space group	P2 <sub>1</sub> /n
Unit cell dimensions	a = 6.0180(10) Å    alpha = 90 ° b = 23.142(5) Å    beta = 103.74(3) ° c = 6.1770(10) Å    gamma = 90 °
Volume	835.6(3) Å <sup>3</sup>
Z	2
Density (calculated)	1.819 Mg m <sup>-3</sup>
Absorption coefficient	1.442 mm <sup>-1</sup>
F(000)	464
Crystal size	0.68 x 0.54 x 0.18 mm
Theta range for data collection	3.51 to 24.99 °
Index ranges	0 ≤ h ≤ 7, -27 ≤ k ≤ 27, -7 ≤ l ≤ 7
Reflections collected	2528
Independent reflections	1377 [R(int) = 0.0375]
Refinement method	Full-matrix least-squares on F <sup>2</sup>
Data / restraints / parameters	1372 / 0 / 107
Goodness-of-fit on F <sup>2</sup>	0.992
Final R indices [I > 2σ(I)]	R1 = 0.0538, wR2 = 0.1443
R indices (all data)	R1 = 0.0604, wR2 = 0.1660
Extinction coefficient	0.052(7)
Largest diff. peak and hole	1.409 and -1.772 e.Å <sup>-3</sup> Near to palladium atom

**Table 4.8** Atomic coordinates ( $\times 10^4$ ) and equivalent isotropic displacement parameters ( $\text{\AA}^2 \times 10^3$ ) for  $[\text{Pd}(\text{hmt})_2\text{Cl}_2]$ , (44)

U(eq) is defined as one third of the trace of the orthogonalized Uij tensor.

	x	y	z	U(eq)
Pd(1)	0	0	0	24(1)
Cl(1)	2654(3)	-346(1)	3034(2)	51(1)
N(1)	1230(6)	845(2)	935(6)	26(1)
N(2)	4667(8)	1455(2)	1635(9)	46(1)
N(3)	1967(9)	1548(2)	3996(7)	43(1)
N(4)	959(10)	1896(2)	193(8)	43(1)
C(1)	3711(9)	884(2)	898(10)	38(1)
C(2)	1004(10)	984(2)	3252(9)	40(1)
C(3)	4392(10)	1559(2)	3896(9)	45(1)
C(4)	3388(11)	1900(2)	169(10)	47(1)
C(5)	9(10)	1327(2)	-558(12)	40(1)
C(6)	763(11)	1990(2)	2460(10)	46(1)



**Table 4.9** Bond lengths [Å] and angles [°] for [Pd(hmt)Cl<sub>2</sub>], (44)

Pd(1)-N(1)#1	2.122(4)	N(2)-C(4)	1.464(8)
Pd(1)-N(1)	2.122(4)	N(2)-C(1)	1.468(7)
Pd(1)-Cl(1)	2.2980(14)	N(3)-C(2)	1.457(7)
Pd(1)-Cl(1)#1	2.2980(14)	N(3)-C(6)	1.466(8)
N(1)-C(1)	1.501(6)	N(3)-C(3)	1.475(8)
N(1)-C(2)	1.505(6)	N(4)-C(6)	1.450(7)
N(1)-C(5)	1.522(7)	N(4)-C(4)	1.465(8)
N(2)-C(3)	1.465(8)	N(4)-C(5)	1.466(7)
<hr/>			
N(1)#1-Pd(1)-N(1)	180.0	C(2)-N(3)-C(6)	108.9(4)
N(1)#1-Pd(1)-Cl(1)	91.80(11)	C(2)-N(3)-C(3)	109.1(4)
N(1)-Pd(1)-Cl(1)	88.20(10)	C(6)-N(3)-C(3)	107.6(5)
N(1)#1-Pd(1)-Cl(1)#1	88.20(11)	C(6)-N(4)-C(4)	108.6(5)
N(1)-Pd(1)-Cl(1)#1	91.80(10)	C(6)-N(4)-C(5)	109.0(5)
Cl(1)-Pd(1)-Cl(1)#1	180.0	C(4)-N(4)-C(5)	108.5(4)
C(1)-N(1)-C(2)	108.4(4)	N(2)-C(1)-N(1)	111.6(4)
C(1)-N(1)-C(5)	106.6(4)	N(3)-C(2)-N(1)	111.8(4)
C(2)-N(1)-C(5)	106.3(4)	N(2)-C(3)-N(3)	111.9(4)
C(1)-N(1)-Pd(1)	109.6(3)	N(4)-C(4)-N(2)	111.7(4)
C(2)-N(1)-Pd(1)	110.6(3)	N(4)-C(5)-N(1)	111.8(4)
C(5)-N(1)-Pd(1)	115.1(3)	N(4)-C(6)-N(3)	112.3(4)
C(3)-N(2)-C(4)	108.1(4)		
C(3)-N(2)-C(1)	108.6(4)		
C(4)-N(2)-C(1)	109.3(4)		

---

Symmetry transformations used to generate equivalent atoms: #1  $-x, -y, -z$

4.6.9 Crystallographic data for [PdCl( $\eta^3$ -C<sub>4</sub>H<sub>7</sub>)(hmt)], (46)<sup>141</sup>**Table 4.10** Crystal data and structure refinement for [PdCl( $\eta^3$ -C<sub>4</sub>H<sub>7</sub>)(hmt)]

Empirical formula	C <sub>10</sub> H <sub>19</sub> ClN <sub>4</sub> Pd	
Formula weight	337.14	
Temperature	100(2) K	
Wavelength	0.71073 Å	
Crystal system	Triclinic	
Space group	P $\bar{1}$	
Unit cell dimensions	a = 7.6747(5) Å	$\alpha$ = 115.176(3) °.
	b = 8.8855(5) Å	$\beta$ = 93.231(3) °.
	c = 9.9329(6) Å	$\gamma$ = 92.194(4) °.
Volume	610.58(6) Å <sup>3</sup>	
Z	2	
Density (calculated)	1.834 Mg m <sup>-3</sup>	
Absorption coefficient	1.717 mm <sup>-1</sup>	
F(000)	340	
Crystal size	0.80 x 0.80 x 0.10 mm <sup>3</sup>	
Theta range for data collection	3.36 to 27.48 °.	
Index ranges	-9 ≤ h ≤ 9, -11 ≤ k ≤ 11, -11 ≤ l ≤ 12	
Reflections collected	4230	
Independent reflections	2766 [R(int) = 0.0757]	
Completeness to theta = 27.48 °	98.8 %	
Absorption correction	Multi-scan	
Max. and min. transmission	0.8470 and 0.3403	
Refinement method	Full-matrix least-squares on F <sup>2</sup>	
Data / restraints / parameters	2766 / 0 / 203	
Goodness-of-fit on F <sup>2</sup>	1.070	
Final R indices [I > 2σ(I)]	R1 = 0.0485, wR2 = 0.1227	
R indices (all data)	R1 = 0.0518, wR2 = 0.1243	
Extinction coefficient	0.033(4)	
Largest diff. peak and hole	2.397 and -1.527 e.Å <sup>-3</sup>	
	Near to palladium atom	

**Table 4.11** Atomic coordinates ( $\times 10^4$ ) and equivalent isotropic displacement parameters ( $\text{\AA}^2 \times 10^3$ ) for  $[\text{PdCl}(\eta^3\text{-C}_4\text{H}_7)(\text{hmt})]$ 

$U(\text{eq})$  is defined as one third of the trace of the orthogonalized  $U^{ij}$  tensor.

	x	y	z	$U(\text{eq})$
Pd(1)	1171(1)	-1541(1)	929(1)	11(1)
Cl(1)	-1866(1)	-1882(1)	128(1)	14(1)
N(1)	2039(5)	-3376(5)	-1121(4)	11(1)
N(2)	4003(5)	-5666(5)	-2169(4)	14(1)
N(3)	3645(5)	-3717(5)	-3304(4)	13(1)
N(4)	1245(5)	-5762(5)	-3577(4)	14(1)
C(1)	3323(6)	-4459(6)	-808(5)	13(1)
C(2)	2963(6)	-2536(6)	-1928(5)	14(1)
C(3)	596(6)	-4549(6)	-2182(5)	13(1)
C(4)	4854(6)	-4745(6)	-2906(5)	15(1)
C(5)	2520(6)	-6732(6)	-3176(5)	15(1)
C(6)	2161(6)	-4821(6)	-4272(5)	15(1)
C(7)	3674(6)	-477(7)	2080(5)	19(1)
C(8)	2474(6)	-451(6)	3121(5)	15(1)
C(9)	933(7)	383(6)	3055(6)	17(1)
C(10)	2637(7)	-1493(7)	3974(6)	22(1)

**Table 4.12** Bond lengths [Å] and angles [°] for [PdCl( $\eta^3$ -C<sub>4</sub>H<sub>7</sub>)(hmt)]

Pd(1)-C(9)	2.100(5)	N(2)-C(5)	1.475(6)
Pd(1)-C(8)	2.136(4)	N(3)-C(2)	1.465(6)
Pd(1)-C(7)	2.141(5)	N(3)-C(6)	1.474(6)
Pd(1)-N(1)	2.159(4)	N(3)-C(4)	1.477(6)
Pd(1)-Cl(1)	2.3856(10)	N(4)-C(6)	1.473(6)
N(1)-C(2)	1.495(5)	N(4)-C(5)	1.474(6)
N(1)-C(3)	1.506(6)	N(4)-C(3)	1.476(6)
N(1)-C(1)	1.513(5)	C(7)-C(8)	1.417(7)
N(2)-C(1)	1.462(6)	C(8)-C(9)	1.432(7)
N(2)-C(4)	1.467(6)	C(8)-C(10)	1.502(7)
C(9)-Pd(1)-C(8)	39.51(18)	C(2)-N(3)-C(4)	107.9(3)
C(9)-Pd(1)-C(7)	68.30(19)	C(6)-N(3)-C(4)	108.2(4)
C(8)-Pd(1)-C(7)	38.69(18)	C(6)-N(4)-C(5)	108.5(4)
C(9)-Pd(1)-N(1)	167.08(17)	C(6)-N(4)-C(3)	107.9(4)
C(8)-Pd(1)-N(1)	129.43(16)	C(5)-N(4)-C(3)	107.7(3)
C(7)-Pd(1)-N(1)	98.78(17)	N(2)-C(1)-N(1)	112.3(3)
C(9)-Pd(1)-Cl(1)	95.75(14)	N(3)-C(2)-N(1)	112.9(4)
C(8)-Pd(1)-Cl(1)	130.65(13)	N(4)-C(3)-N(1)	112.5(4)
C(7)-Pd(1)-Cl(1)	162.21(15)	N(2)-C(4)-N(3)	112.7(4)
N(1)-Pd(1)-Cl(1)	96.97(10)	N(4)-C(5)-N(2)	112.3(4)
C(2)-N(1)-C(3)	107.8(3)	N(4)-C(6)-N(3)	113.0(3)
C(2)-N(1)-C(1)	107.1(3)	C(8)-C(7)-Pd(1)	70.5(3)
C(3)-N(1)-C(1)	106.1(3)	C(7)-C(8)-C(9)	113.4(4)
C(2)-N(1)-Pd(1)	110.2(3)	C(7)-C(8)-C(10)	122.4(5)
C(3)-N(1)-Pd(1)	114.4(3)	C(9)-C(8)-C(10)	123.0(4)
C(1)-N(1)-Pd(1)	110.8(3)	C(7)-C(8)-Pd(1)	70.8(3)
C(1)-N(2)-C(4)	108.2(4)	C(9)-C(8)-Pd(1)	68.9(3)
C(1)-N(2)-C(5)	108.6(4)	C(10)-C(8)-Pd(1)	118.9(3)
C(4)-N(2)-C(5)	108.4(4)	C(8)-C(9)-Pd(1)	71.6(3)
C(2)-N(3)-C(6)	107.8(3)		

4.6.10 Crystallographic data for  $[\text{Pd}_2\text{Cl}_2(\eta^3\text{-C}_4\text{H}_7)_2(\mu\text{-hmt})]$ , (47)**Table 4.13** Crystal data and structure refinement for  $[\text{Pd}_2\text{Cl}_2(\eta^3\text{-C}_4\text{H}_7)_2(\mu\text{-hmt})]$ , (47)

Empirical formula	$\text{C}_{14}\text{H}_{26}\text{Cl}_2\text{N}_4\text{Pd}_2$	
Formula weight	534.09	
Temperature	293(2) K	
Wavelength	0.71073 Å	
Crystal system	Monoclinic	
Space group	C2/c	
Unit cell dimensions	$a = 14.698(3)$ Å	$\alpha = 90^\circ$
	$b = 15.946(3)$ Å	$\beta = 112.19(3)^\circ$
	$c = 8.545(2)$ Å	$\gamma = 90^\circ$
Volume	1854.4(7) Å <sup>3</sup>	
Z	4	
Density (calculated)	1.913 Mg m <sup>-3</sup>	
Absorption coefficient	2.229 mm <sup>-1</sup>	
F(000)	1056	
Crystal size	0.74 x 0.28 x 0.12 mm	
Theta range for data collection	2.55 to 25.04 °	
Index ranges	0 ≤ h ≤ 17, 0 ≤ k ≤ 19, -10 ≤ l ≤ 9	
Reflections collected	1707	
Independent reflections	1640 [R(int) = 0.0178]	
Refinement method	Full-matrix least-squares on F <sup>2</sup>	
Data / restraints / parameters	1635 / 0 / 102	
Goodness-of-fit on F <sup>2</sup>	1.012	
Final R indices [I > 2σ(I)]	R1 = 0.0335, wR2 = 0.0899	
R indices (all data)	R1 = 0.0362, wR2 = 0.0960	
Extinction coefficient	0.0046(4)	
Largest diff. peak and hole	0.863 and -0.713 e.Å <sup>-3</sup> Near to palladium atom	

**Table 4.14** Atomic coordinates ( $\times 10^4$ ) and equivalent isotropic displacement parameters ( $\text{\AA}^2 \times 10^3$ ) for  $[\text{Pd}_2\text{Cl}_2(\eta^3\text{-C}_4\text{H}_7)_2(\mu\text{-hmt})]$ , (47)

U(eq) is defined as one third of the trace of the orthogonalized  $U^{\text{ij}}$  tensor.

	x	y	z	U(eq)
Pd(1)	3174(1)	2736(1)	3128(1)	28(1)
Cl(1)	1768(1)	1910(1)	1629(1)	41(1)
N(1)	4236(2)	1862(2)	2796(4)	25(1)
N(2)	5484(2)	776(2)	4010(4)	31(1)
C(1)	2409(3)	3731(3)	3681(6)	48(1)
C(2)	3317(4)	4046(3)	3718(6)	45(1)
C(3)	4136(4)	3627(3)	4836(6)	51(1)
C(4)	3378(6)	4639(3)	2397(8)	72(2)
C(5)	3785(3)	1302(2)	1297(5)	29(1)
C(6)	4750(3)	1312(2)	4288(5)	30(1)
C(7)	5000	2383(3)	2500	27(1)
C(8)	5000	264(3)	2500	36(1)

**Table 4.15** Bond lengths [Å] and angles [°] for [Pd<sub>2</sub>Cl<sub>2</sub>(η<sup>3</sup>-C<sub>4</sub>H<sub>7</sub>)<sub>2</sub>(μ-hmt)], (47)

Pd(1)-C(1)	2.099(4)	N(2)-C(8)	1.465(4)
Pd(1)-C(2)	2.140(4)	N(2)-C(5)#1	1.463(5)
Pd(1)-C(3)	2.142(5)	C(1)-C(2)	1.414(7)
Pd(1)-N(1)	2.189(3)	C(2)-C(3)	1.392(7)
Pd(1)-Cl(1)	2.3767(12)	C(2)-C(4)	1.501(8)
N(1)-C(7)	1.494(4)	C(5)-N(2)#1	1.463(5)
N(1)-C(5)	1.494(5)	C(7)-N(1)#1	1.494(4)
N(1)-C(6)	1.496(4)	C(8)-N(2)#1	1.465(4)
N(2)-C(6)	1.464(5)		
C(1)-Pd(1)-C(2)	39.0(2)	C(6)-N(2)-C(8)	109.0(3)
C(1)-Pd(1)-C(3)	67.5(2)	C(6)-N(2)-C(5)#1	109.2(3)
C(2)-Pd(1)-C(3)	37.9(2)	C(8)-N(2)-C(5)#1	107.9(3)
C(1)-Pd(1)-N(1)	168.2(2)	C(2)-C(1)-Pd(1)	72.1(2)
C(2)-Pd(1)-N(1)	129.8(2)	C(3)-C(2)-C(1)	114.1(5)
C(3)-Pd(1)-N(1)	101.0(2)	C(3)-C(2)-C(4)	122.5(5)
C(1)-Pd(1)-Cl(1)	96.31(14)	C(1)-C(2)-C(4)	122.0(5)
C(2)-Pd(1)-Cl(1)	131.01(13)	C(3)-C(2)-Pd(1)	71.1(3)
C(3)-Pd(1)-Cl(1)	161.92(14)	C(1)-C(2)-Pd(1)	69.0(3)
N(1)-Pd(1)-Cl(1)	95.41(8)	C(4)-C(2)-Pd(1)	117.8(3)
C(7)-N(1)-C(5)	107.8(2)	C(2)-C(3)-Pd(1)	71.0(3)
C(7)-N(1)-C(6)	107.5(2)	N(2)#1-C(5)-N(1)	112.3(3)
C(5)-N(1)-C(6)	107.3(3)	N(2)-C(6)-N(1)	111.7(3)
C(7)-N(1)-Pd(1)	106.6(2)	N(1)-C(7)-N(1)#1	112.4(4)
C(5)-N(1)-Pd(1)	112.6(2)	N(2)-C(8)-N(2)#1	112.2(4)
C(6)-N(1)-Pd(1)	114.8(2)		

Symmetry transformations used to generate equivalent atoms: #1  $-x+1, y, -z+1/2$

---

# Chapter Five

Studies on complexes of  
rhodium(II) carboxylates  
with  
hexamethylenetetramine

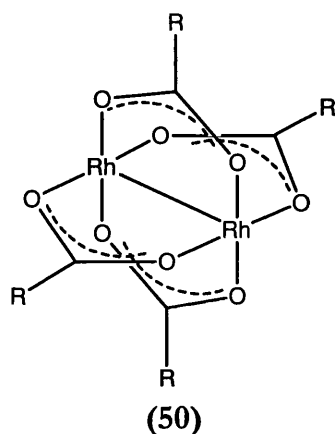


## 5.1 Introduction

Reactions of hexamethylenetetramine with a number of transition metal tetracarboxylate complexes have been reported. For example the chain polymers  $[\text{Ni}_2(\text{O}_2\text{CCH}_3)_4(\text{hmt})]_n$ <sup>180</sup> and  $[\text{Cu}_2(\text{O}_2\text{CCH}_3)_4(\text{hmt})]_n$ <sup>47</sup> have been prepared *via* reaction of hexamethylenetetramine with two equivalents of the metal acetate complex. The synthesis of non-polymeric complexes, however, has not been reported, nor have reactions of dirhodium carboxylates with hexamethylenetetramine. This chapter describes progress made in this area with the synthesis of the 1:2 adduct,  $[\text{Rh}_2(\text{O}_2\text{CR})_4(\text{hmt})_2]$  and the 2:1 adduct  $[\{\text{Rh}_2(\text{O}_2\text{CR})_4\}_2(\mu\text{-hmt})]$ . Derivatives of  $[\text{Rh}_2(\text{O}_2\text{CR})_4]$  have interesting redox chemistry and are frequently subjected to cyclic voltammetric studies. In this chapter the results of electrochemical investigations of  $[\text{Rh}_2(\text{O}_2\text{CR})_4]$  with axial ligands hexamethylenetetramine, triethylamine and  $[\text{Pd}(\eta^3\text{-C}_3\text{H}_7)(\text{hmt})\text{Cl}]$  are described. To put this work in context the remainder of this introduction describes the synthesis of a number of dirhodium tetracarboxylate complexes, particularly those containing amine or nitrogen-donor ligands, along with an introduction to their redox chemistry, as determined by cyclic voltammetry.

### 5.1.1 Dirhodium tetracarboxylate complexes

Although it is not common for rhodium to be found in the dipositive oxidation state dirhodium tetracarboxylate complexes  $[\text{Rh}_2(\text{O}_2\text{CR})_4]$  (**50**) are well known.



These dimeric compounds contain a Rh-Rh bond and adopt a lantern structure with  $D_{4h}$  symmetry. The most commonly studied of these complexes is  $[\text{Rh}_2(\text{O}_2\text{CCH}_3)_4]$ , which is prepared *via* the reaction of  $\text{RhCl}_3 \cdot \text{H}_2\text{O}$  with sodium acetate trihydrate and glacial acetic acid in ethanol.<sup>181</sup> Recrystallisation from methanol results in formation of the 1:2 adduct  $[\text{Rh}_2(\text{O}_2\text{CCH}_3)_4(\text{CH}_3\text{OH})_2]$ , where methanol occupies the axial sites of the complex. Heating this compound *in vacuo* results in removal of the methanol and the formation of  $[\text{Rh}(\text{O}_2\text{CCH}_3)_4]$  with no axial ligands. Exchange of the bridging acetate groups may be used to prepare other tetracarboxylate complexes, for example, dissolution of  $[\text{Rh}_2(\text{O}_2\text{CCH}_3)_4]$  in an excess of refluxing propionic acid followed by cooling results in the precipitation of  $[\text{Rh}_2(\text{O}_2\text{CCH}_2\text{CH}_3)_4]$ .<sup>182</sup> Many other examples have been reported, including those with bulky bridging ligands, such as  $[\text{Rh}_2\{\text{O}_2\text{C}(2\text{-PhC}_6\text{H}_4)_4\}(\text{CH}_3\text{CN})_2]$ <sup>183</sup> and  $[\text{Rh}_2(\text{O}_2\text{C}\{1\text{-adamanty}\}_4)(\text{CH}_3\text{OH})_2]$ ,<sup>183</sup> **Figure 5.1.**

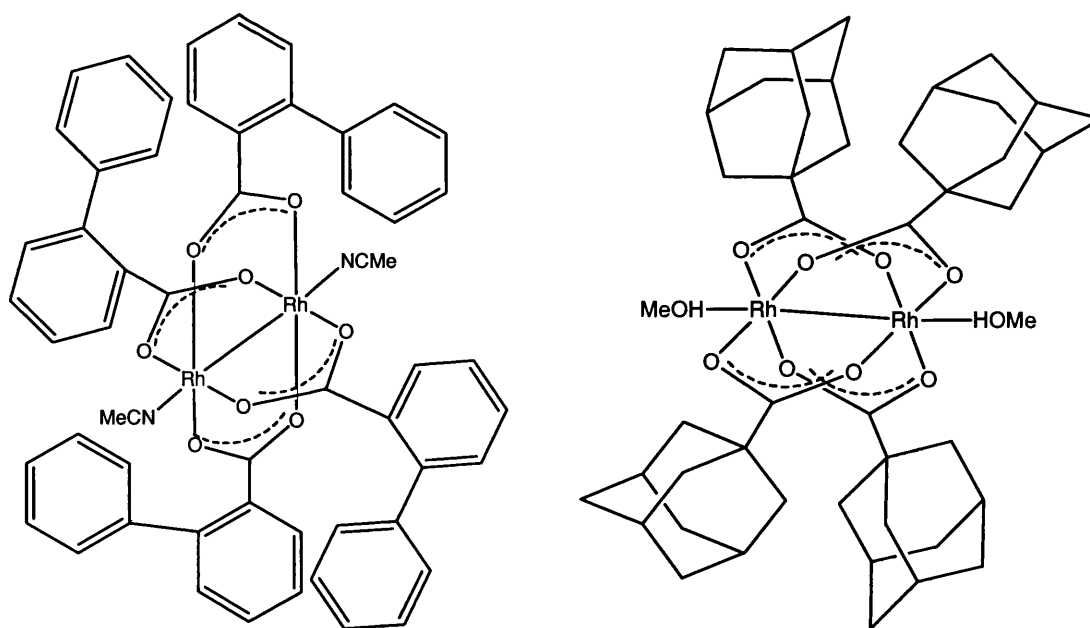


**Figure 5.1** Examples of dirhodium tetracarboxylate complexes with bulky bridging ligands

Although the majority of these complexes have been isolated with solvent molecules in the axial sites, two complexes have been structurally characterised which formally have vacant axial sites; although in practice these are occupied by

the oxygen atoms of a carboxylate ligand from another  $[\text{Rh}_2(\text{O}_2\text{CR})_4]$  unit. As a consequence infinite chains are formed, as illustrated in **Figure 5.2**.<sup>184, 185</sup>

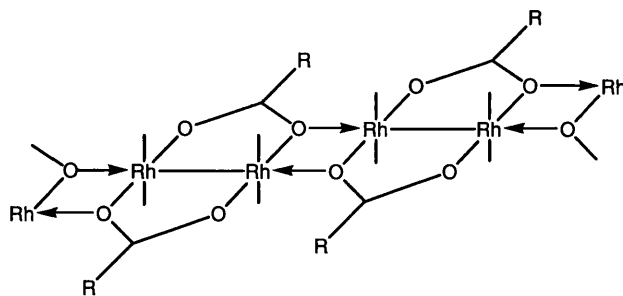


**Figure 5.2** Chains formed by  $[\text{Rh}_2(\text{O}_2\text{CR})_4]$ ,  $\text{R} = \text{C}_3\text{H}_7$  or  $\text{CF}_3$  <sup>184, 185</sup>

### 5.1.2 Bonding in $[\text{Rh}_2(\text{O}_2\text{CR})_4]$ complexes<sup>186</sup>

This qualitative consideration of the bonding in  $[\text{Rh}_2(\text{O}_2\text{CR})_4]$  complexes considers formulation of the metal-metal bond *via* *d*-orbital overlap using molecular orbital theory. When two metal atoms approach each other only five non-zero overlaps are possible due to the symmetry properties. These five and their resulting bonding/anti-bonding orbitals are shown in **Table 5.1**.

**Table 5.1** Overlaps of *d*-orbitals and their resulting molecular orbitals

<i>d</i> -orbital overlap	resulting molecular orbitals
$d_z^2 + d_z^2$	$\sigma$
$d_z^2 - d_z^2$	$\sigma^*$
$d_{xz} + d_{xz}$	$\pi$
$d_{xz} - d_{xz}$	$\pi^*$
$d_{yz} + d_{yz}$	$\pi$
$d_{yz} - d_{yz}$	$\pi^*$
$d_{xy} + d_{xy}$	$\delta$
$d_{xy} - d_{xy}$	$\delta^*$
$d_{x^2-y^2} + d_{x^2-y^2}$	$\delta$
$d_{x^2-y^2} - d_{x^2-y^2}$	$\delta^*$

Since the  $d_{x^2-y^2}$  orbitals are predominantly involved in metal-ligand bonding they are not considered in the metal-metal bonding model. Thus, four bonding and four anti-bonding orbitals are available for the Rh-Rh bond:  $\sigma$ ,  $\sigma^*$ ,  $\pi$ ,  $\pi^*$ ,  $\delta$  and  $\delta^*$ . Hückel's molecular orbital theory states that molecular orbital energies are proportional to overlap integrals and since the overlaps increase  $\delta \ll \pi < \sigma$ , the expected order of the orbitals in order of increasing energy is:

$$\sigma < \pi \ll \delta < \delta^* \ll \pi^* < \sigma^*$$

In  $[\text{Rh}_2(\text{O}_2\text{CR})_4]$  compounds the rhodium ions are in the +2 oxidation state so each has seven  $d$ -electrons available for the Rh-Rh bond. This gives an electronic configuration of  $\sigma^2 \pi^4 \delta^2 \delta^{*2} \pi^{*4}$ . Since, bond order =

$$(\text{number of electrons in bonding orbital} - \text{number in anti-bonding orbitals})/2$$

then the bond order for  $[\text{Rh}_2(\text{O}_2\text{CR})_4]$  is 1.0. Upon oxidation an electron is lost from an anti-bonding orbital, thus a Rh(II)Rh(III) compound has a bond order of 1.5.

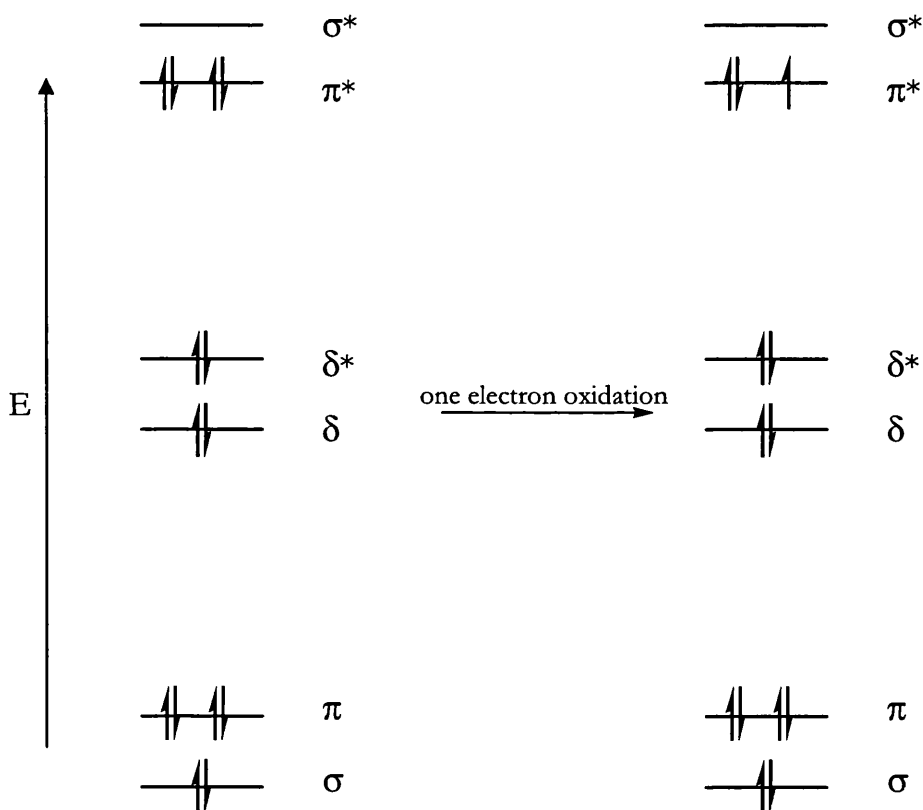


Figure 5.3 Effect of oxidation on the electronic configuration of  $[\text{Rh}_2(\text{O}_2\text{CR})_4]$

### 5.1.3 Lewis base adducts of $[\text{Rh}_2(\text{O}_2\text{CR})_4]$ compounds

#### 5.1.3.1 A general overview of 1:2 adducts

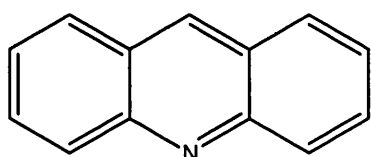
Reactions of  $[\text{Rh}_2(\text{O}_2\text{CR})_4]$  compounds with Lewis bases to form 1:2 adducts,  $[\text{Rh}_2(\text{O}_2\text{CR})_4\text{L}_2]$ , are well known. Complexes with  $\text{L} = \text{H}_2\text{O}$ , THF, MeCN, DMSO,  $\text{NH}_3$  and en have been prepared in pure form by treating solid  $[\text{Rh}_2(\text{O}_2\text{CCH}_3)_4]$  with a slight excess of the pure gaseous or liquid ligand.<sup>187</sup> Studies of the solid state structures of  $[\text{Rh}_2(\text{O}_2\text{CCH}_3)_4\text{L}_2]$  complexes using X-ray crystallography reveal a marked similarity between the Rh-Rh bond lengths, **Table 5.2**, which varies over a small range, 0.074 Å. In these complexes the ligands, L, are bound in the sites *trans* to the Rh-Rh bond (axial ligation); the relatively long Rh-L bond length is consistent with the lability of the axial ligands.<sup>182</sup> Kinetic and thermodynamic studies on axial ligation of dirhodium tetracarboxylate complexes have demonstrated that the 1:2 adducts are formed in two steps, *via* a 1:1 intermediate.<sup>188, 189, 190, 191</sup> These studies have also shown that the second axial ligand is less readily bound to the second rhodium atom.

**Table 5.2** Bond lengths [Å] for selected  $[\text{Rh}_2(\text{O}_2\text{CCH}_3)_4\text{L}_2]$

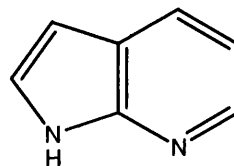
L	Rh-Rh	average Rh-L	reference
H <sub>2</sub> O	2.386(3)	2.308(3)	192
CO	2.4191(3)	2.095(2)	193
MeCN	2.384(1)	2.254(7)	194
DMSO	2.406(1)	2.451(2)	195
MeOH	2.3777(6)	2.288(3)	196
pyridine	2.3963(2)	2.227(3)	197
PPh <sub>3</sub>	2.4505(2)	2.4771(5)	198

### 5.1.3.2 1:2 adducts with nitrogen-donor ligands

In addition to the simple adducts of  $[\text{Rh}_2(\text{O}_2\text{CCH}_3)_4]$  many other 1:2 adducts of a range of dirhodium tetracarboxylate complexes have been prepared. A general survey shows nitrogen donor ligands are the most common ligating species.<sup>186</sup> The most common adducts are those with aromatic nitrogen heterocycles as axial ligands, these comprise over 70 % of the 1:2 adducts for which solid state X-ray structures have been reported.<sup>199</sup> Of these complexes adducts with pyridine or pyridine based ligands are particularly common. Examples include the simple pyridine complexes  $[\text{Rh}_2(\text{O}_2\text{CCH}_3)_4(\text{py})_2]$ <sup>200</sup> and  $[\text{Rh}_2(\text{O}_2\text{CPh})_4(\text{py})_2]$ ,<sup>201</sup> and complexes with larger pyridine based ligands such as,  $[\text{Rh}_2(\text{O}_2\text{CCH}_2\text{CH}_3)_4(\text{L})_2]$  (L = acridine **(51)** or 7-azaindole **(52)**).<sup>202</sup> The adduct formed with 7-azaindole is interesting since it contains two potential donor sites but binds through the pyridyl nitrogen atom, rather than the amine.

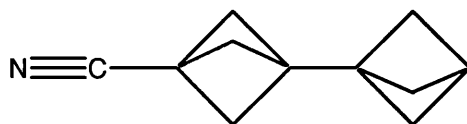


**(51)**



**(52)**

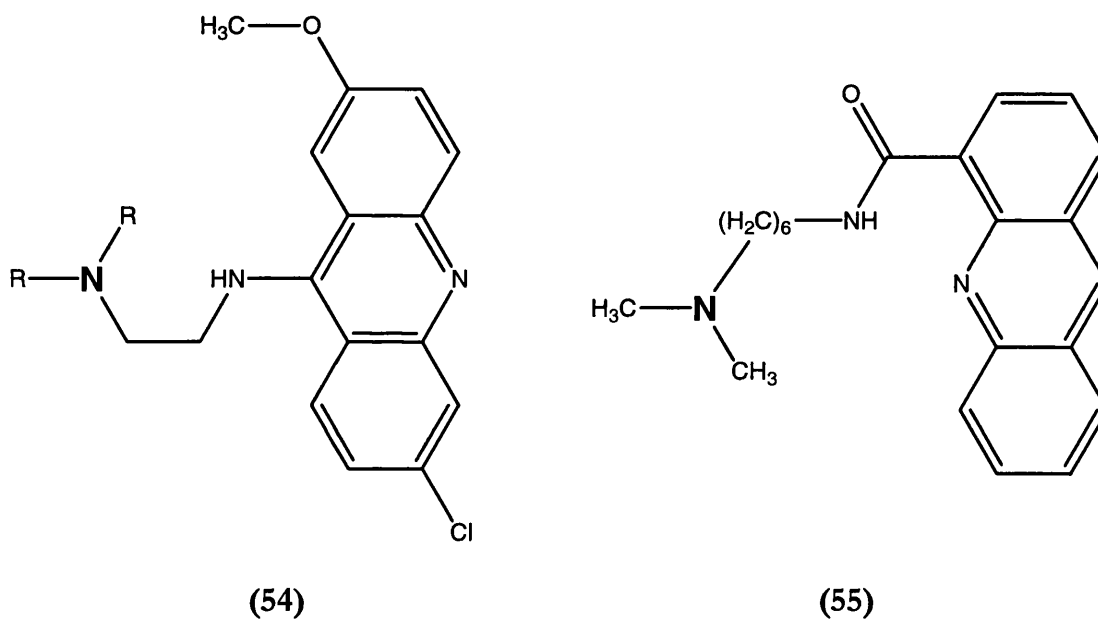
Other examples of 1:2 adducts of  $[\text{Rh}_2(\text{O}_2\text{CCH}_3)_4]$  with nitrogen-donor ligands include compounds containing nitrile donor ligands such as acetonitrile<sup>194</sup> and the more bulky nitrile ligand **(53)**.<sup>203</sup>



**(53)**

Of obvious relevance to the work discussed in this chapter are 1:2 adducts of  $[\text{Rh}_2(\text{O}_2\text{CR})_4]$  compounds with amine ligands. Interestingly, only a limited number of these have been prepared. The simplest of these complexes are

$[\text{Rh}_2(\text{O}_2\text{CCH}_3)_4(\text{NHEt}_2)_2]$ <sup>204</sup> and  $[\text{Rh}_2(\text{O}_2\text{C}^t\text{Bu})_4(\text{NEt}_3)_2]$ . The latter was prepared by evaporation of a solution of  $[\text{Rh}_2(\text{O}_2^t\text{Bu})_4]$  in triethylamine.<sup>205</sup> There are only four other crystallographically characterised examples of  $[\text{Rh}_2(\text{O}_2\text{CR})_4]$  compounds with amines as axial ligands. Three of these contain the large ligands **(54)**<sup>206</sup> and **(55)**,<sup>207</sup> which are found in the complexes  $[\text{Rh}_2(\text{O}_2\text{CCH}_3)_4(\mathbf{54})_2]$  ( $\text{R} = \text{CH}_3$ ),  $[\text{Rh}_2(\text{O}_2\text{CCH}_3)_4(\mathbf{55})_2]$ , and  $[\text{Rh}_2(\text{O}_2\text{CCH}_2\text{CH}_3)_4(\mathbf{54})_2]$ , ( $\text{R} = \text{H}$ ), (the nitrogen atom that coordinates to the rhodium ion is shown in bold).



Although ligands **(54)** and **(55)** contain a number of potential binding sites the isolated products contain each ligand bound to the rhodium atom in only one fashion. This observation is in contrast to that made of the products formed in the reaction of  $[\text{Rh}_2(\text{O}_2\text{CCH}_3)_4]$  with 2-amino-6-methylpyridine, a ligand which has the potential to bind through an amine nitrogen or an aromatic nitrogen. In this case the crystal structure contains two different dirhodium adducts, **Figure 5.4**, compound **(56)** where the ligand is bound by the amino nitrogen atoms, and compound **(57)** with the ligand coordinated by the pyridyl nitrogen atoms.<sup>208</sup>

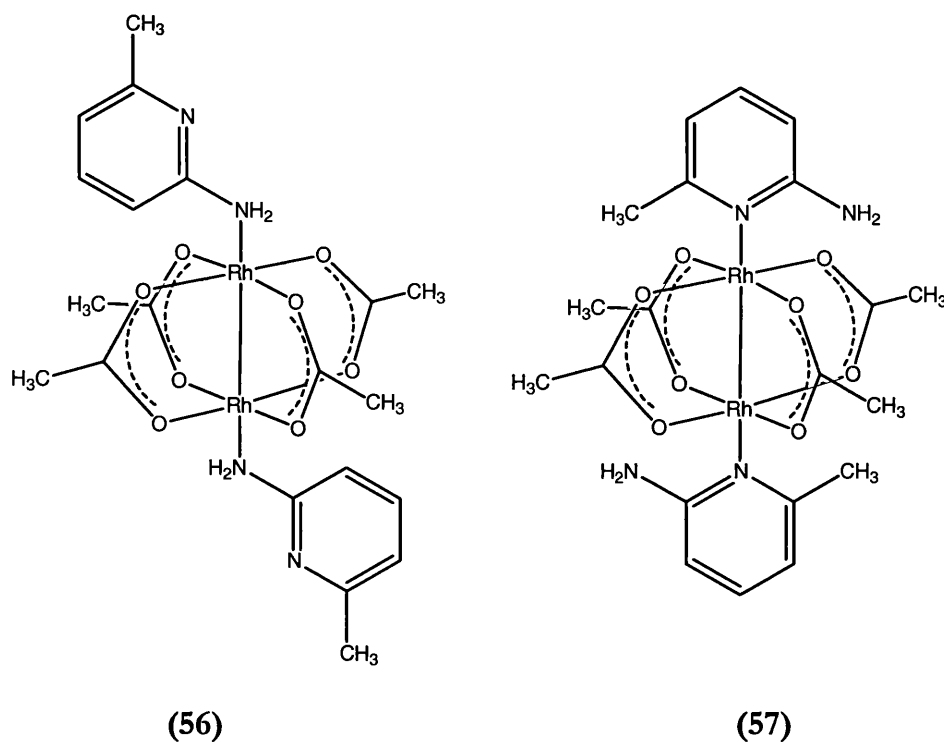


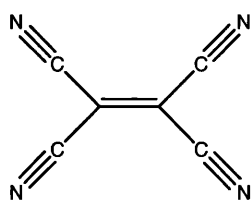
Figure 5.4 Complexes isolated from the reaction of  $[\text{Rh}_2(\text{O}_2\text{CCH}_3)_4]$  with 2-amino-6-methylpyridine

In principle, a Lewis base with two (or more) binding sites might coordinate to several dirhodium units, forming a polymeric structure. The following section discusses examples of such compounds.

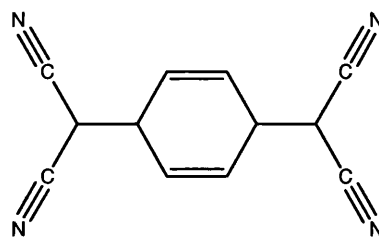
### 5.1.3.3 Polymeric complexes of $[\text{Rh}_2(\text{O}_2\text{CR})_4]$ with nitrogen donor ligands

A wide range of nitrogen-donor ligands have been observed in polymeric  $[\text{Rh}_2(\text{O}_2\text{CR})_4\text{L}]_n$  species. Reported examples include complexes with bifunctional aromatic nitrogen donor ligands, such as  $[\text{Rh}_2(\text{O}_2\text{CCH}_2\text{CH}_3)_4(\text{phz})]_n$  (phz = phenazine),<sup>202</sup> In contrast the tetradentate nitrile ligands, (58)<sup>209</sup> and (59),<sup>210</sup> have been shown to bind to four  $[\text{Rh}_2(\text{O}_2\text{CR})_4]$  units creating much larger structures. Ligand (58) has also been observed acting as a bidentate bridging ligand in a chain polymer with a “ $\text{Rh}_2(\text{O}_2\text{CCH}_3)_4\text{L}$ ” repeating unit.<sup>211</sup>





(58)



(59)

As well as tetradentate nitrile ligands, a number of polydentate pyridine based ligands have been reacted with  $[\text{Rh}_2(\text{O}_2\text{CCH}_3)_4]$  to form chain polymers. The most relevant examples are those containing pyridine based ligands with amine substituents, such as 2-(aminomethyl)pyridine<sup>212</sup> and 2,6-diaminopyridine.<sup>208</sup> In the latter case the ligand has three potential binding sites, however, the observed mode of binding is through the pyridyl nitrogen and only one primary amine nitrogen. A second example, in this instance with a potentially tetradentate ligand (4-amino-5(aminomethyl)-2-methylpyrimidine, aamp,)<sup>213</sup> forms the chain structure illustrated in **Figure 5.5**.

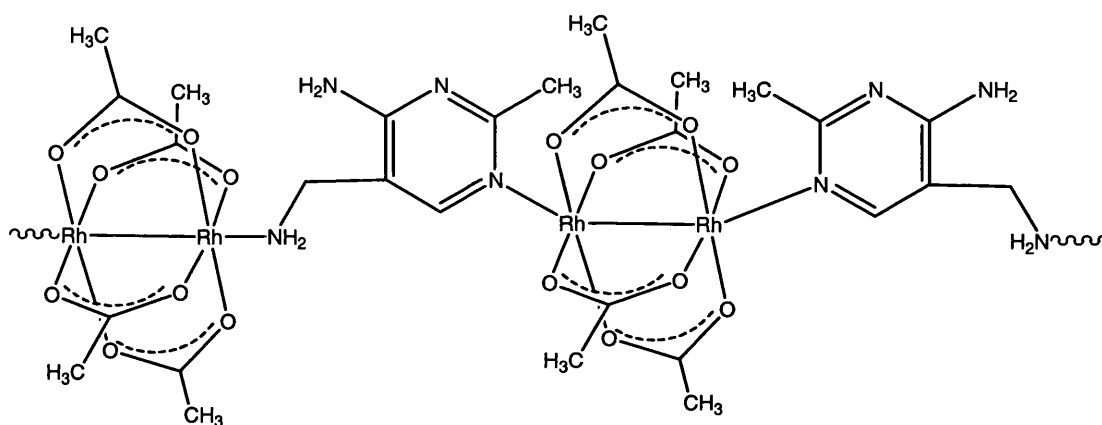


**Figure 5.5** Repeating unit of polymeric  $[\text{Rh}_2(\text{O}_2\text{CCH}_3)_4(\text{aamp})]_n$ <sup>213</sup>

The area of  $[\text{Rh}_2(\text{O}_2\text{CCR})_4(\text{L})]_n$  polymers based only on amine donors is relatively unexplored, with the only solid state X-ray structure of a polymer linked by two amine functionalities being dirhodium tetracpropionate moieties linked by 2,3,5,6-tetramethyl-*p*-phenylenediamine ligands.<sup>202</sup> Reactions of a range of  $[\text{Rh}_2(\text{O}_2\text{CR})_4]$

complexes with macrocyclic nitrogen-donor ligands (Figure 5.6) have been studied, however, and are believed to lead to polymeric compounds, although there is no X-ray crystallographic evidence to support this argument.<sup>214</sup> The adducts  $[\text{Rh}_2(\text{O}_2\text{CR})_4(\mathbf{60})]_n$ ,  $[\{\text{Rh}_2(\text{O}_2\text{CR})_4\}_3(\mathbf{61})_2]_n$  and  $[\{\text{Rh}_2(\text{O}_2\text{CR})_4\}_3(\mathbf{62})_2]_n$  have been reported. The 1:1 stoichiometry of  $[\text{Rh}_2(\text{O}_2\text{CR})_4(\mathbf{60})]_n$  is consistent with a chain polymeric structure with two of the four nitrogen donor atoms coordinated to different  $[\text{Rh}_2(\text{O}_2\text{CR})_4]$  units, and the other two nitrogen atoms non-metallated. The products containing the tridentate ligands have a stoichiometry which suggests that each ligand is coordinated to three different dirhodium units, thus resulting in a network polymer structure.<sup>214</sup>

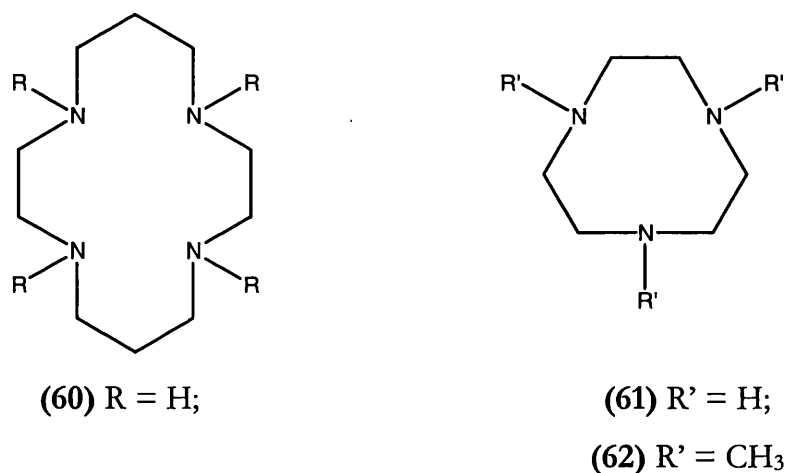
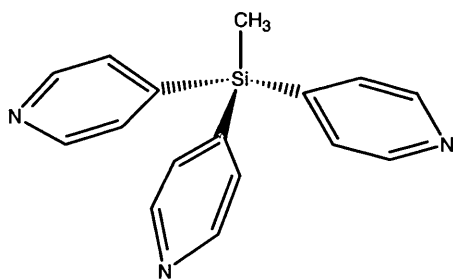


Figure 5.6 Macrocyclic nitrogen-donor ligands

Since the current work utilises the potentially tetradentate ligand hexamethylenetetramine then other polydentate nitrogen donor ligands, not just amines, are of interest. Of particular significance is the nitrogen-donor ligand (63) that has rigidly orientated donor groups rather like hexamethylenetetramine.



(63)

The reaction of **(63)** with  $[\text{Rh}_2(\text{O}_2\text{CCF}_3)_4]$  in benzene produces a compound characterised by X-ray crystallography as a discrete pyramid shaped hexanuclear complex -  $\{[\text{Rh}_2(\text{O}_2\text{CCF}_3)_4]_3\text{CH}_3\text{Si}(\text{C}_5\text{H}_4\text{N})_3(\eta^1\text{-C}_6\text{H}_5)_3\}$ .<sup>215</sup> It is thought that in solution this complex is a building block for larger and more complex supramolecular networks.<sup>215</sup>

#### 5.1.3.4 Adducts of $[\text{Rh}_2(\text{O}_2\text{CR})_4]$ with metallo-ligands

Earlier in this thesis (Chapters Three and Four) attempts to prepare multimetallic complexes with hexamethylenetetramine as a bridging ligand were described. There are a number of reports of the preparation of adducts of  $[\text{Rh}_2(\text{O}_2\text{CR})_4]$  compounds with metallo-ligands. Examples include the chain polymers  $[\{\text{Rh}_2(\text{O}_2\text{CPh})_4\} \{\mu^2\text{-[Fe(CN)}_6\text{]}\}]^{3-n}$ , and  $[\{\text{Rh}_2(\text{O}_2\text{CCH}_3)_4\} \{\mu^2\text{-[Ir(CN)}_3\text{Cp}^*]\}]^-$  which contain nitrile bridges.<sup>216,217</sup> A nitrile bridged two-dimensional polymer is also known;  $[\{\text{Rh}_2(\text{O}_2\text{CCH}_3)_4\} \{\mu^4\text{-[Co(CN)}_6\text{]}\}]^{3-}$ .<sup>218</sup> Illustrated in **Figure 5.7** is a 1:2 adduct containing one dirhodium unit and two rhenium moieties bridged by a 4,4'-bipyridyl ligand, prepared by addition of a THF solution of  $[\text{Re}(\text{CO})_3(2,2'\text{-bpy})(4,4'\text{-bpy})](\text{CF}_3\text{SO}_3)$  to a solution of  $[\text{Rh}_2(\text{OCCH}_3)_4]$  in THF. Cyclic voltammetry studies on this complex suggest that the interactions between the dirhodium unit and the rhenium moieties are easily disrupted by donor solvents such as acetonitrile.<sup>219</sup>

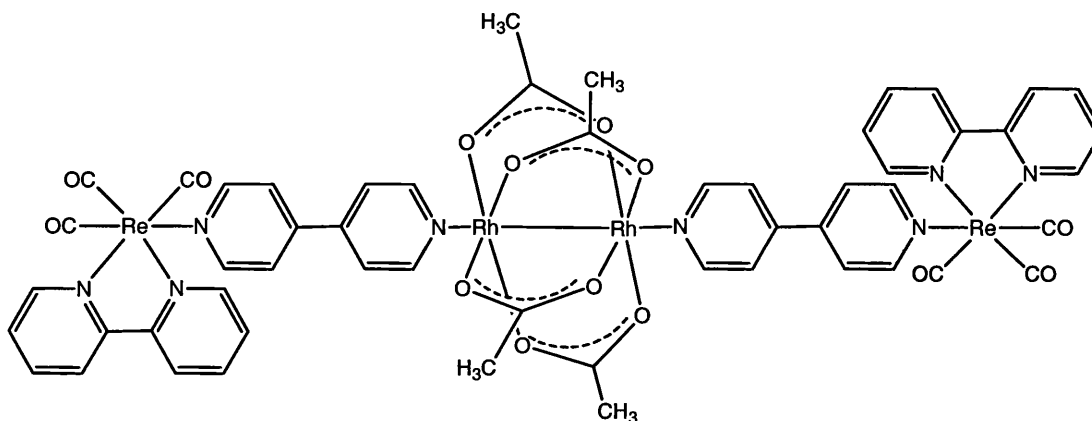


Figure 5.7 1:2 adduct of  $[\text{Rh}_2(\text{O}_2\text{CR})_4]$  with a rhenium containing ligand

#### 5.1.4 Electrochemical studies on $[\text{Rh}_2(\text{O}_2\text{CR})_4\text{L}_2]$ complexes

The electrochemistry of dirhodium tetracarboxylate complexes has been widely studied in recent years and is a convenient way to monitor axial ligation. In fact, one of the earliest systematic studies on dirhodium tetracarboxylate compounds reported both the effects of the axial ligand, L, and of substituent, R, upon the electrochemistry of  $[\text{Rh}_2(\text{O}_2\text{CR})_4\text{L}_2]$  compounds.<sup>220</sup> This study observed a reversible one-electron oxidation of  $[\text{Rh}_2(\text{O}_2\text{CR})_4]$  ( $\text{R} = \text{CMe}_3, \text{Pr}, \text{Et}, \text{Me}, \text{PhCH}_2, \text{MeOCH}_2, \text{PhOCH}_2, \text{MeCHCl}$ ) at a platinum electrode, to give stable Rh(II)-Rh(III) dimers. The researchers observed a linear relationship between the half-wave potentials and the nature of R (using Taft's polar substituent parameters<sup>221</sup>), indicating stabilisation of the higher oxidation state of rhodium by the more electron donating substituents.<sup>220</sup> This was further confirmed by the fact that an oxidation step was not observed for  $[\text{Rh}_2(\text{O}_2\text{CF}_3)_4]$  (within solvent limits), consistent with the strong electron-withdrawing substituents stabilising the Rh(II) oxidation state. Of more significance to the research described in this chapter are the experiments which identified the effects of axial donor ligands on the redox chemistry of  $[\text{Rh}_2(\text{O}_2\text{CR})_4\text{L}_2]$ .<sup>220</sup> In this work the axial ligands are provided by the solvent in which  $[\text{Rh}_2(\text{O}_2\text{CR})_4]$  is dissolved, after first being desolvated by drying at  $80^\circ\text{C}$  *in vacuo*. The donor ability of each solvent was quantified using the empirical parameter: Guttmann's donor number,<sup>222</sup> and these values were plotted against the half-wave potential for the oxidation of the

complex. The resulting plot showed that the higher the donor number the lower the  $E_{1/2}$ . Thus as the donor ability of the solvent increases so does the ease of oxidation. Electrochemical studies have also been carried out on 1:2 and 1:1 adducts of  $[\text{Rh}_2(\text{O}_2\text{C}_4\text{H}_7)_4]$  with Lewis bases including MeCN, py, DMSO and piperidine. These show that the 1:2 adducts were more easily oxidised than the 1:1 adducts.<sup>190</sup> These studies have demonstrated that it is possible to predict the ease with which an adduct will be oxidised depending upon its axial ligand. Hexamethylenetetramine may be considered as having a donor number similar to triethylamine (donor number  $61.0 \text{ kcal mol}^{-1}$ ) and therefore the adduct  $[\text{Rh}_2(\text{O}_2\text{CR})_4(\text{hmt})_2]$  might be expected to undergo a one-electron oxidation at a relatively low  $E_{1/2}$ . Correspondingly, dichloromethane has a donor number of less than  $1.0 \text{ kcal mol}^{-1}$ , thus,  $E_{1/2}$  for  $[\text{Rh}_2(\text{O}_2\text{CR})_4]$  in this non-coordinating solvent is expected to be much higher than that observed for  $[\text{Rh}_2(\text{O}_2\text{CR})_4(\text{hmt})_2]$ , and in fact most other  $[\text{Rh}_2(\text{O}_2\text{CR})_4\text{L}_2]$  complexes. Observations of the redox chemistry of the adduct formed between  $[\text{Rh}_2(\text{O}_2\text{CR})_4]$  and  $[\text{Pd}(\eta^3\text{-C}_3\text{H}_7)(\text{hmt})\text{Cl}]$  will be particularly interesting, since a comparison of the  $E_{1/2}$  value for the oxidation of this species compared with that of  $[\text{Rh}_2(\text{O}_2\text{CR})_4(\text{hmt})_2]$  will indicate which has the better donor ability. Consequently, it will be possible to determine the nature/extent (if any) of the interaction between the rhodium and palladium ions across the hexamethylenetetramine bridge.

## 5.2 Results and discussion

### 5.2.1 Synthetic investigations

The emerald green compound  $[\text{Rh}_2(\text{O}_2\text{CCH}_2\text{CH}_3)_4(\text{CH}_3\text{CH}_2\text{CO}_2\text{H})_2]$  was produced *via* ligand exchange after refluxing  $[\text{Rh}_2(\text{O}_2\text{CCH}_3)_4]$  in an excess of propionic acid for 24 h. Heating the complex under vacuum produced the pale green desolvated complex  $[\text{Rh}_2(\text{O}_2\text{CCH}_2\text{CH}_3)_4]$ . The reaction of this complex with two equivalents of hexamethylenetetramine in dichloromethane gave a pink solution. The pink solution was reduced to dryness *in vacuo* and the product

extracted into ice-cold toluene. The  $^1\text{H}$  NMR spectrum of the resulting pink solid exhibits three resonances at 298 K: a broad singlet at 5.03 ppm attributable to hexamethylenetetramine and a triplet (0.85 ppm) and quartet (2.02 ppm) assigned to the protons of the propionate ligands. The integral ratios of the hexamethylenetetramine resonance (24H) to the propionate proton resonance (20H) indicate synthesis of the 1:2 adduct. The broad signal for hexamethylenetetramine in the  $^1\text{H}$  NMR spectrum indicates an exchange process is occurring, as observed for the adducts discussed in Chapters Three and Four. In the  $^1\text{H}$  NMR spectrum recorded at 223 K different environments are observed for the propionate ligands, suggesting the presence of two distinct species. This is confirmed by analysis of the hexamethylenetetramine signals at 223 K, where three distinct sets of signals are observed **Figure 5.8**. A singlet and AB quartet are observed, and ascribed to the 2:1 adduct, as well as a singlet attributable to non-coordinated hexamethylenetetramine, signals with a 2:8:2 ratio are ascribed to the complex illustrated in **Figure 5.9**. At this temperature the solution contains a mixture of  $[\text{Rh}_2(\text{O}_2\text{CCH}_2\text{CH}_3)_4(\text{hmt})_2]$  and  $[\{\text{Rh}_2(\text{O}_2\text{CCH}_2\text{CH}_3)_4\}_2(\mu\text{-hmt})]$ . Attempts to separate the two complexes by fractional crystallisation were unsuccessful. Section 5.2.2 describes electrochemical experiments on the two complexes.

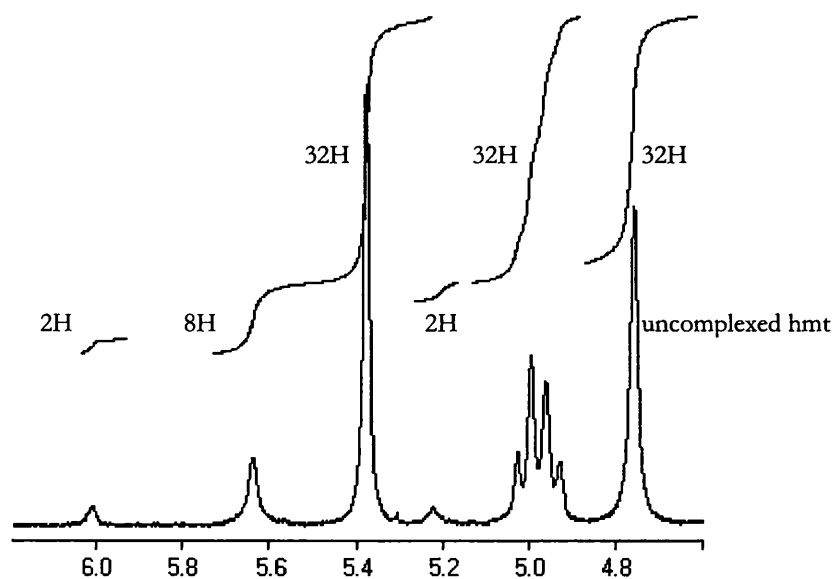


**Figure 5.8**  $^1\text{H}$  NMR spectrum at 223 K, of  $[\text{Rh}_2(\text{O}_2\text{CCH}_2\text{CH}_3)_4(\text{hmt})_2]$  and  $[\{\text{Rh}_2(\text{O}_2\text{CCH}_2\text{CH}_3)_4\}_2(\mu\text{-hmt})]$  between 4.6 and 6.2 ppm

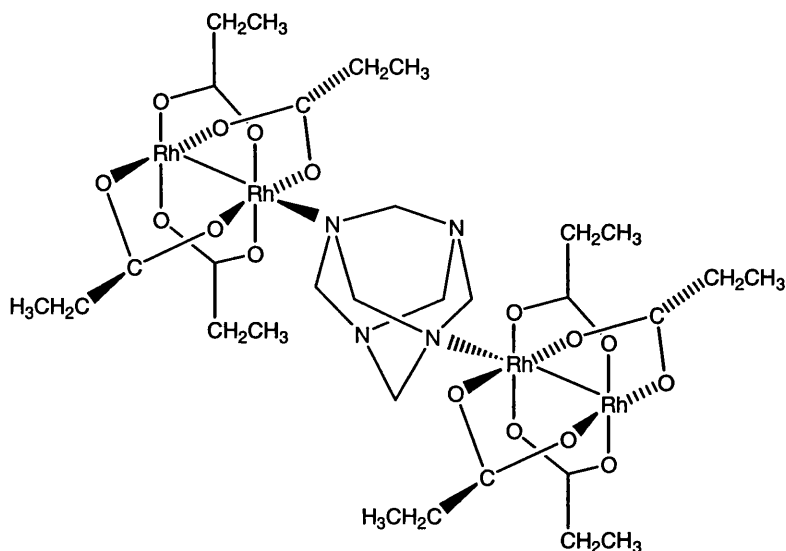


Figure 5.9 The complex  $[\{\text{Rh}_2(\text{O}_2\text{CCH}_2\text{CH}_3)_4\}_2(\mu\text{-hmt})]$

### 5.2.2 Electrochemical Investigations

The electrochemical behaviour of a number of adducts of  $[\text{Rh}_2(\text{O}_2\text{CCH}_2\text{CH}_3)_4]$  has been studied in DCM (0.1 M or 0.2 M supporting electrolyte) using cyclic voltammetry. The redox behaviour of  $[\text{Rh}_2(\text{O}_2\text{CCH}_2\text{CH}_3)_4]$  is well known, however, for comparative purposes an initial electrochemical experiment was performed on  $[\text{Rh}_2(\text{O}_2\text{CCH}_2\text{CH}_3)_4]$  in dichloromethane. The resulting cyclic voltammogram exhibits a single oxidation peak on the forward scan and a coupled reverse reduction peak on the return scan, giving a half-wave potential of 1.32 V (scan rate,  $100 \text{ mV s}^{-1}$ ). The reversible one-electron oxidation of ferrocene in the same cell had a separation between  $E_{\text{pa}}$  and  $E_{\text{pc}}$  of  $125 \text{ mV} \pm 5 \text{ mV}$ . This value is higher than the 59 mV expected for a one-electron transfer because of the internal resistance of the cell. The peak separation ( $E_{\text{pa}} - E_{\text{pc}}$ ) observed for  $[\text{Rh}_2(\text{O}_2\text{CCH}_2\text{CH}_3)_4]$  in this cell is 130 mV, corresponding to a one-electron transfer, as expected. Cyclic voltammograms were obtained at a variety of scan rates from  $20 - 500 \text{ mV s}^{-1}$ . In this range the  $E_{1/2}$  does not vary significantly and the ratio of the forward and reverse currents is unity. These factors confirm the occurrence of a fully reversible one-electron oxidation. **Figure 5.10** illustrates the cyclic voltammogram observed when less than two mole equivalents of hexamethylenetetramine are added to the

electrochemical cell containing  $[\text{Rh}_2(\text{O}_2\text{CCH}_2\text{CH}_3)_4]$ . The addition results in the appearance of an oxidation peak at 1.18 V on the forward scan, coupled with a reduction peak at 1.13 V on the reverse scan, *i.e.*  $E_{1/2}$  1.16 V. It is assumed that this is the one-electron oxidation of the adduct  $[\{\text{Rh}_2(\text{O}_2\text{CCH}_2\text{CH}_3)_4\}_2(\mu\text{-hmt})]$ . The proximity of the peaks for each complex ( $[\text{Rh}_2(\text{O}_2\text{CCH}_2\text{CH}_3)_4]$  and  $[\{\text{Rh}_2(\text{O}_2\text{CCH}_2\text{CH}_3)_4\}_2(\mu\text{-hmt})]$ ) hindered any further observations in this case.

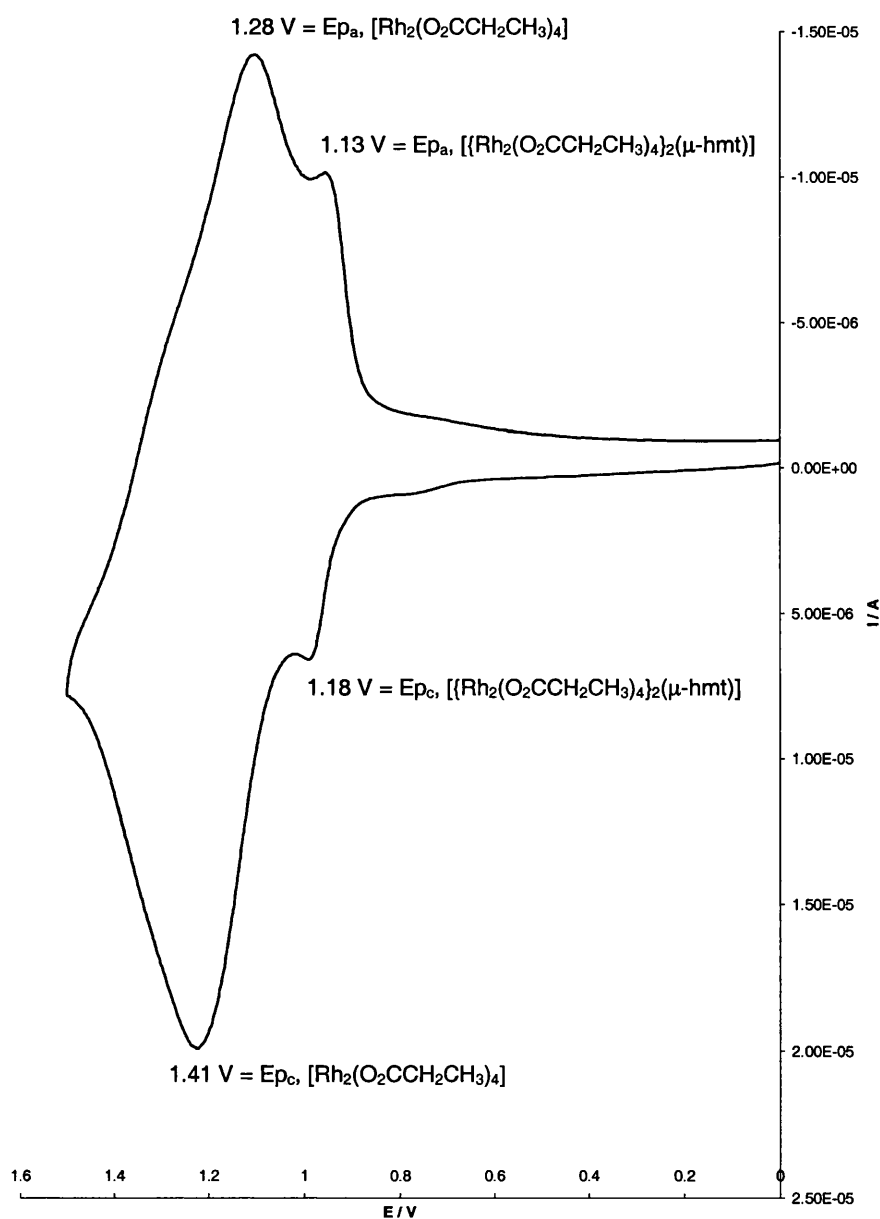


Figure 5.10 Cyclic voltammogram recorded in DCM (0.1 M  $\text{TBABF}_4$  supporting electrolyte) for  $[\text{Rh}_2(\text{O}_2\text{CCH}_2\text{CH}_3)]$  and hexamethylenetetramine



In a separate experiment, the addition of a small excess of two mole equivalents of hexamethylenetetramine to a cell containing  $[\text{Rh}_2(\text{O}_2\text{CCH}_2\text{CH}_3)_4]$  resulted in cyclic voltammograms exhibiting peaks for the reversible one-electron oxidation of the 1:2 adduct  $[\text{Rh}_2(\text{O}_2\text{CCH}_2\text{CH}_3)_4(\text{hmt})_2]$ , **Figure 5.11**. The observed half-wave potential is 0.95 V, lower than that observed for  $[\text{Rh}_2(\text{O}_2\text{CCH}_2\text{CH}_3)_4]$  because the improved donor ability of hexamethylenetetramine (compared with DCM) makes oxidation easier. The peak-to-peak separation of the forward and reverse waves is  $85 \text{ mV} \pm 15 \text{ mV}$ , corresponding to a one-electron transfer process, since  $E_{\text{pa}} - E_{\text{pc}}$  for ferrocene in the same cell is 80 mV. The ratio of the forward and reverse currents at scan rates 20, 50 and  $100 \text{ mV s}^{-1}$  is unity.

The cyclic voltammogram of hexamethylenetetramine under the same conditions exhibits a peak at 1.62 V attributable to the irreversible oxidation of the organic molecule, since no return wave is observed. The recording of consecutive scans at  $100 \text{ mV s}^{-1}$  reveals a drop in current consistent with the coating of the electrode by the species produced on oxidation.

Interestingly, the  $E_{1/2}$  for  $[\text{Rh}_2(\text{O}_2\text{CCH}_2\text{CH}_3)_4(\text{hmt})_2]$  is lower than that for  $[\{\text{Rh}_2(\text{O}_2\text{CCH}_2\text{CH}_3)_4\}_2(\mu\text{-hmt})]$  (1.16 V) which indicates that a monodentate hexamethylenetetramine ligand is a better donor than a bridging hexamethylenetetramine ligand. This is simply explained as on complexation of one nitrogen atom the remaining nitrogen atoms become poorer donors. This is a straightforward effect based on the argument that bonding to the Rh(II) ion causes an inductive effect, withdrawing electron density from the lone pairs of the three non-metallated nitrogen atoms, thus making them poorer donors.

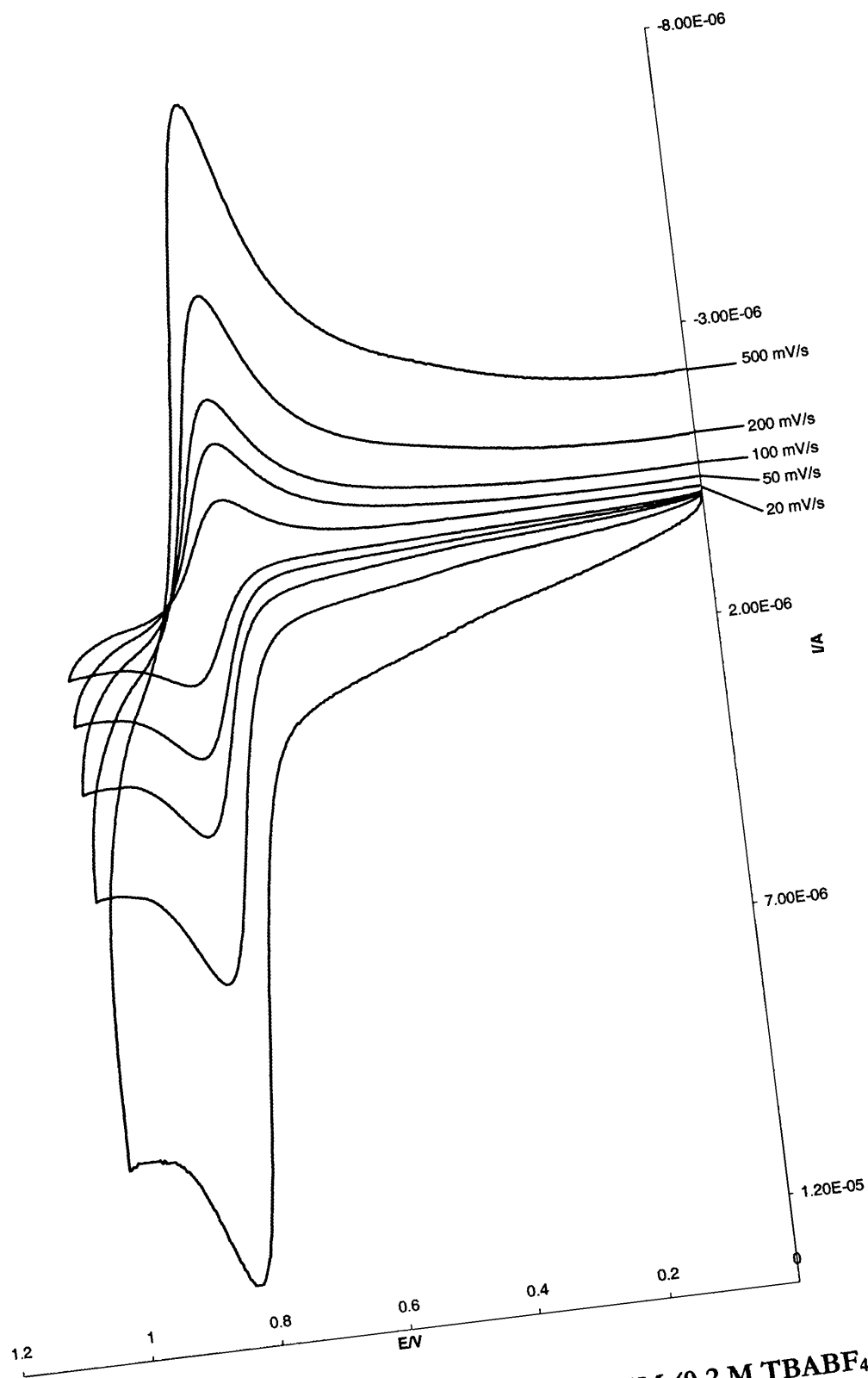


Figure 5.11 Cyclic voltammogram recorded in DCM (0.2 M TBABF<sub>4</sub> supporting electrolyte) [Rh<sub>2</sub>(O<sub>2</sub>CCH<sub>2</sub>CH<sub>3</sub>)(hmt)<sub>2</sub>] over a range of scan rates

For comparison purposes the electrochemistry of  $[\text{Rh}_2(\text{O}_2\text{CCH}_2\text{CH}_3)_4(\text{NEt}_3)_2]$  was investigated. First, the adduct  $[\text{Rh}_2(\text{O}_2\text{CCH}_2\text{CH}_3)_4(\text{NEt}_3)_2]$  was prepared by dissolution of  $[\text{Rh}_2(\text{O}_2\text{CCH}_2\text{CH}_3)_4]$  in an excess of neat triethylamine, followed by evaporation of the solvent in air. This produced a mixture of the green starting material and the purple 1:2 adduct. This observation indicates that triethylamine does not bind very well to  $[\text{Rh}_2(\text{O}_2\text{CCH}_2\text{CH}_3)_4]$ , a result which was further confirmed by the electrochemical experiment. The green/purple mixture was dissolved in DCM in the electrochemical cell to produce a green solution. The resulting cyclic voltammogram exhibits three oxidation peaks on the forward scan, at 1.09, 1.21 and 1.43 V. The peak at 1.43 V is coupled with a peak at 1.28 V on the reverse scan. The observed half-wave potential, 1.36 V was attributed to the one-electron oxidation of the starting material,  $[\text{Rh}_2(\text{O}_2\text{CCH}_2\text{CH}_3)_4]$ . A cyclic voltammogram of triethylamine alone confirms the peak at 1.09 V as that of the irreversible oxidation of the amine. Thus, the peak at 1.21 V is attributed to the 1:2 adduct. Cooling the cell to 223 K resulted in a pink solution, indicative of coordination of triethylamine to the dirhodium complex, unfortunately the broad nature of the peaks at this temperature prevented any accurate measurements of potential or currents.

The electrochemistry of the 1:2 adduct of  $[\text{Rh}_2(\text{O}_2\text{CCH}_2\text{CH}_3)_4]$  with the metalloligand  $[\text{PdCl}(\eta\text{-C}_4\text{H}_7)(\text{hmt})]$  was also investigated. The adduct was prepared in situ *via* addition of  $[\text{PdCl}(\eta\text{-C}_4\text{H}_7)(\text{hmt})]$  to an electrochemical cell containing  $[\text{Rh}_2(\text{O}_2\text{CCH}_2\text{CH}_3)_4]$  in DCM (0.2 M TBABF<sub>4</sub>), until a pink solution was observed. The cyclic voltammograms obtained at this point showed a *pseudo*-reversible one-electron oxidation with an  $E_{1/2}$  of 1.01 V. Over a range of scan rates (20-500 mV s<sup>-1</sup>) the ratio of the forward and reverse peak currents is  $0.71 \pm 0.08$ . The most interesting feature of these cyclic voltammograms, however, is that the half-wave potential for the oxidation is slightly higher than that observed for  $[\text{Rh}_2(\text{O}_2\text{CCH}_2\text{CH}_3)_4(\text{hmt})_2]$ , implying that unmetallated hexamethylenetetramine is a better donor ligand than  $[\text{PdCl}(\eta\text{-C}_4\text{H}_7)(\text{hmt})]$ . This may be explained using the same rationale as described earlier for the oxidation

of  $[\{\text{Rh}_2(\text{O}_2\text{CCH}_2\text{CH}_3)_4\}_2(\mu\text{-hmt})]$  at a higher potential than  $[\text{Rh}_2(\text{O}_2\text{CCH}_2\text{CH}_3)_4(\text{hmt})_2]$ .

### 5.3 Conclusions

The complexes  $[\text{Rh}_2(\text{O}_2\text{CCH}_2\text{CH}_3)_4(\text{hmt})_2]$  and  $[\{\text{Rh}_2(\text{O}_2\text{CCH}_2\text{CH}_3)_4\}_2(\mu\text{-hmt})]$  have been synthesised. Although these complexes were not isolated in pure form, low temperature  $^1\text{H}$  NMR spectroscopy at 223 K confirms their synthesis. The redox properties of both complexes have been investigated using cyclic voltammetry. Using these electrochemical results, the donor ability of a number of ligands has been determined. The donor ability of the ligands investigated is  $\text{hmt} > [\text{PdCl}(\eta^3\text{-C}_4\text{H}_7)(\text{hmt})] > [\text{Rh}_2(\text{O}_2\text{CCH}_2\text{CH}_3)_4(\text{hmt})]$ . A simple rationale for this ordering has been suggested.

### 5.4 Experimental

#### 5.4.1 Reaction of $[\text{Rh}_2(\text{O}_2\text{CCH}_2\text{CH}_3)_4]$ with two equivalents of hexamethylenetetramine

$[\text{Rh}_2(\text{O}_2\text{CCH}_2\text{CH}_3)_4]$  (50 mg, 0.10 mmol) was dissolved in dichloromethane (6 cm<sup>3</sup>) and hexamethylenetetramine (31 mg, 0.22 mmol) was added. The resulting pink solution was stirred under nitrogen for 2 h, reduced *in vacuo* to half volume then cooled overnight. The solution was reduced to dryness *in vacuo*, washed with ice-cold toluene and dried under vacuum. Yield 0.42 mg.

$\delta_{\text{H}}$  (400 MHz; CDCl<sub>3</sub>; 298 K) 0.85 (12H, t, CH<sub>3</sub>), 2.02 (8H, q, CH<sub>2</sub>), 5.03 (12H, s, hmt).

$\delta_{\text{H}}$  (400 MHz; CDCl<sub>3</sub>; 223 K) 0.83 (t, CH<sub>3</sub>), 0.85 (t, CH<sub>3</sub>), 2.05 (q, CH<sub>2</sub>), 2.07 (q, CH<sub>2</sub>), 4.76 (s, hmt), 4.98 (AB q, hmt), 5.31 (s, hmt), 5.22 (s, hmt), 5.64 (s, hmt), 6.01 (s, hmt).

#### **5.4.2 General electrochemical procedure**

Cyclic voltammetry studies were conducted using an Eco Chemie Autolab PSTAT10 with supplied software, from Windsor Scientific. A standard three-electrode cell geometry was used throughout. The working electrode was glassy carbon and the counter electrode platinum wire. A silver wire was used as the pseudo-reference electrode. The electrolytic solutions were 0.1 M or 0.2 M TBABF<sub>4</sub> (tetra-*n*-butylammonium tetrafluoroborate) in dichloromethane. Argon was bubbled through each solution to ensure removal of dissolved oxygen before measurements were recorded. In order to calibrate voltammograms ferrocene was added at the end of each experiment. Potentials are reported assuming the FeCp<sub>2</sub>/FeCp<sub>2</sub><sup>+</sup> couple occurs at 0.60 V.

## 5.4.3 Cyclic voltammetry: results

Compound	Scan rate mV/s	$E_{1/2}$ V	$\Delta E$ V	$i_{pa}/i_{pc}$
[Rh <sub>2</sub> (O <sub>2</sub> CCH <sub>2</sub> CH <sub>3</sub> ) <sub>4</sub> ]	20	1.34	0.13	1.00
	50	1.33	0.13	1.00
	100	1.32	0.12	1.00
	200	1.31	0.12	1.00
	500	1.30	0.13	1.00
[{Rh <sub>2</sub> (O <sub>2</sub> CCH <sub>2</sub> CH <sub>3</sub> ) <sub>4</sub> } <sub>2</sub> ( $\mu$ -hmt)]	100	1.16	–	<sup>a</sup>
[Rh <sub>2</sub> (O <sub>2</sub> CCH <sub>2</sub> CH <sub>3</sub> ) <sub>4</sub> (hmt) <sub>2</sub> ]	20	0.95	0.07	1.0
	50	0.95	0.08	1.03
	100	0.95	0.08	1.02
	200	0.95	0.09	<sup>c</sup>
	500	0.95	0.10	<sup>c</sup>
hexamethylenetetramine	100	1.62 <sup>b</sup>	–	–
[Rh <sub>2</sub> (O <sub>2</sub> CCH <sub>2</sub> CH <sub>3</sub> ) <sub>4</sub> {PdCl( $\eta^3$ -C <sub>4</sub> H <sub>7</sub> )(hmt)} <sub>2</sub> ]	20	1.00	0.11	0.63
	50	1.00	0.12	0.66
	100	1.01	0.13	0.74
	200	1.01	0.13	0.79
	500	1.02	0.17	0.77

<sup>a</sup>Could not be reliably determined due to peak overlap. <sup>b</sup>Irreversible oxidation  $E_{pa}$  given. <sup>c</sup>Could not be reliably determined.

# References

---

1. A. Butlerow, *Ann.*, 1859, **111**, 250.
2. J. F. Walker, *Formaldehyde*, Reinhold, New York, 1964, 3<sup>rd</sup> Ed., Ch. 20.
3. E. M. Smolin and L. Rapoport, *The Chemistry of Heterocyclic Compounds: s-Triazines and Derivatives*, Interscience, New York and London, 1959, Ch. X.
4. F. Meissner, *British Patent* 722434, 1955.
5. Belstein, **1**, 583.
6. H. A. Schiotz and K. Guttu, *Acta Obstetrica et Gynecologica Scandinavica*, 2002, **81**, 743.
7. L. N. Becka and D. W. J. Cruickshank, *Proc. R. Soc. London, Ser. A*, 1963, **273**, 435.
8. R. G. Dickinson and A. L. Raymond, *J. Am. Chem. Soc.*, 1923, **45**, 22.
9. P. Duden and M. Scharf, *Ann.*, 1895, 218.
10. G. Lösekann, *Chem. Ztg.*, 1890, **14**, 1409.
11. J. H. van't Hoff, *Ansichten über organische Chemie*, Braunschweig, 1881, Vol. I, p.121.
12. M. Dominkiewicz, *Arch. Chem Farm.*, 1939, **4**, 1.
13. V. Schomaker and P. A. Shaffer, Jr., *J. Am. Chem. Soc.*, 1947, **69**, 1555.
14. A. F. Andresen, *Acta Cryst.*, 1957, **10**, 107.
15. S. P. Kampermann, T. M. Sabine, B. M. Craven and R. K. McMullan, *Acta Cryst.*, 1995, **A51**, 489.
16. S. P. Kampermann, J. P. Ruble and B. M. Craven, *Acta Cryst.*, 1994, **B50**, 737.
17. T. C. W. Mak, W. K. Li and W. H. Yip, *Acta Cryst.*, 1983, **C39**, 134.
18. P. K. Hon, T. C. W. Mak and J. Trotter, *Inorg. Chem.*, 1979, **18**, 2916.
19. T. C. W. Mak, M. F. C. Ladd and D. C. Povey, *J. Chem. Soc., Perkin Trans.*, **2**, 1979, 593.
20. F. Hanic and V. Šubtová, *Acta Cryst.*, 1969, **B25**, 405.

21. K. Y. Hui, P. C. Chan and T. C. W. Mak, *Inorg. Chim. Acta*, 1984, **84**, 25.
22. H. H. Richmond, G. S. Myers and George F. Wright, *J. Am. Chem. Soc.*, 1948, **70**, 3659.
23. A. T. Nielsen, D. W. Moore, M. D. Ogan and R. L. Atkins, *J. Org. Chem.*, 1979, **44**, 1678.
24. M. L. Boyd and C. A. Winkler, *Can. J. Res.*, 1947, **25B**, 387.
25. S. Bose, *J. Ind. Chem. Soc.*, 1957, **34**, 663.
26. M. A. Azim and M. Shafi, *J. Nat. Sci. Math.*, 1966, **6**, 203.
27. Y. Ogata and A. Kawasaki, *Bull. Chem. Soc. Jpn.*, 1964, **37**, 514.
28. R. K. Wood and W. F. Stevens, *J. Appl. Chem.*, 1964, **14**, 325.
29. J. R. Polley, C. A. Winkler and R. V. V. Nicholls, *Can. J. Research*, 1947, **25B**, 525.
30. E. Slowick and R. Kelley, *J. Am. Pharm. Assoc.*, 1942, **31**, 15.
31. *Reagents for Organic Synthesis*, Fieser and Fieser, Wiley, 1<sup>st</sup> Ed., 427.
32. N. Blažević, D. Kolbah, B. Belin, V. Šunjić and F. Kajfež, *Synthesis*, 1979, 161.
33. S. J. Angyal, *Org. React.*, 1954, **8**, 197.
34. J. C. Duff, *J. Chem. Soc.*, 1941, 547.
35. T. L. Davis, *The Chemistry of Powder and Explosives*, John Wiley & Sons, New York, 1943, Vol. II, p. 451.
36. W. E. Bachmann and J. C. Sheenan, *J. Am. Chem. Soc.*, 1949, **71**, 1842.
37. W. Bachmann and N. Deno, *J. Am. Chem. Soc.*, 1951, **73**, 2777.
38. P. M. Graham, R. D. Pike, M. Sabat, R. D. Bailey and W. T. Pennington, *Inorg. Chem.*, 2000, **39**, 5121.
39. L. Carlucci, G. Ciani, D. M. Proserpio and A. Sironi, *Inorg. Chem.*, 1997, **36**, 1736.
40. M. L. Tong, S. L. Zheng and X. M. Chen, *Chem.-Eur. J.*, 2000, **6**, 3729.
41. Y. Q. Zhu, B. L. Li, Z. Xu, H. B. Liu and K. B. Yu, *Trans. Met. Chem.*, 2001, **26**, 369.



42. Y. Zhang, J. Li, H. Hou, M. Nishiura and T. Imamoto, *J. Mol. Struct.*, 1999, **510**, 191.
43. Y. Zhang, J. Li, M. Nishiura and T. Imamoto, *J. Mol. Struct.*, 2000, **520**, 259.
44. Y. Zhang, J. Li, M. Nishiura and T. Imamoto, *J. Mol. Struct.*, 2000, **523**, 257.
45. M. K. Ammar, T. Jouini and A. Driss, *J. Chem. Cryst.*, 2000, **30**, 265.
46. J. B. Hill, S. J. Eng, W. T. Pennington and G. H. Robinson, *J. Organomet. Chem.*, 1993, **445**, 11.
47. V. J. Pickhardt, *Acta Cryst.*, 1981, **B37**, 1753.
48. R. Meyer, *Explosives*, Verlag Chemie, 2nd Ed.
49. A. T. Nielsen, *Chem. Energ. Mat.*, 1991, 95.
50. E. B. Fleischer, *J. Am. Chem. Soc.*, 1964, **86**, 3889.
51. L. A. Paquette, R. J. Ternansky, D. W. Balogh and G. Kentgen, *J. Am. Chem. Soc.*, 1964, **108**, 1343.
52. J. C. Gallucci, C. W. Doecke and L. A. Paquette, *J. Am. Chem. Soc.*, 1983, **105**, 5446.
53. A. T. Nielsen, Naval Weapons Center Technical Paper No. NWC TP 5452, February, 1973.
54. D. A. Cichra, J. R. Holden and C. R. Dickinson, Naval Surface Weapons Center Technical Report No. NSWC TR-79-273.
55. A. T. Nielsen, A. R. Nissan, J. D. Vanderah, *J. Org. Chem.*, 1990, **55**, 1459.
56. M. R. Crampton, J. Hamid, R. Millarand G. Ferguson, *J. Chem. Soc. Perkin Trans. 2*, 1993, 925.
57. Y. X. Ou, H. P. Jia, B. R. Chen, G. Y. Fang, L. H. Liu, F. P. Zheng, Z. L. Pan and C. Wang, *Science in China Series B – Chemistry*, 1999, **42**, 217.
58. M. F. Foltz, C. L. Loon, F Garcia and A. L. Nichols, *Propellants, Explosives and Pyrotechnics*, 1994, **19**, 19.
59. J. Nelson, V. Mckee, G. Morgan, *Prog. Inorg. Chem.*, 1998, **47**, 167.
60. A. M. Sargeson, *Pure Appl. Chem.*, 1984, **56**, 1603.
61. *Advanced Inorganic Chemistry*, F. A. Cotton and G. Wilkinson Eds., Wiley Interscience, 1988, 5<sup>th</sup> Ed.

62. K. H. Reddy, G. Krishnaiah and Y. Sreenivasulu, *Polyhedron*, 1991, **10**, 2785.
63. M. P. Suh and S. G. Kang, *Inorg. Chem.*, 1988, **27**, 2544.
64. I. I. Creaser, R. J. Geue, J. MacB. Harrowfield, A. J. Herlt, A. M. Sargeson, M. R. Snow and J. Springborg, *J. Am. Chem. Soc.*, 1982, **104**, 6016.
65. J. MacB. Harrowfield and A. M. Sargeson, *J. Am. Chem. Soc.*, 1974, **96**, 2634.
66. J. MacB. Harrowfield, A. J. Herlt, P. A. Lay and A. M. Sargeson, *J. Am. Chem. Soc.*, 1983, **105**, 5503.
67. H. A. Boucher, G. A. Lawrance, P. A. Lay, A. M. Sargeson, A. M. Bond, D. F. Sangster and J. C. Sullivan, *J. Am. Chem. Soc.*, 1983, **105**, 4652.
68. M. P. Suh, W. Shin, D. Kim and S. Kim, *Inorg. Chem.*, 1984, **23**, 618.
69. M. P. Suh and D. Kim, *Inorg. Chem.*, 1985, **24**, 3712.
70. K. Marouka, A. B. Concepcion, N. Murase, M. Oishi, N. Hirayama and H. Yamamoto, *J. Am. Chem. Soc.*, 1993, **115**, 3943.
71. G. A. Bottomley, I. J. Clark, I. I. Creaser, L. M. Engelhardt, R. J. Geue, K. S. Hagen, J. MacB. Harrowfield, G. A. Lawrance, P. A. Lay, A. M. Sargeson, A. J. See, B. W. Skelton, A. H. White and F. R. Wilner, *Aust. J. Chem.*, 1994, **47**, 143.
72. I. I. Creaser, J. MacB. Harrowfield, A. M. Sargeson, B. W. Skelton and A. W. White, *Aust. J. Chem.*, 1993, **46**, 465.
73. P. Comba, I. I. Creaser, L. R. Gahan, J. MacB. Harrowfield, G. A. Lawrance, L. L. Martin, A. W. H. Mau, A. M. Sargeson, W. H. F. Sasse and M. R. Snow, *Inorg. Chem.*, 1986, **25**, 384.
74. P. A. Anderson, I. I. Creaser, C. Dean, J. MacB. Harrowfield, E. Horn, L. L. Martin, A. M. Sargeson, M. R. Snow and E. R. T. Tiekink, *Aust. J. Chem.*, 1993, **46**, 449.
75. A. M. Sargeson, *Pure. Appl. Chem.*, 1978, **50**, 905.
76. A. M. Bond, G. A. Lawrance, P. A. Lay, A. M. Sargeson, *Inorg. Chem.*, 1983, **22**, 2010.

77. *Handbook of Preparative Inorganic Chemistry*, Academic Press, Georg Brauer Ed., 2<sup>nd</sup> Ed, Vol. II.
78. G. W. Watt, *Inorganic Syntheses*, **III**, 194.
79. P. Spacu, C. Gheorghiu, M. Brezeanu and S. Popescu, *Rev. Chem. (Bucharest)*, 1958, **3**, 127.
80. T. Okawara, *J. Synth. Org. Chem. Japan*, 1999, **57**, 280.
81. A. Vogel, *Vogel's Textbook of Practical Organic Chemistry*, Longman, 4<sup>th</sup> Ed., p. 366.
82. J. MacB. Harrowfield, G. A. Lawrance and A. M. Sargeson, *J. Chem. Edu.*, 1985, **65**, 804.
83. L. Moroder, A. Hallett, E. Wiinsch, Okeller and G. Wersin, *Hoppe-Seyler's Z. Physiol. Chem*, 1972, 1652.
84. P. F. Pagoria, A. R. Mitchell, R. D. Schmidt, C. L. Coon and E. S. Jessop, *Nitration Recent Laboratory and Industrial Developments, A.C.S. Symposium Series 623*, 1996, 150.
85. R. J. Geue, T. W. Hambley, J. M. Harrowfield, A. M. Sargeson and M. R. Snow, *J. Am. Chem. Soc.*, 1984, **106**, 5478.
86. M. A. Bennett, T. N. Huang, T. W. Matheson and A. K. Smith, *Inorg. Synth.*, 1982, **21**, 75.
87. M. A. Bennett and A. K. Smith, *J. Chem. Soc. Dalton Trans.*, 1974, 233.
88. G. Winkhaus and H. Singer, *J. Organomet. Chem.*, 1967, **7**, 487.
89. R. A. Zelonka and M. C. Baird, *Can. J. Chem.*, 1972, **50**, 3063.
90. M. A. Bennett, G. B. Robertson and A. K. Smith, *J. Organomet. Chem.*, 1972, **43**, C41.
91. F. B. McCormick and W. B. Gleason, *Acta Cryst.*, 1987, **C44**, 603.
92. D. R. Robertson and T. A. Stephenson, *J. Organomet. Chem.*, 1976, **116**, C29.
93. H. Werner and R. Werner, *Chem. Ber.*, 1982, **115**, 3766.
94. D. R. Robertson and T. A. Stephenson, *J. Organomet. Chem.*, 1977, **142**, C31.
95. D. R. Robertson and T. A. Stephenson, *J. Orgaanomet. Chem.*, 1977, **141**, 325.

96. P. Laruerta, J. Latorre, M. Sanaú, F. A. Cotton and W. Schwotzer, *Polyhedron*, 1988, **7**, 1311.
97. M. A. Bennett, T. R. B. Mitchell, M. R. Stevens and A. C. Willis, *Can. J. Chem.*, 2001, **79**, 655.
98. E. C. Morrison, C. A. Palmer and D. A. Tocher, *J. Organomet. Chem.*, 1988, **349**, 405.
99. D. A. Tocher, R. A. Gould, T. A. Stephenson, M. A. Bennett, J. P. Ennett, T. W. Matheson, L. Sawyer and V. K. Shah, *J. Chem. Soc. Dalton Trans.*, 1983, 1571.
100. F. Faranone, G. A. Loprete and G. Tresoldi, *Inorg. Chim. Acta*, 1979, **34**, L251.
101. M. A. Bennett, M. I. Bruce and T. W. Matheson in *Comprehensive Organometallic Chemistry*, G. Wilkinson, Ed., Pergamon: Oxford, 1982, **4**, 796.
102. H. Le Bozec, D. Touchard and P. H. Dixneuf, *Adv. Organomet. Chem.*, 1989, **29**, 163.
103. G. Consiglio and F. Morandini, *Chem. Rev.*, 1987, **87**, 761.
104. E. L. Muetterties, J. R. Bleeke and E. J. Wucherer, *Chem. Rev.*, 1982, **82**, 499.
105. L. Carter, D. L. Davies, J. Fawcett and D. R. Russell, *Polyhedron*, 1993, **12**, 1123.
106. P. Pertici, S. Bertozzi, R. Lazzaroni, G. Vitulli and M. A. Bennett, *J. Organomet. Chem.*, 1988, **354**, 117.
107. P. Pertici, E. Pitzalis, G. U. Barretta, F. Marchetti and P. Salvadori, *Gazz. Chim. Ital.*, 1995, **125**, 27.
108. M. J. Begley, S. Harrison and A. H. Wright, *Acta Cryst.*, 1991, **C47**, 318.
109. G. Sánchez, J. García, J. Pérez, G. García, G. López and G. Villora, *Thermochim. Acta*, 1997, **293**, 153 .
110. G. García, I. Solano, G. Sánchez, M. Santana, G. López, J. Casabó, E. Molins and C. Miravittles, *J. Organomet. Chem.*, 1994, **467**, 119.

111. P. Pertici, P. salvadori, A. Biasci, G. Vitulli, M. A. Bennett and L. A. P. Kane-Maguire, *J. Chem. Soc. Dalton Trans.*, 1988, 315.
112. R. S. Bates, M. J. Baegley and A. H. Wright, *Polyhedron*, 1990, **12**, 1113.
113. R. Crabtree and A. Pearman, *J. Organomet. Chem.*, 1977, **141**, 325.
114. G. García, I. Solano, G. Sánchez and G. López, *Polyhedron*, 1995, **14**, 1855.
115. M. R. Churchill, S. A. Julis and F. J. Rotella, *Inorg. Chem.*, 1977, **16**, 1137.
116. C. White, S. J. Thompson and P. M. Maitlis, *J. Chem. Soc. Dalton Trans.*, 1977, 1654.
117. C. White and P. M. Maitlis, *J. Chem. Soc. A*, 1971, 3322.
118. J. W. Kang, K. Moseley and P. M. Maitlis, *J. Am. Chem. Soc.*, 1969, **91**, 5970.
119. K. Isobe, P. M. Bailey and P. M. Maitlis, *J. Chem. Soc. Dalton Trans.*, 1981, 2003.
120. W. D. Jones and V. L. Kuykendall, *Inorg. Chem.*, 1991, **30**, 2615.
121. D. S. Gill and P. M. Maitlis, *J. Organomet. Chem.*, 1975, **87**, 359.
122. F. Faranone, V. Marsala and G. Tresoldi, *J. Organomet. Chem.*, 1978, **152**, 337.
123. W. Rigby, J. A. McCleverty and P. M. Maitlis, *J. Chem. Soc. Dalton Trans.*, 1979, 382.
124. G. García, G. Sánchez, I. Romero, I. Solano, M. D. Santana and G. López, *J. Organomet. Chem.*, 1991, **408**, 241.
125. G. Sánchez, J. García, J. Pérez, G. García and G. López, *Thermochim. Acta*, 1997, **307**, 127.
126. L. Porri, M. C. Galazzi, A. Columbo and G. Allegra, *Tetrahedron Lett.*, 1965, 4187.
127. A. Columbo and G. Allegra, *Acta Cryst.*, 1971, **B27**, 1653.
128. D. N. Cox and R. Roulet, *Inorg. Chem.*, 1990, **29**, 1360.
129. R. A. Head, J. F. Nixon, J. R. Swain and C. M. Woodard, *J. Organomet. Chem.*, 1974, **76**, 393.
130. D. N. Cox, R. W. H. Small and R. Roulet, *J. Chem. Soc. Dalton Trans.*, 1991, 2013.

131. J. W. Steed and D. A. Tocher, *J. Organomet. Chem.*, 1994, **471**, 221.
132. J. W. Steed and D. A. Tocher, *J. Organomet. Chem.*, 1991, **412**, C34.
133. J. W. Steed and D. A. Tocher, *Polyhedron*, 1992, **11**, 2729.
134. R. Aronson, M. R. J. Elsegood, J. W. Steed and D. A. Tocher, *Polyhedron*, 1991, **10**, 1727.
135. C. S. Allardyce, P. J. Dyson, D. J. Ellis and S. L. Heath, *J. Chem. Soc. Chem. Commun.*, 2001, 1396.
136. B. Chaudret, F. Jalón and M. Pérez-Manrique, *New. J. Chem.*, 1990, **14**, 331.
137. W. S. Sheldrick and H. S. Hagen-Eckhard, *J. Organomet. Chem.*, 1991, **410**, 73.
138. Z. Otwinowski and W. Minor in *Methods in Enzymology*, C. W. Carter Jr. and R. M. Sweet Eds., Academic Press, New York, 1996 .
139. G. M. Sheldrick, SHELXL-86, *Acta Cryst.*, 1990, **A46**, 467.
140. G. M. Sheldrick, SHELXL-93, University of Gottingen, 1993.
141. Structure determination performed by J. W. Steed at Kings College, London.
142. R. J. Goodfellow, J. G. Evans, P. L. Goggin and D. A. Duddell, *J. Chem. Soc. A*, 1968, 1604.
143. A. W. Verstuyft, L. W. Cary and J. H. Nelson, *Inorg. Chem.*, 1975, **14**, 1495.
144. H. Dietl, H. Reinheimer, J. Moffat and P. M. Maitlis, *J. Am. Chem. Soc.*, 1938, **92**, 2276.
145. P. M. Maitlis, P. Espinet and M. J. H. Russell 'Palladium: Introduction and General Principles' in *Comprehensive Organometallic Chemistry*, G. Wilkinson, Ed., Pergamon: Oxford, 1982, **6**, 238.
146. J. R. Holden and N. C. Baenziger, *Acta Cryst.*, 1956, **9**, 194.
147. M. S. Kharasch, R. C. Seyler and F. R. Mayo, *J. Am. Chem. Soc.*, 1938, **60**, 882.
148. M. M. Olmstead, P. W. Wei, A. S. Ginwalla and A. L. Balch, *Inorg. Chem.*, 2000, **39**, 4555.

149. X. M. Luo, X. H. Chen, S. S. S. Raj, H. K. Fun and L. G. Zhu, *Acta Cryst.*, 1999, **C55**, 1220.
150. D. R. Jensen, J. S. Pugsley and M. S. Sigman, *J. Am. Chem. Soc.*, 2001, **123**, 7475.
151. T. J. Hubin, J. M. McCormack, N. W. Alcock and D. H. Busch, *Inorg. Chem.*, 1998, **37**, 6549.
152. P. Nilsson, M. Larhead and A. Halberg, *J. Am. Chem. Soc.*, 2001, **123**, 8217.
153. A. Constable, W. S. McDonald and B. L. Shaw, *J. Chem. Soc. Dalton Trans.*, 1979, 496.
154. A. E. Smith, *Acta Cryst.*, 1965, **18**, 331.
155. F. R. Hartley, *The Chemistry of Platinum and Palladium*, Applied Science, London, 1973.
156. P. M. Maitlis, *The Organic Chemistry of Palladium, Volume I Metal Complexes*, Academic Press, NY, 1971.
157. P. M. Maitlis, P. Espinet and M. J. H. Russell 'Allylic complexes of Pd(II)' in *Comprehensive Organometallic Chemistry*, G. Wilkinson, Ed., Pergamon: Oxford, 1982, **6**, 385.
158. J. C. W. Chien and H. C. Dehm, *Chem. Ind.*, 1961, 745.
159. K. C. Ramey and G. L. Statton, *J. Am. Chem. Soc.*, 1966, **88**, 4387.
160. J. Chatt, N. P. Johnson and B. L. Shaw, *J. Chem. Soc.*, 1964, 1625.
161. A. J. Deeming, M. N. Meah and M. B. Hursthouse, *J. Chem. Soc. Dalton Trans.*, 1998, 235.
162. P. Ganis, G. Maglio, A. Musco and A. L. Segre, *Inorg. Chim. Acta*, 1969, **3**, 266.
163. J. W. Faller and M. Incorvia, *J. Organomet. Chem.*, 1970, **19**, P13.
164. B. M. Trost and D. L. Van Vranken, *Chem. Rev.*, 1996, **96**, 395.
165. Y. Tatsumo, T. Yashida and S. Otsuka, *Inorg. Synth.*, 1979, **19**, 220.
166. B. T. Khan, K. M. Mohan, S. R. A. Kahn, K. Venkatasubramanian and T. Satyanarayana, *Polyhedron*, 1996, **15**, 63.
167. G. Bandoli and D. A. Clemente, *Acta Cryst.*, 1980, **B37**, 490.

168. J. P. Sutter, M. Pfeffer, A. De Cian and J. Fischer, *Organometallics*, 1992, **11**, 386.
169. P. A. van der Schaaf, J. P. Sutter, M. Grellier, G. P. M. van Mier, A. L. Spek, G. van Koten and M. Pfeffer, *J. Am. Chem. Soc.*, 1994, **116**, 5134.
170. N. W. Murrall and A. J. Welch, *J. Organomet. Chem.*, 1986, **301**, 109.
171. Y. Kitano, T. Kajimoto, M. Kashiwagi and Y. Kinoshita, *J. Organomet. Chem.*, 1971, **33**, 123.
172. *gNMR 4.1* Cherwell Scientific Ltd. © Ivory Soft.
173. S. Hansson, P. O. Norrby, M. P. T. Sjögren, B. Åkermark, M. E. Cucciolito, F. Giordano and A. Vitagliano, *Organometallics*, 1993, **12**, 4940.
174. F. De Candia, G. Maglio, A. Musco and G. Paiaro, *Inorg. Chim. Acta*, 1968, **2**, 233.
175. A. Albinati, R. W. Kunz, C. J. Ammann and P. S. Pregosin, *Organometallics*, 1991, **10**, 1800.
176. F. G. Riddell and P. Murray-Rust, *J. Chem. Soc., Chem. Commun.*, 1970, 1075.
177. P. Murray-Rust, *J. Chem. Soc. Perkin Trans.*, 1974, 1136.
178. G. M. Sheldrick, SHELXL-86, *Acta Cryst.*, 1990, **A46**, 467.
179. G. M. Sheldrick, SHELXL-93, University of Gottingen, 1993.
180. S. Wang, M. L. Hu and S. W. Ng, *Acta Cryst.*, 2002, **E58**, m242.
181. G. A. Rempel, P. Legzdins, H. Smith and G. Wilkinson, *Inorg. Synth.*, 1972, **13**, 90.
182. T. R. Felthouse, *Prog. Inorg. Chem.*, 1982, **29**, 73.
183. F. A. Cotton and J. L. Thompson, *Inorg. Chim. Acta*, 1984, **81**, 193.
184. F. A. Cotton and K. -B. Shiu, *Rev. Chim. Mater.*, 1986, **23**, 14.
185. F. A. Cotton, E. V. Dikarev and X. Feng, *Inorg. Chim. Acta*, 1995, **237**, 19.
186. F. A. Cotton and R. A. Walton, *Multiple Bonds Between Metal Atoms*, 1993, 2<sup>nd</sup> Ed., Oxford University Press, New York .
187. S. A. Johnson, H. R. Hunt and H. M. Neumann, *Inorg. Chem.*, 1963, **2**, 960.
188. K. Das and J. L. Bear, *Inorg. Chem.*, 1976, **15**, 2093.
189. K. Das, E. L. Simmons and J. L. Bear, *Inorg. Chem.*, 1977, **16**, 1268.



190. R. S. Drago, S. P. Tanner, R. M. Richman and J. R. Long, *J. Am. Chem. Soc.*, 1979, **101**, 2897.
191. L. Rainen, R. A. Howard, A. P. Kimball and J. L. Bear, *Inorg. Chem.*, 1975, **14**, 2752.
192. F. A. Cotton, B. G. DeBoer, M. D. LaPrade, J. R. Pipal and D. A. Ucko, *J. Am. Chem. Soc.*, 1970, **92**, 2926.
193. G. G. Christoph and Y. B. Koh, *J. Am. Chem. Soc.*, 1979, **101**, 1422.
194. F. A. Cotton and J. L. Thompson, *Acta Cryst.*, 1981, **B37**, 2235.
195. F. A. Cotton and T. R. Felthouse, *Inorg. Chem.*, 1980, **19**, 323.
196. V. Noinville, B. Viossat and Nguyen-Huy Dung, *Acta. Cryst.*, 1993, **C49**, 1297.
197. Y. B. Koh and G. G. Christoph, *Inorg. Chem.*, 1978, **17**, 2590.
198. G. G. Christoph, J. Halpern, G. P. Khare, Y. B. Koh and C. Romanowski, *Inorg. Chem.*, 1981, **20**, 3029.
199. The United Kingdom Chemical Database Service, D. A. Fletcher, R. F. McMeeking and D. J. Parkin, *Chem. Inf. Comput. Sci.*, 1996, **36**, 746.
200. Y. B. Koh and G. G. Christoph, *Inorg. Chem.*, 1978, **17**, 2590.
201. N. Mehmet and D. A. Tocher, *Inorg. Chim. Acta*, 1991, **188**, 71.
202. F. A. Cotton and T. R. Felthouse, *Inorg. Chem.* 1981, **20**, 600.
203. T. Janecki, Shu Shi, P. Kaszynski and J. Michi, *Collect. Czech. Chem. Commun.*, 1993, **58**, 89.
204. Y. B. Koh and G. G. Christoph, *Inorg. Chem.*, 1979, **18**, 1122.
205. M. Handa, M. Watanabe, D. Yoshioka, S. Kawabata, R. Nukada, M. Mikuriya and K. Kasuga, *Bull. Chem. Soc. Jpn.*, 1999, **72**, 2681.
206. D. M. L. Goodgame, C. J. Page and D. J. Williams, *Inorg. Chim. Acta*, 1988, **153**, 219.
207. D. M. L. Goodgame, C. A. O'Mahoney, C. J. Page and D. J. Williams, *Inorg. Chim. Acta*, 1990, **175**, 141.
208. H. Kitamura, T. Ozawa, K. Jitsukawa, H. Masuda, Y. Aoyama and H. Einaga, *Inorg. Chem.*, 2000, **39**, 3294.

209. F. A. Cotton and Youngmee Kim, *J. Am. Chem. Soc.*, 1993, **115**, 8511.
210. H. Miyasaka, C. S. Campos-Fernandez, R. Clerac and K. R. Dunbar, *Angew. Chem. Int. Ed. Engl.*, 2000, **39**, 3831.
211. F. A. Cotton, Y. Kim and J. Lu, *Inorg. Chim. Acta*, 1994, **221**, 1.
212. C. A. Crawford, E. F. Day, W. E. Streib, J. C. Huffman and G. Christou, *Polyhedron*, 1994, **13**, 2933.
213. K. Aoki and H. Yamazaki, *J. Am. Chem. Soc.*, 1984, **106**, 3691.
214. A. J. Holder, M. Schröder and T. A. Stephenson, *Polyhedron*, 1987, **6**, 461.
215. F. A. Cotton, E. V. Dikarev, M. A. Petrukhina, M. Schmitz and P. J. Stang, *Inorg. Chem.*, 2002, **41**, 2903.
216. Youngmee Kim, Sung-Jin Kim and Wonwoo Nam, *Acta Cryst.*, 2001, **C57**, 266.
217. S. M. Contakes, K. K. Klausmeyer and T. B. Rauchfuss, *Inorg. Chem.*, 2000, **39**, 2069.
218. Jian Lu, W. T. A. Harrison and A. J. Jacobson, *Chem. Commun.*, 1996, 399.
219. Wen-Mei Xue, F. E. Kuhn and E. Herdtweck, *Polyhedron*, 2001, **20**, 791.
220. K. Das, K. M. Kadish and J. L. Bear, *Inorg. Chem.*, 1978, **17**, 930.
221. R. W. Taft in '*Steric Effects in Organic Chemistry*', M. S. Newman Ed., Wiley, New York, 1967.
222. V. Gutmann, *Coord. Chem. Rev.*, 1976, **18**, 225.